ISBN 0-612-15600-1

UNIVERSITÉ D'OTTAWA
UNIVERSITY OF OTTAWA

For Ingrid and Ryan...

*Yes I broke some rules...but I got the sound I wanted.*

-Claude Debussy

# Table of Contents


**Acknowledgments.** i

**List of figures.** ii

**List of schemes.** v

**Abbreviations and symbols.** x

**Abstract.** xii

**Chapter 1: Discovery and Practical Applications of the Gilvocarcins.** 1

1.1 Isolation and structure elucidation. 1

1.2 Biological activity. 3

**Chapter 2: Previous Syntheses of the Gilvocarcins.** 7

2.1 Aglycones. 7

2.1.1 Findlay's synthesis. 8

2.1.2 Jung's synthesis. 10

2.1.3 Martin's intramolecular biaryl coupling. 11

2.1.4 The Hart synthesis. 13

2.1.5 The McGee-Hua approach. 15

2.1.6 McKenzie's synthesis of defucogilvocarcin M. 16

2.1.7 The Parker synthesis. 18

2.2 Glycones. 19

**Chapter 3: Synthesis of the Gilvocarcin Ring System via the Diels-Alder Cycloaddition.** 22

3.1 The Intramolecular Approach. 22

3.1.1 Retrosynthetic analysis. 22

3.1.2 Model systems. 24
3.2 The Intermolecular Approach. 26
3.2.1 Retrosynthetic analysis. 26
3.2.2 Model systems. 28

**Chapter 4: *o*-Quinodimethanes.** 30
4.1 *o*-Quinodimethane preparation and reactivity. 30
4.2 Synthetic applications. 35

**Chapter 5: Photochemical Synthesis of 1,4-Dioxygenated-*o*-quinodimethanes.** 38
5.1 Previous syntheses of 1,4-dioxygenated-*o*-quinodimethanes. 38
5.2 Synthesis of the aldehydic precursors. 40
5.3 Intermolecular cycloaddition studies. 48
5.4 Electrocyclization vs dimerization. 79
5.5 The effect of lithium chloride on the cycloaddition reaction. 85
5.6 Attempted intramolecular cycloadditions. 93
5.7 Conclusions. 97
5.8 Experimental section. 98

**Chapter 6: Acyl Cyanides as Carbonyl Heterodienophiles.** 125
6.1 Photocyclization of *o*-alkylacetophenones, benzaldehydes and benzoyl cyanides. 125
6.2 The synthesis of other aroyl cyanide

*o*-QDM precursors. 131

6.3 Preliminary cycloaddition studies. 137

6.4 Mixed cycloaddition studies. 144

6.5 Cycloaddition with thermally generated *o*-quinodimethanes. 156

6.6 Relative reactivity and competition experiments. 168

6.7 Sulfur dioxide trapping experiments. 176

6.8 Conclusions. 184

6.9 Experimental section. 184

**Chapter 7: Acyl Cyanides as Carbonyl Heterodienophiles: Synthetic Applications of the Cycloadducts.** 221

7.1 Introduction. 221

7.2 An isoquinolone synthesis. 222

7.3 An isocoumarin synthesis. 229

7.4 Synthesis of naphthols and naphthoquinones. 230

7.5 Attempted cyclization of naphthoquinone **16a**. 240

7.6 Photochemical behavior of naphthoquinone **16a**. 243

7.7 Attempted synthesis of the defucogilvocarcin M ring system by anionic carbamoyl transfer. 247

7.8 Conclusions. 251

7.9 Experimental section. 251

**Chapter 8: Recommendations for Further Research.** 267

8.1 Further studies based on 1,4-dioxygenated-*o*-quinodimethanes. 267

8.2 Quinone methide electrocyclization. 270
8.3 Quinone photochemistry. 278
8.4 Extension of the remote metallation approach. 280
8.5 Experimental section. 281

**Claims to original research.** 286
**Publications** 289
**References.** 290

# Acknowledgments

I would like to thank the following people who either directly or indirectly contributed to the body of work covered in this thesis:

Ingrid and Ryan Connors: For offering me more frendship, moral support, and understanding than I deserve.

My parents: For their love and encouragment.

Jean-Claude Bradley: For laughing at the same things I do.

Elizabeth Tran: For her valuable contributions as an NSERC summer student.

Yvonne Lear, Shawna Mackinnon, Terry Connolly, Rob Ben and Manfred Jung: For many entertaining and informative conversations.

Professor Tony Durst: For his patience, advice and philosophical insights; and for giving me the freedom to make my own discoveries.

# List of Figures

**Chapter 5:**


5.1 $^1$H-NMR spectrum of **11**. 42

5.2 $^1$H-NMR spectrum of **14a**. 44

5.3 $^1$H-NMR spectrum of **14b**. 46

5.4 $^1$H-NMR spectrum of **14c**. 47

5.5 $^1$H-NMR spectrum of **16** and **17**. 50

5.6 Chemical shifts and coupling constants for **16** and **17**. 51

5.7 $^1$H-NMR spectrum of **19** and **20**. 53

5.8 Chemical shifts and coupling constants for **19** and **20**. 54

5.9 $^1$H-NMR spectrum of **21** and **22**. 56

5.10 Chemical shifts and coupling constants for **21** and **22**. 57

5.11 Chemical shifts and coupling constants for **23-25**. 60

5.12 $^1$H-NMR spectrum of **23**. 62

5.13 $^1$H-NMR spectrum of **24** and **25**. 63

5.14 Chemical shifts and coupling constants for **26-28**. 65

5.15 $^1$H-NMR spectrum of **26**. 66

5.16 $^1$H-NMR spectrum of **27** and **28**. 67

5.17 Chemical shifts and coupling constants for **29** and **30**. 70

5.18 $^1$H-NMR spectrum of **29**. 71

5.19 $^1$H-NMR spectrum of **30**. 72

5.20 $^1$H-NMR spectrum of **31**. 76

5.21 $^1$H-NMR spectrum of **32**. 77

5.22 Chemical shifts and coupling constants for **31** and **32**. 78

5.23 $^1$H-NMR spectrum of **37**. 81

5.24 $^1$H-NMR spectrum of **38**. 82

5.25 Chemical shifts and coupling constants for **37** and **38**. 83

5.26 Diene HOMO-dienophile LUMO interactions. 85
5.27 Lewis acid catalysed cycloadditions of **18b**. 87
5.28 Extraction of LiCl in benzene by **14b**. 88
5.29 $^1$H-NMR of **14b/23** with varying LiCl concentration. 90
5.30 Effect of LiCl on other cycloadditions of **18b**. 91
5.31 $^1$H-NMR spectrum of **14d**. 95

**Chapter 6:**

6.1 $^1$H-NMR spectrum of **6a**. 129
6.2 $^{13}$C-NMR spectrum of **6a**. 130
6.3 $^1$H-NMR spectrum of **1b**. 133
6.4 $^{13}$C-NMR spectrum of **1b**. 134
6.5 $^1$H-NMR spectrum of **1e**. 135
6.6 $^1$H-NMR spectrum of **1d**. 136
6.7 $^1$H-NMR spectrum of **6b**. 138
6.8 $^{13}$C-NMR spectrum of **6b**. 139
6.9 $^1$H-NMR spectrum of **6c**. 142
6.10 $^{13}$C-NMR spectrum of **6c**. 143
6.11 $^1$H-NMR spectrum of **7a**. 146
6.12 $^{13}$C-NMR spectrum of **7a**. 147
6.13 $^1$H-NMR spectrum of **7d**. 150
6.14 $^{13}$C-NMR spectrum of **7d**. 152
6.15 $^1$H-NMR spectrum of **7e**. 154
6.16 $^{13}$C-NMR spectrum of **7e**. 155
6.17 $^1$H-NMR spectrum of **10a**. 160
6.18 $^{13}$C-NMR spectrum of **10a**. 161
6.19 ORTEP diagram of **10a**. 162

6.20 $^{1}$H-NMR spectrum of **10b**. 164
6.21 $^{13}$C-NMR spectrum of **10b**. 165
6.22 $^{1}$H-NMR spectrum of **11a**. 167
6.23 $^{1}$H-NMR spectrum of **14a** and **14b**. 171
6.24 $^{1}$H-NMR spectrum of the products from the cycloaddition of **2a** and benzoyl fluoride. 177
6.25 a) $^{1}$H-NMR spectrum of **19a**. b) Aromatic expansion. 179

**Chapter 7:**

7.1 $^{1}$H-NMR spectrum of **7a**. 224
7.2 $^{13}$C-NMR spectrum of **7a**. 225
7.3 $^{1}$H-NMR spectrum of **13a**. 232
7.4 $^{1}$H-NMR spectrum of **13c**. 235
7.5 $^{13}$C-NMR spectrum of **13c**. 236
7.6 $^{1}$H-NMR spectrum of **16c**. 238
7.7 $^{13}$C-NMR spectrum of **16c**. 239
7.8 $^{1}$H-NMR spectrum of **25**. 246

# List of Schemes


**Chapter 2:**

2.1 The Findlay-Danishefsky defucogilvocarcin V synthesis. 8

2.2 Jung's defucogilvocarcin V synthesis. 11

2.3 Martin's defucogilvocarcin M and E syntheses. 12

2.4 Hart's defucogilvocarcin M synthesis. 14

2.5 McGee's defucogilvocarcin V synthesis. 15

2.6 McKenzie's defucogilvocarcin M synthesis. 17

2.7 Parker's *o*-methyldefucogilvocarcin synthesis. 18

2.8 Suzuki's (+)-gilvocarcin M synthesis. 20

**Chapter 3:**

3.1 Previous disconnection strategies. 22

3.2 Intramolecular Diels-Alder antithesis. 23

3.3 Proposed 1,4-dioxygenated-*o*-QDM 5. 24

3.4 Intramolecular model system. 25

3.5 Intermolecular Diels-Alder antithesis. 27

3.6 Intermolecular model system. 28

**Chapter 4:**

4.1 Endo vs exo adducts: α,α'-disubstituted-*o*-QDM. 31

4.2 Macdonald and Durst's podophyllotoxin synthesis. 32

**Chapter 5:**

5.1 Kraus' α,α'-dioxygenated-*o*-quinodimethane. 38

5.2 Kraus' pleurotin model. 39

5.3 Saa's 1-aryl-1-hydroxy-2-methoxybenzocyclobutenes. 40

5.4 Synthesis of aldehyde **11**. 41
5.5 Synthesis of aldehyde **14a**. 43
5.6 Synthesis of aldehydes **14b** and **14c**. 45
5.7 Sterically congested photoenols. 48
5.8 Synthesis of **16** and **17**. 49
5.9 Synthesis of **19** and **20**. 52
5.10 Synthesis of **21** and **22**. 55
5.11 Synthesis of **23, 24** and **25**. 59
5.12 Synthesis of **26, 27** and **28**. 64
5.13 Synthesis of **29** and **30**. 69
5.14 Cycloaddition of **18b** with alkynyl dienophiles. 74
5.15 Dimerization of 2-methylbenzaldehyde. 79
5.16 Photochemical dimerization of **14b**. 80
5.17 Synthesis of **14d** and **14e**. 93
5.18 Attempted photocycloaddition of **14d**. 96
5.19 Attempted photocycloaddition of **14e**. 97

**Chapter 6:**

6.1 Benzocyclobutenol formation from hindered photoenols. 125
6.2 Proposed electrocyclic ring closure of **2a**. 126
6.3 Photochemical dimerization of **1a**. 127
6.4 Synthesis of substituted aroyl cyanides **1b-1e**. 131
6.5 Photochemical dimerization of **1b**. 137
6.6 Photochemical dimerization of **1c**. 140
6.7 Abortive photochemical dimerization of **1d**. 144
6.8 Irradiation of **1a** and benzoyl cyanide. 145
6.9 Irradiation of **1b** and benzoyl cyanide. 148

6.10 Irradiation of **1c** and benzoyl cyanide. 149
6.11 Photoenolization of **1b** in the presence of **1e**. 151
6.12 Photocycloaddition of **2a** and acetyl cyanide. 153
6.13 Proposed mechanistic pathways leading to **7a**. 157
6.14 Cycloaddition of **9a** with benzoyl cyanide. 158
6.15 Cycloaddition of **9b** with benzoyl cyanide. 163
6.16 Cycloaddition of **9a** with acetyl cyanide. 168
6.17 Competition between phenylglyoxal and benzoyl cyanide. 169
6.18 Effect of *o*-substitution on heterodienophile reactivity. 172
6.19 Kessar's dimerization sequence. 173
6.20 Attempted cycloaddition of **2a** and benzoyl cyanide. 174
6.21 Cycloadditions with neutral acylating agents. 175
6.22 Charlton and Durst's benzothiophenedioxides. 177
6.23 Irradiation of **1a** in the presence of $SO_2$. 178
6.24 Irradiation of **1b** in the presence of $SO_2$. 180

**Chapter 7:**

7.1 Tandem addition cyclization strategy. 221
7.2 Couture's isoquinolone synthesis. 222
7.3 Synthesis of isoquinolone **7a**. 223
7.4 Synthesis of isoquinolone **7b**. 226
7.5 Versatile isoquinolone synthesis. 227
7.6 Synthesis of **9a** and **9b**. 228
7.7 Synthesis of isocoumarins **10a** and **10b**. 229
7.8 Synthesis of naphthol **13a** via MeLi. 230
7.9 Abortive synthesis of naphthol **13b**. 231
7.10 Synthesis of naphthol **13c**. 233

7.11 Preparation of naphthoquinones **16a** and **16c**. 237
7.12 Attempted cyclization of naphthoquinone **16a**. 240
7.13 Postulated mechanistic sequence leading to **19**. 241
7.14 Alternative sequence leading to **19**. 242
7.15 Kanaoka's *N*-(*o*-tolyl)phthalimide photocyclization. 243
7.16 Photocyclization of naphthoquinone **16a**. 244
7.17 Synthesis of intermediates **13c** and **16c**. 247
7.18 Snieckus' dibenzo[c,d]pyranone synthesis. 248
7.19 Alternative pathways leading to **31**. 249

**Chapter 8:**

8.1 Krause's model vs model **18e**. 267
8.2 Proposed photoenols **18f**, **18g** and **18h**. 268
8.3 s-cis and s-trans rotamers of **18g**. 269
8.4 E,E vs E,Z-photoenols (**18h**). 269
8.5 Cyclization of **17** to **18'**. 270
8.6 Cyclization of **17b** to **18b**. 271
8.7 Retrosynthetic analysis of quinone **16b**. 272
8.8 Synthesis of chalcones **22a** and **22b**. 273
8.9 Synthesis of **23a** and **23b**. 274
8.10 Potential synthesis of **16b** involving TMSCN. 275
8.11 Potential synthesis of **16e**. 276
8.12 Potential isoquinolone analogues of defucogilvocarcin M. 277
8.13 Electrocyclic ring closure leading to **33**. 278
8.14 Photochemical reactivity of quinone **16a**. 278
8.15 Potential DNA alkylating agent. 279
8.16 Quinone methide defucogilvocarcin M analogues. 280

8.17 Remote carbamoyl transfer leading to **36**. 280

8.18 Methylation of hydroquinone **38**. 281

# Abbreviations and Symbols

| | |
|---|---|
| (br) | broad |
| (m) | medium |
| (s) | strong |
| (w) | weak |
| $[M]^+$ | molecular ion |
| BTAH | benzyltrimethylammonium hydroxide |
| BtfI | [bis(trifluoroacetoxy)iodo]benzene |
| CIMS | chemical ionization mass spectrum |
| $cm^{-1}$ | wavenumber |
| $\delta$ | chemical shift |
| d | doublet |
| DMAP | dimethylaminopyridine |
| DMF | dimethylformamide |
| EIMS | electrical ionization mass spectrum |
| eq | equivalents |
| FMO | frontier molecular orbital |
| h | hours |
| hv | electromagnetic irradiation |
| Hz | hertz |
| IR | infrared |
| *J* | coupling constant |
| LDA | lithium diisopropylamide |
| M | molar |
| m | multiplet |
| m/e | mass/charge ratio |

| | |
|---|---|
| MeI | methyl iodide |
| MeOH | methanol |
| min | minute |
| mL | milliliter |
| NaH | sodium hydride |
| $\nu_{max}$ | absorbance |
| NMR | nuclear magnetic resonance |
| *o*-QDM | *o*-quinodimethane |
| $^{o}C$ | degrees celsius. |
| Π | base |
| PDC | pyridinium dichromate |
| ppm | parts per million |
| q | quartet |
| r t | room temperature |
| s | singlet |
| t | triplet |
| TEA | triethylamine |
| THF | tetrahydrofuran |
| t l c | thin layer chromatography |
| TMS | tetramethylsilane |
| TMSCN | trimethylsilylcyanide |
| TsOH | *p*-toluenesulfonic acid |

# Abstract

This thesis describes efforts to develop a synthesis of the defucogilvocarcin M carbon skeleton utilizing either an intramolecular or an intermolecular Diels-Alder cycloaddition as the key step.

Chapters 1 and 2 provide background information regarding the isolation, biological activity, mechanism of action and previous syntheses of the gilvocarcins.

Chapter 3 provides a retrosynthetic analysis of defucogilvocarcin M and describes the intramolecular and the intermolecular Diels-Alder approaches to its synthesis.

Chapter 4 gives a brief review of the *o*-quinodimethane chemistry central to the proposed synthesis.

Chapter 5 describes a photochemical synthesis of 1,4-dioxygenated-*o*-quinodimethanes. The *o*-QDMs were obtained by irradiation of 2-(methoxymethyl)-benzaldehyde (**11**) and the 2-(acyloxymethyl)benzaldehydes **14a-c**.

The intermolecular Diels-Alder reactivity, regioselectivity and stereoselectivity of the photoenols was ascertained by reaction with several dienophiles of varying reactivity.

The catalytic effect of LiCl on the cycloaddition of the photoenol derived from 2-(benzoyloxymethyl)benzaldehyde (**14b**) and methyl acrylate was briefly examined. Marginal effects were also observed with several other dienophiles.

2-(benzoyloxymethyl)benzaldehyde (**14b**) was found to dimerize to compound **37** when irradiated in the absence of a reactive

dienophile, analogous to the known photochemical behavior of *o*-tolualdehyde.

Two model systems, **14d** and **14e**, designed to test the feasibility of an intramolecular photochemical Diels-Alder cycloaddition were synthesized. Photoenolization of the compounds, however, failed to afford cycloaddition products.

Chapter 6 describes the results obtained from a re-evaluation of the photochemistry of 2-methylbenzoyl cyanide (**1a**).

The latter compound as well as a number of other acyl cyanides (**1b-e**) were found to act as carbonyl heterodienophiles in Diels-Alder reactions with photochemically (**1a-c**) and thermally (**8a,b**) generated *o*-quinodimethanes. Several dimerizations and mixed cycloadditions were studied which led to highly substituted 3,4-dihydro-3-cyano-1H-2-benzopyran-1-ones.

Photoenols derived from aroyl cyanides **1a** and **1b** were found to react with $SO_2$ to give 1-Hydroxy-1-cyano-1,3-dihydrobenzo[c]thiophene 2,2-Dioxides **19** and **20**.

Chapter 7 describes efforts to utilize the acyl cyanide cycloadducts as synthetic intermediates.

A versatile isoquinolone synthesis was developed which involved reacting the acyl cyanide cycloadducts **1** and **8** with alkyl amines then cyclizing the amides obtained in aqueous acetic acid.

Two cycloadducts (**1** and **8**) were converted to isocoumarins by dehydrocyanation with KtBuO in THF.

The cycloadducts were shown to react with methyl lithium to give acetophenones and 3-aryl naphthols-via an addition cyclization

sequence. The naphthols were readily oxidized to the naphthoquinones **16a** and **16c**.

Preliminary attempts to convert naphthoquinone **16a** to the defucogilvocarcin ring system by anionic electrocyclic ring closure were unsuccessful.

Irradiation of naphthoquinone **16a** resulted in cyclization to an indenonaphthoquinone derivative. Acid catalysed dehydration gave 5H-benzo[a]fluoren-5-one, a potential DNA intercalating agent.

Attempts to convert naphthoquinone **16c** to the defucogilvocarcin M system by remote metallation and ring to ring carbamoyl transfer are described.

Chapter 8 proposes possible directions for future research.

# Chapter 1

# Discovery and Practical Applications of the Gilvocarcins

## 1.1 Isolation and structure elucidation

The gilvocarcins and chrysomycins are representatives of an emerging class of *C*-aryl glycosides which exhibit significant antitumor as well as antibiotic activity. The members of this family share a common benzonaphthopyranone system attached to different *C*-glycoside moieties.

In 1971 Hatano and Horii[1] reported the isolation, from *Streptomyces collinus* subsp. *albescens*, of the antibiotic B21085. They later published details[2] regarding the isolation and biological activity of B21085 which they christened toromycin (1). Subsequently in 1981 Takahashi's group[3] isolated, from *Streptomyces gilvotanareus*, gilvocarcin V (1) whose structure and stereochemistry was deduced

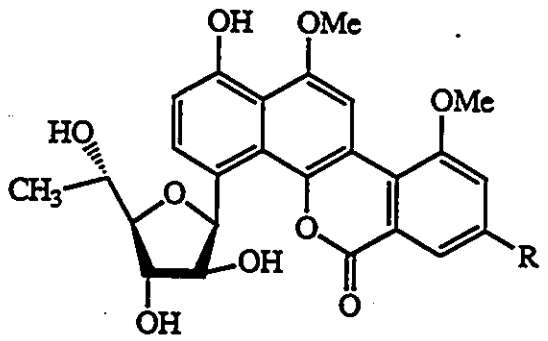


1 R = $CH{=}CH_2$
2 R = $CH_3$
3 R = $CH_2CH_3$

on the basis of a comparison of the $^{1}H$ and $^{13}C$-NMR spectra with those of the known antibiotic gilvocarcin M[4]. Jain and co-workers[5] (1983) provided additional confirmation with their report of the isolation of **1** from the streptomycete AAC-324. They independently assigned the structure of gilvocarcin V, based on proton and carbon NMR spectral evidence, and the structure of several degradation products including gilvocarcin E[6] (**3**).

Chrysomycin V (**4**) and chrysomycin M (**5**), both isolated from *Streptomyces* sp. A-419[7] (Strelitz 1955), share the same tetracyclic aglycone chromophore as the gilvocarcin series. Their structures were reported by Weiss et al[8] in 1982 on the basis of carbon and proton NMR experiments.

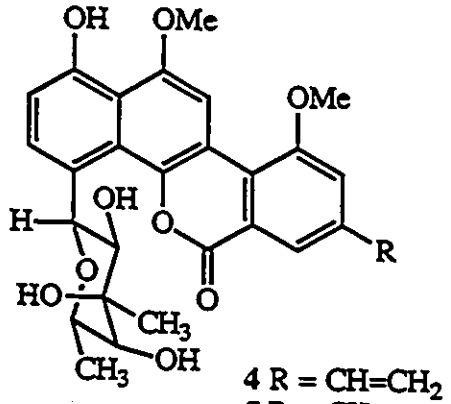


**4** R = CH=CH$_2$
**5** R = CH$_3$

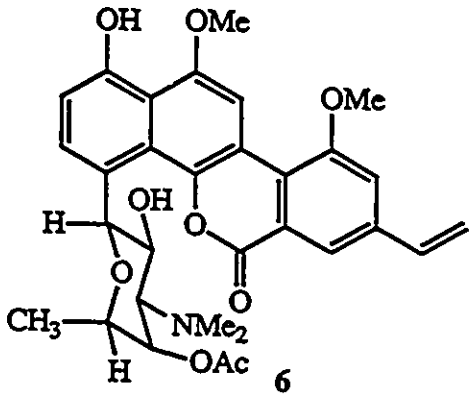


**6**

Ravidomycin[9] (**6**), Isolated from the fermentation broth of *Streptomyces ravidus*, was assigned the structure depicted above (Findlay et al 1981) on the basis of chemical and spectroscopic data.[10]

The aglycones common to compounds **1** through **6** have also been subjected to extensive study. The tetracyclic chromophore has been repeatedly isolated during degradation studies and defucogilvocarcin V

(7), in particular, has recently been isolated by Misra and co-workers[11] from *Streptomyces arenae* 2064. The latter report is of considerable interest from a biogenetic viewpoint suggesting that the sugar moieties may be installed after the formation of the chromophore.

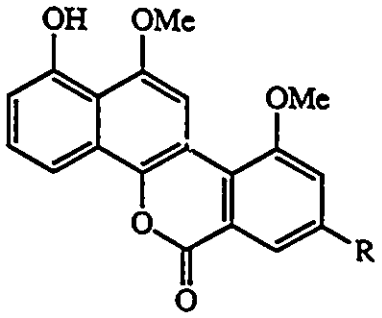


7 R = $CH{=}CH_2$
8 R = $CH_3$

## 1.2 Biological activity

The gilvocarcins are active against gram positive organisms and weakly active against gram negative bacteria, as well as various species of fungi and tumors.[12] Defucogilvocarcin V (7) has antitumor activity similar to its congener (1) but exhibits greater selectivity than its *C*-glycoside counterparts with respect to antimicrobial action.

While gilvocarcin V is known to inhibit DNA synthesis,[13] its precise mechanism of action is only partially understood. In side by side assays for photoinitiated DNA damage, it has been demonstrated to be $10^3$ to $10^5$ times more active than 8-methoxy psoralen.[14] The impressive potencies of some of the gilvocarcins where single strand DNA breaks have been indicated (concentrations as low as 0.01 μg/mL have been detected), together with the minimal toxicity observed in

vivo ($LD_{50}$ ~ 1000 mg/kg) render them attractive as potential anticancer agents.

Elespuru and Gonda have established a connection between in vitro DNA strand nicking by gilvocarcin V and irradiation with low energy light.[14] They utilized prophage induction experiments employing *Escherichia coli* strain BR 513 which contains a chromosomally integrated lambda-lacZ fusion phage under control of the lambda repressor. The lacZ gene encodes β-galactosidase which is produced in response to DNA damage and ensuing derepression of prophage (prophage induction). Both chrysomycin V (4) and gilvocarcin V showed strong prophage induction after 15 to 20 min. exposure of solutions to fluorescent light (induction was most efficient when a UVA lamp with a stronger emission in the 320 to 420 nm region was used) and no activity when the procedure was repeated in the dark. The wavelength dependance of the induction assay for gilvocarcin V was strongly correlated with its absorption spectrum.[15] Gilvocarcin M (2), by contrast, showed no prophage induction on light exposure which would seem to suggest that the vinyl group present in gilvocarcin V, chrysomycin V, ravidomycin and defucogilvocarcin V is essential for antitumor activity.

In connection with the relationship between the vinyl group and biological activity, McGee and Misra[15] have identified 9 as having resulted from an in vitro [2+2] photocycloaddition between the vinyl group of gilvocarcin V and a thymidine residue from DNA. The anomalous pyranose residue was explained as having arisen as a result of acid catalysed

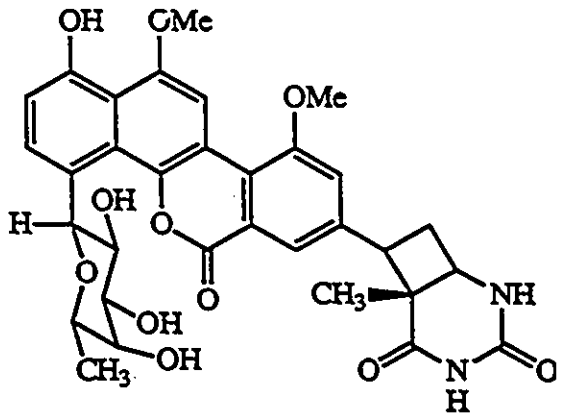

9

isomerization of the fucosyl moiety during the digestion of the host DNA.

Other factors have also been suggested which might contribute to the biological activity of the gilvocarcins, specifically, type I and type II photochemical effects.

Type I photochemistry involves the production of radical ions or free radicals by interaction of a photosensitizer triplet with substrate. This includes the generation of superoxide ions which disproportionate to hydrogen peroxide in aqueous systems then, in the presence of iron, to hydroxy radicals. The deleterious effects of such radicals in vivo has been well documented.[16]

Type II photochemistry involves the generation of singlet oxygen via photosensitizers with long lived triplet states. The singlet oxygen produced reacts readily with electron rich substrates, a property which has been ascribed to the activity of cytotoxic hematoporphoryn derivatives.[17]

Riesz[18] has undertaken a detailed ESR study of the photochemistry of gilvocarcin V and found that it proceeds by both type

I and type II pathways. Gilvocarcin V was determined to photoreduce DMSO, resulting in the production of methyl radicals, and to photoreduce oxygen, yielding singlet oxygen with moderate efficiency. In contrast to these observations rose bengal, a singlet oxygen generator, and plumbagin, a redox cycling quinone, failed to induce bacteriophage lambda in *E. coli* in the same manner as gilvocarcin V. Consequently it has been concluded that the DNA damaging effects seen in the gilvocarcins must also require that it intercalate into the host DNA.

# Chapter 2

# Previous Syntheses of the Gilvocarcins

## 2.1 Aglycones

The gilvocarcin aglycones (**1**,**2**) exhibit significant antibacterial and antitumor activities as well as low toxicity, properties which have garnered them much attention as potential anticancer agents.[1-4] The compounds have also aroused considerable interest amongst synthetic organic chemists perhaps owing to the challenge inherent in the highly functionalized tetracyclic framework.

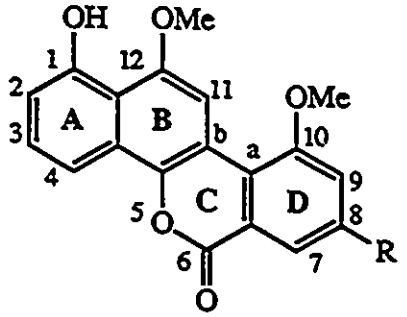


**1** R = $CH{=}CH_2$
**2** R = $CH_3$

To date most of the synthetic endeavors have centered around elaboration of the C10(a)-C10(b) bond, from naphthalenic and aryl precursors, employing nucleophile-electrophile partners at C10(b) in ring B and C10(a) in ring D, or the reverse. Another approach involved disconnection along the C11 and C12 bond and reconnection via a chromium carbene benzannulation. Fewer reports have appeared directed at synthesis of the parent *C*-aryl glycosides.

### 2.1.1 Findlay's synthesis

Findlay's synthesis[19] of defucogilvocarcin V (scheme 2.1), which was later improved upon by Danishefsky's group[20], began with 1,5-dihydroxynaphthalene (3) and bromovanillin (4).

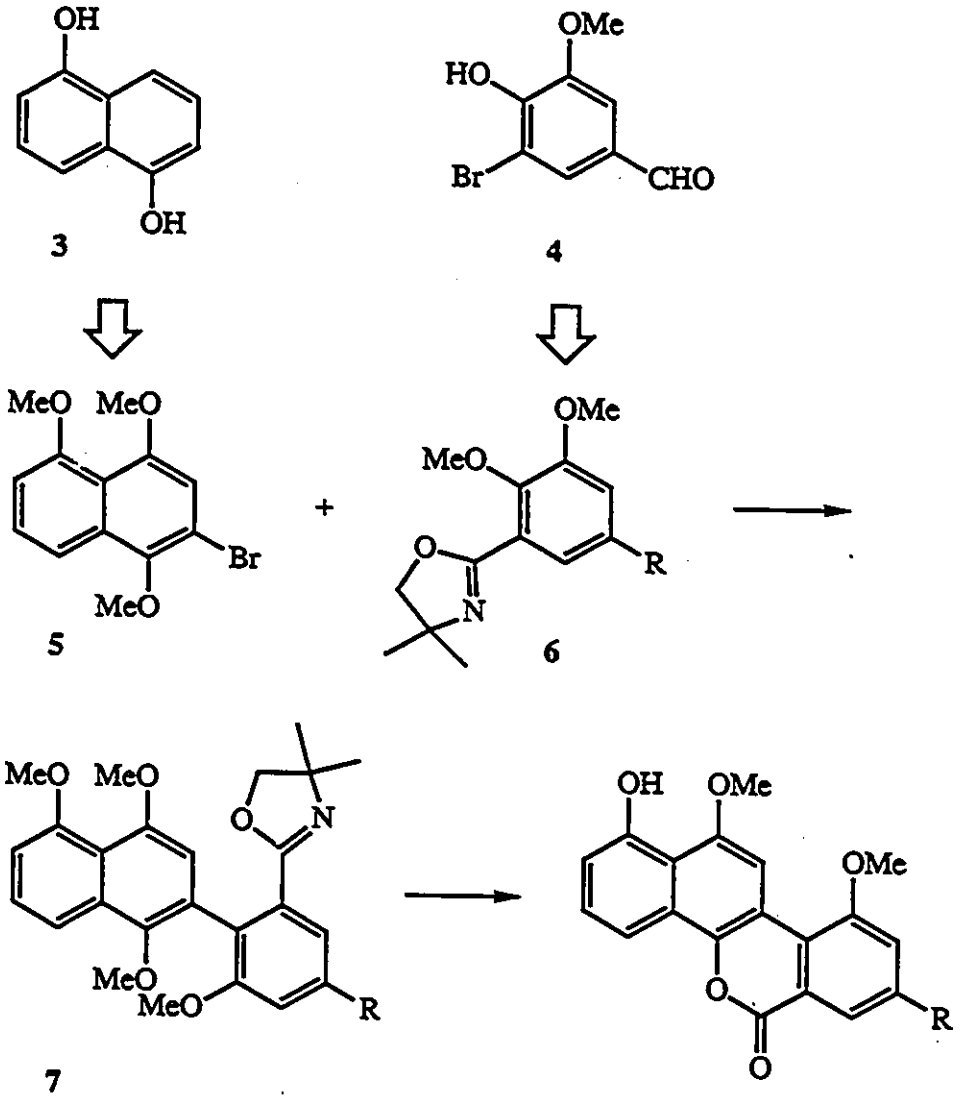


Scheme 2.1: The Findlay-Danishefsky synthesis of Defucogilvocarcin V

The key step in their approach involved the union of the Grignard reagent derived from the appropriately substituted naphthalene **5** with the oxazoline **6**, via a nucleophilic aromatic substitution, leading to the phenyl naphthalene **7**. Compound **5** was prepared from **3** by a sequence involving acetylation, bromination, and oxidation to the quinone followed by subsequent reduction and permethylation. Compound **6** was constructed by *O*-methylation of **4**, followed by Wittig olefination, carboxylation via the Grignard, then protection as the oxazoline. This latter step proved incompatible with the vinyl functionality which had to be masked by catalytic hydrogenation prior to the carboxylate protection step. The Grignard reaction between **5** and **6** furnished **7** in 81 % yield, which was subsequently deprotected and cyclized to the lactone in refluxing acetic/hydriodic acid, then permethylated leading to the 8-ethyl derivative of **1**. The vinyl group was reintroduced by benzylic bromination followed by elimination of the phenylselenoxide derivative.

Danishefsky's synthesis[20] was conceptually similar to Findlay's in that the crucial C10(a)-C10(b) bond was generated employing the Meyer's coupling reaction. Where Danishefsky's approach differed was in the

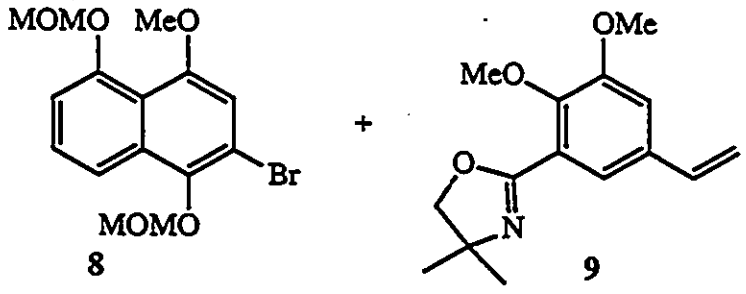

distribution of the protecting groups in the naphthalenic partner of the precursor pair for the coupling reaction. The MOM ethers present in compound **8** allowed for simultaneous deprotection and lactonization in the final stage of the synthesis. In addition, the vinyl group was present from the earliest stages of the synthesis eliminating the bromination-oxidative deselenation steps employed in Findlay's synthesis.

### 2.1.2 Jung's synthesis

Jung's synthesis[21] of defucogilvocarcin M, depicted in scheme 2.2, shares with both Findlay's and Danishefsky's approach the strategem involving a nucleophilic coupling between a naphthalene nucleus and a highly functionalized aryl electrophile. The crucial step in this case employed a Suzuki biaryl coupling[22] of the boronic acid derived from **12**, obtained by lithiation and quenching with trimethyl borate, and the aryl iodide **13**.

Compound **12** was prepared via a five step sequence from **10** involving bromination and oxidation to the quinone, followed by benzylation, reduction to the hydroquinone, and permethylation.

Compound **13** was constructed employing a five step progression from the phenol **11** entailing oxidation to the monocarboxylic acid, permethylation, and $LiAlH_4$ reduction to the benzyl alcohol, followed by o-lithation, iodination and oxidation to the methyl carboxylate.

The Suzuki coupling proceeded in 61 % yield giving compound **14**, which was then converted to **15** in three steps involving oxidation to the quinone, reduction to the hydroquinone, followed by lactonization and methylation.

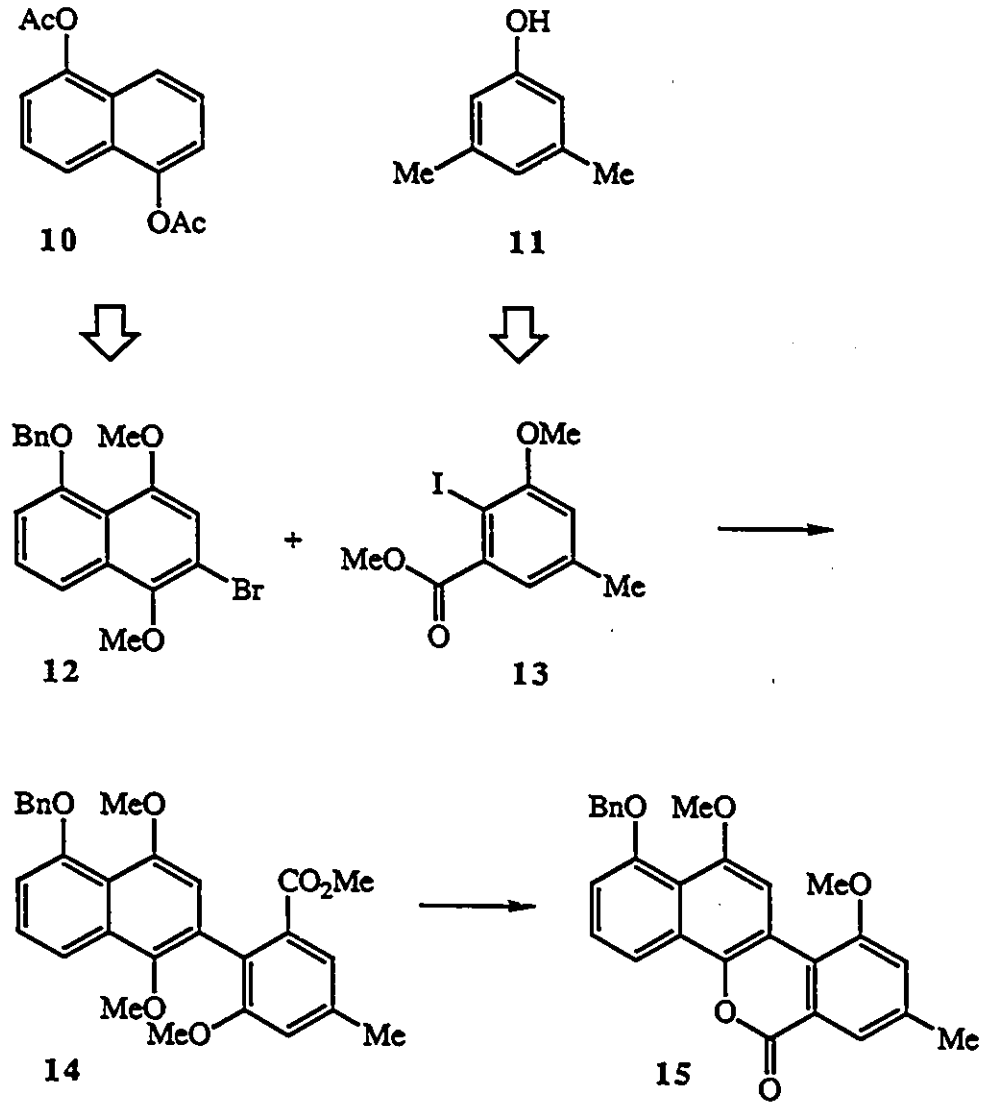


Scheme 2.2: Jung's Synthesis of Defucogilvocarcin M

### 2.1.3 Martin's intramolecular biaryl coupling

Martin's approach[23] involved an intramolecular incarnation of the Suzuki biaryl coupling, the rationale being that in the case of the intramolecular reaction, only one of the partners would require

activation thereby streamlining the procedure and possibly improving the overall yield.

The synthesis, outlined in scheme 2.3, started with the readily available precursors **16** and **17**. The advanced intermediate **18** was constructed in

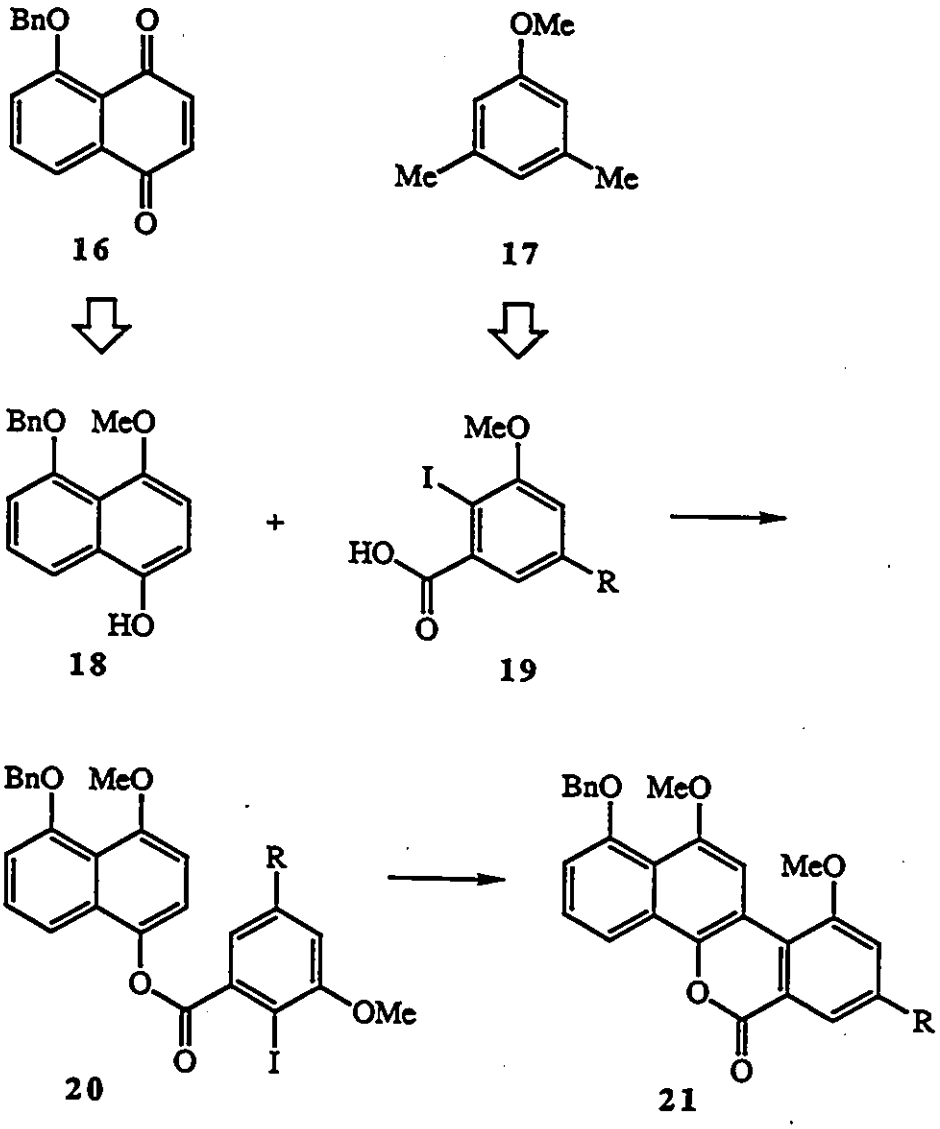


Scheme 2.3: The Martin Synthesis of Defucogilvocarcin M and E

three steps from **16** involving a simultaneous reduction and regioselective monoacetylation, employing Zn in acetic anhydride in the presence of pyridine, followed by methylation of the remaining phenolic hydroxyl group and subsequent hydrolysis of the acetate.

The eastern portion was prepared utilizing an efficient four step sequence from **17** entailing oxidation to the monocarboxylate and exhaustive methylation followed by regioselective *o*-thallation, iodination and hydrolysis to the carboxylic acid.

Compound **20**, readily prepared by DCC coupling of **18** and **19**, then underwent the biaryl coupling leading to **21** in 75 to 80 % yields.

### 2.1.4 The Hart synthesis

The preceding syntheses were all predicated on a strategy encompassing a nucleophilic naphthalene precursor and an aryl electrophile. Hart's synthesis[24], illustrated in scheme 2.4, reversed this protocol wherein the nucleophilic center, which originated in the eastern end (oxazoline **24**), underwent a conjugate addition to the α,β unsaturated tetralone **23**.

Compound **23** was prepared from **16** via a three step sequence involving sodium hydrosulfite reduction to the hydroquinone, regioselective methylation of the least hindered phenolic hydroxyl group employing methyl sulfate, followed by electrochemical oxidation to the tetralone.

Oxazoline **24** was synthesized in four steps from **22** beginning with tandem Grignard reactions utilizing methyl sulfate and ethyl chloroformate as electrophiles, followed by saponification of the ethyl ester and oxazoline formation.

The conjugate addition was carried out in the presence of methyl aluminum bis-(2,6-di-*tert*-butyl-4-methylphenoxide) furnishing the aryl tetralone **25** in 72 % yield. The tetracyclic lactone **26** was formed on acid hydrolysis of the oxazoline protecting group.

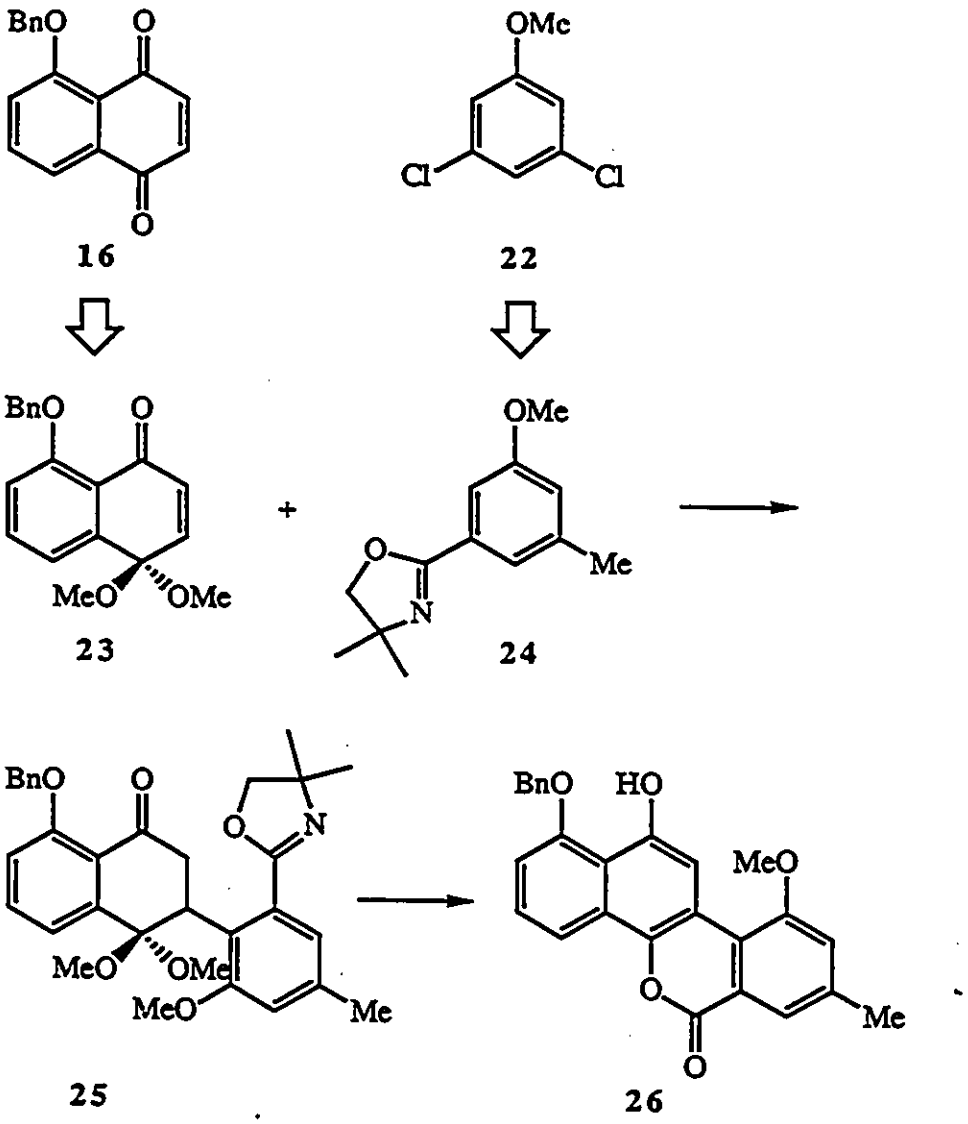


Scheme 2.4: Hart's Synthesis of Defucogilvocarcin M

### 2.1.5 The McGee-Hua approach

The efforts of McGee[25] and Hua[26] delineate the second major strategy employed in the synthesis of the gilvocarcin carbon skeleton.

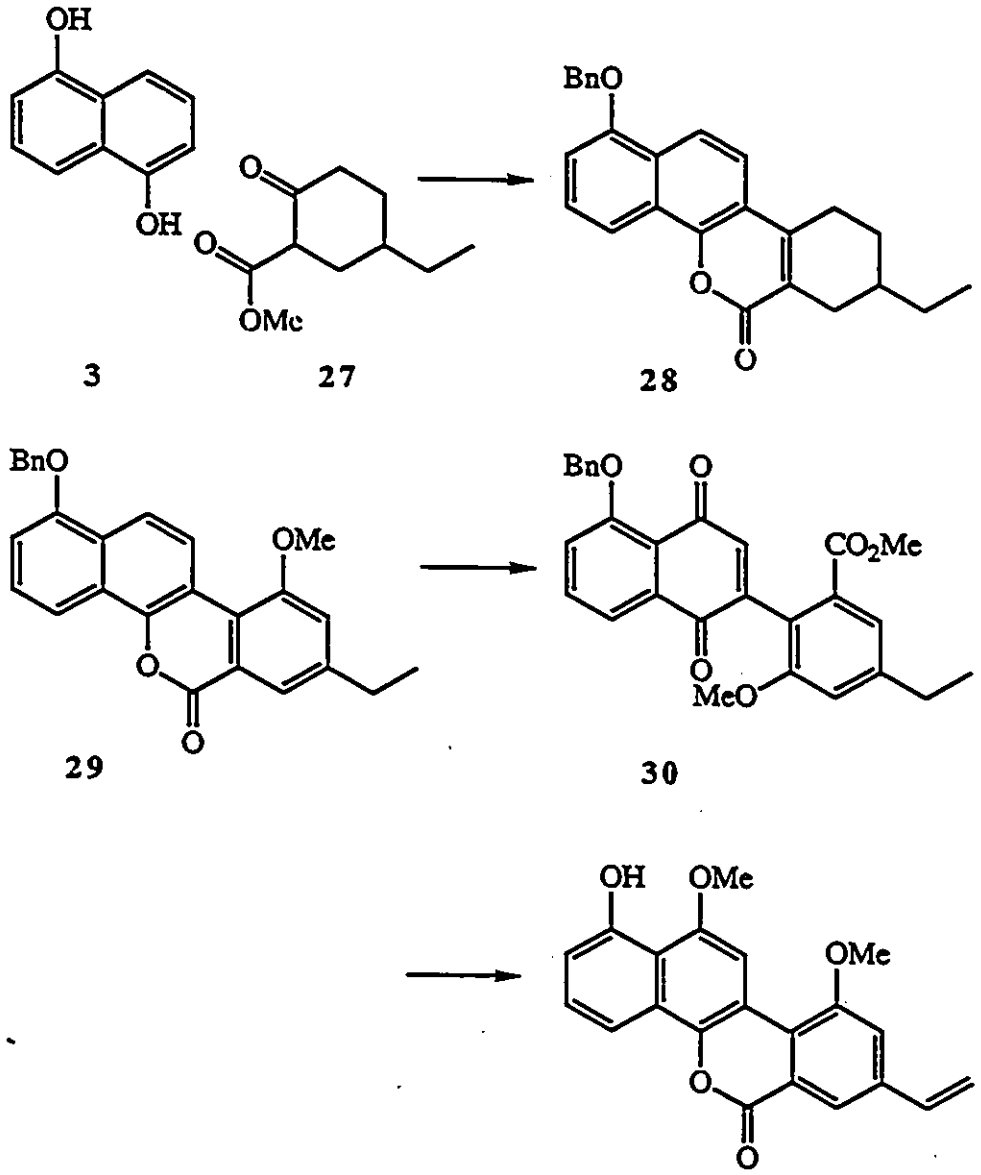


Scheme 2.5: McGee's Synthesis of Defucogilvocarcin V via Pechmann Condensation

McGee's approach, depicted in scheme 2.5, which involved a Pechmann condensation between 1,5-dihydroxynaphthalene **3** and the cyclohexanone derivative **27**, was impressive in that it assembled the entire gilvocarcin framework in a single step.

Compound **28**, which formed in 56 % yield, was subsequently oxidized in the allylic position of ring D with selenium dioxide and PCC, then converted to the dimethylacetal and aromatized with DDQ giving lactone **29**. Subsequent steps included Fremy's salt oxidation to the quinone **30**, sodium hydrosulfite reduction with lactonization followed by deprotection of the benzyl ether, then an allylic bromination dehydrobromination sequence leading to defucogilvocarcin V.

Hua[26] improved upon McGee's synthesis[25] somewhat by condensing the naphthalene derivative **31**, obtained by deprotection of the acetate, with **27** in $CF_3COOH$-$H_2SO_4$, furnishing the tetracyclic lactone **32** in 81 % yield.

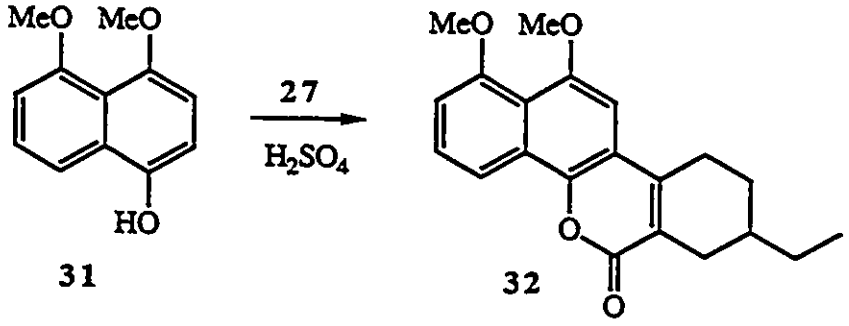


31 32

## 2.1.6 McKenzie's synthesis of defucogilvocarcin M

McKenzie's synthesis[27] of defucogilvocarcin M represents a more linear approach to construction of the tetracyclic ring system, in contrast to the convergent strategies previously described. The key steps, outlined in scheme 2.6, included a Meerwein arylation employing

the diazonium salt derived from the aniline **33**, followed by a directed Diels-Alder cycloaddition leading to the aryl naphthalene **35**.

The aniline **33** was prepared in four steps from 3-methyl-6-nitroanisole by catalytic reduction of the nitro function, conversion to the pivamide, ortho-lithiation and carboxylation, followed by esterification in acidic methanol.

The aryl naphthalene **35** was subsequently condensed with thiophenol and desulfurized by catalytic hydrogenation, which afforded the lactone **36** after methylation with diazomethane.

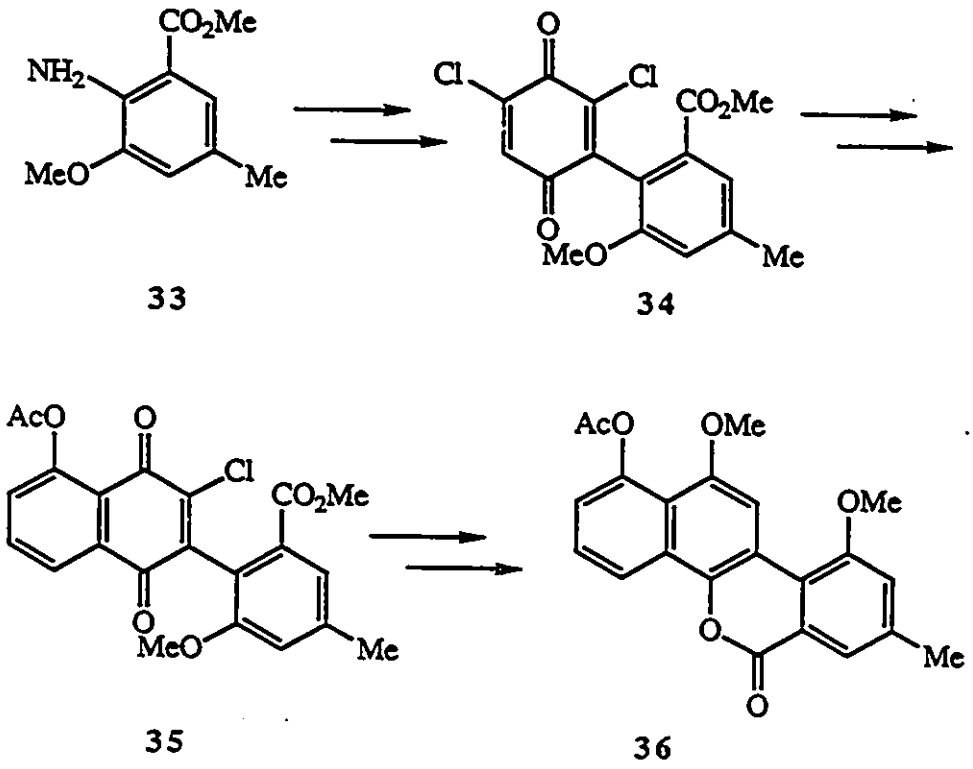


Scheme 2.6: McKenzie's Linear Sequence to Defucogilvocarcin M

The crucial steps, namely the Meerwein arylation and the Diels-Alder reaction proceeded in 55 % and 80 % yields respectively.

### 2.1.7 The Parker synthesis

The Parker synthesis[28] was an elegant approach in which the key step involved a Dotz chromium carbene benzannulation between the appropriately substituted acetylene **40** and the methoxyphenyl chromium carbene complex **39.**

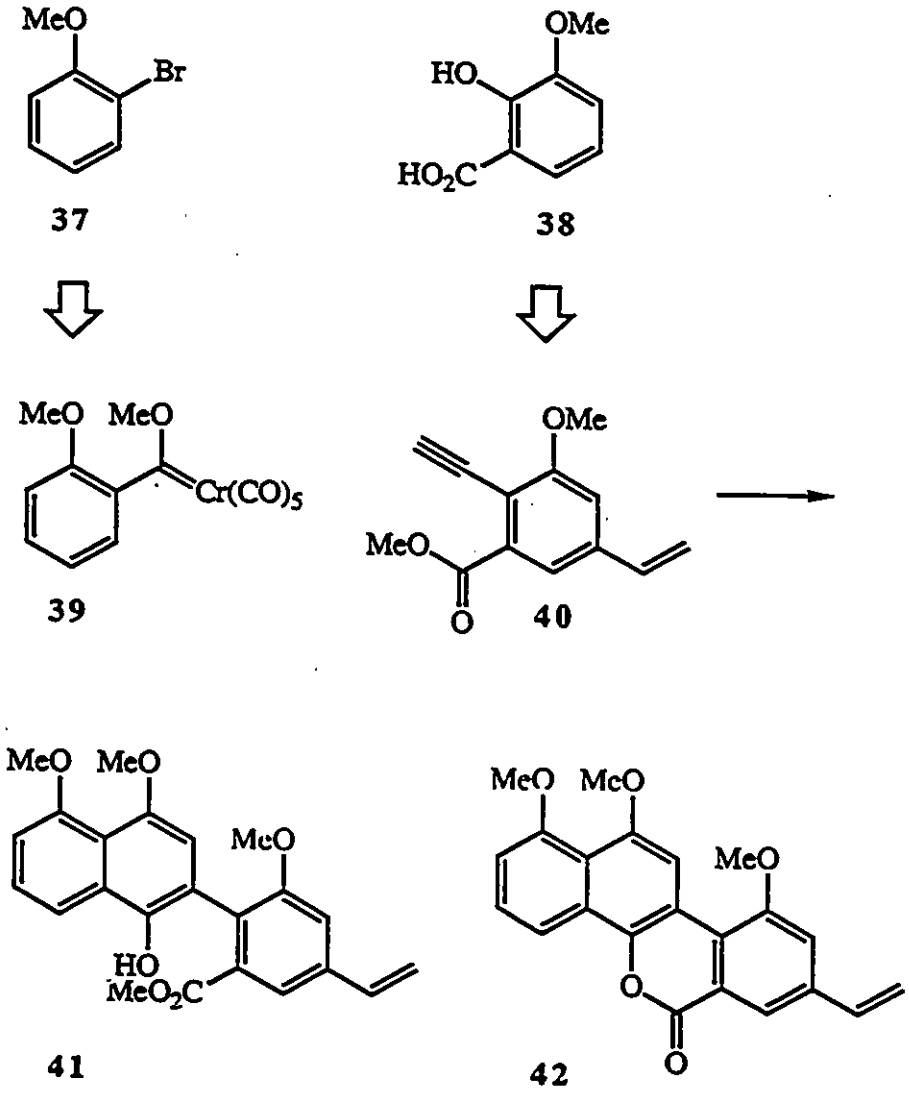


Scheme 2.7: Parker's Synthesis of 1-*O*-Methyldefucogilvocarcin V

The chromium carbene complex was readily available from 2-bromoanisole by halogen-metal exchange followed by treatment with chromium hexacarbonyl, then methylation via trimethyloxonium tetrafluoroborate.

The highly substituted acetylene **40** was prepared from 3-methoxysalicylic acid by reaction with hexamethylenetetramine in $CF_3COOH$ forming the aldehyde, followed by esterification, activation of the phenolic hydroxyl group as the triflate, Pd(II) coupling with TMS-acetylene, and Peterson olefination.

The benzannulation proceeded giving compound **41** in 43 % yield, which was subsequently converted to the lactone **42** in benzene, in the presence of TsOH.

## 2.2 Glycones

The majority of the synthetic work to date has focused on the aglycones, fewer reports have appeared dealing with the fully intact structure.

Recently Suzuki[29] has reported the successful synthesis and stereochemical assignment of gilvocarcin M, which is highlighted in scheme 2.8. The synthesis followed a linear progression beginning with the acetate of L-fucose **43**, which was converted to the aryl *C*-glycoside in 87 % yield ($\alpha/\beta$=8/1), by treatment with **44** in the presence of $Cp_2HfCl_2$-$AgClO_4$ in $CH_2Cl_2$. Conversion to the triflate followed by metalation and benzyne formation yielded, on treatment with 2-methoxyfuran, the naphthol **46**,

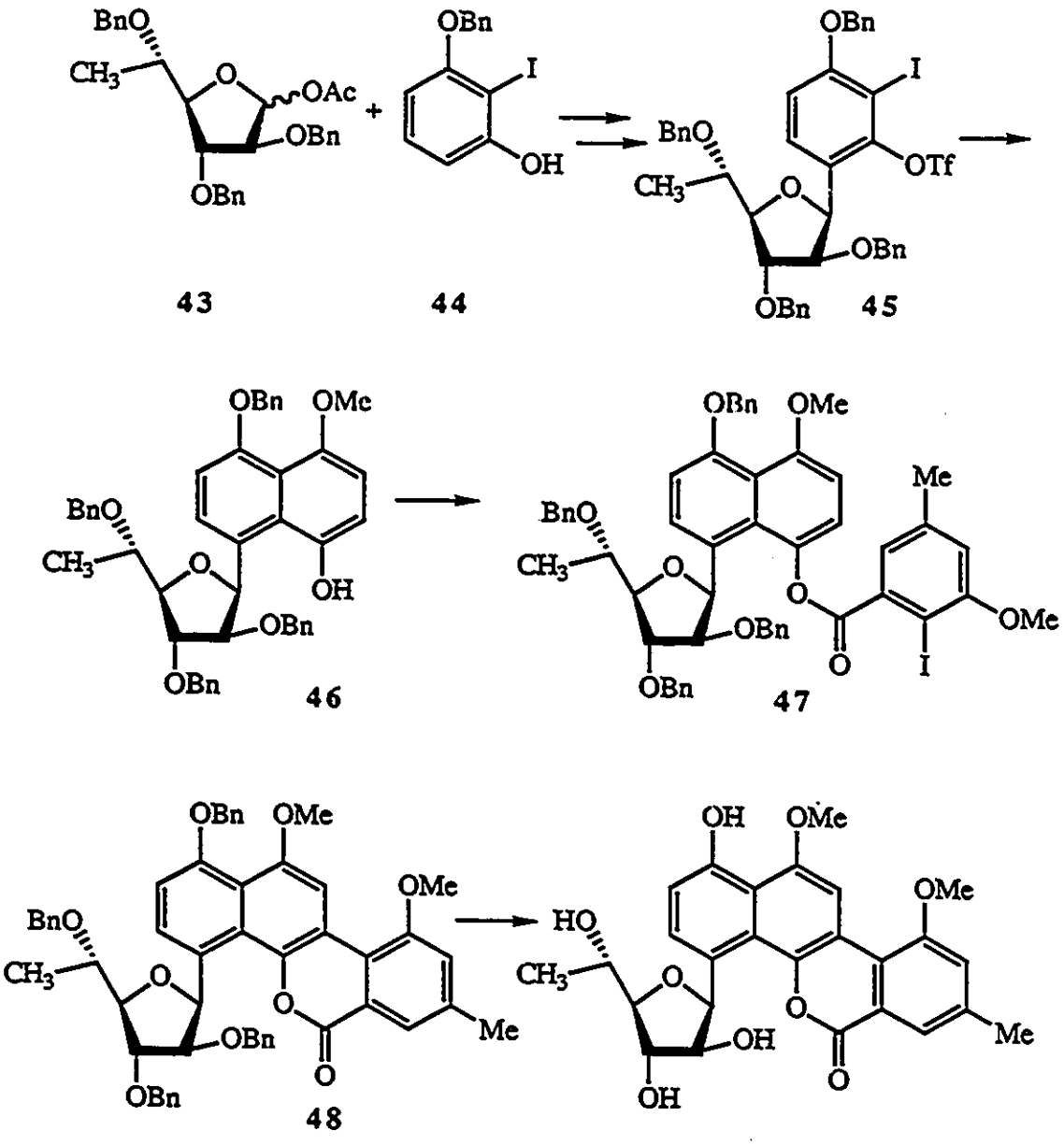


Scheme 2.8: Suzuki's Synthesis of (+)-Gilvocarcin M

which was attached to the eastern portion via reaction with the appropriate acid chloride, leading to compound **47**. Compound **47**, analogous to the precursor prepared by Martin et al.[23] in their synthesis of the aglycone, underwent intramolecular Suzuki biaryl

coupling in 90 % yield, which after deprotection, furnished the target (+)-gilvocarcin M in a total of six steps.

The synthetic compound was found to have an optical rotation opposite to that previously established in the literature[3] which confirmed that the natural product was in fact the enantiomer of **49**, incorporating D-fucose rather than L-fucose.

# Chapter 3

# Synthesis of the Gilvocarcin Ring System via the Diels-Alder Cycloaddition

## 3.1 The Intramolecular Approach

### 3.1.1 Retrosynthetic analysis

As was discussed in chapter 2, previous syntheses of the gilvocarcin aglycones were based either on a C10(a)-C10(b) disconnection, requiring a naphthalene and an aryl progenitor, or on a C11-C12 disconnection, starting with the precursors to rings **A** and **D** (scheme 3.1).

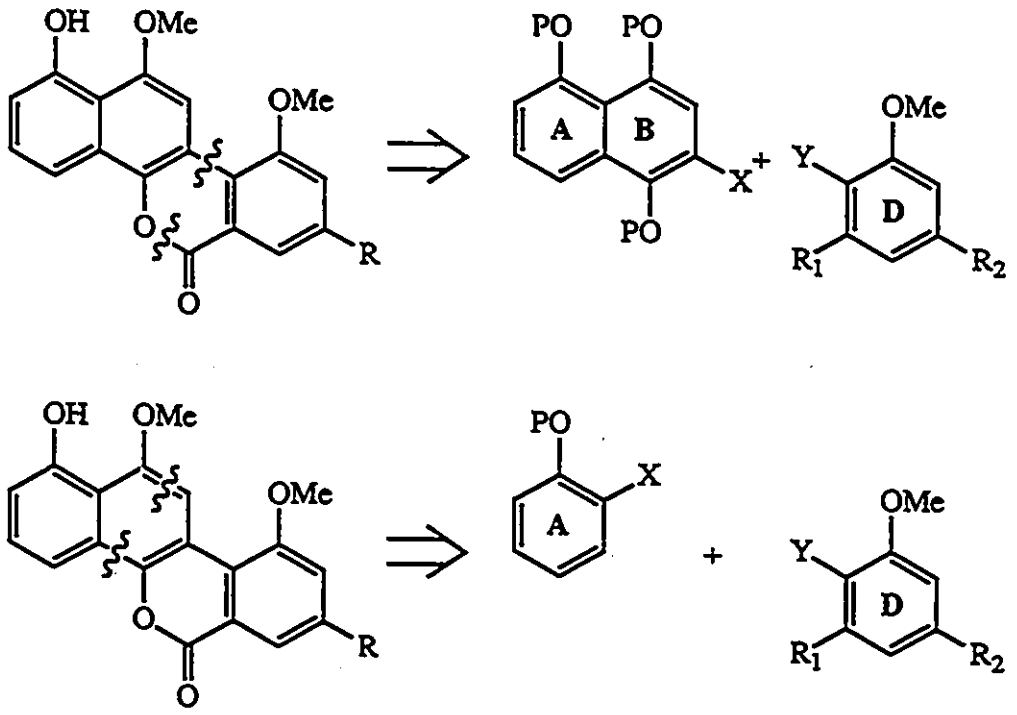


Scheme 3.1: Previous Disconnection Strategies

Given the rich synthetic background of the intramolecular Diels Alder reaction applied to the construction of polycyclic natural products,[30] it followed that the methodology should be applicable to assembly of the tetracyclic gilvocarcin framework. The proposed antithesis, depicted in scheme 3.2,

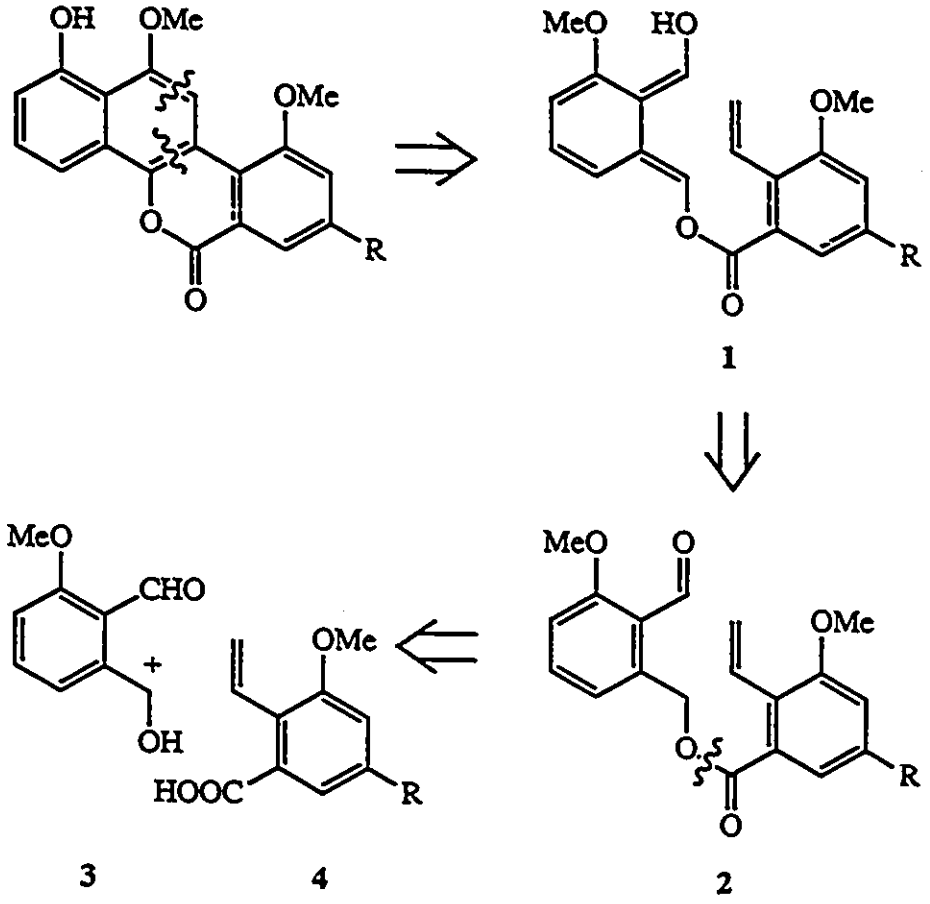


Scheme 3.2: Intramolecular Diels-Alder Antithesis

is contingent on a bilateral series of disconnections beginning at the C11-C12 and C4(b)-C10(b) junctions leading to the *o*-quinodimethane **1**,

available via photoenolization of the aldehyde **2**, followed by dismantling of the C5-C6 ester linkage resulting in compounds **3** and **4**.

### 3.1.2 Model systems

In order to fully explore the potential of this approach, two general areas should be addressed, namely:

1) The feasibility of generating the 1,4-dioxygenated-*o*-quinodimethane **1** by photoenolization of an *o*-(benzoyloxymethyl) benzaldehyde, as well as its reactivity toward dienophiles.

2) The efficiency of intramolecular cycloaddition of styryl precursors such as **1**, upon photoenolization.

A program directed at addressing these criteria should begin with minimally configured structures which balance ease of synthesis with the required functional domains.

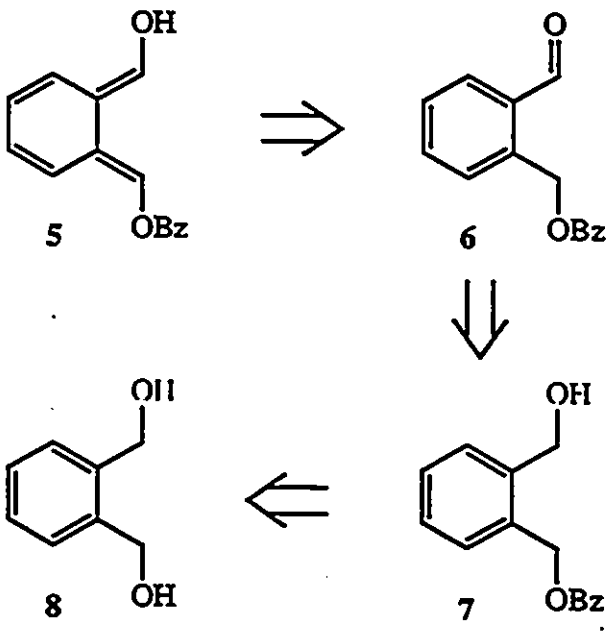


Scheme 3.3: Retrosynthetic Analysis of Proposed 1,4-Dioxygenated *o*-Quionoid 5

Scheme 3.3 illustrates the retrosynthetic analysis for the proposed 1,4-dioxygenated-*o*-quinodimethane **5**, derived from the appropriately substituted aldehyde **6**, which should be readily obtained from *o*-xylenol. Intermolecular cycloaddition studies of **5** with a variety of dienophiles would provide some insight into its reactivity, in preparation for the intramolecular version.

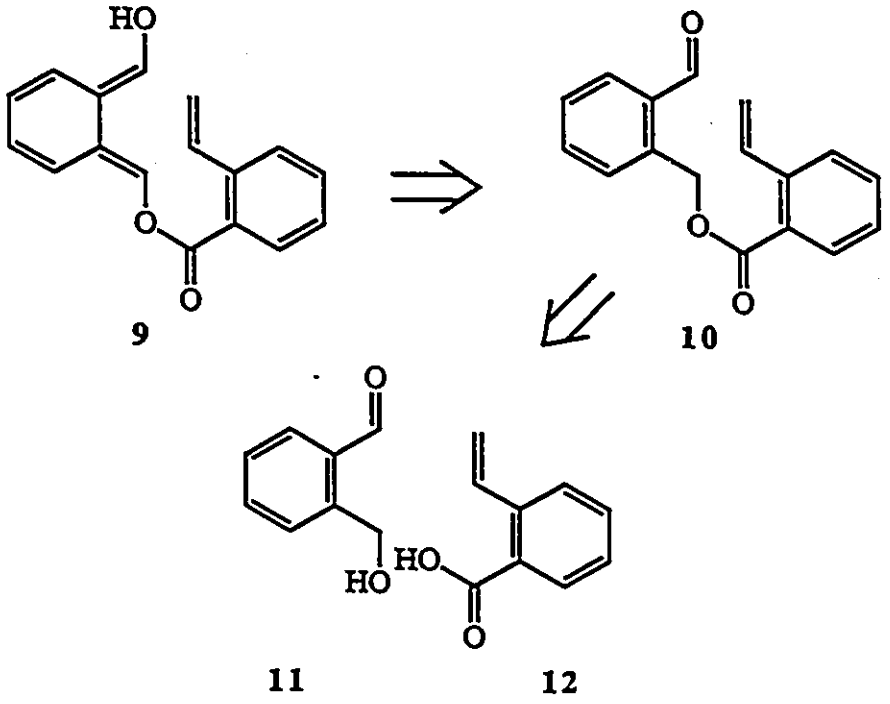


Scheme 3.4: Retrosynthetic Analysis of Proposed Intramolecular Model

The model proposed to investigate the feasibility of the intramolecular cycloaddition is depicted in scheme 3.4 where the *o*-xylylene **9**, obtained by photoenolization of **10** should be obtainable via a short progression from the readily available starting materials **11** and **12**.

## 3.2 The Intermolecular Approach

### 3.2.1 Retrosynthetic analysis

Another potentially useful variation of the strategy outlined in scheme 3.2 would invoke the possibility of applying an intermolecular cycloaddition to construct the naphthalene component of the system. The central challenge inherent in this approach would be the regioselective formation of a 3-aryl naphthol. The retrosynthetic analysis illustrated in scheme 3.5 highlights the direction proposed to accomplish the task.

The antithesis shows two alternative disconnections of ring C, path a and b, wherein the former, ring C would be generated via an electrocyclic ring closure of the quinone **14** giving the pyran **13a**. In path b, the formation of ring C would involve a remote metallation and carbamoyl transfer of the naphthalene **13b**. Compound **13b** should be available from **14** by a sequence involving reduction to the hydroquinone, formation of the monocarbamate, and conversion to the methyl ether.

The quinone **14**, would be available by oxidation of the 3-aryl-naphthol **15**. The synthesis of compound **15**, and the problem of regioselectivity would be addressed by employing an intermolecular hetero Diels-Alder reaction of an *o*-quinodimethane such as **17**, with an appropriately substituted heterodienophile **18**.

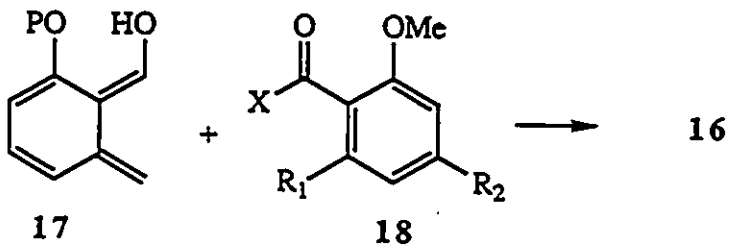

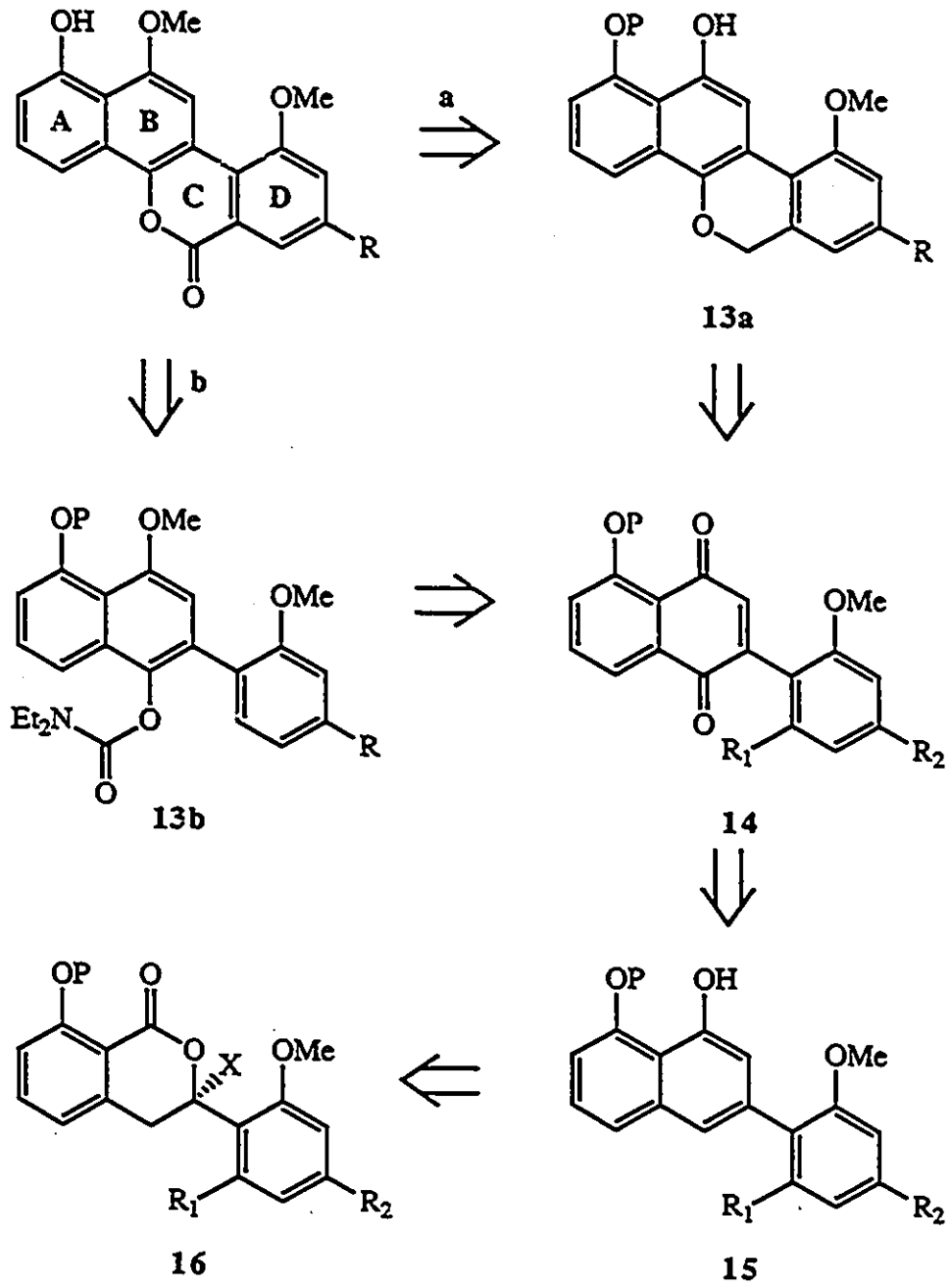


Scheme 3.5: Intermolecular Diels-Alder Antithesis

Conversion of compound **16** to the naphthol **15** should be accomplished readily by one carbon homologation to the aryl acetophenone followed by ring closure to the naphthol.

The advantages of the latter approach, specifically as it progresses to compound **13b**, include a considerable simplification of the precursors of both the western and eastern moieties, especially the latter which has required a large number of steps to prepare in previous syntheses, as well as the potential for synthesis of derivatives.

### 3.2.2 Model systems

The model system proposed to test the feasibility of the intermolecular approach is depicted in scheme 3.6.

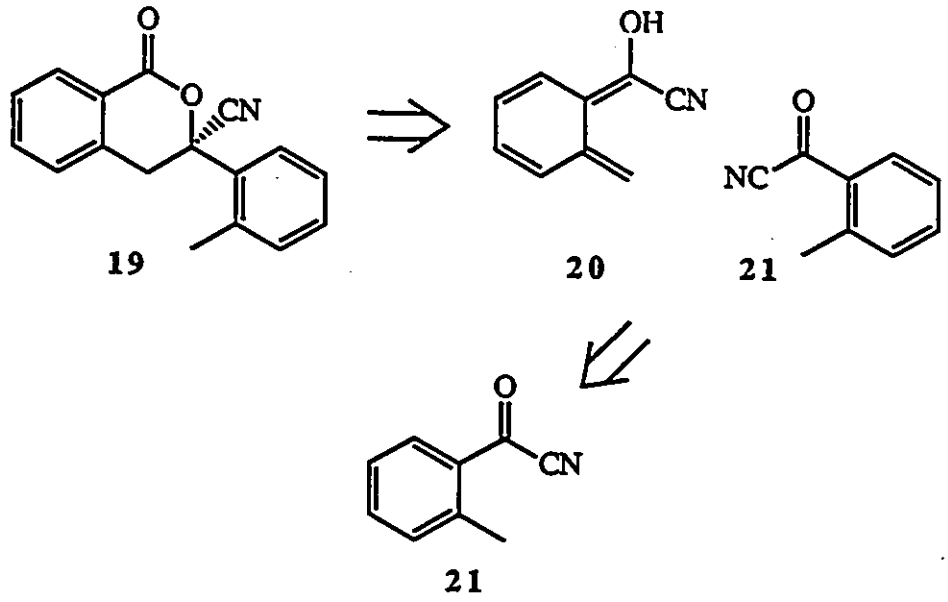


Scheme 3.6: Intermolecular Model System

Compound **19** possesses the structural requirements, analogous to compound **16**, necessary to act as a prototype for the intermolecular sequence and should be readily obtained by cycloaddition of the

*o*-quinodimethane **20** with heterodienophile **21**. *o*-QDM **20** would be accessible by photoenolization of the aroyl cyanide **21**.

# Chapter 4

# *o*-Quinodimethanes

## 4.1 *o*-Quinodimethane preparation and reactivity

Over the past thirty six years since their discovery, *o*-quinodimethanes have become valuable tools to the synthetic chemist.[30] Cava[31] was the first to propose the intermediacy of the *o*-xylylene **2** in the formation of *trans*-α-α'-dibromobenzocyclobutene from α,α,α',α'-tetrabromo-*o*-xylene.

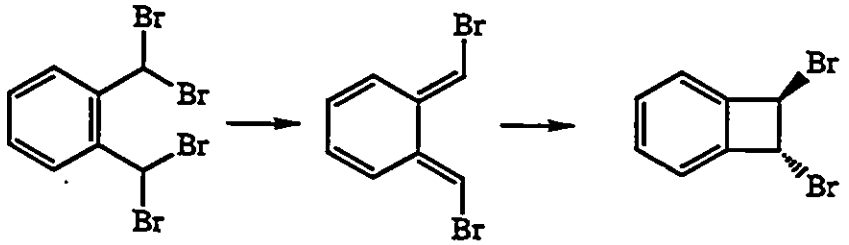


**1** **2** **3**

*o*-Quinodimethanes (*o*-QDM) such as **2**, are useful synthetically because of their ability to participate in Diels-Alder cycloadditions. The cycloaddition is suprafacial for both diene and dienophile, exhibiting a 1,2-regiochemical preference over the 1,3 addition with substituted partners.

Secondary orbital and steric interactions are competing influences which determine whether the cycloaddition proceeds in an endo or exo fashion. Charlton and Durst[32] have studied the stereoselectivity in the Diels-Alder reaction of phenyl and oxy-substituted *o*-quinodimethanes and found that the α-oxygenated species

undergo cycloaddition via an endo transition state leading to the *cis*-1,2-disubstituted tetralins. Conversely, the α-phenyl congener was observed to yield primarily 1,2-trans products indicating that the cycloaddition had passed through an exo transition state and that steric effects had predominated. Perhaps most interesting was the case of an (E,E)- α-phenyl-α'-methoxy-*o*-QDM, depicted in scheme 4.1, which, on cycloaddition with dimethyl maleate, furnished exo over endo products. This was in contrast to the analogous reaction with maleic anhydride, which gave primarily endo addition.

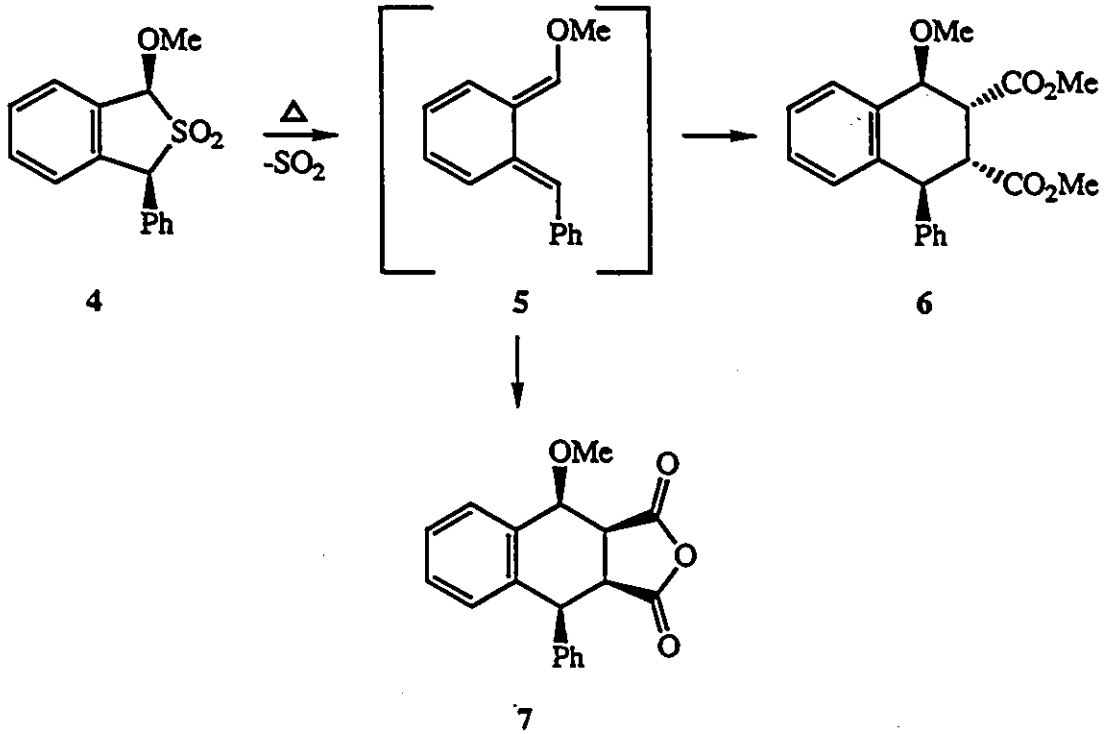


4 5 6 7

Scheme 4.1: Endo vs Exo Cycloadducts for α,α'-Disubstituted-*o*-QDM

The stereochemical outcome for the intramolecular cycloaddition can be affected by the influence of the tethering group. Macdonald and

Durst[33] capitalized on this effect in their synthesis of podophyllotoxin where compound **8**, on thermolysis in nitromethane, formed the tetralin **10**, possessing the opposite stereochemistry of that observed for intermolecular reactions. This product was successfully converted to the natural product **11**.

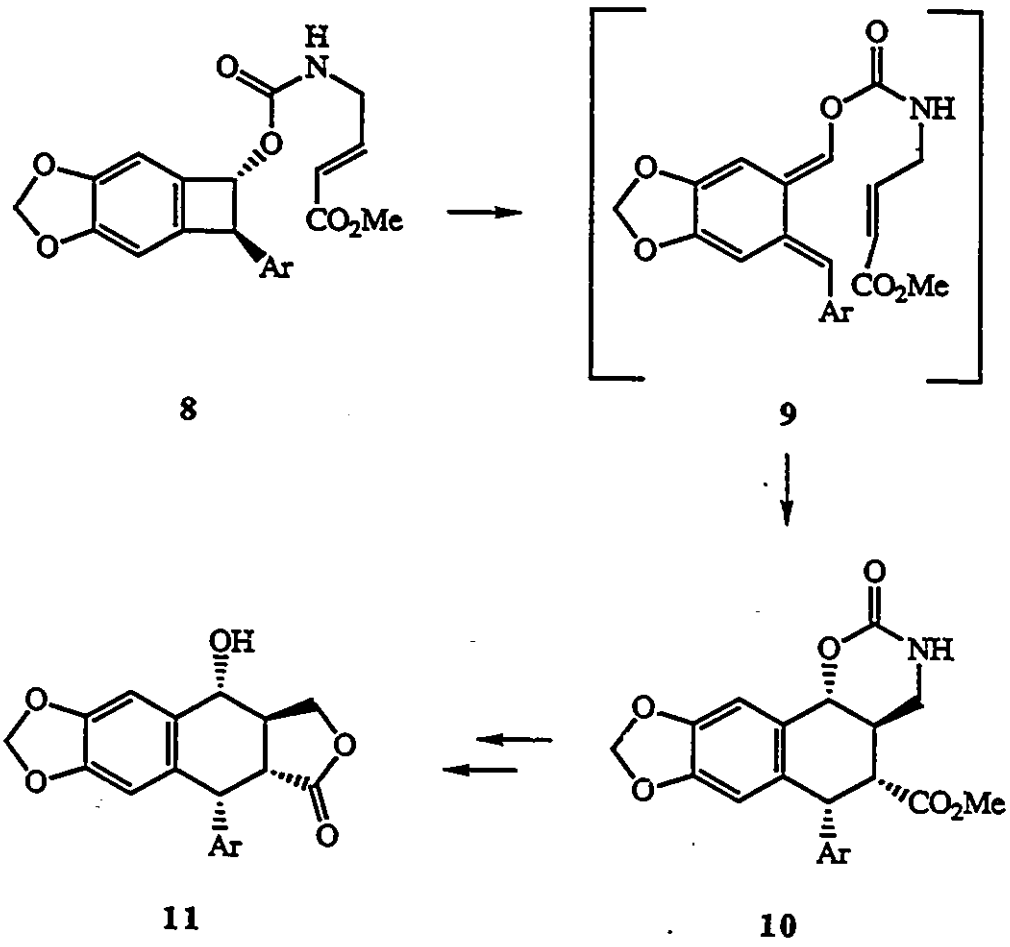


Scheme 4.2: Macdonald and Durst's Podophyllotoxin Synthesis

Understandably, given the usefulness of *o*-quinodimethanes as synthetic intermediates, the literature is replete with reports describing the preparation of its precursors.[30] The myriad of

approaches to the intermediate can be organized into four general categories, namely: electrocyclic ring opening, 1,4-elimination processes, extrusion reactions and photoenolization.

**i) Electrocyclic ring opening**

The most frequently used method of generating *o*-quinodimethanes is the thermal conrotatory ring opening of benzocyclobutenes.[34]

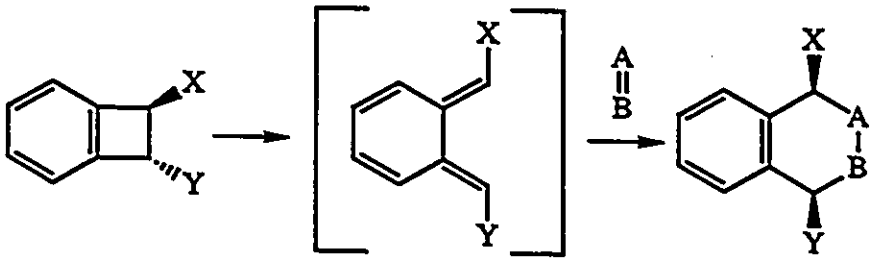


12 13 14

Houk et al[35] has applied a combination of experimental and theoretical techniques to the question of torquoselectivity for the ring opening and determined that the propensity for outward rotation of the X or Y groups increases in proportion to their electron donor ability. Conversely, the presence of acceptor groups is attended by an increase in the proclivity for inward rotation.

The major drawback of this method of preparing *o*-quinodimethanes is the difficulty involved in synthesizing the benzocyclobutene precursors, nevertheless, the protocol has seen wide application.

**ii) 1,4-Elimination processes**

This methodology involves a 1,4-elimination process which has been induced by pyrolysis,[36] treatment with base,[37] reducing metals,[38]

and most notably, by fluorodesilylation, a procedure applied elegantly by Ito et al.[39]

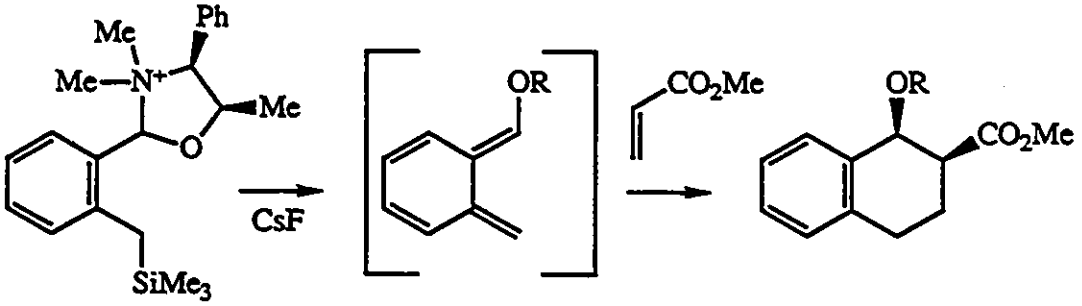


15 16 17

### iii) Extrusion reactions

The reactions which fall under this classification include Diels-Alder cycloreversions,[40] photochemical expulsion of carbon monoxide from 2-indanones,[41] and the cheletropic extrusion of sulfur dioxide from sulfones and sultines.[42]

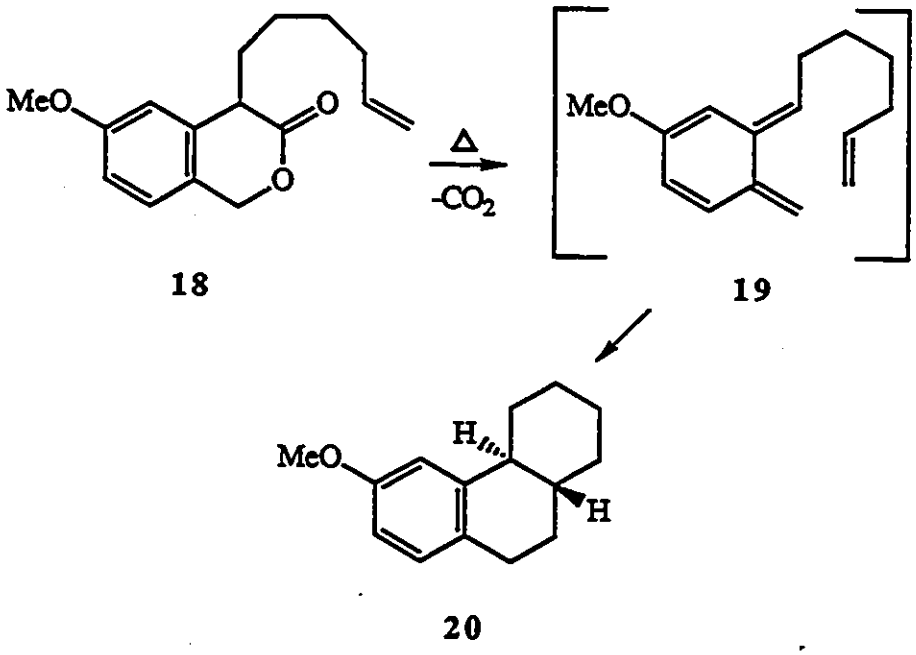


18 19 20

Oppolzer,[30] for example, thermolyzed the 3-isochromanone **18**, generating the *o*-quinodimethane **19**, which subsequently cyclized to the trans-fused ring system **20**.

**iv) Photoenolization**

Photoenolization involves H abstraction, which occurs from the $n\pi^*$ excited state, and enolization of *o*-alkyl-arylketones and aldehydes.[43] Glinski and Durst[44] utilized this approach in their synthesis of racemic epiisopodophyllotoxin.

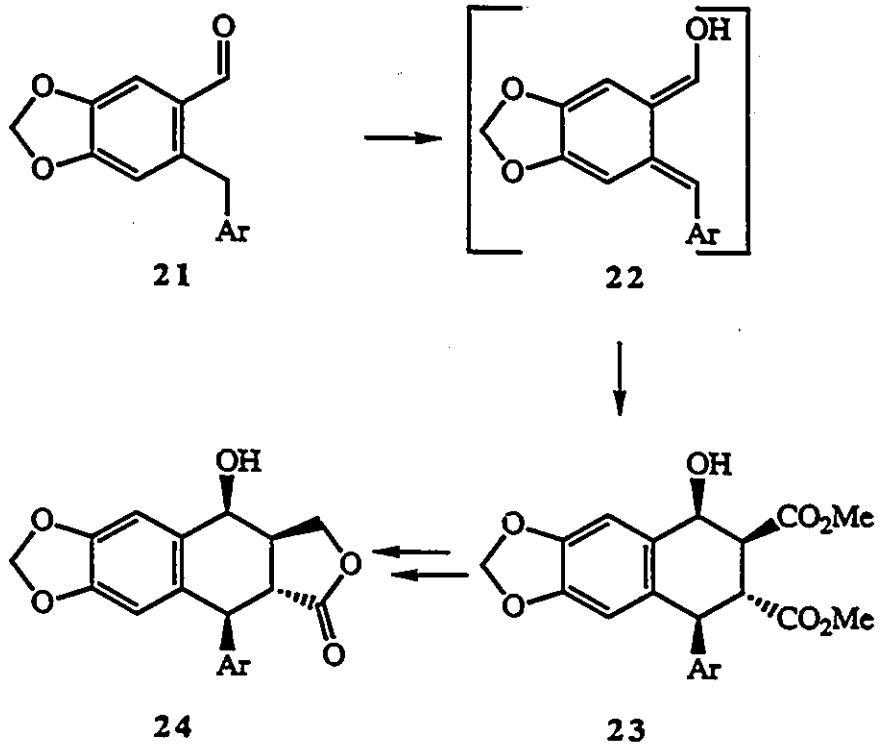


**21** **22** **24** **23**

## 4.2 Synthetic applications

The literature abounds with synthetic sequences employing *o*-quinodimethanes. In addition to the examples highlighted in the preceding section, only two syntheses of special relevance will be presented. Oppolzer's synthesis of *d*-chelidonine[45] incorporated a similar series of disconnections as was proposed for the

intramolecular approach to the defucogilvocarcin framework described in chapter 3.

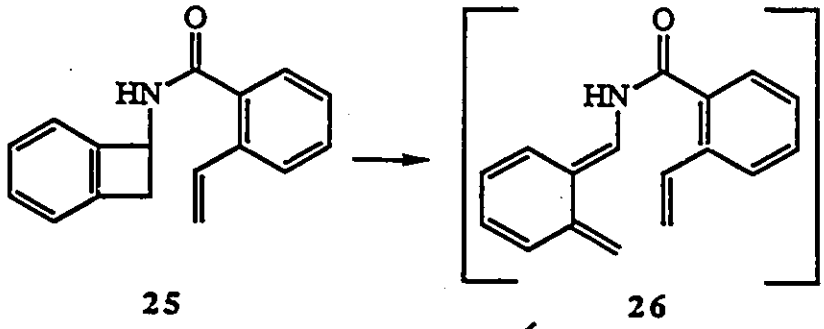

25 26

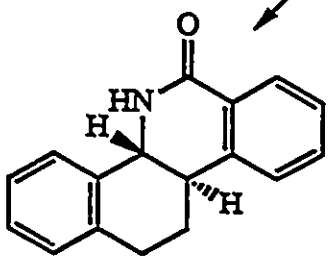

27

The model system **27** was prepared, via the *o*-xylylene **26**, by thermolysis of the benzocyclobutene **25** for 16 hr in bromobenzene.

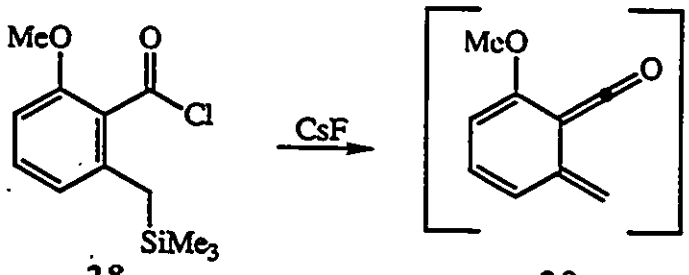

28 29

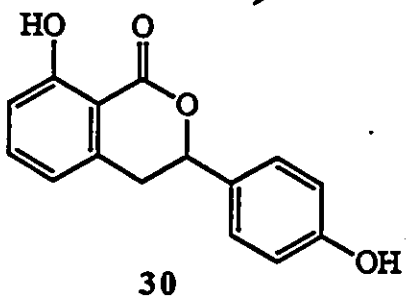

30

Recently Kessar[46] has described the synthesis of racemic hydrangenol, phyllodulcin, tetrahydropalmatine and canadine by cycloaddition of the appropriate aldehydes with *o*-quinodimethanes generated by fluorodesilylation of various *o*-((trimethylsilyl)methyl)benzoyl chloride derivatives. Thus compound **28** underwent fluorodesilylation yielding the ketene **29**, which was trapped with *p*-methoxy benzaldehyde and subsequently converted to hydrangenol **30**.

# Chapter 5

# Photochemical Synthesis of 1,4-Dioxygenated-*o*-quinodimethanes

## 5.1 Previous syntheses of 1,4-dioxygenated-*o*-quinodimethanes

At the outset of this project, no reports of photochemically generated α,α'-dioxygenated-*o*-quinodimethanes had appeared in the literature. Kraus and Chen[47] were the first to demonstrate

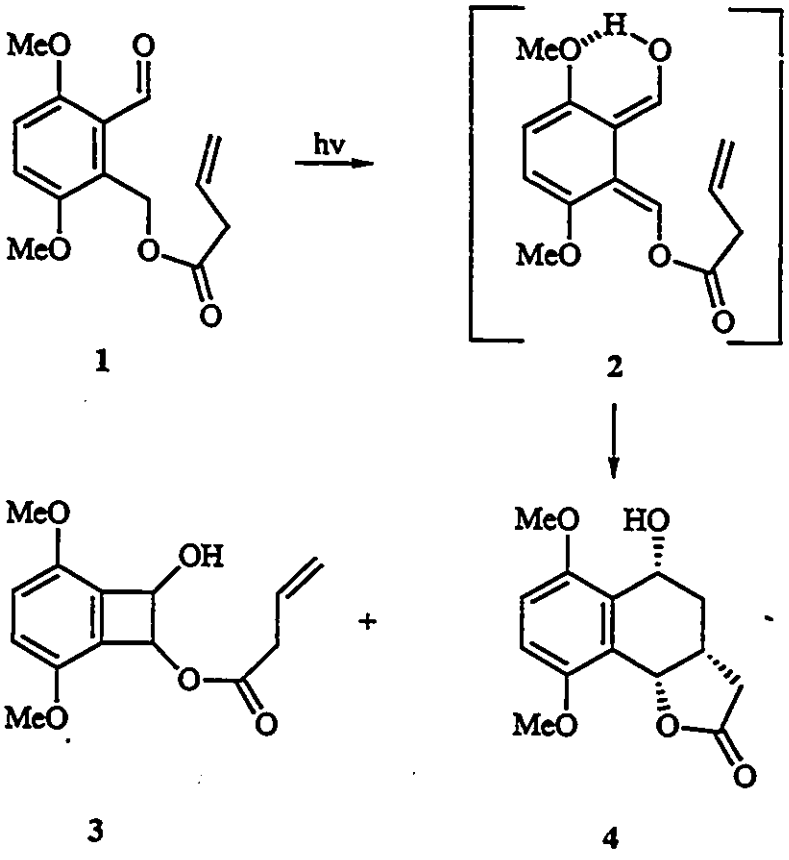


Scheme 5.1: Kraus' α,α'-dioxygenated-*o*-quinodimethane

that benzylic heteroatom substituents do not adversely affect the photoenolization of *o*-methylbenzaldehydes during model studies directed at developing a route to the anticancer agent pleurotin. Irradiation of **1** in benzene solution furnished the benzocyclobutenol **3** and the tricyclic lactone **4** in 31 and 33 % yields respectively. Compound **3** was converted to **4** in 95 % yield by refluxing in benzene at 130 °C for 38 h. In addition, compound **5** (scheme 5.2) formed the tetracyclic lactone **6** after irradiation and thermolysis.

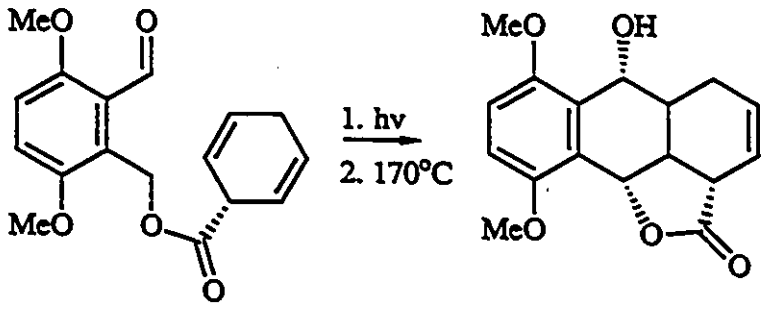


**5** **6**

Scheme 5.2

Wagner and co-workers[48] have also explored this area and recently reported that a variety of *o*-(alkoxymethyl)phenyl ketones efficiently form cyclobutenols on irradiation, and that the mechanism involves thermal electrocyclic ring closure of the photoenols.

Saa and co-workers,[49] in an effort to procure 2-arylbenzocyclobutenols for the synthesis of lignans, have studied the photochemical behavior of several highly congested phenolic *o*-(methoxymethyl)benzophenones. On irradiation, the benzophenones

smoothly formed 1-aryl-1-hydroxy-2-methoxybenzocyclobutenes in high chemical yields (scheme 5.3). Semiempirical (AM1) calculations

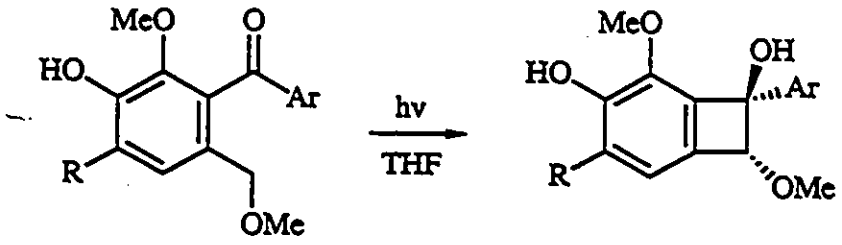


7 8

Scheme 5.3: Saa's 1-aryl-1-hydroxy-2-methoxybenzocyclobutenes

on the thermal ring opening of a number of benzocyclobutene derivatives showed that the α,α'-dioxygenated-*o*-quinodimethanes were 5-7 kcal/mol more stable than the corresponding benzocyclobutenols, suggesting that the latter species were not derived from photoenol precursors.

## 5.2 Synthesis of the aldehydic precursors

In chapter 3 a program was outlined which was designed to explore the feasibility of applying an intramolecular Diels-Alder cycloaddition to construction of the tetracyclic defucogilvocarcin framework. The program was predicated on two criteria: the first being the degree of α,α'-dioxygenated-*o*-quinodimethane reactivity attainable in an intermolecular Diels-Alder cycloaddition, and the second encompassing the intramolecular reactivity.

The first α,α'-dioxygenated-*o*-quinodimethane precursor selected for study of the intermolecular cycloaddition was

2-(methoxymethyl)benzaldehyde (**11**), the synthesis of which, is depicted in scheme 5.4.

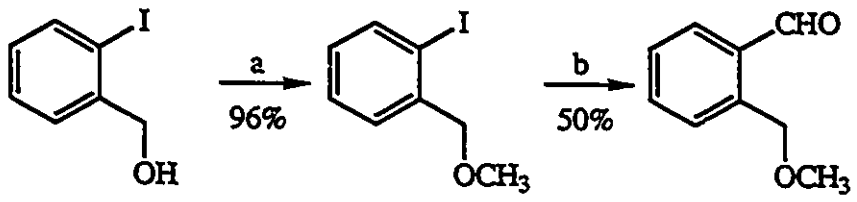


**9** **10** **11**

Scheme 5.4: a) NaH/THF 0°C, MeI b) Mg/THF, DMF

The methyl ether **10**, a yellow oil, was prepared from the commercially available benzyl alcohol **9** in 96 % yield by treatment of **9** with sodium hydride in THF at 0°C followed by quenching with methyl iodide.

The aldehyde **11** was prepared in a straightforward manner by conversion of the aryl iodide **10** to its Grignard reagent (Mg/THF), followed by quenching with DMF. Compound **11** exhibited characteristic signals in its proton NMR spectrum (fig. 5.1), most notably the singlets at δ 3.46, 4.85 and 10.19 ppm assigned to the methoxy, methylene and aldehyde protons, as well as the expected IR absorption at $\nu_{max}$ 1721 $cm^{-1}$. Aldehyde **11** was prone to auto-oxidation at room temperature but could be stored indefinitely, under nitrogen atmosphere, at freezer temperatures.

The second series of *o*-QDM precursor aldehydes selected were acylated versions of **11**. *o*-(Acetoxymethyl)benzaldehyde was prepared

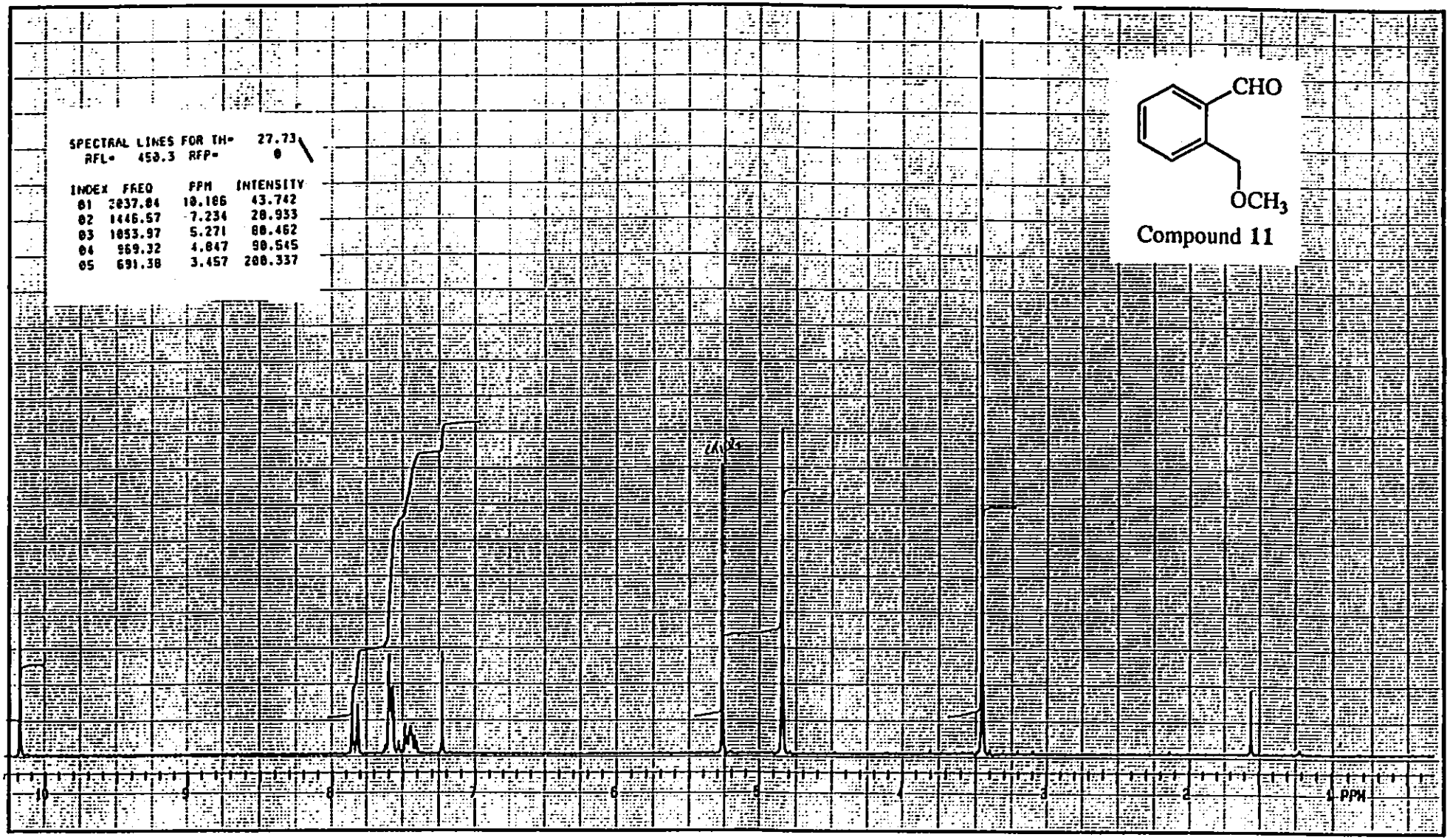


Figure 5.1: $^{1}$H-NMR of compound **11**.

in two steps, as illustrated in scheme 5.5, from commercially available *o*-xylenol. Thus the monoacylated benzyl alcohol **13a**,

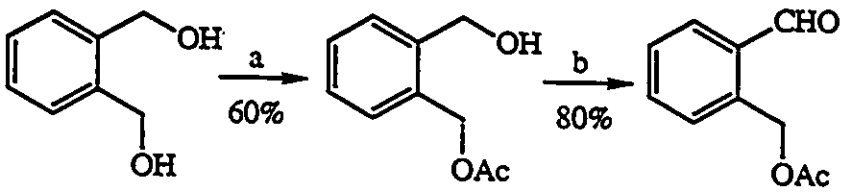


**12** **13a** **14a**

Scheme 5.5: a) NaH/THF 0°C, $Ac_2O$ b) $PDC/CH_2Cl_2$

a viscous colorless oil, [IR $\nu_{max}(cm^{-1})$ 3601, 1736] was prepared in 60 % yield by treatment of the mono-oxyanion (NaH/THF) of **12** with one equivalent of acetic anhydride or acetyl chloride, and subsequently purified by flash chromatography.

Compound **14a**, [IR $\nu_{max}(cm^{-1})$ 1740, 1698] was obtained by oxidation of **13a** ($PDC/CH_2Cl_2$) and was efficiently purified via the bisulfite adduct. It proved convenient to store **14a** as the bisulfite adduct and to hydrolyze it prior to use. The $^1$H-NMR spectrum (fig. 5.2) showed the expected aldehyde signal at δ 10.13 ppm, in addition to the acetate signal at δ 2.09 ppm and the methylene signal at δ 5.50 ppm.

Two additional aldehydes (scheme 5.6), bearing sterically more demanding hydroxyl protecting groups, were synthesized employing the same strategy as was utilized for **14a**. Thus the monobenzoyl-*o*-xylenols

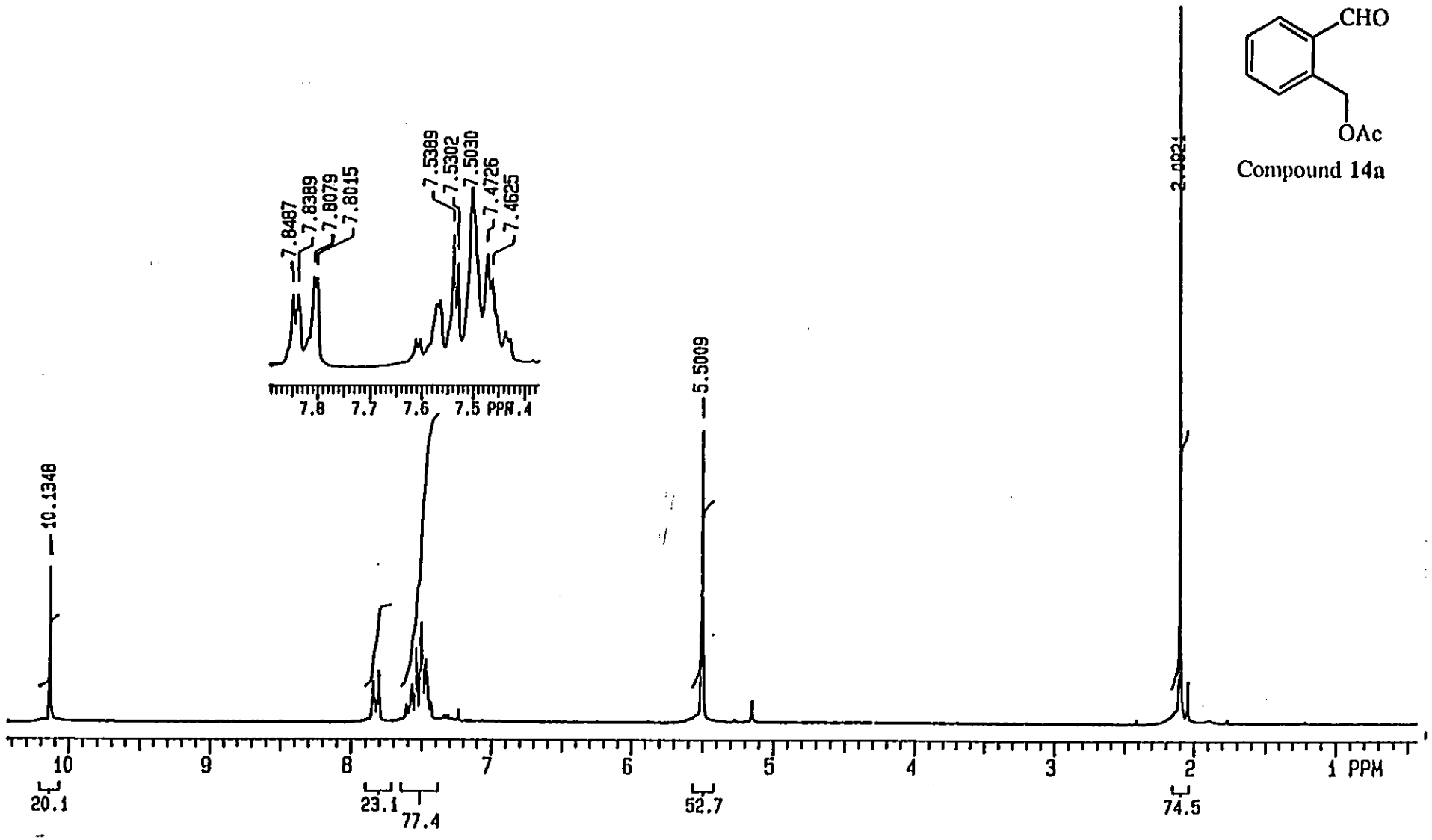


Figure 5.2: $^{1}$H-NMR of compound 14a.

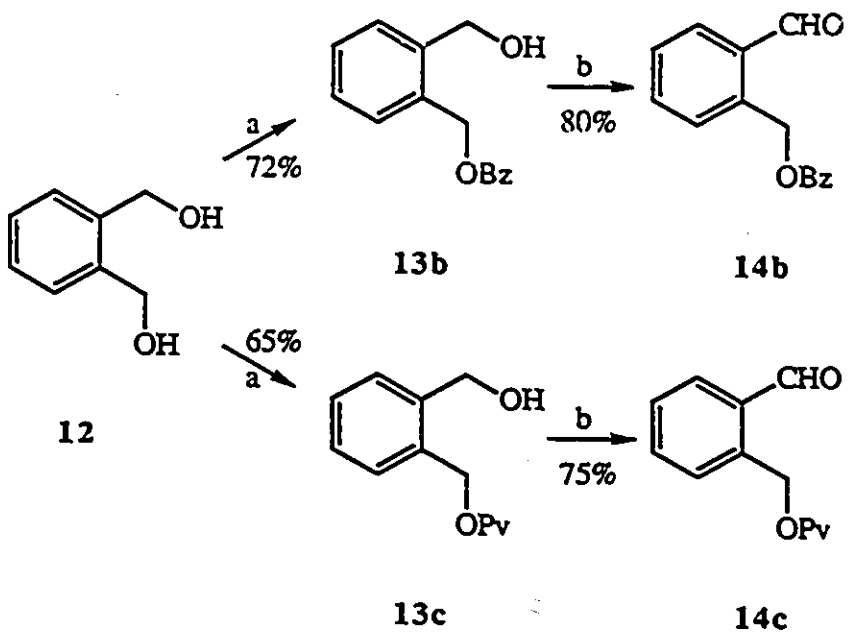


Scheme 5.6: a) NaH/THF 0°C, RCOCl b) $PDC/CH_2Cl_2$

**13b** [IR $\nu_{max}(cm^{-1})$ 3602, 1717] and **13c** [IR $\nu_{max}(cm^{-1})$ 3602, 1723] were prepared in 72 and 65 % yields respectively, and subsequently oxidized ($PDC/CH_2Cl_2$) to aldehydes **14b** and **14c** in 80 and 75 % yields. Both aldehydes exhibited spectral characteristics consistent with their structural assignment. The $^1$H-NMR spectrum of compound **14b** (fig. 5.3), for example, showed two singlets at δ 5.80 and 10.22 ppm, assigned to the benzylic methylene and aldehyde protons, while the analogous signals in the $^1$H-NMR spectrum of **14c** (fig. 5.4) appeared at δ 5.50 and 10.15 ppm.

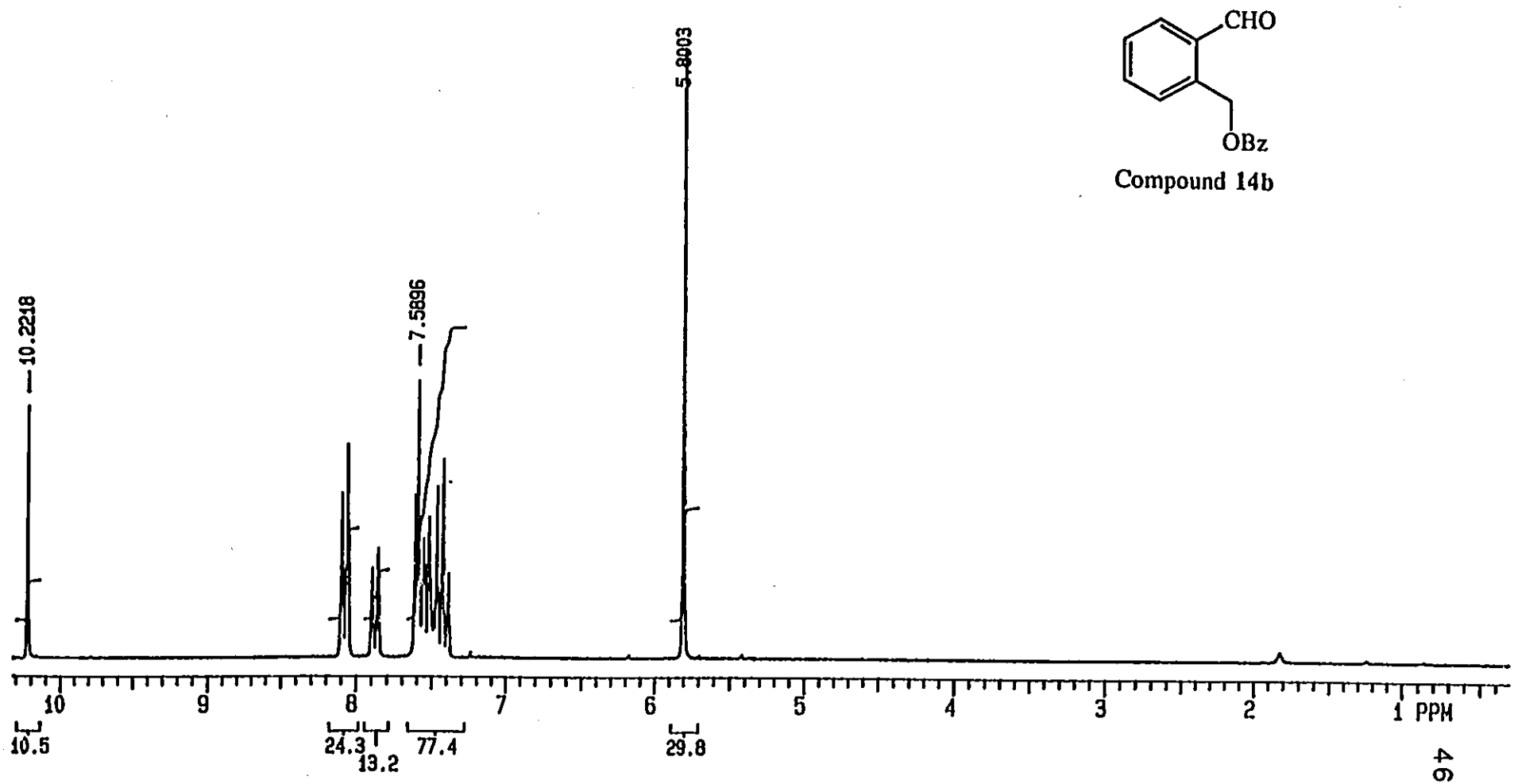


Figure 5.3: $^{1}$H-NMR of compound **14b**.

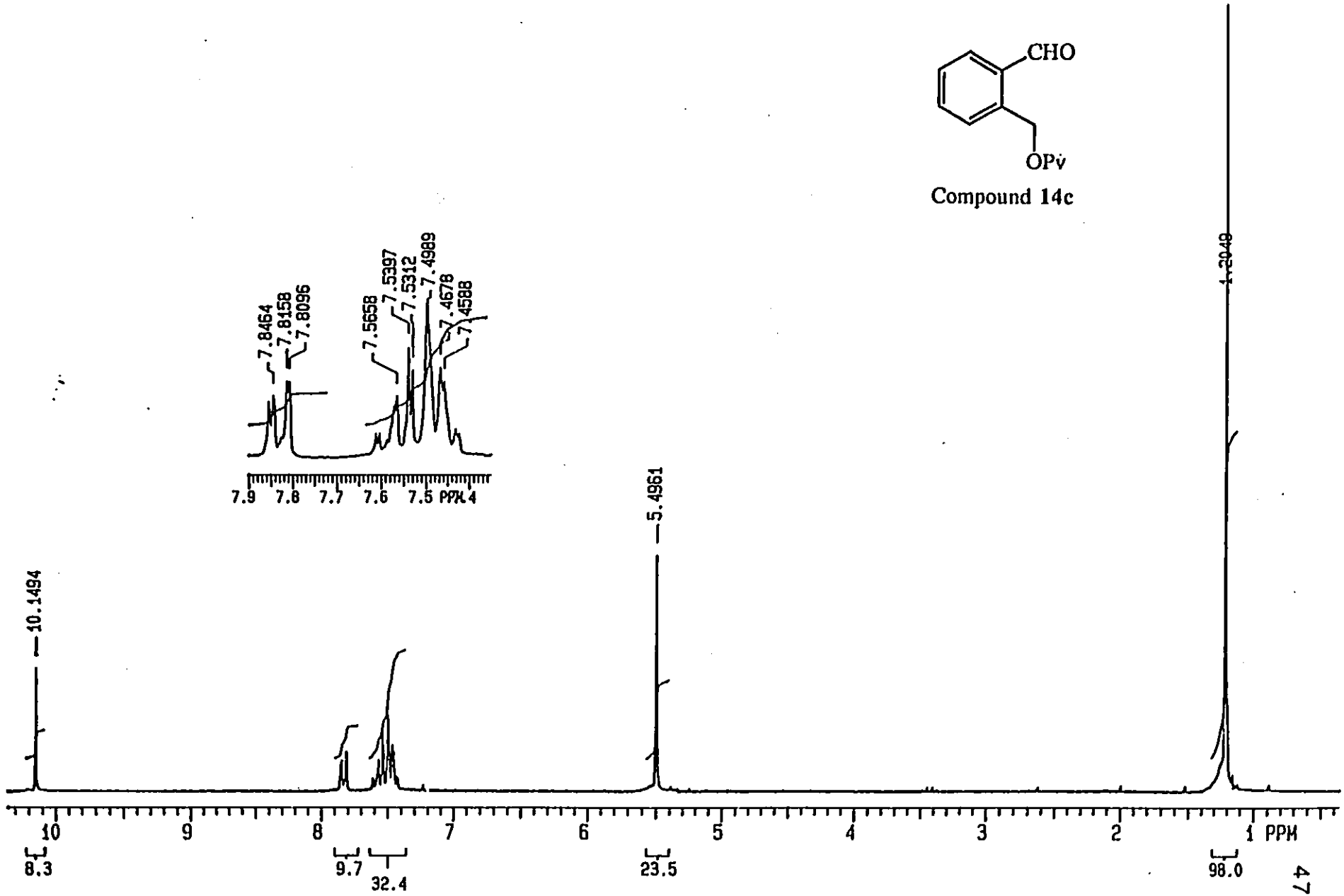


Figure 5.4: $^{1}$H-NMR of compound 14c.

## 5.3 Intermolecular cycloaddition studies

Kraus and Chen,[47] as was described earlier in this chapter, obtained approximately equal amounts of benzocyclobutenol and cycloadduct when either **1** or **5** was irradiated in benzene solution (schemes 5.1,2). Wagner[48] reported that various *o*-(alkoxymethyl)-arylketones, when irradiated in acetonitrile solution, also underwent cyclization to the benzocyclobutenols. Both of these results are consistent with Matsuura's observation[50] that steric congestion in photoenols, derived from aryl ketones, favours cyclobutenol formation (scheme 5.7). Given that the photoenols derived from aldehydes **11** and **14a-14c** are not sterically crowded, it was not anticipated that benzocyclobutenol formation would compete effectively with cycloaddition.

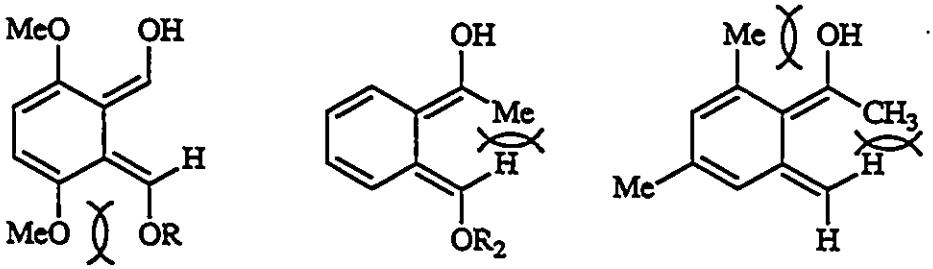


Kraus Wagner Matsuura

Scheme 5.7

In the event, irradiation of aldehyde **11** and 3 equivalents of dimethyl fumarate in benzene solution, afforded what appeared to be a

2:1 mixture of the diastereomeric cycloadducts **16** (14 %) and **17** (7 %) in 21 % combined yield (scheme 5.8). The adducts were purified by

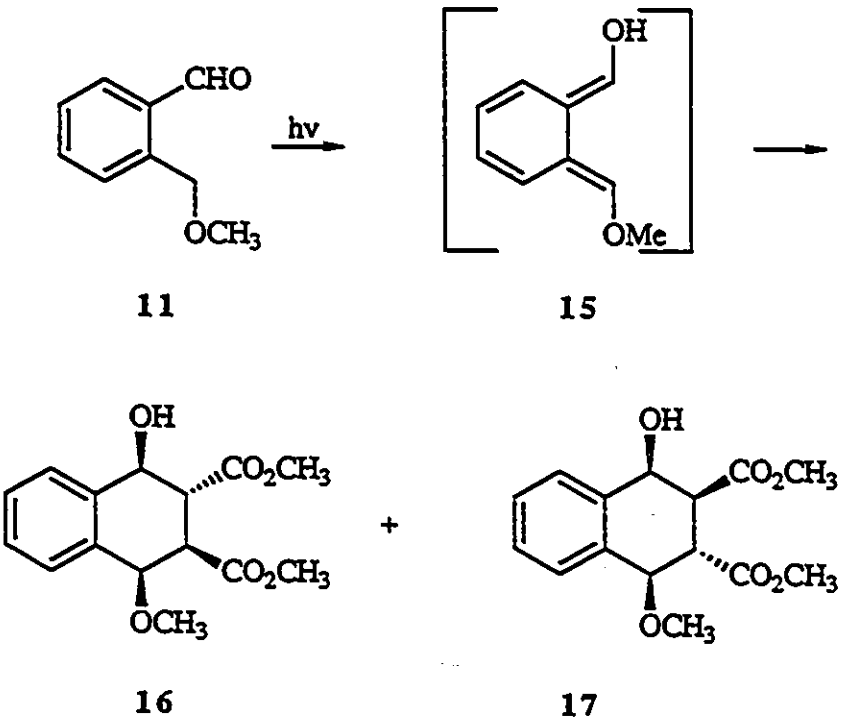


Scheme 5.8

flash chromatography and exhibited spectral characteristics in accord with the assigned structures. The $^1$H-NMR spectrum of the 2:1 mixture of **16** and **17**, illustrated in fig. 5.5, showed upfield signals at δ 3.23 and 3.30 ppm, corresponding to the benzylic methoxy protons, and four signals at δ 3.70, 3.72, 3.76, and 3.78 ppm, all representative of the carbomethoxy hydrogens. The region between δ 4.50 and 5.10 ppm contained the signals which arose from the benzylic protons;

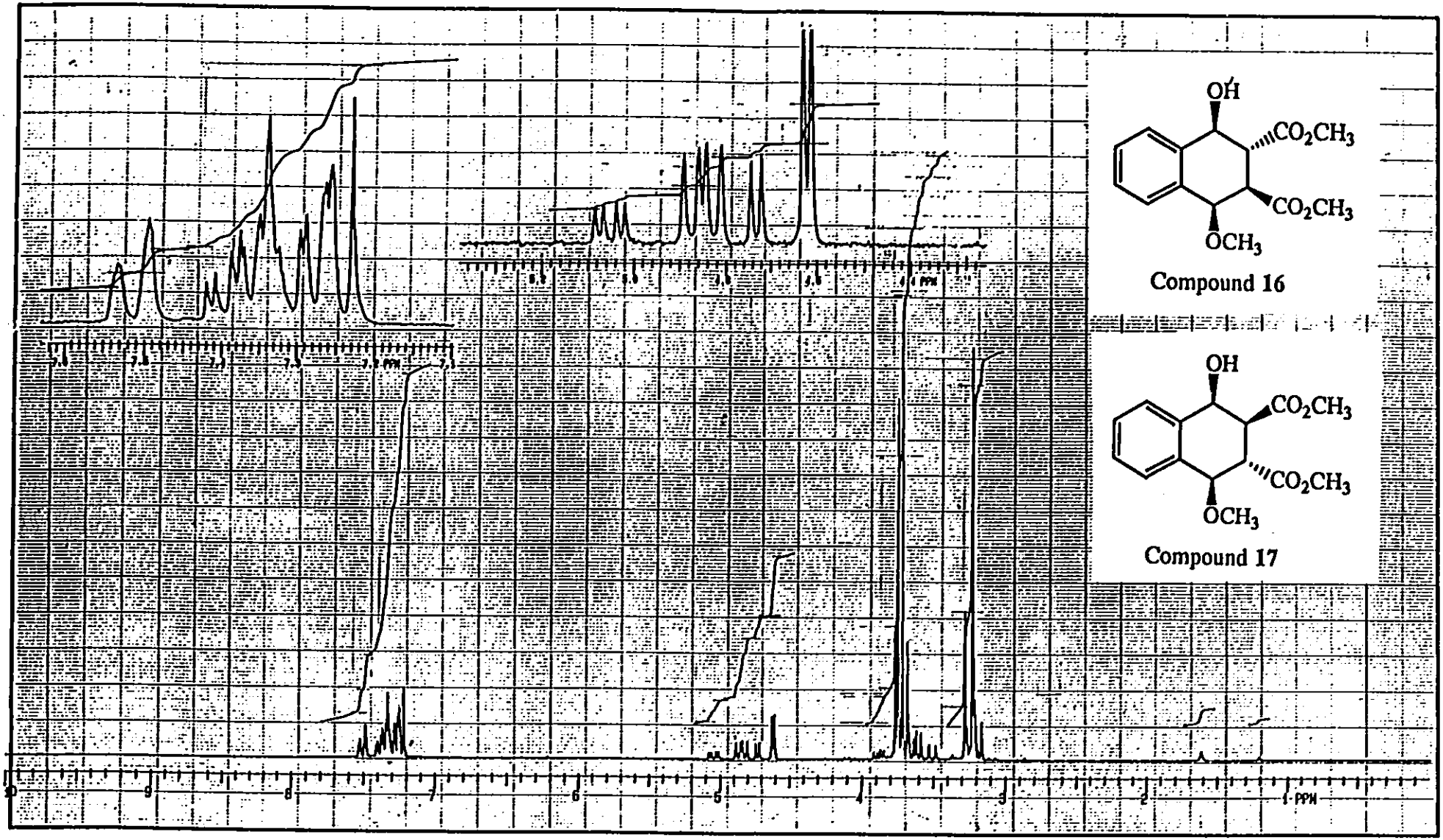


Figure 5.5: $^1$H-NMR of compounds 16 and 17.

an analysis of the chemical shifts and the coupling constants observed for **16** and **17** is presented in fig. 5.6

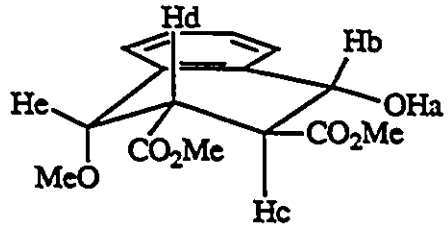


**16**

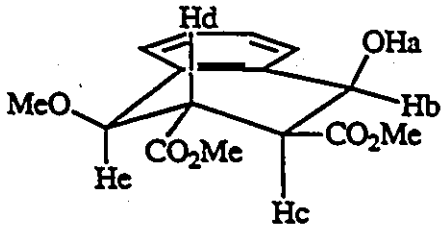


**17**

Chemical Shifts (ppm)

| | Ha | Hb | Hc | Hd | He |
|---|---|---|---|---|---|
| **16** | 3.50 | 4.85 | 3.65 | 3.20 | 4.62 |
| **17** | - | 5.05 | 3.90 | 3.20 | 4.74 |

Coupling Constants (Hz)

| | Jab | Jbc | Jcd | Jde |
|---|---|---|---|---|
| **16** | 9.5 | 6.4 | 10.0 | 3.0 |
| **17** | 9.2 | 4.0 | 9.0 | 4.5 |

Figure 5.6: Chemical Shifts and Coupling Constants for **16** and **17**

Presumably, cycloaddition occurred with the E,E-photoenol (**15**) acting as the diene given that Z,E-photoenols rapidly undergo sigmatropic rearrangement to their precursors[51] and cycloaddition to E,Z-disubstituted-*o*-quinodimethanes is known to occur more slowly.[52] The predominance of **16** (methoxy-endo) over **17** was not unexpected and is consistent with the Alder endo rule.[32,53]

The next *o*-QDM precursor studied was aldehyde **14a**. It was anticipated that the less electron donating protecting group might have a beneficial effect on the cycloaddition, in keeping with literature precedents.[32,54] Diethyl fumarate was selected as the dienophile for practical reasons as any excess could easily be removed during workup by evaporation under high vacuum.

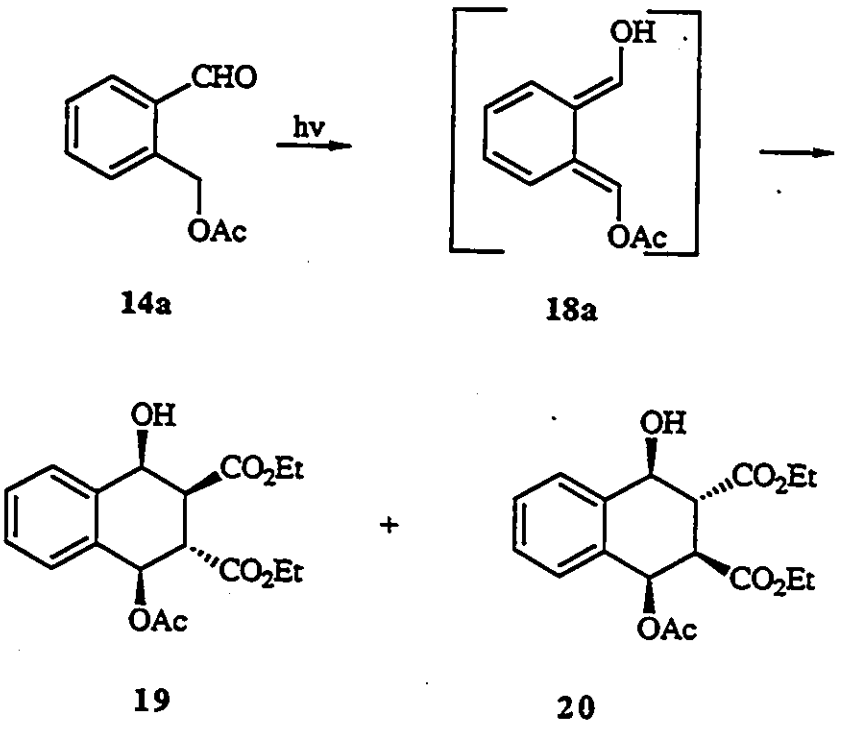


Scheme 5.9

As depicted in scheme 5.9, irradiation of **14a** and 3 equivalents of diethyl fumarate in benzene solution followed by flash chromatography of the product mixture furnished a mixture, assumed to be **19** and **20** in 78 % yield, as a 2:1 mixture of diastereomers. The compounds were identified readily. For example, the IR spectrum exhibited two diagnostic absorptions at $\nu_{max}$ 3520 (br) and 1732 (s) $cm^{-1}$

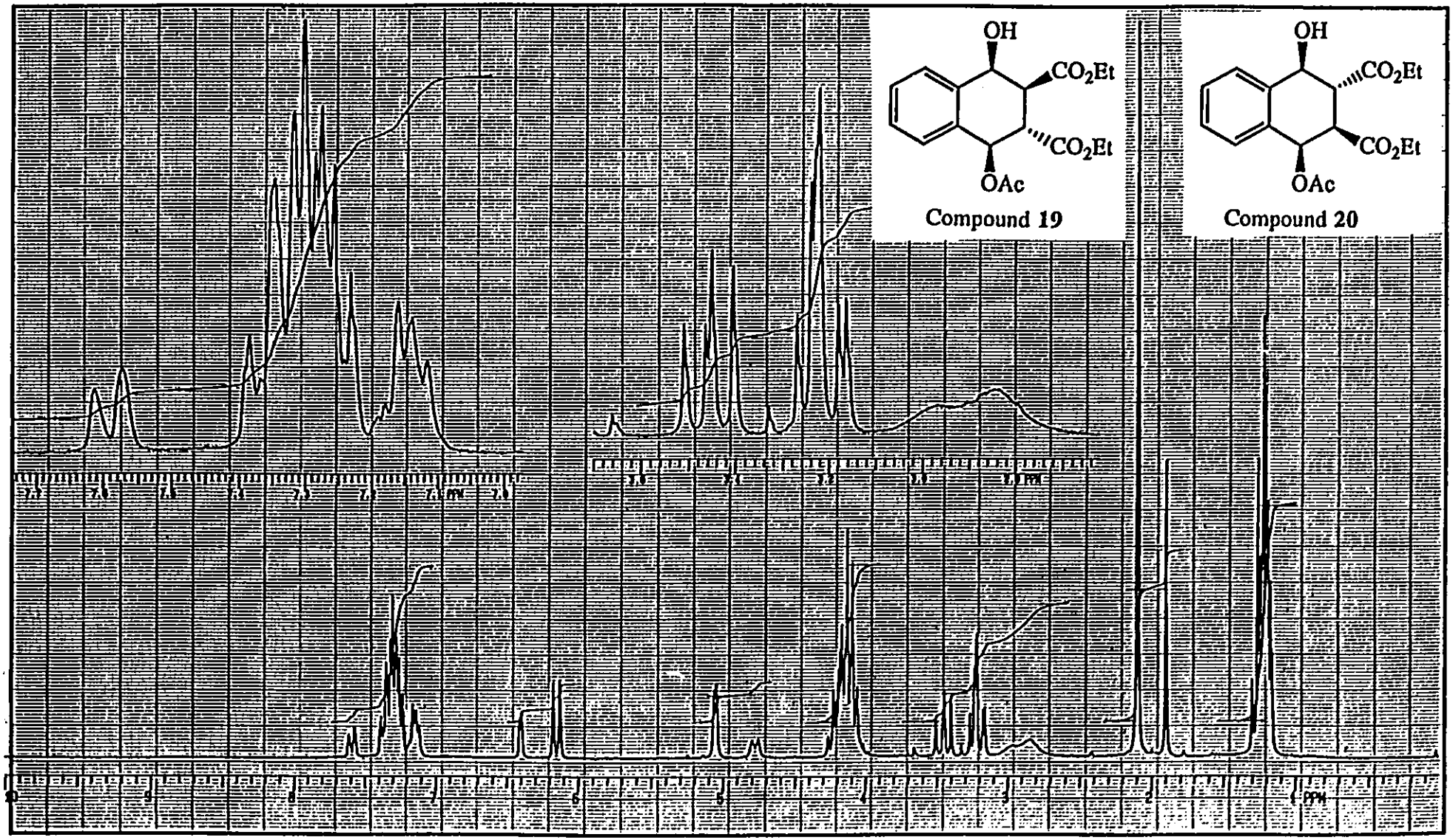


Figure 5.7: $^{1}$H-NMR of compounds **19** and **20**.

and the $^1$H-NMR spectrum (fig. 5.7) showed characteristic signals, which are summarized in fig. 5.8.

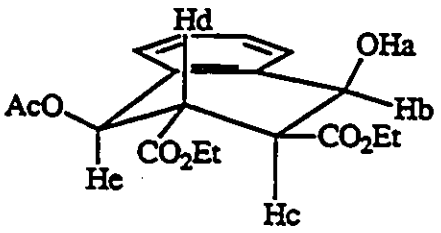


19

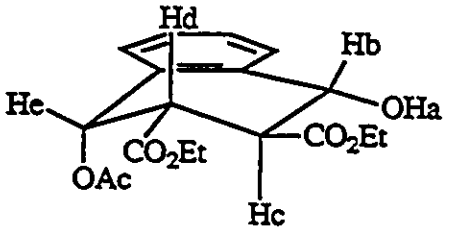


20

Chemical Shifts (ppm)

| | Ha | Hb | Hc | Hd | He |
|---|---|---|---|---|---|
| 19 | 2.85 | 5.06 | 3.20 | 3.45 | 6.16 |
| 20 | 2.95 | 4.78 | - | - | 6.40 |

Coupling Constants (Hz)

| | Jab | Jbc | Jcd | Jde |
|---|---|---|---|---|
| 19 | - | 3.1 | 13.8 | 9.2 |
| 20 | - | 9.0 | - | 3.2 |

Figure 5.8: Chemical Shifts and Coupling Constants for 19 and 20

The region in the $^1$H-NMR spectrum (fig. 5.7) between δ 4.50 and 6.50 ppm contained signals corresponding to the benzylic protons which illustrated the proportions of the diastereomers **19** and **20**. The increased yield obtained for this cycloaddition (78 %) as compared to aldehyde **11** (21 %) confirmed the positive effect of the less electron donating protecting group (fewer side reactions with **18a**).

Aldehyde **14b**, which readily recrystallized from dichloromethane/hexane, was stable when stored at freezer temperatures under nitrogen. When **14b** and 3 equivalents of diethyl fumarate were irradiated in benzene solution and the crude product mixture resolved by flash chromatography, adducts, assumed to be **21** and **22** (scheme 5.10), were obtained in 73 % yield, as a 3:1 mixture of diastereomers.

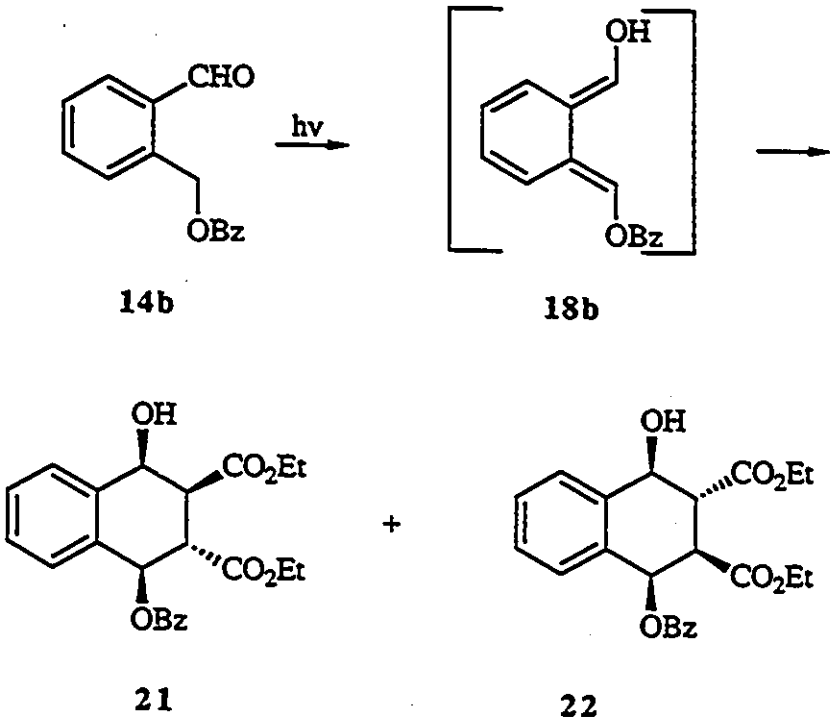


Scheme 5.10

Besides the diagnostic $[M+1]^+$ ion (m/e 413) obtained in the chemical ionization mass spectrum (CIMS), the mixture exhibited characteristic IR absorptions at $\nu_{max}$ 3579 (br) and 1732 (s) $cm^{-1}$ (hydroxyl, carbonyl functions). The $^1H$-NMR spectrum, illustrated

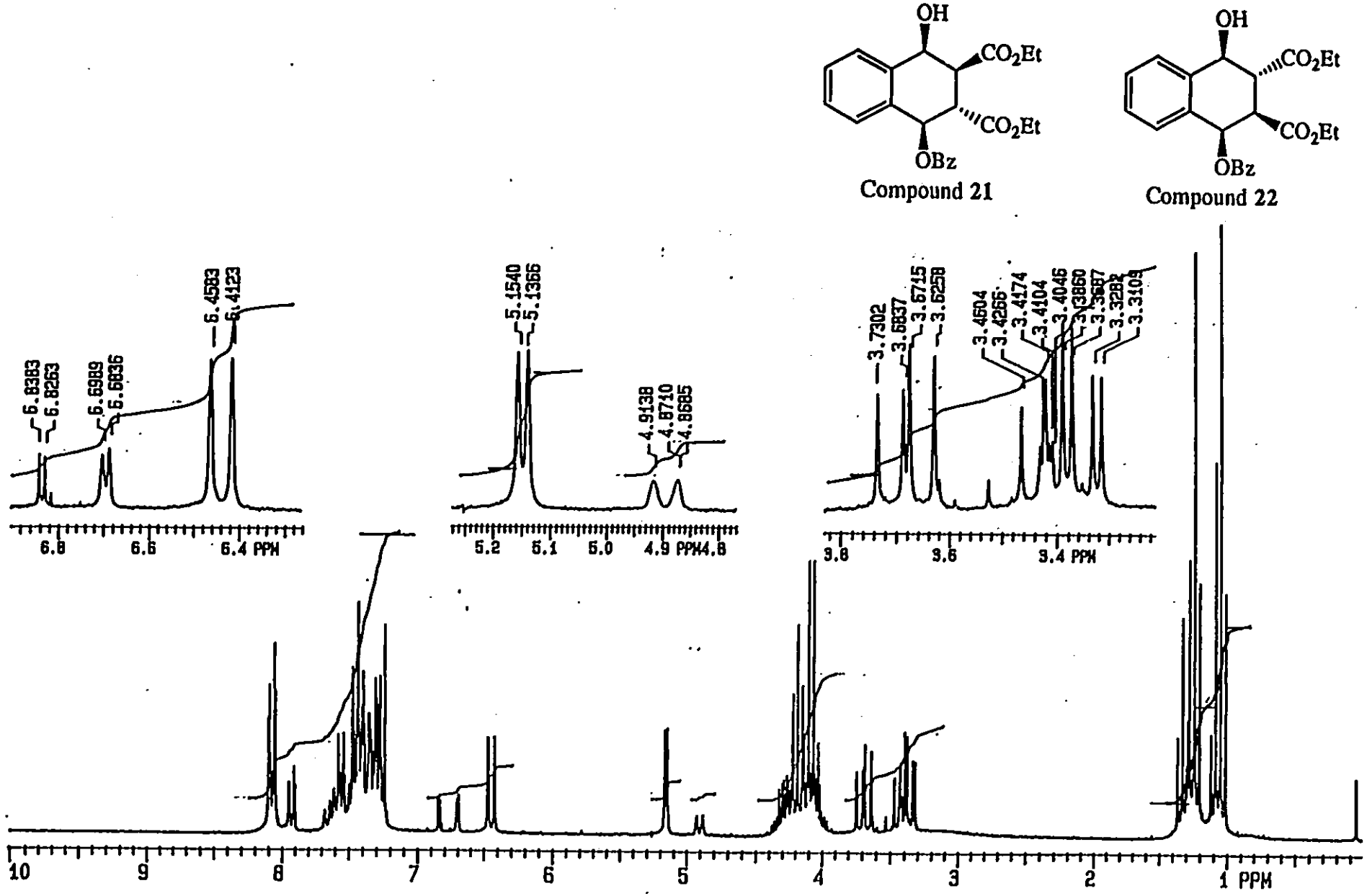


Figure 5.9: $^{1}$H-NMR of compounds **21** and **22**.

in fig. 5.9, was equally informative with the essential information summarized in fig. 5.10.

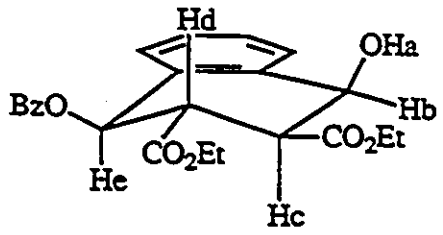


21

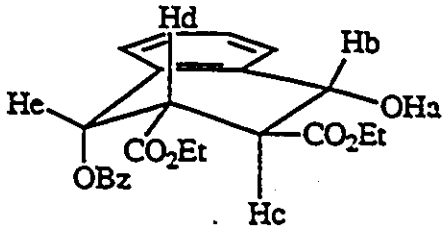


22

Chemical Shifts (ppm)

| | Ha | Hb | Hc | Hd | He |
|---|---|---|---|---|---|
| 21 | - | 5.15 | 3.35 | 3.68 | 6.44 |
| 22 | - | 4.89 | - | - | 6.69 |

Coupling Constants (Hz)

| | Jab | Jbc | Jcd | Jde |
|---|---|---|---|---|
| 21 | - | 3.5 | 11.7 | 9.2 |
| 22 | - | 9.1 | - | 3.1 |

Figure 5.10: Chemical Shifts and Coupling Constants for 21 and 22

As was the case for the $^1$H-NMR spectrum of compounds **19** and **20**, the region between δ 4.50 and 7.00 ppm was useful in assessing the *endo:exo* (**21**:**22**) ratio of the tetralins, in this case 3:1. In going from **14a** to **14b**, the modest increase in the *endo* to *exo* product ratio was ascribed to the greater steric bulk of the benzoyl protecting group. Similar steric influences, on the stereochemistry of Diels-Alder

reactions of *o*-xylylenes, have been observed with other α,α'-disubstituted-*o*-quinodimethanes (chapter 4).

To summarize, it had now been established that the photoenols **15**, **18a**, and **18b** (schemes 5.8-10) all underwent cycloaddition with the reactive dienophiles diethyl or dimethyl fumarate. The relatively electron rich photoenol **15** gave a poor yield of adducts (21 %) with a 2:1 *endo/exo* ratio, whereas the less electron rich photoenols **18a** and **18b** gave good yields (ca. 75 %) of cycloadducts with *endo/exo* ratios of 2:1 and 3:1 respectively.

In considering the next direction to be taken in this study, several factors were evaluated:

The poor yield obtained in the cycloaddition of **15** excluded aldehyde **11** from any further study.

While aldehydes **14a** and **14b** gave comparable yields of cycloaddition products, the crystallinity of **14b**, as well as the likelihood of crystallinity in any derived cycloadducts, rendered it a more attractive substrate for further study. In addition, the greater structural similarity of **14b** to the proposed intramolecular models (chapter 3) served to further distance **14a** from any additional consideration.

In view of the preceding points, aldehyde **14b** was selected for more in depth study. In an effort to assess the scope of the cycloaddition, **14b** would be photoenolized in the presence of several other dienophiles of varying reactivity. Where unsymmetrical dienophiles were used, trends indicative of the stereochemistry and regioselectivity of the cycloaddition could be determined.

Scheme 5.11 illustrates the products obtained when **14b** was irradiated in the presence of 3 equivalents of methyl acrylate in benzene solution.

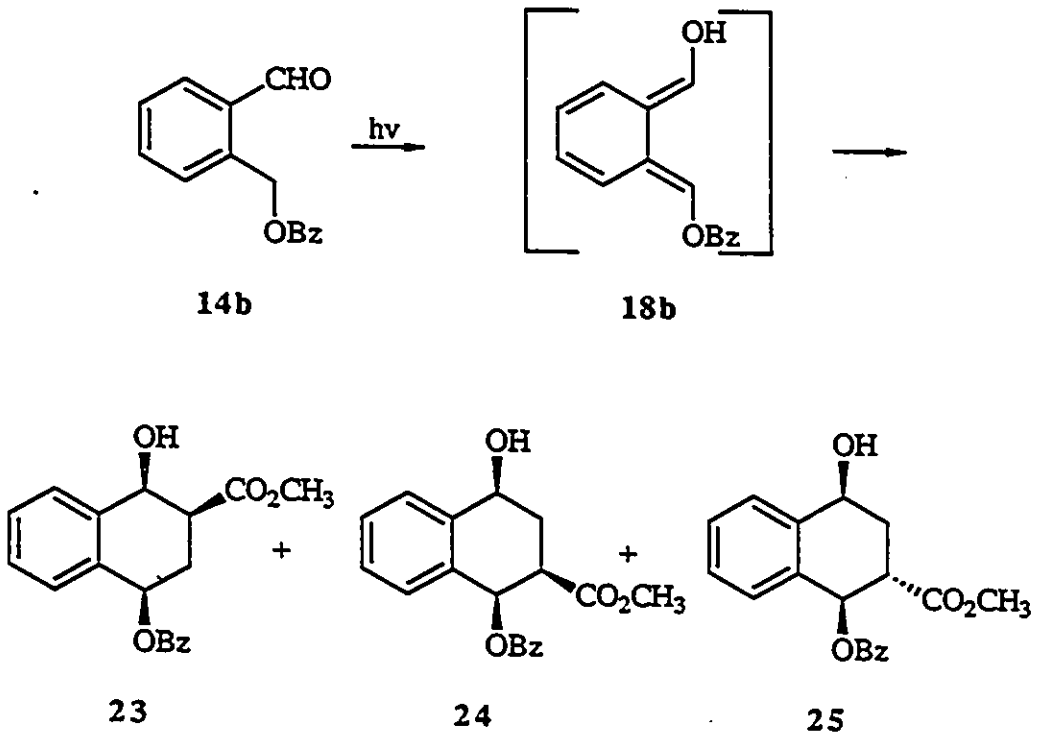


Scheme 5.11: Products obtained on irradiation of **14b** in the presence of 3 equivalents of methyl acrylate

The product mixture was purified by flash chromatography (10:1 chloroform:ether) furnishing the major regioisomer **23** in 50 % yield, and an equimolar mixture, assumed to be the diastereomeric tetralins **24** and **25** in 15 % yield.

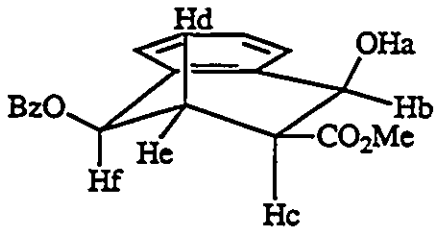


23

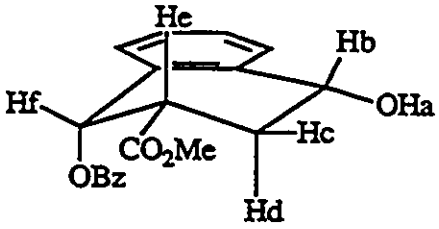


24

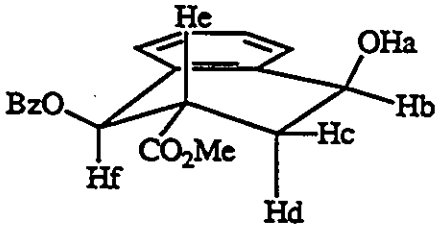


25

Chemical Shifts (ppm)

| | Ha | Hb | Hc | Hd | He | Hf |
|---|---|---|---|---|---|---|
| 23 | 3.20 | 5.04 | 3.00 | 2.53 | 2.53 | 6.20 |
| 24 | - | 4.83 | 2.62 | 2.33 | 3.08 | 6.61 |
| 25 | - | 4.90 | 2.33 | 2.33 | 3.49 | 6.52 |

Coupling Constants (Hz)

| | Jab | Jbc | Jbd | Jcd | Jce | Jde | Jdf | Jef |
|---|---|---|---|---|---|---|---|---|
| 23 | 5.9 | 3.6 | - | 10.8 | 3.6 | - | 8.8 | 6.5 |
| 24 | - | 6.2 | 9.9 | 13.6 | 3.4 | 12.2 | - | 3.7 |
| 25 | - | 4.3 | 4.3 | - | 4.9 | 9.0 | - | 8.4 |

Figure 5.11: Chemical shifts and coupling constants for 23-25

Compound **23** showed a diagnostic $[M+1]^+$ ion in its CIMS, as well as a broad absorbance in its IR spectrum at 3564 $cm^{-1}$, and a strong absorbance at 1720 $cm^{-1}$. The mixture of **24** and **25** also gave a

$[M+1]^+$ ion of m/e 327 in its CIMS in addition to characteristic absorptions in their IR spectrum at 3588 and 1732 $cm^{-1}$. A summary of the relevant chemical shifts and coupling constants extracted from the $^1$H-NMR spectra (fig. 5.12, 5.13) of compounds **23** to **25** is presented in figure 5.11. The proton NMR spectrum of compound **23** (fig. 5.12) clearly supports its structural assignment as is demonstrated by the signal at δ 3.67 (s, 3H) ppm, denoting the carbomethoxy hydrogens, and the signals at δ 5.04 (dd, 1H, $J$ = 3.6, 5.9 Hz) and 6.20 (dd, 1H, $J$ = 6.5, 8.8 Hz) ppm, attributable to the northern and southern benzylic protons respectively. The $^1$H-NMR spectrum of the *m*-cis/*m*-trans isomeric mixture (fig. 5.13) was similarly informative as was indicated by the pair of signals at δ 3.59 (s, 3H) and 3.63 (s, 3H) ppm, ascribed to the carbomethoxy hydrogens, and the signals centered at δ 4.85 (northern benzylic protons) and 6.55 ppm (southern benzylic hydrogens). The pair of doublets centered at δ 6.55 ppm, in particular, nicely illustrated the stereochemistry and the 1:1 ratio of the isomers **24** and **25**.

The preponderance of the *o-endo* adduct **23** over the *m*-cis **24** and *m*-trans **25** isomers (regioselectivity 3:1) was not unexpected in terms of FMO theory[53] and has precedents with the related photoenol derived from *o*-methylbenzaldehyde.[55] In view of the effect of steric crowding on the stereochemistry of addition to other α,α'-disubstituted-*o*-quinodimethanes[56] (vide infra), the question arose as to whether similar effects on the stereoselectivity and regioselectivity would be observed with our substrates. To address this question, an *o*-(acyloxymethyl)benzaldehyde (**14c**), bearing the sterically more demanding pivaloyl protecting group, was photolyzed.

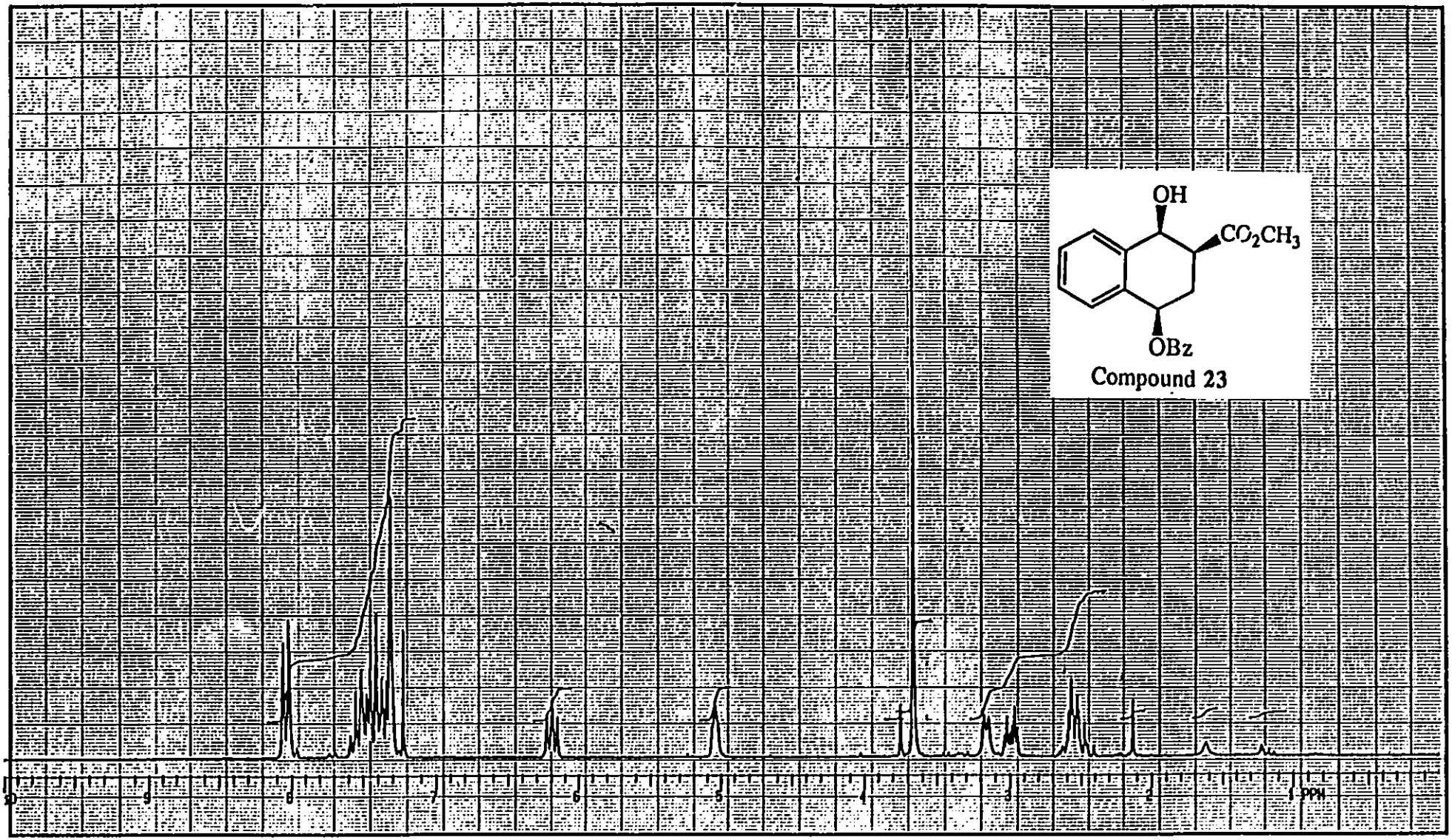


Figure 5.12: $^1$H-NMR of compound **23**.

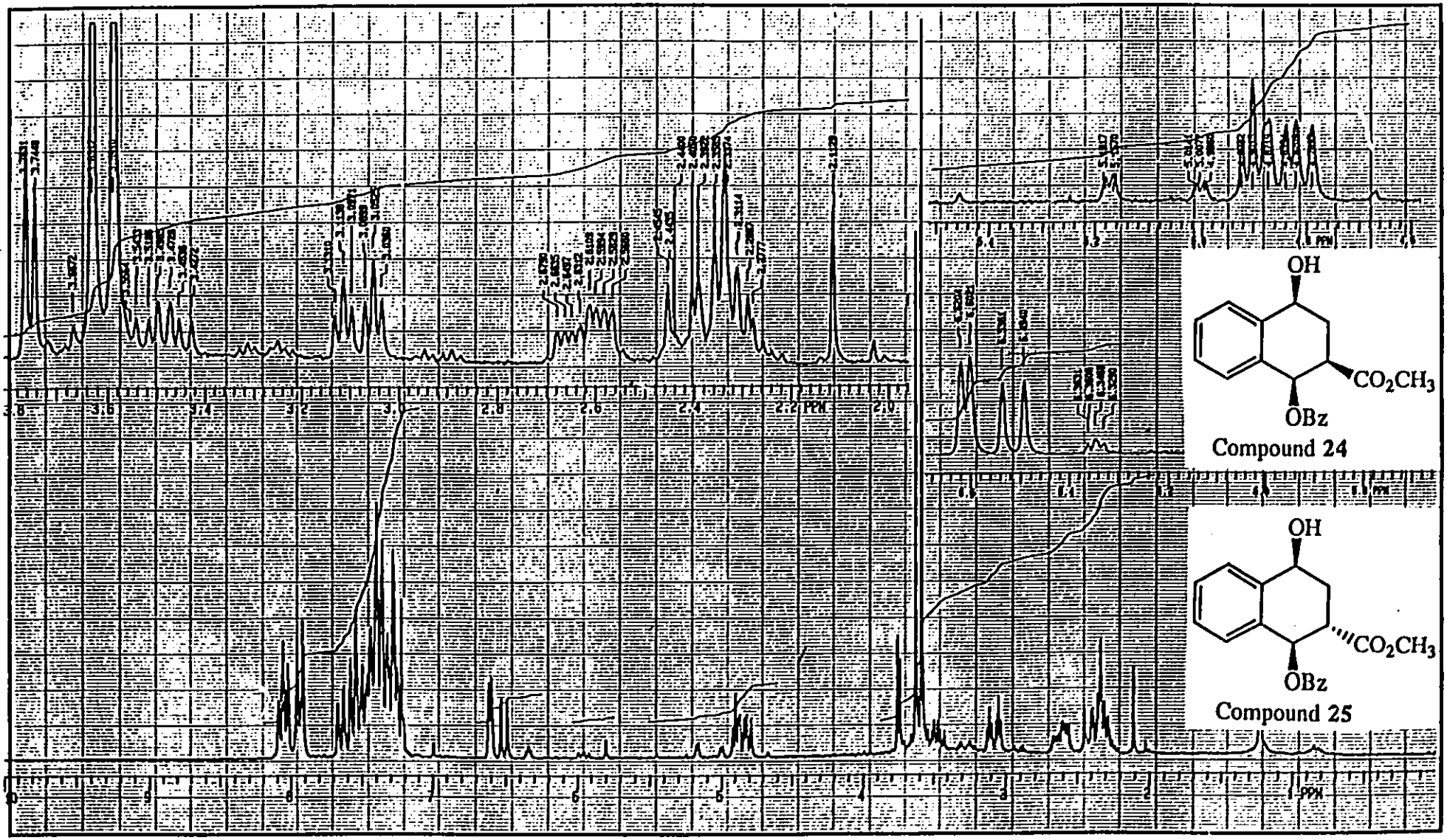


Figure 5.13: $^{1}$H-NMR of compounds **24** and **25**.

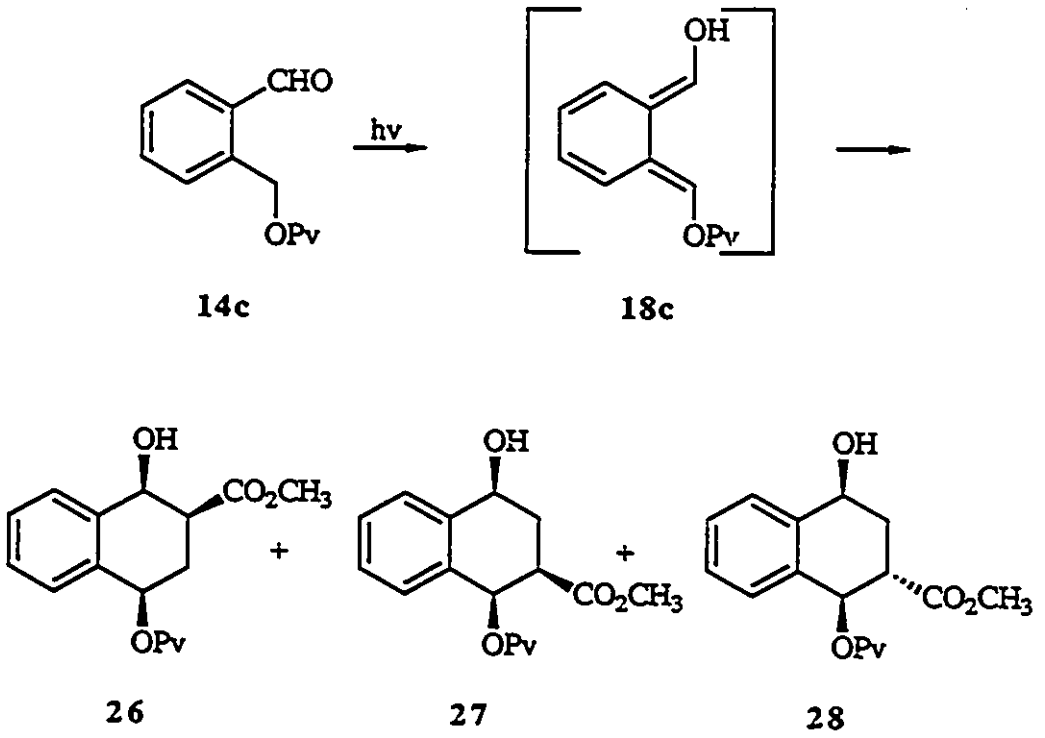


Scheme 5.12: Products obtained on irradiation of **14c** in the presence of 3 equivalents of methyl acrylate

As depicted in scheme 5.12, aldehyde **14c**, when irradiated under the same conditions as employed for **14b**, furnished the *o*-endo adduct **26** in 47 % yield, along with a 3:2 mixture, presumably the *m*-cis **27** and *m*-trans **28** regioisomers, in 8 % combined yield. A summary of the $^1$H-NMR (fig. 5.15, 5.16) spectral assignments is tabulated in fig. 5.14.

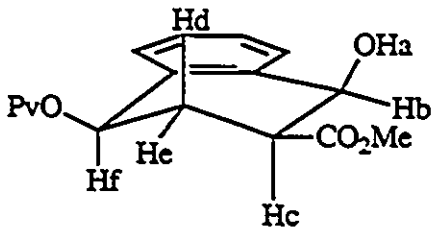


26

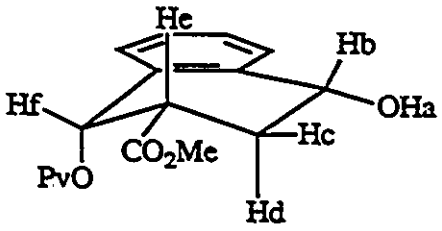


27

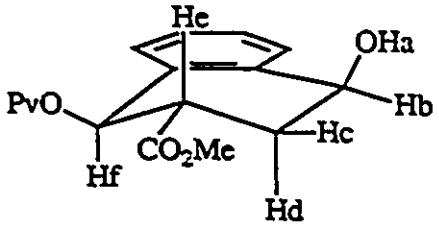


28

Chemical Shifts (ppm)

| | Ha | Hb | Hc | Hd | He | Hf |
|---|---|---|---|---|---|---|
| 26 | 3.06 | 5.02 | 2.87 | 2.27 | 2.45 | 5.91 |
| 27 | - | 4.83 | 2.52 | 2.23 | 2.96 | 6.33 |
| 28 | - | 4.75 | 2.13 | 2.36 | 3.31 | 6.20 |

Coupling Constants (Hz)

| | Jab | Jbc | Jbd | Jcd | Jce | Jde | Jdf | Jef |
|---|---|---|---|---|---|---|---|---|
| 26 | 5.3 | 4.4 | - | 12.6 | 3.1 | 12.8 | 10.1 | 6.5 |
| 27 | - | 6.0 | - | 14.1 | 2.9 | 12.2 | - | 4.0 |
| 28 | - | - | - | - | 4.9 | 9.7 | - | 9.5 |

Figure 5.14: Chemical shifts and coupling constants for 26-28

The $^1$H-NMR spectrum of compound **26** (fig. 5.15) was essentially identical to that of **23** (fig. 5.12), except for the signal at δ 1.24 (s, 9H)

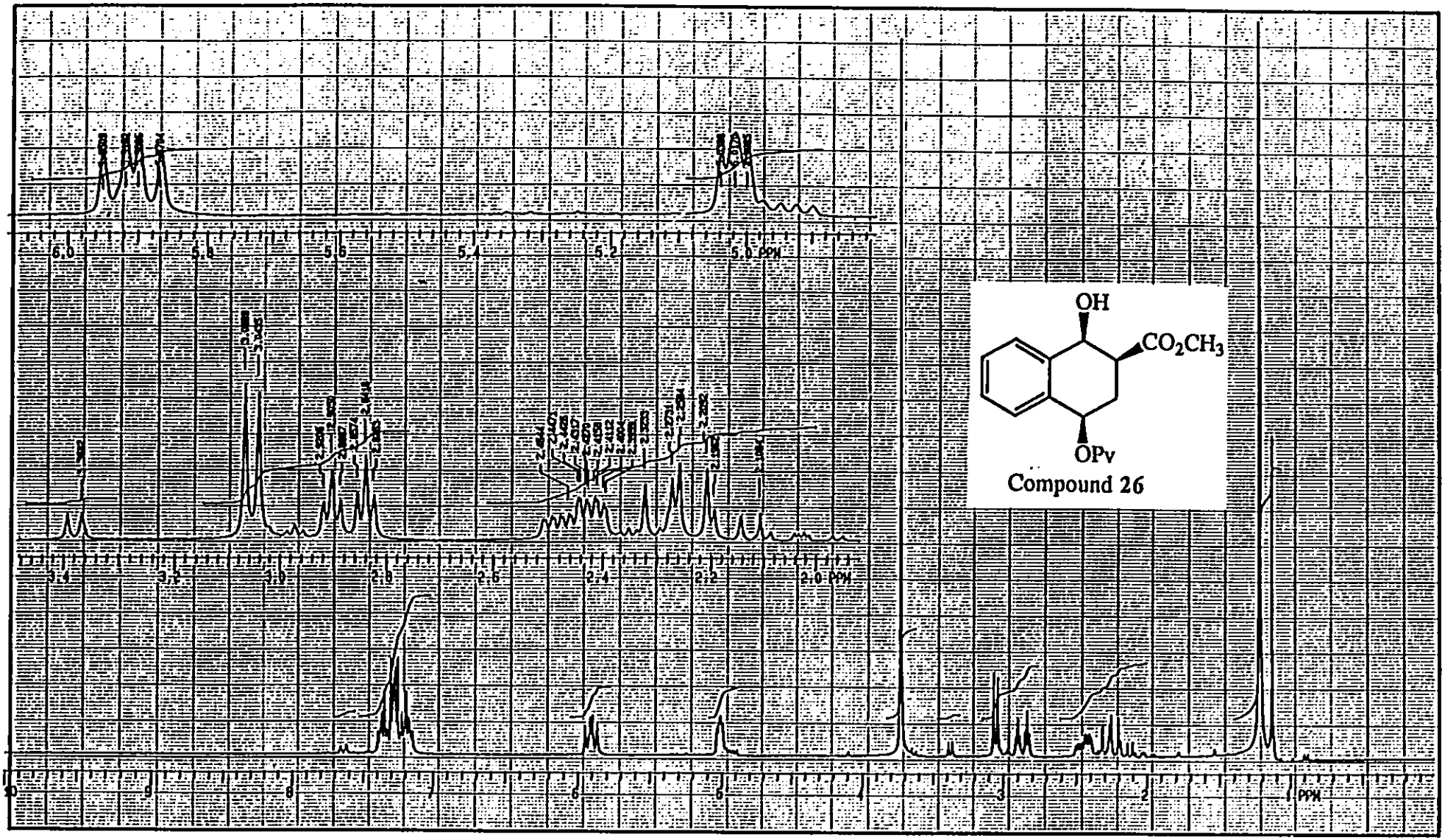


Figure 5.15: $^1$H-NMR of compound 26.

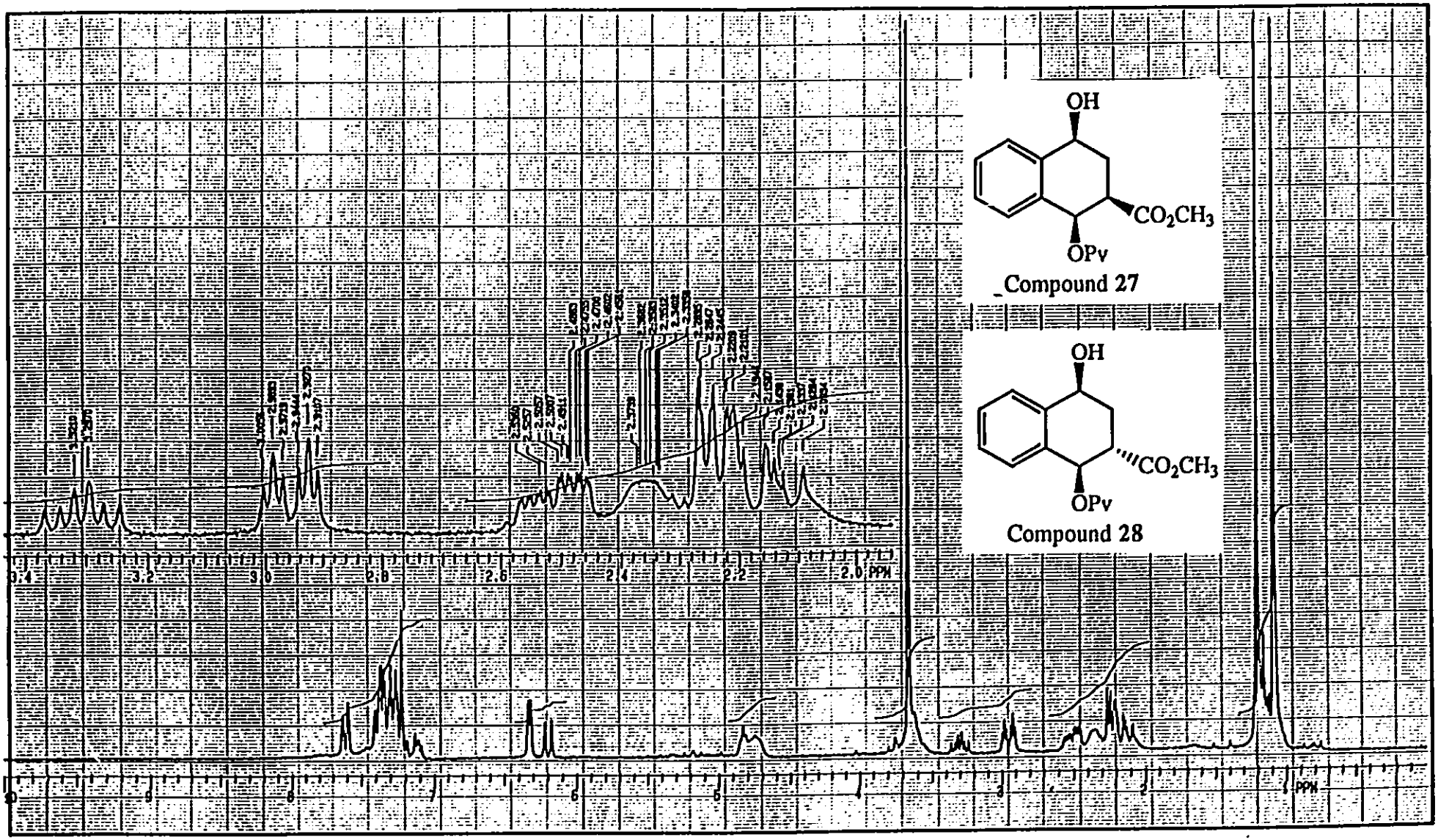


Figure 5.16: $^1$H-NMR of compounds 27 and 28.

ppm ascribed to the pivaloyl hydrogens. The ABMX system, centered at δ 2.30 ppm (fig. 5.15), was informative with its large geminal coupling constant (*J* de 12.8 Hz), its two cis coupling constants (*J* ce, *J* ef 3.1, 6.5 Hz) and its two trans coupling constants (*J* cd, *J* df 12.6, 10.1). The peaks arising from the benzylic protons were equally diagnostic with the signal at δ 5.02 (dd, 1H, *J* = 4.4, 5.3 Hz) ppm corresponding to the northern hydrogen, and the signal at δ 5.91 (dd, 1H, *J* = 6.5, 10.1 Hz) ppm originating from the southern counterpart.

Similar assignments were made with the $^1$H-NMR spectrum of the *m*-cis and *m*-trans isomers (fig. 5.16), except for major differences observed for the southern benzylic protons of (**27**) δ 6.33 (d, 1H, *J* = 4.0 Hz) and (**28**) δ 6.20 (d, 1H, *J* = 9.5 Hz) ppm, as well as the acidic α-proton He (fig. 5.14), whose signal occurred at δ 2.96 (dt, 1H, *J* = 3.3, 12.2 Hz) ppm for compound **27** and δ 3.31 (td, 1H, *J* = 4.9, 9.7 Hz) for **28**.

While there was a marginal increase in the regioselectivity for this cycloaddition (6:1 *o*-endo:*m*-cis/*m*-trans) over the 3:1 ratio obtained in the photoenolization of **14b**, no significant effect on the proportion (3:2 *m*-cis:*m*-trans) of the *m*-cis and *m*-trans isomers was observed; It was evident that steric influences would not play an important role with our substrates in terms of affecting the regioselectivity or the stereoselectivity.

The next dienophile selected for cycloaddition was methyl crotonate which, when irradiated in the presence of **14b**, furnished a 33 % yield of the adducts **29** and **30** as a 2:1 mixture of regioisomers (scheme 5.13). Compounds **29** and **30** were purified by flash chromatography and in addition to the diagnostic $[M+1]^+$ ions observed

in their CIMS, showed characteristic IR absorptions at 3599 and 1725 $cm^{-1}$ for **29** and 3592 and 1723 $cm^{-1}$ for **30**.

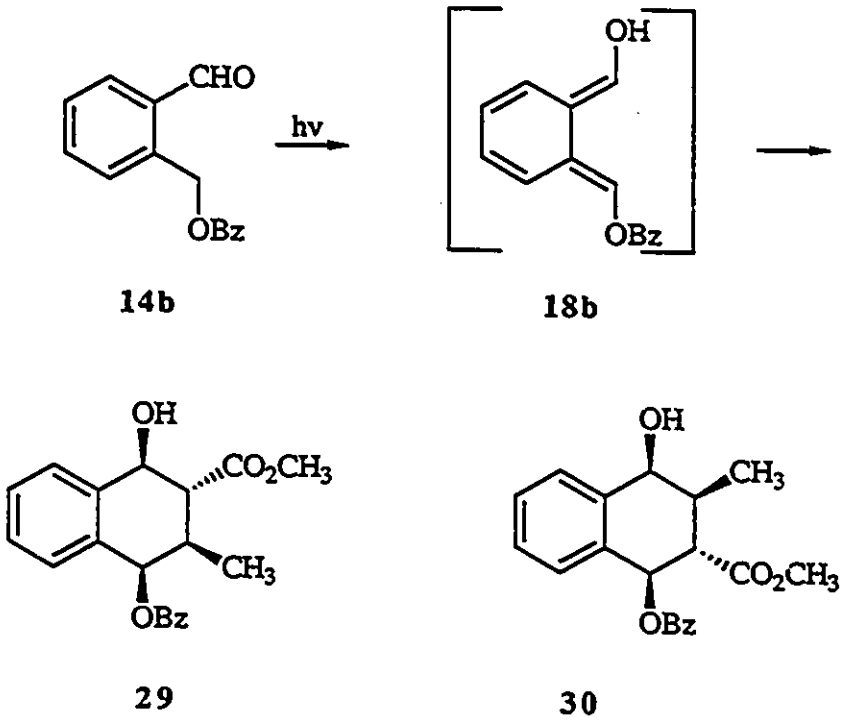


Scheme 5.13

A summary of the chemical shifts and coupling constants observed in the $^1$H-NMR spectra (fig. 5.18, 5.19) of compounds **29** and **30** is presented in fig. 5.17. The proton NMR spectrum of the exo adduct **29** (fig. 5.18) was amenable to straightforward analysis. For example the signals at δ 3.06 (dd, 1H, $J$ = 10.4, 11.9 Hz) and 5.06 (t, 1H, $J$ = 8.7 Hz) ppm, corresponding to the acidic α-proton Hc (fig. 5.17) and the benzylic hydrogen Hb respectively, verified the trans relationship between Hb, Hc, and Hd. In addition, the signals present at δ 2.38 (dq, 1H, $J$ = 3.4, 11.7 Hz) and 6.26 (d, 1H, $J$ = 3.2 Hz) ppm, ascribed to Hd and

He respectively, confirmed the cis-trans relationship between He, Hd and Hc.

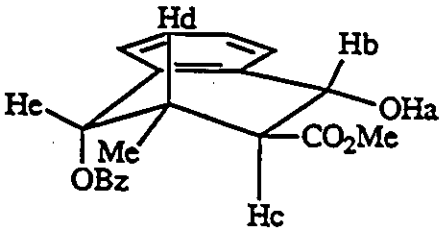


29

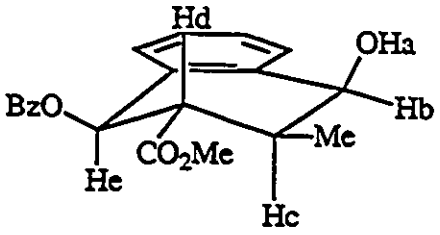


30

Chemical Shifts (ppm)

| | Ha | Hb | Hc | Hd | He | Me |
|---|---|---|---|---|---|---|
| 29 | 2.77 | 5.06 | 3.06 | 2.38 | 6.26 | 1.04 |
| 30 | 1.90 | 4.61 | 2.30 | 3.27 | 6.51 | 1.17 |

Coupling Constants (Hz)

| | Jab | Jbc | Jcd | Jde | Jcm | Jdm |
|---|---|---|---|---|---|---|
| 29 | 8.3 | 10.4 | 11.9 | 3.2 | - | 6.8 |
| 30 | 4.7 | 3.3 | 11.8 | 9.7 | 6.9 | - |

Figure 5.17: Chemical shifts and coupling constants for 29 and 30

The $^1$H-NMR spectrum of compound **30** (fig. 5.19) was similar to that of **29** with several notable exceptions. The assignment of the substitution pattern for **30** was predicated on the observation of both an upfield shift in δ for Hb and a downfield shift in δ for He (fig. 5.17). A similar effect on the chemical shifts of

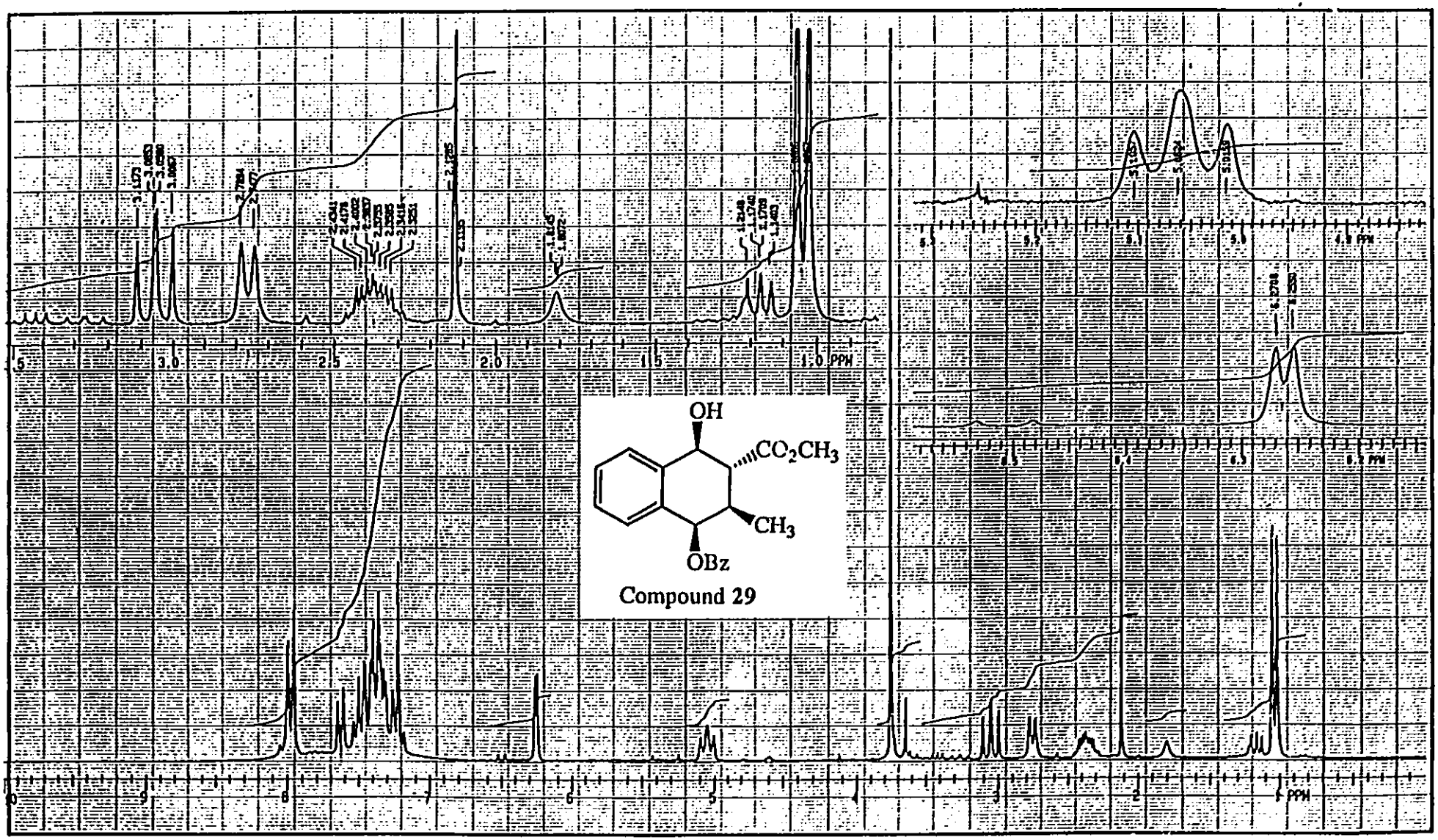


Figure 5.18: $^1$H-NMR of compound 29.

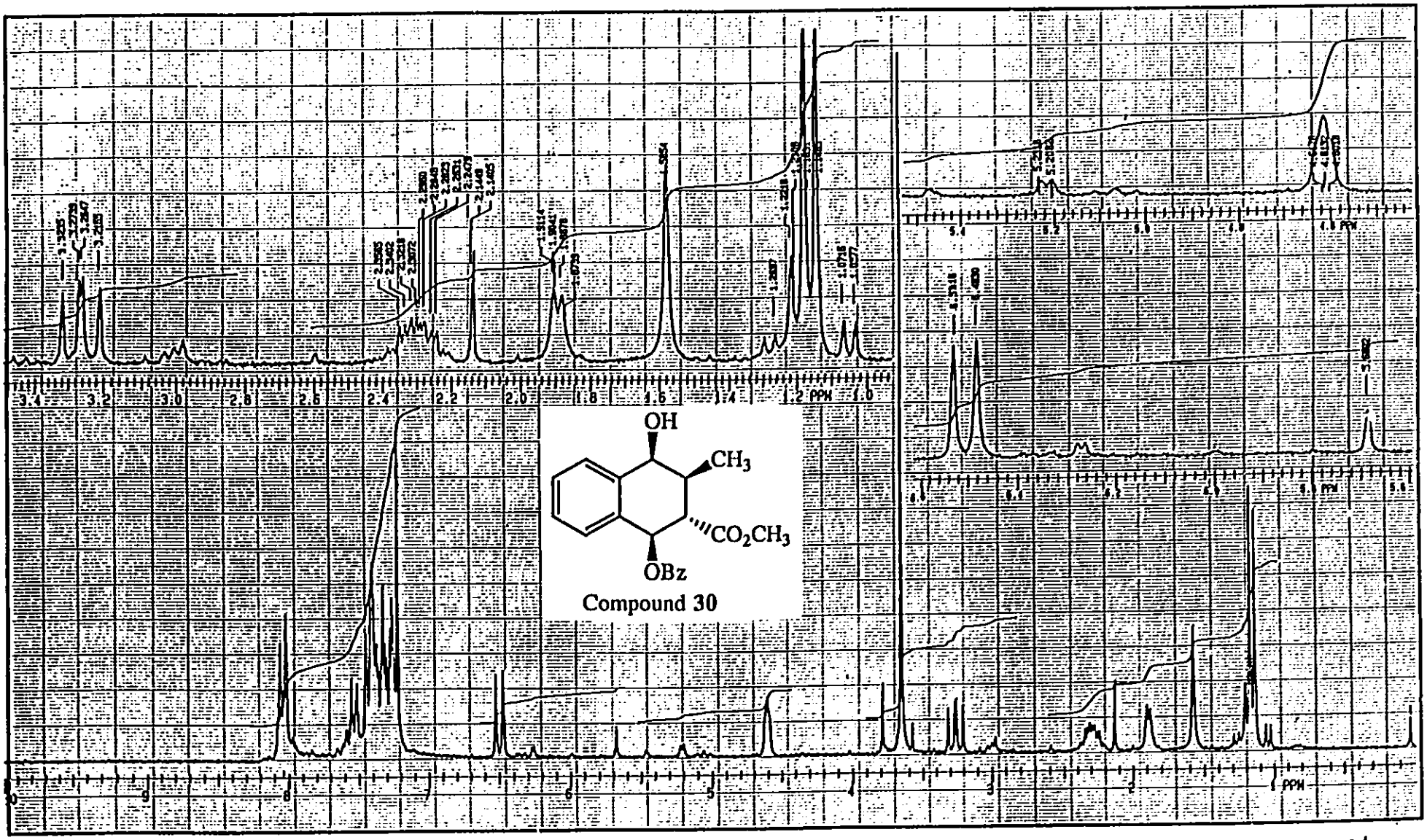


Figure 5.19: $^{1}$H-NMR of compound 30.

the benzylic hydrogens, between regioisomers, had been observed with adducts **23-25** and **26-28**. The signals at δ 6.51 (d, 1H, *J* = 9.7 Hz) and 3.27 (dd, 1H, *J* = 9.8, 11.8 Hz) ppm, corresponding to He and Hd respectively, confirmed the trans-trans relationship between He, Hd and Hc. In addition, the signals at δ 4.61 (t, 1H, *J* = 0.9 Hz) and 2.30 (dq, 1H, *J* = 3.3, 6.9, and 12.1) ppm, arising from Hb and Hc respectively, verified the cis-trans relationship between Hb, Hc and Hd.

The most notable aspect of this cycloaddition was the stereochemistry of carbomethoxytetralins **29** and **30** which in both cases was 1,2-trans. This indicated that cycloaddition had proceeded through *exo* transition states, in contrast to the *endo* transition state predicted by empirical precedence. Mann and Piper[57] reported the isolation of *exo* adducts when an α-phenyl-*o*-quinodimethane was reacted with dimethyl maleate or methyl crotonate. Shorter reaction times favoured greater proportions of the *endo* adduct leading the authors to the conclusion that the cycloaddition was reversible and that the accumulation of *exo* adduct represented a thermodynamic partition. Charlton, Kozma and Durst[56] also reported the isolation of *exo* adducts when thermally generated α-substituted and α,α'-disubstituted-*o*-quinodimethanes were reacted with dimethyl fumarate or maleate. Charlton and Durst's thermolyses were carried out at lower temperatures than Mann and Piper's cycloadditions, excluding the possibility of a thermodynamic partition. Charlton, in a subsequent review,[30a] concluded that at least in some cases, despite favorable secondary orbital effects, *exo* addition to α-substituted-*o*-quinodimethanes occurs and is likely due to steric influences.

The last series of dienophiles examined included the alkynes depicted in scheme 5.14.

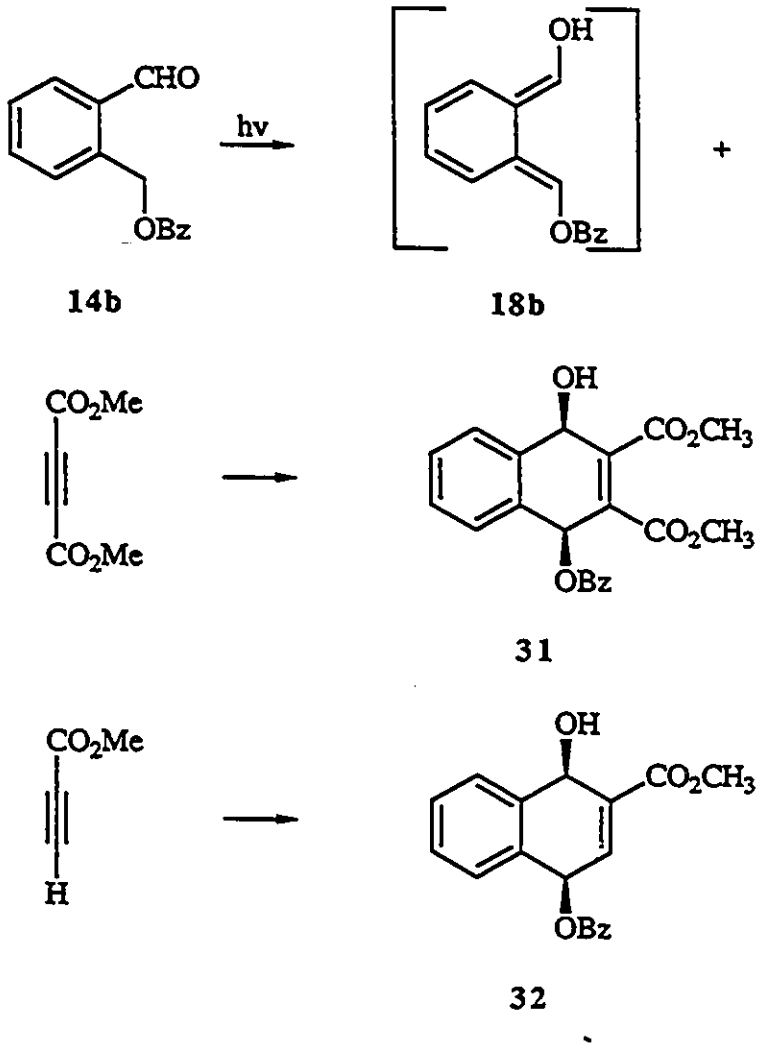


Scheme 5.14: Cycloaddition attempts with alkynyl dienophiles

Photoenolization of **14b**, in the presence of 3 equivalents of dimethylacetylene dicarboxylate, furnished **31** in 56 % yield, after purification by flash chromatography.

The CIMS of compound **31** gave no molecular ion but showed a fragment at m/e 365 corresponding to a loss of $H_2O$ ($[M+1]^+$-18); the IR spectrum exhibited characteristic absorptions at 3528 (br, OH), 1728 (s, C=O), and 1732 (s, C=O) $cm^{-1}$. Analysis of the $^1$H-NMR spectrum (fig. 5.20) was straightforward, however, the signal at δ 5.42 (dd, 1H, $J$ = 2.3, 7.4 Hz) deserves further note. In addition to exhibiting a 7.4 Hz $^3J_{HH}$ coupling to the hydroxyl proton (δ 3.47 ppm), it exhibited an unusual $^5J_{HH}$ transannular coupling (2.4 Hz) to the second benzylic hydrogen Hc at δ 6.85 (d, 1H, $J$ = 2.4 Hz) ppm.

Irradiation of **14b**, in the presence of 3 equivalents of methyl propiolate, furnished the *o*-adduct **32** in 20 % yield after flash chromatography ; no trace of the *m*-regioisomer was isolated from the product mixture.

The EIMS of **32** gave a small molecular ion at m/e 324 and the IR spectrum showed characteristic absorptions at 3548 (br, OH) and 1720 (s, C=O) $cm^{-1}$. The $^1$H-NMR spectrum (fig. 5.21) clearly supported the assigned structure. Both signals arising from the benzylic hydrogens Hb and Hd were triplets (or dd) which, as with compound **31**, was likely due to overlapping $^3J_{HH}$ and $^5J_{HH}$ couplings. The most informative chemical shifts and coupling constants, both for adducts **31** and **32**, are summarized in figure 5.22.

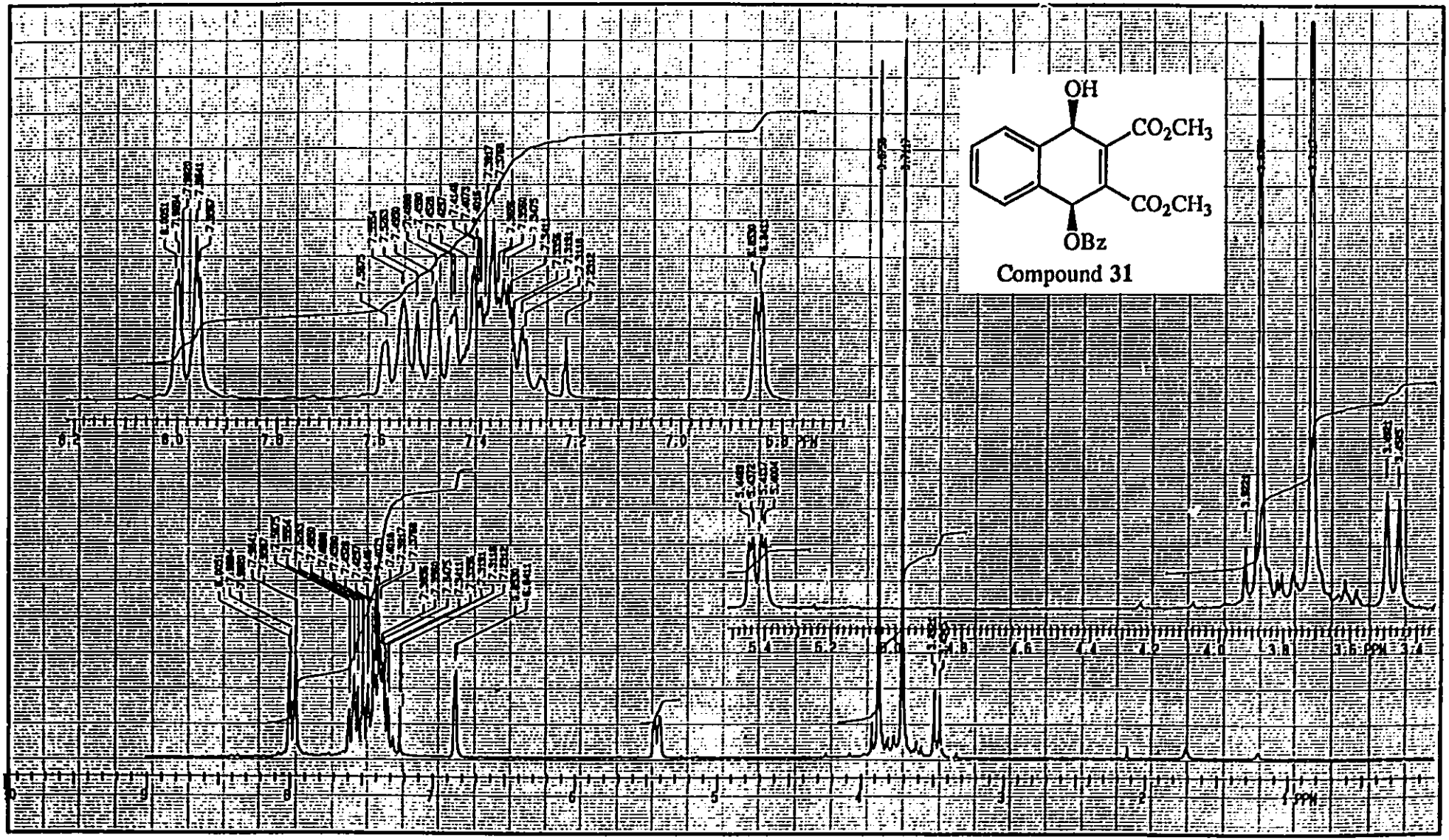


Figure 5.20: $^1$H-NMR of compound 31.

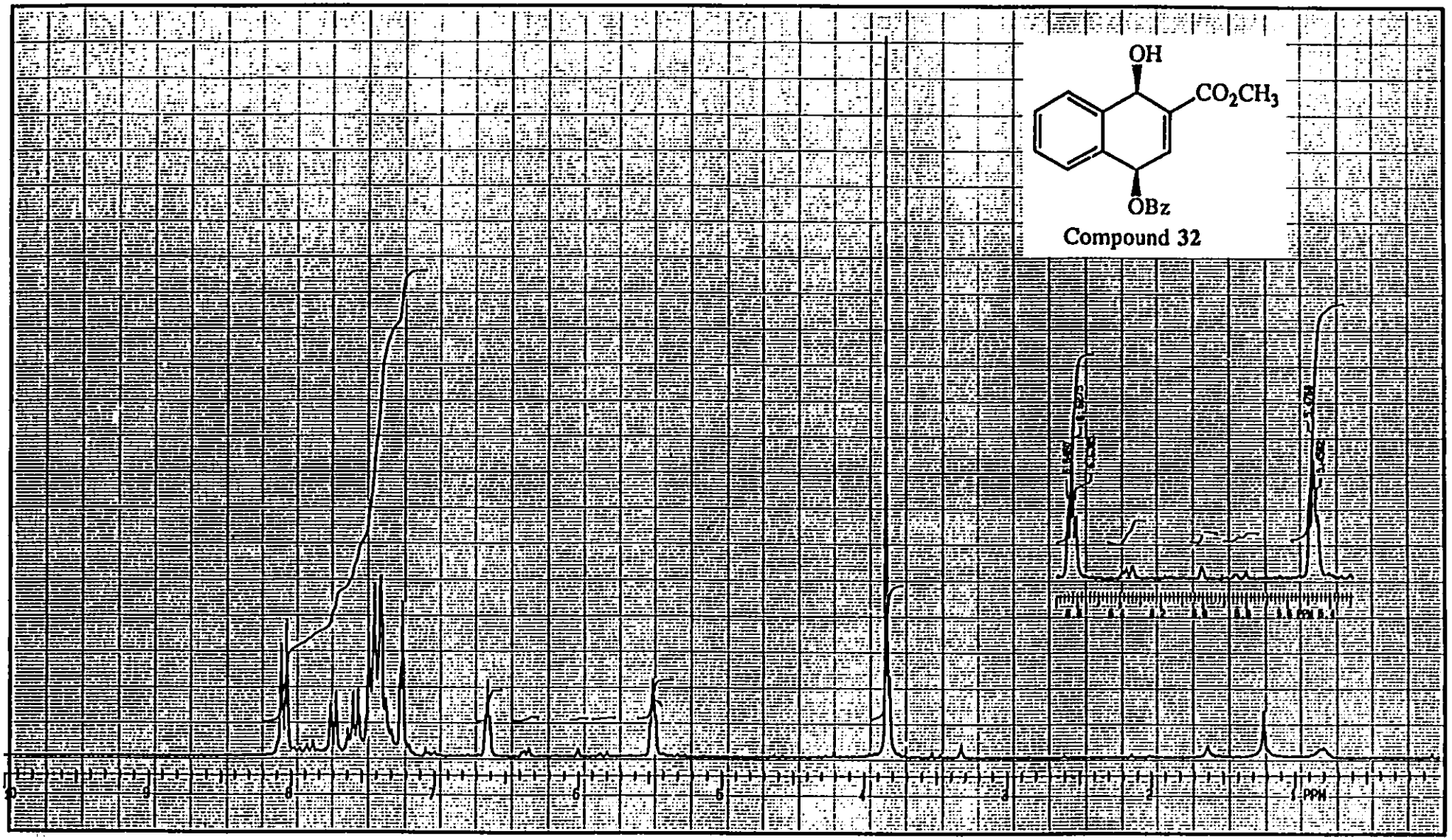


Figure 5.21: $^1$H-NMR of compound 32.

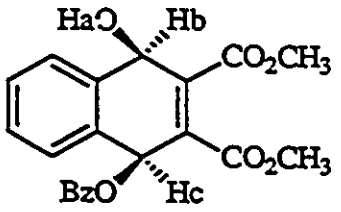


31

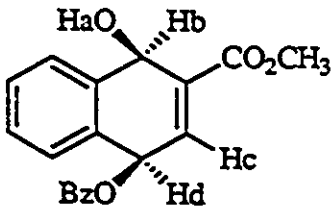


32

Chemical Shifts (ppm)

| | Ha | Hb | Hc | Hd |
|---|---|---|---|---|
| 31 | 3.47 | 5.42 | 6.85 | - |
| 32 | 3.82 | 5.48 | 7.23 | 6.63 |

Coupling Constants (Hz)

| | Jab | Jbc | Jbd | Jcd |
|---|---|---|---|---|
| 31 | 7.5 | 2.3 | - | - |
| 32 | 3.7 | - | 3.8 | 3.8 |

Figure 5.22: Chemical shifts and coupling constants for 31 and 32

## 5.4 Electrocyclization vs dimerization

The photoenols derived from aldehydes **11** and **14a-c** are not significantly sterically encumbered, thus it was not surprising that benzocyclobutenols were not isolated from any of the product mixtures containing the cycloadducts. Sammes[58] reportedly isolated small quantities (10 %) of benzocyclobutenol upon photolysis of benzene solutions of 2-methylbenzaldehyde. The major products consisted of dimers arising from pinacolization and self-cycloaddition where the ground state aldehyde had acted as a heterodienophile (scheme 5.15).

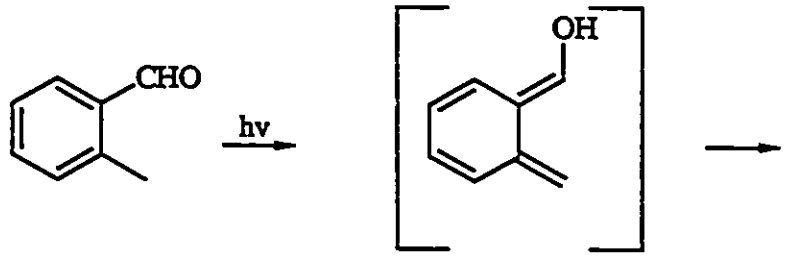


33 34

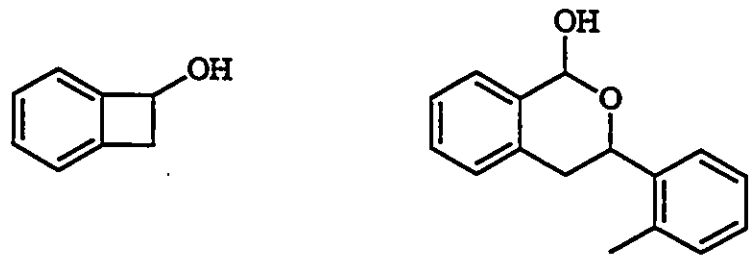


35 36

Scheme 5.15: Sammes' products isolated upon photoenolization of 2-methylbenzaldehyde

Closer examination of the side products accompanying compound **32** suggested that a similar dimerization had occurred during photoenolization of aldehyde **14b**. Indeed, irradiation of a 0.1 M benzene solution of **14b** furnished the assumed dimer **37** (scheme 5.16) in 73 % yield as a mixture of the *endo* and *exo* isomers.

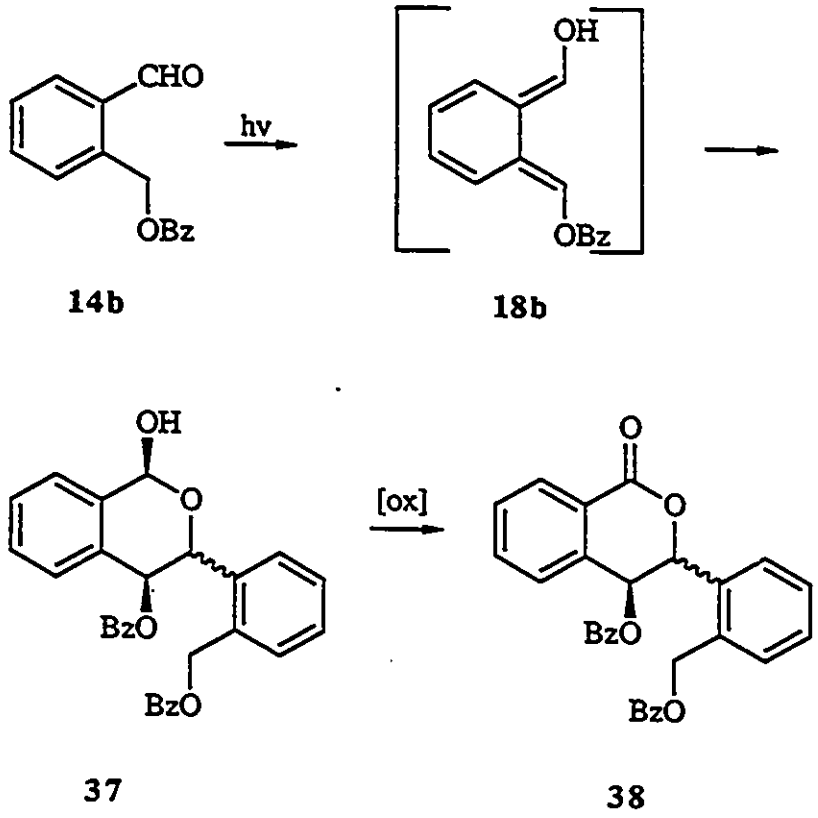


Scheme 5.16: Photochemical dimerization of **14b**

The IR spectrum of the mixture exhibited absorptions at 3572 and 1719 $cm^{-1}$ corresponding to the hydroxyl and carbonyl functions respectively; the $^1$H-NMR spectrum (fig. 5.23) showed characteristic signals which are summarized in figure 5.25.

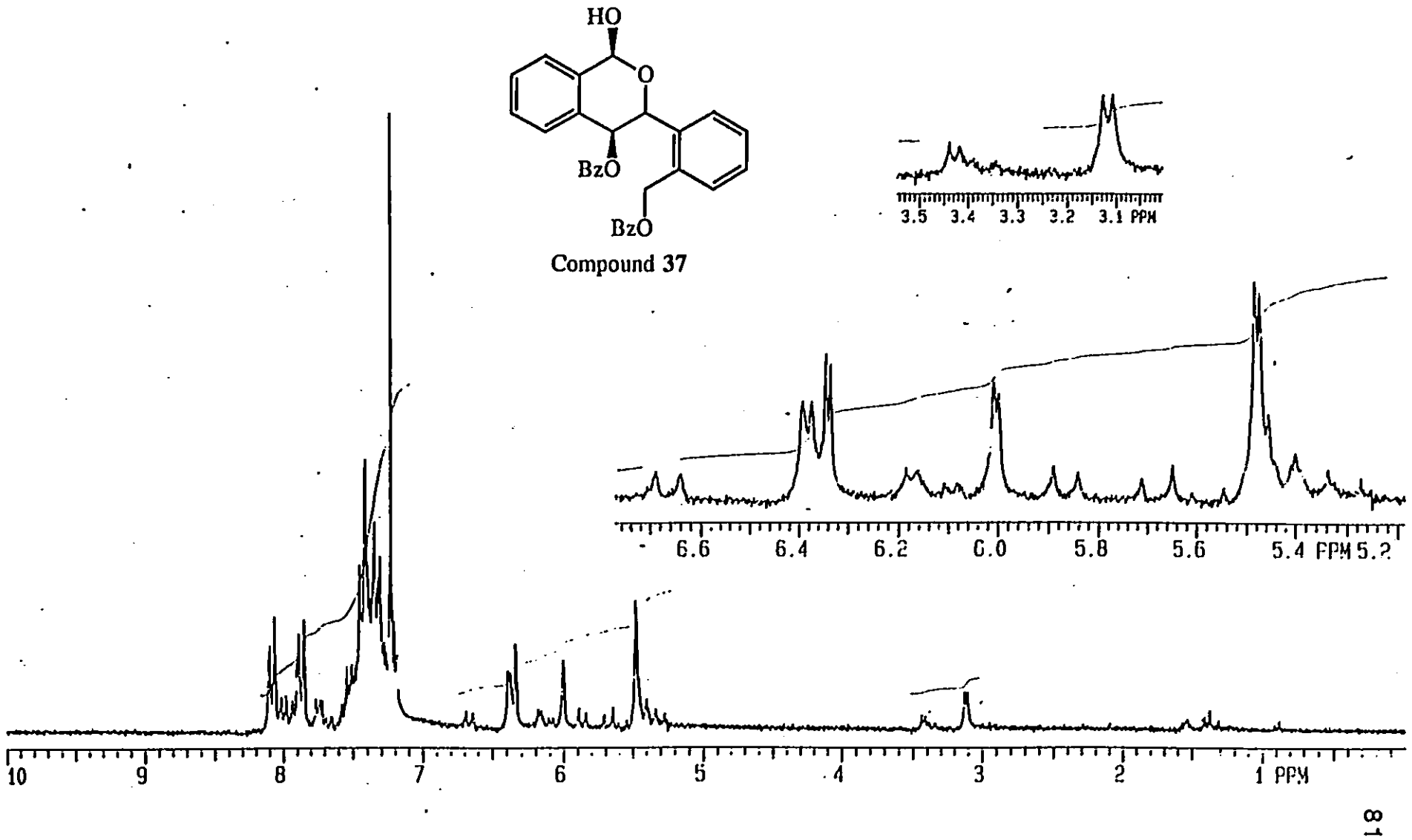


Figure 5.23: $^{1}$H-NMR of compound 37.

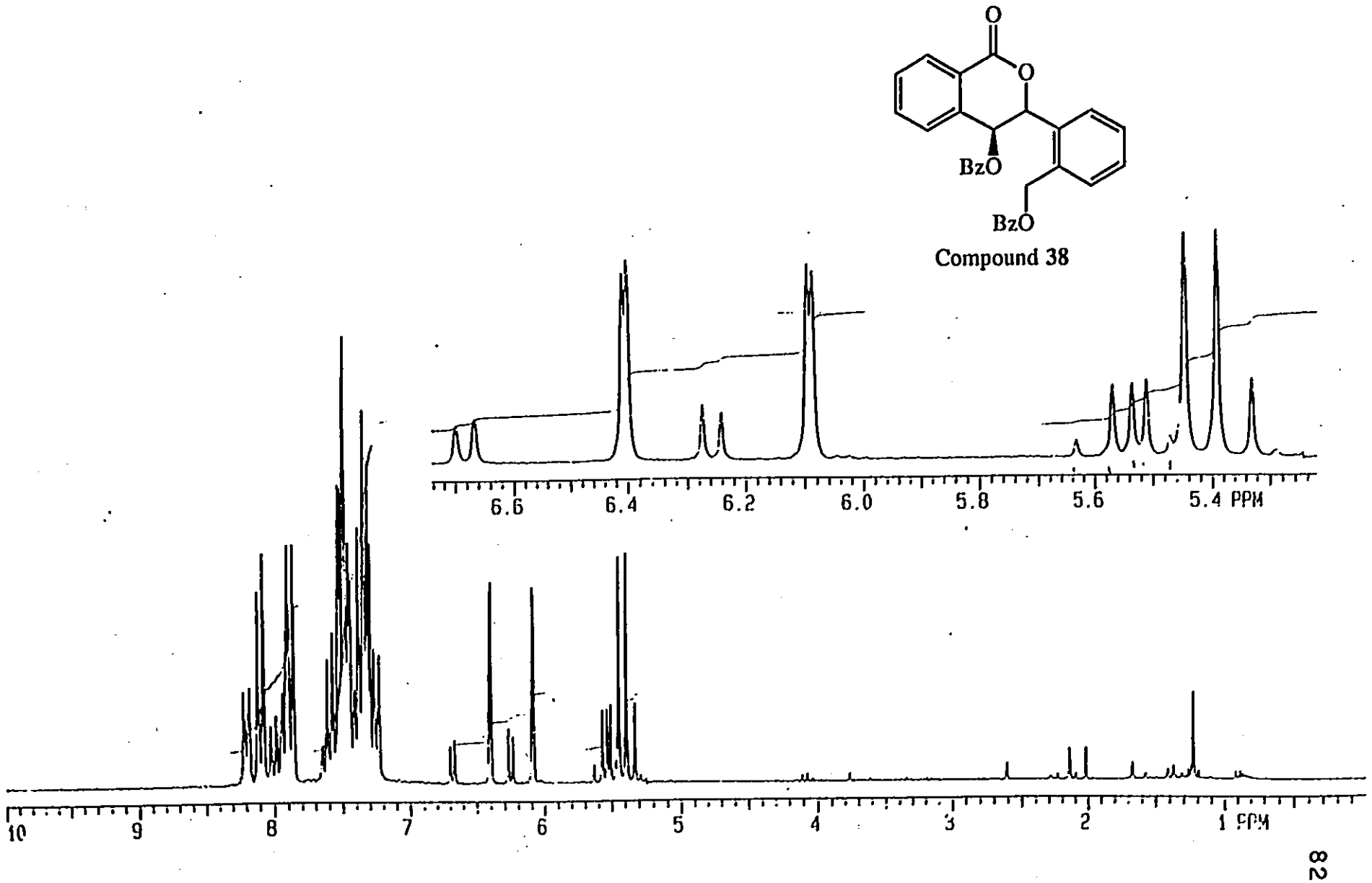


Figure 5.24: $^{1}$H-NMR of compound **38**.

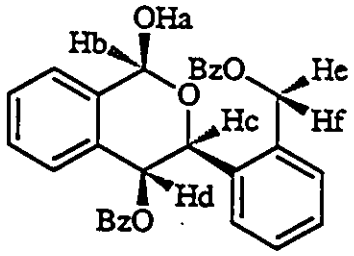


37-*cis*

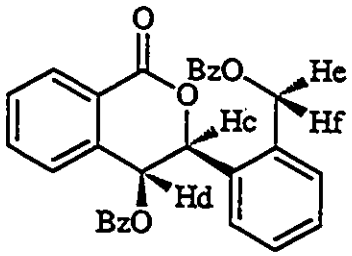


38-*cis*

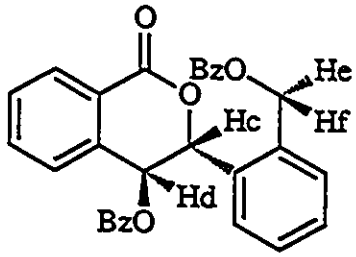


38-*trans*

Chemical Shifts (ppm)

| | Ha | Hb | Hc | Hd | Hef |
|---|---|---|---|---|---|
| 37 | 3.42 | 6.37 | 6.01 | 6.35 | 5.47 |
| 38c | - | - | 6.26 | 6.68 | 5.55 |
| 38t | - | - | 6.09 | 6.41 | 5.42 |

Coupling Constants (Hz)

| | Jab | Jcd | Jef |
|---|---|---|---|
| 37 | 4.3 | 1.6 | 1.3 |
| 38c | - | 1.7 | 12.6 |
| 38t | - | 6.5 | 13.0 |

Figure 5.25: Chemical shifts and coupling constants for **37** and **38**

The small coupling constant (1.6 Hz) obtained for Hc and Hd in compound **37**-*cis*, the major isomer, (fig. 5.25) verified the cis relationship. The increased yield of **37**-*cis* indicated that the hetero Diels-Alder cycloaddition had proceeded predominantly through an endo transition state as a result of secondary orbital interactions between the *o*-QDM **18b** and aldehyde **14b**.

Oxidation of **37** (PDC, $CH_2Cl_2$) furnished **38** in 82 % yield as a 3:1 mixture of the cis and trans isomers. The CIMS of **38** showed a prominent molecular ion at m/e 479 $[M+1]^+$ and the IR spectrum gave a strong absorption at 1724 $cm^{-1}$. The $^1$H-NMR spectrum of **38** (fig. 5.24) was highly informative and is summarized in figure 5.25. The quartet centered at δ 5.42 ppm, with its large geminal coupling constant (12.6 Hz), was assigned to the benzylic protons He and Hf of the cis isomer. The doublets at δ 6.09 and 6.41 ppm were ascribed to hydrogens Hc and Hd respectively; the small coupling constant ($J$ = 1.7 Hz) confirmed their cis relationship. Similar assignments were made for the trans isomer, specifically, the quartet at δ 5.55 ppm was ascribed to hydrogens He and Hf and the signals at δ 6.26 and 6.69 ppm were attributed to Hc and Hd respectively.

The isolation of **38** as a 3:1 ratio of cis and trans isomers suggested that **37** exists as a 3:1 ratio of the endo and exo isomers. It is also possible that some acid catalysed thermodynamic equilibration of the lactol may have occurred during the oxidation. Attempts to separate the endo and exo isomers of **37** were unsuccessful.

## 5.5 The effect of lithium chloride on the cycloaddition reactions

The beneficial effects of Lewis acid catalysts on the Diels-Alder cycloaddition with respect to reaction rates, regioselectivity and stereoselectivity (*endo*:*exo* ratios and asymmetrical bias with chiral dienophiles) has been well documented.[59a] For example, coordination of the nonbonding electrons of an α,β-unsaturated carbonyl or nitrile on the dienophile to a Lewis acid results in a substantial lowering of the frontier orbital energies, an increase in the difference in the magnitudes of the LUMO coefficients of the alkene moiety, and an increase in the magnitude of the LUMO coefficient of the carbonyl carbon (fig. 5.26, Houk and Strozier[59b]).

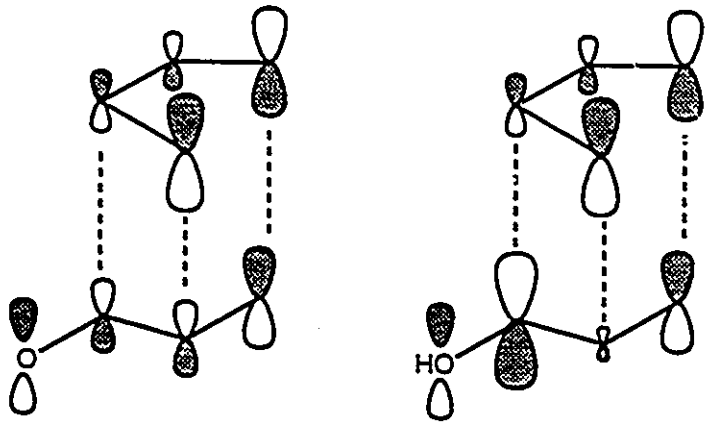


Figure 5.26: Diene HOMO-dienophile LUMO interactions in endo transition states with A-acrolein B-acrolein-$H^+$ as described by Houk and Strozier.

The narrowing of the energy gap between the HOMO of the diene and the LUMO of the dienophile, resulting from lowering of the frontier orbital energies of the latter, greatly facilitates cycloaddition and, typically, rate enhancements of $10^5$ have been observed.[60]

The increased difference in the magnitudes of the LUMO coefficients of the alkene (dienophile) enhances the regioselectivity during cycloaddition, for example, 2-phenyl-, chloro- and methyl-butadiene react with methyl acrylate to give para:meta ratios of 70-80:30-20 in the uncatalysed reactions and >97:<3 in $AlCl_3$-catalysed reactions.[59a]

The increased magnitude of the LUMO coefficient of the carbonyl carbon (dienophile) results in greater *endo* selectivity during cycloaddition, due to increased secondary orbital interactions with the diene HOMO. In addition, greater asymmetric induction is observed in cycloadditions with chiral dienophiles because of the tighter transition states induced by the increased secondary orbital interactions.[59b]

In view of the numerous examples of the beneficial effect of Lewis acid catalysis on Diels-Alder reactions which exist in the literature,[60] the question arose as to whether the reaction of diene **18b** with methyl acrylate could be similarly affected. To address the question, **14b** and three equivalents of methyl acrylate in benzene solution were irradiated in the presence of several Lewis acids (1.0 eq). The results are compiled in table 1.

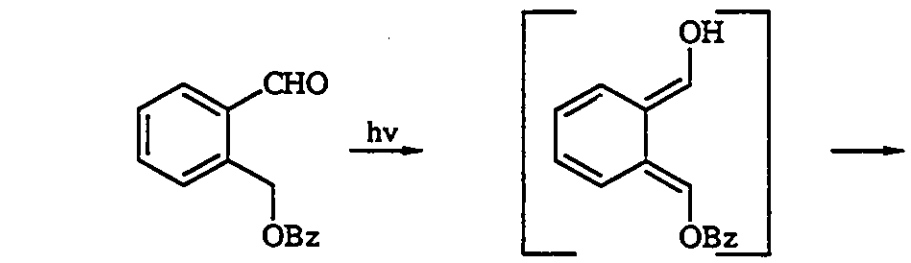


**14b** **18b**

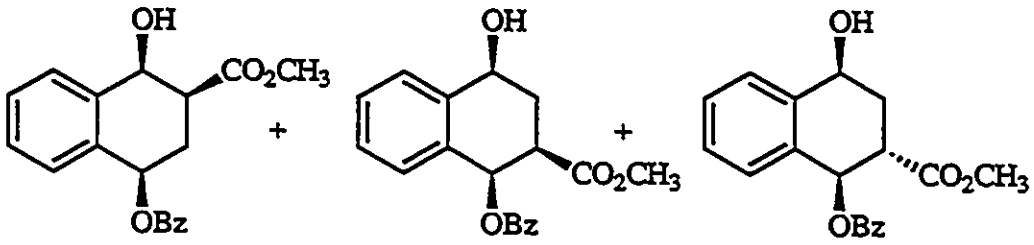


**23** **24** **25**

Table 1: Product distribution of 23-25

| Lewis acid | 23 | 24 | 25 |
|---|---|---|---|
| none | 50 | 8 | 7 |
| LiCl | 81 | 8 | 7 |
| MgC | 48 | 8 | 7 |
| $AlCl_3$ | 58 | 8 | 7 |
| $FeCl_3$ | - | - | - |

Figure 5.27: Products obtained on cycloaddition of **18b** with methyl acrylate in the presence of several Lewis acids

$AlCl_3$, a commonly used Lewis acid, had a minimal effect on the product distribution as was the case for $MgCl_2$. $FeCl_3$ completely inhibited the photoenolization as **14b** was recovered intact from the

reaction mixture. LiCl, a mild Lewis acid, had a pronounced effect on the cycloaddition specifically increasing the yield of the *o-endo* adduct **23** from 50 % in the uncatalysed reaction, to 81 %; no effect on the yield or the ratio of the *m*-cis **24** and *m*-trans **25** isomers was observed.

When the reaction was run in the absence of a catalyst, the products normally were accompanied by a significant amount of polar, polymeric material likely derived from methyl acrylate. The $^1$H-NMR spectrum of the crude product mixture of the LiCl catalysed reaction, however, showed no sign of the polymeric contaminant.

LiCl is essentially insoluble in benzene. To reconcile this fact with the catalytic effect observed, it was postulated that the LiCl was extracted into benzene solution by complexation to **14b** (fig. 5.28), in a manner not unlike that of a crown ether.

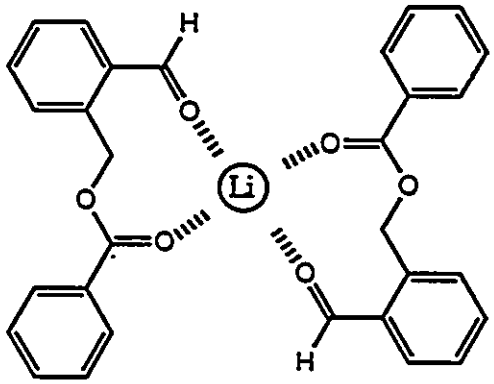


Figure 5.28: Extraction of LiCl in benzene by **14b**

In an attempt to verify the postulate, a series of cycloadditions were run in parallel, each pretreated in the following manner:

A) No LiCl added.

B) Excess LiCl added.

C) Benzene saturated with LiCl at RT and filtered prior to the addition of **14b** and methyl acrylate.

D) Benzene saturated with LiCl at 80 °C and filtered hot prior to the addition of **14b** and methyl acrylate.

E) Solution of **14b** in benzene saturated with LiCl at 80°C and filtered hot prior to the addition of methyl acrylate.

F) Solution of methyl acrylate in benzene saturated with LiCl at 80°C and filtered hot prior to the addition of **14b**.

G) Solution of **14b** and methyl acrylate in benzene saturated with LiCl at 80°C and filtered hot.

The mixtures (all 0.1 M **14b** in benzene) were irradiated side by side, then stopped prematurely (45 min.) and the product ratios assessed by $^1$H-NMR. The $^1$H-NMR spectra, illustrated in figure 5.29, clearly show the sharp contrast between amount of product formed in the uncatalysed reaction (A) and the amount of product formed in the LiCl catalysed reaction (B). The mole ratio obtained by comparing the integrations of the signals at δ 5.80 (benzylic hydrogens of **14b**) and 5.04 ppm (northern benzylic proton of **23**) was 85:15 (**14b**:**23**) for A compared to 56:44 (**14b**:**23**) for B.

Reactions C and D, which were filtered prior to irradiation, showed no significant increase in the proportion of **23**. This was expected because of the insolubility of LiCl in benzene.

Reaction E showed the most pronounced effect with a ratio of 50:50 **14b**:**23** verifying that LiCl had been extracted into benzene

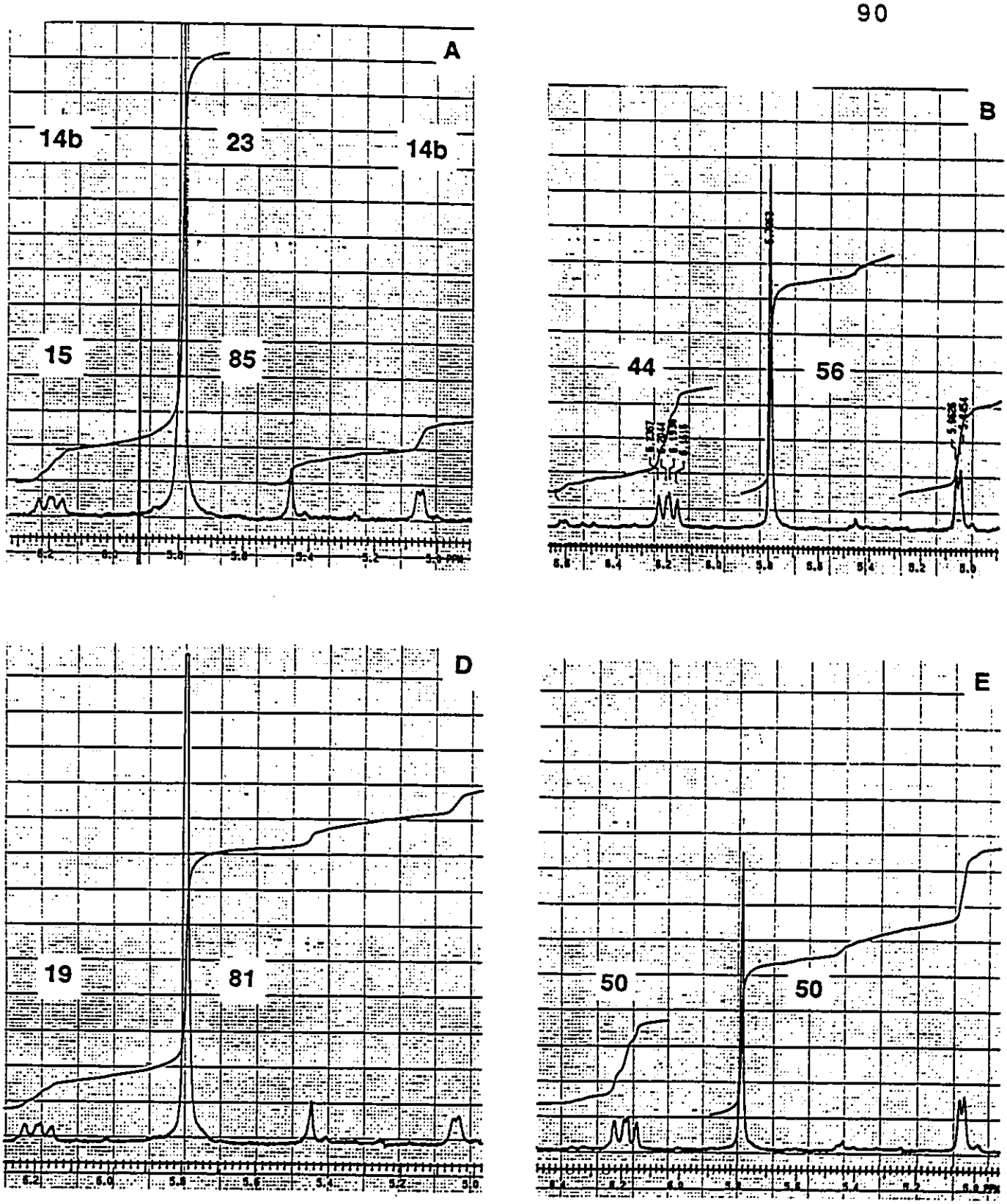


Figure 5.29: $^{1}$H-NMR of compounds **14b/23** with varying [LiCl].

solution by **14b**. Reaction F also showed some improvement (66:34), but not to the extent observed for E.

Having established the catalytic effect of LiCl on the cycloaddition of **18b** with methyl acrylate, attention was next directed at assessing its effect with other dienophiles. The cycloadditions, described previously, which involved diethyl fumarate, methyl crotonate, dimethylacetylene dicarboxylate and methyl propiolate were repeated in the presence of excess LiCl.

The results, as indicated in figure 5.30, were dissapointing with only a marginal improvement in yield observed for diethyl fumarate, and no improvement observed for methyl crotonate and methyl propiolate. One exception was dimethylacetylene dicarboxylate which furnished adduct **31** in 85 % yield when the reaction was carried out in the presence of LiCl as compared to 56 % uncatalysed.

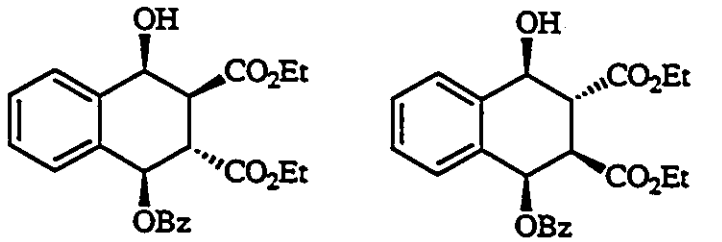


21




22

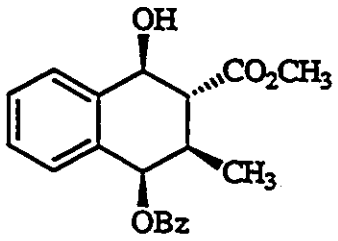


29

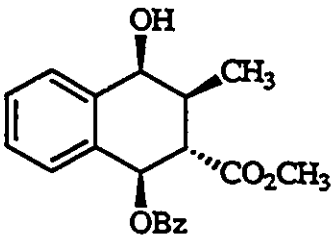


30

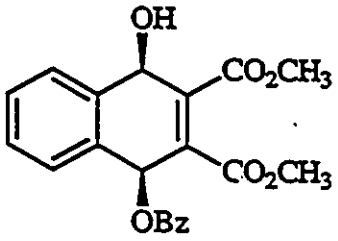


31

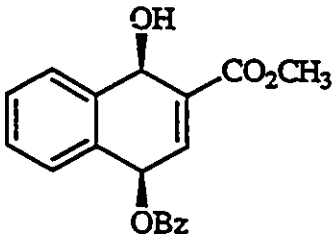


32

Table 2

| Status | 21 | 22 | 29 | 30 | 31 | 32 |
|---|---|---|---|---|---|---|
| Uncatalysed | 54 | 19 | 22 | 11 | 56 | 20 |
| Catalysed | 72 | 18 | 21 | 16 | 85 | 20 |

Figure 5.30: Effect of LiCl on the cycloaddition of **18b** with diethyl fumarate, methyl crotonate, dimethylacetylene dicarboxylate and methyl propiolate

## 5.6 Attempted intramolecular cycloadditions

Having garnered sufficient insight into the reactivity of α,α'-dioxygenated-*o*-quinodimethanes in the intermolecular Diels-Alder reaction, attention was next directed at the intramolecular cycloadditions. In chapter 3 a model system (**14e**) was proposed which was designed to investigate the feasibility of intramolecular cycloaddition. Scheme 5.17 depicts the strategy employed to synthesize the styrene as well as the additional aliphatic system **14d**.

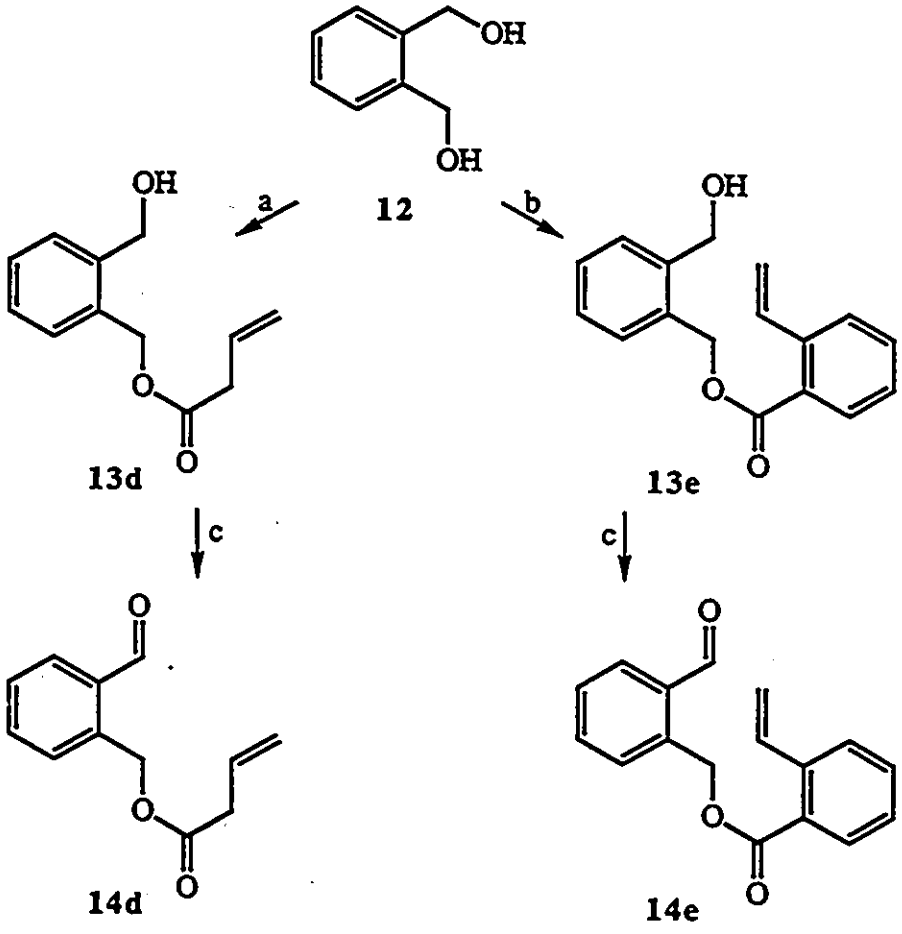


Scheme 5.17: a) NaH/THF 0°C, vinylacetyl chloride b) NaH/THF 0°C, 2-vinylbenzoyl chloride c) PDC/$CH_2Cl_2$

The methodology employed for the preparation of compounds **14d** and **14e** was essentially identical to that used for **14a-c**, for example **13d**, a colorless oil, [IR $\nu_{max}(cm^{-1})$ 3530, 1723] was obtained in 48 % yield after flash chromatography, and was subsequently oxidized to **14d**, a yellow oil, [IR $\nu_{max}(cm^{-1})$ 1698, 1733] in 84 % yield.

The $^1$H-NMR spectrum of **14d** (fig. 5.31) reinforced its structural assignment with key signals including two singlets at δ 5.56 ppm (benzylic methylene) and δ 10.16 ppm (aldehyde H), as well as three multiplets at δ 3.17 ppm (α-methylene protons), 5.18 ppm (vinyl $CH_2$) and 5.94 ppm (vinyl CH).

Disappointingly, aldehyde **14d**, when irradiated in 0.1 M benzene solution, failed to furnish the desired cycloadduct **38** (scheme 5.18) but instead yielded an intractable mixture of polymeric products, as judged by examination of the $^1$H-NMR spectrum.

The failure of intermediate **18d** to undergo cycloaddition was likely due to a combination of two factors: first, the low reactivity of the unactivated alkene dienophile which should have slowed the addition, and second, the preferred s-cis conformation[61] of the ester which should have isolated the alkene moiety from the *o*-quinodimethane. This failure did not auger well for the cycloaddition of aldehyde **14e** which was expected to suffer these same limitations.

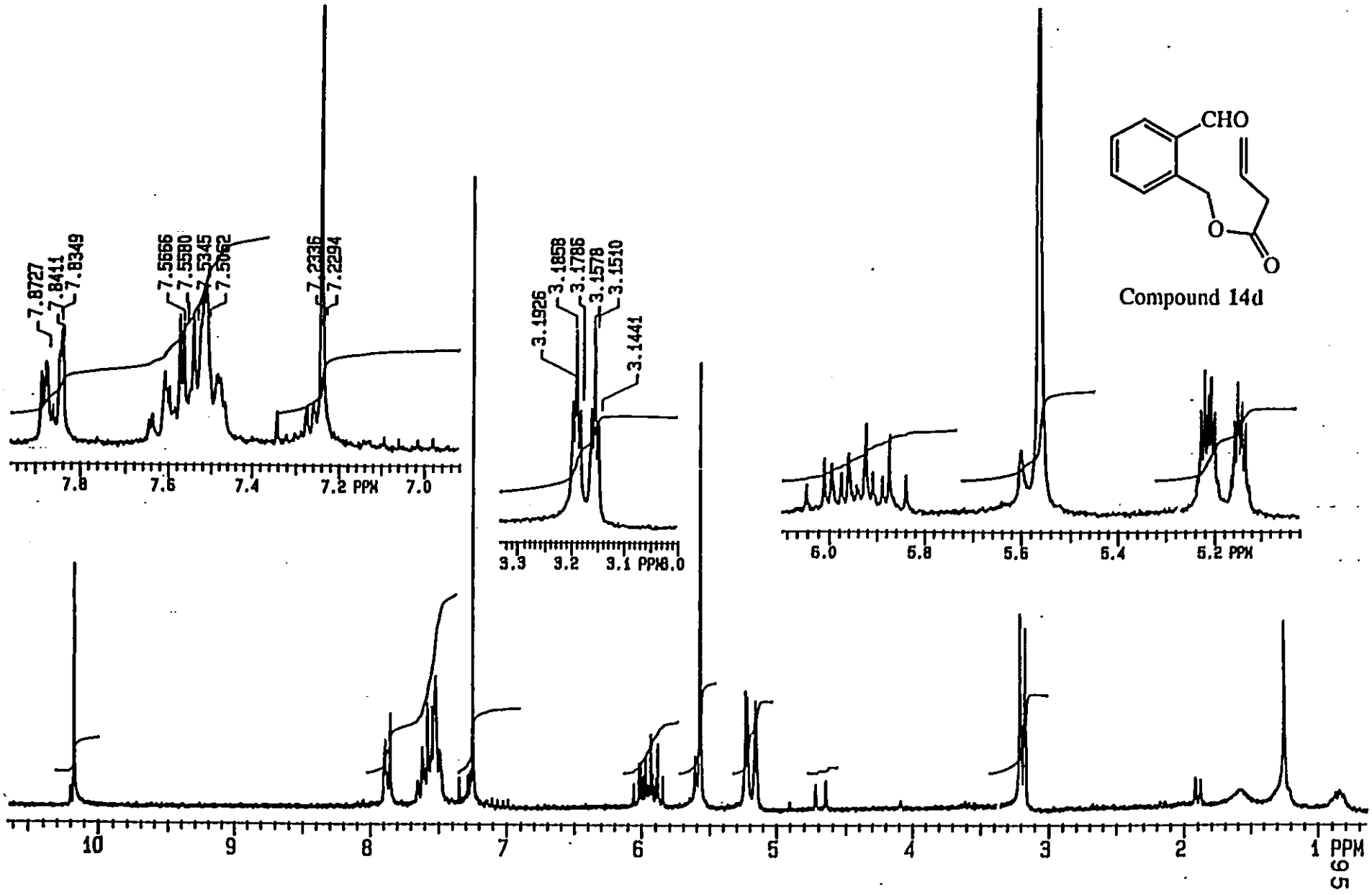


Figure 5.31: $^{1}$H-NMR of compound **14d**.

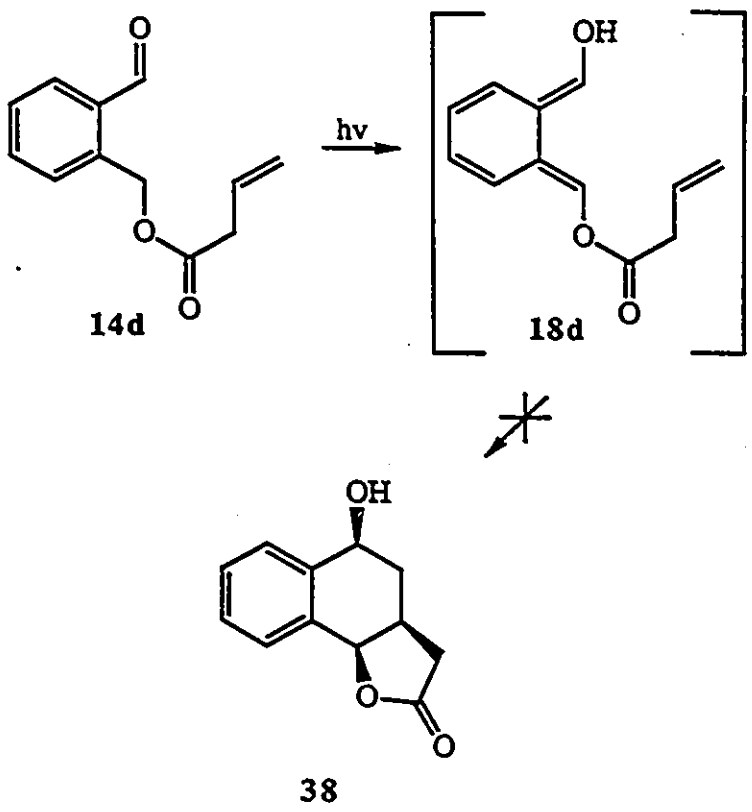


Scheme 5.18: Attempted photochemical cycloaddition of **14d**

In the event, irradiation of a 0.1 M benzene solution of aldehyde **14e** failed to produce the anticipated cycloadduct **39** (scheme 5.19), but instead, furnished a complex mixture; tlc analysis of the product mixture showed a long polar smear devoid of resolved spots while the $^1$H-NMR spectrum exhibited broad unresolved signals characteristic of a polymeric mixture. The failure of the E,E-enols **18d** and **18e** to undergo cycloaddition stands in sharp contrast to the results obtained by Krause et al. Given the buttressing effect of the methoxy groups of Krause's intermediate (**2**), it's possible that cycloaddition occurred via the E,Z-enol. The absence of a similar E,Z-directing group on **14d** or **14e** should have resulted in the preferential formation of the E,E-

enols, which in combination with the s-trans conformation of the ester, should have slowed cycloaddition, and increased side reactions.

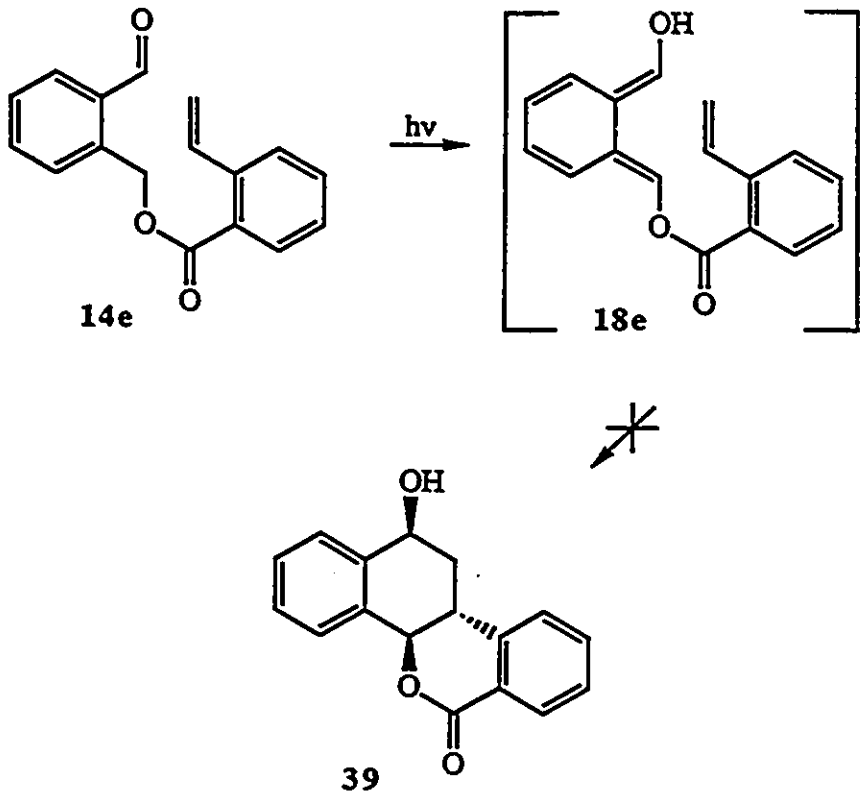


Scheme 5.19: Attempted photochemical cycloaddition of **14e**

## 5.7 Conclusions

The disheartening results obtained for aldehydes **14d** and **14e** suggested that intramolecular cycloaddition may not be feasible employing an ester tether. An investigation of substrates incorporating an ether tether was postponed to a later date. The encouraging results obtained with the intermolecular cycloadditions suggested that an alternative intermolecular strategy may also be feasible.

## 5.8 Experimental section

**General:** Melting points were determined by use of a Gailenkamp digital melting point apparatus and are uncorrected. Mass spectra were obtained using an AEIMS 9025 or a Kratos concept 2H instrument. IR spectra were recorded in chloroform solution employing a Bomem-Michelson MB-100 FT/IR spectrophotometer with the abbreviations: broad (br), strong (s), medium (m) and weak (w). $^{1}H$ and $^{13}C$ NMR spectra were obtained either on a Varian XL-300 or a Gemini-200 spectrometer with the chemical shifts reported in ppm relative to TMS. The multiplicities of the NMR signals were reported employing the following abbreviations, singly or in combination: singlet (s), doublet (d), triplet (t), quartet (q), multiplet (m).

Solvents for the extractions and chromatographic purifications were routinely distilled prior to use. THF was dried by distillation from a benzophenone ketyl. Reagent grade benzene and acetonitrile were used as received. Thin layer chromatography (tlc) was carried out using Kieselgel 60 $F_{254}$ precoated 0.25 mm plates. Visualization was facilitated by UV irradiation as well as $I_2$, alkaline $KMnO_4$, and dinitrophenylhydrazine (DNP) stains.

Irradiations were carried out through a 1mm pyrex filter employing a water-jacketed 450 W Hanovia medium pressure mercury lamp, immersed in a water bath. The samples were contained in 30 mL quartz test tubes and suspended 10 cm from the light source. The procedures carried out for the cycloadditions in the presence of Lewis acids were identical save for the addition of 0.01 to 1.0 eq of the Lewis acid.

### 5.7.1 Preparation of 10

A solution of 10.0 g (42.7 mmol) *o*-iodobenzyl alcohol in 20 ml dry THF, contained in a dropping funnel, was added to an ice cooled, stirred suspension of 2.5 g (64.1 mmol) NaH (60 % dispersion in mineral oil) in 50 mL THF over the course of 5 min. After gas evolution had ceased, a solution of 4.0 mL (9.1 g, 64.1 mmol) of methyl iodide in 10 mL THF was introduced over 5 min. After addition was complete, the mixture was removed from the ice bath and stirred for 2 h after which time tlc analysis (3:1 hexane:ethyl acetate) indicated no starting material remained. The mixture was poured into 100 mL of saturated $NH_4Cl$ solution and the layers separated. The aqueous phase was extracted with two 40 mL aliquots of ethyl acetate, the organic phases combined and partitioned over 40 mL brine. Drying over $MgSO_4$ and concentration on a rotovap produced 10.2 g (96 %) of a yellow oil.

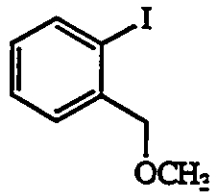


$C_8H_9IO$ 248.06

**10**

**MS** (EI) : 248 $[M]^+$, 217, 121, 55.

**IR** ($CH_2Cl_2$) $\nu_{max}(cm^{-1})$ 1121 .

**$^1$H-NMR** ($CDCl_3$) δ(ppm) 3.44 (s, 3H); 4.42 (s, 2H);
6.95 (t, 1H, *J* = 7.5 Hz); 7.33 (t, 1H, *J* = 7.0 Hz);
7.40 (d, 1H, *J* = 7.5 Hz); 7.80 (d, 1H, *J* = 7.0 Hz)

### 5.7.2 Preparation of 11

1.0 g (40.8 mmol) of magnesium metal was added to a stirred solution of 9.2 g (37.1 mmol) 2-(methoxymethyl)iodobenzene and 100 mg of iodine in 80 mL dry THF under nitrogen atmosphere. The mixture was heated to rf for 2 h then cooled to 0°C in an ice bath. A solution of 3.2 mL (3.0 g, 40.8 mmol) DMF in 10 mL of THF, contained in a dropping funnel, was subsequently introduced over 10 min and the mixture allowed to warm to rt. After stirring for 16 h, tlc analysis (hexane: ethyl acetate 7:1) indicated complete conversion of the starting materials. The reaction mixture was quenched with 50 mL of saturated $NH_4Cl$ solution, the layers separated and the aqueous phases extracted with two 30 mL portions of ethyl acetate. The combined organic phases were then dried over $MgSO_4$ and concentrated on a rotovap producing 5.0 g of of a brown oil. Vacuum distillation (BP 121-124 °C 0.9 mm) furnished 2.7 g (50 %) of a yellow oil.

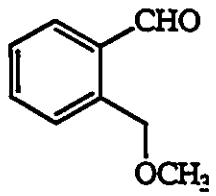


$C_9H_{10}O_2$ 150.20

**11**

**MS** (EI) : 150 $[M]^+$, 132, 118, 101, 57.

**IR** ($CH_2Cl_2$) $\nu_{max}(cm^{-1})$ 1721, 1125.

**$^1$H-NMR** ($CDCl_3$) δ(ppm) 3.46 (s, 3H); 4.85 (s, 2H); 7.45 (t, 1H, $J$ = 7.5 Hz); 7.56 (m, 2H); 7.83 (d, 1H, $J$ = 7.5 Hz); 10.19 (s, 1H).

### 5.7.3 Preparation of 13a

A solution of 8.0 g (58.0 mmol) of *o*-xylenol in 20 mL dry THF was added dropwise over 10 min to an ice cooled, stirred suspension of 2.6 g (63.8 mmol) of NaH (60 % dispersion in mineral oil) in 60 mL THF under nitrogen atmosphere. The mixture was removed from the ice bath and stirred for 2 h, until gas evolution had ceased. The mixture was again cooled to 0°C, and a solution of 5.9 g (58.0 mmol) of acetic anhydride in 20 mL THF was added, via dropping funnel, over 10 min. The flask was removed from the ice bath and stirred for 2 h, at which time tlc analysis (hexane:ethyl acetate 1:1) indicated complete reagent conversion, then poured into 100 mL of saturated $NH_4Cl$ solution. After separation, the aqueous phase was extracted with two 50 mL portions of ether and the combined organic phases partitioned over brine. The product solution was further dried over $MgSO_4$ then concentrated on a rotovap yielding 10.3 g of a brown oil. Flash chromatography employing hexane:ethyl acetate 2:1 as eluent furnished 6.3 g (60 %) of a colorless oil.

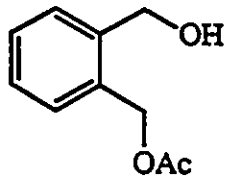


$C_{10}H_{12}O_3$ 180.20

**13a**

**MS** (CI/ISO) : 181 $[M+1]^+$, 163, 121.

**IR** ($CH_2Cl_2$) $\nu_{max}(cm^{-1})$ 3601 (br), 1736 (s), 1023 (m).

**$^1$H-NMR** ($CDCl_3$) δ(ppm) 2.04 (s, 3H); 2.87 (s, 1H); 4.67 (s, 2H); 5.16 (s, 2H); 7.22-7.42 (m, 4H).

### 5.7.4 Preparation of 13b

A solution of 5.0 g (36.2 mmol) of *o*-xylenol in 40 mL dry THF was added, dropwise, to an ice cooled, stirred suspension of 1.6 g (39.9 mmol) of NaH (60 % dispersion in mineral oil) in 40 mL THF over 5 min under nitrogen atmosphere. After complete addition, the flask was removed from the ice bath and stirred at rt for 2 h until gas evolution ceased. The mixture was again cooled to 0°C and a solution of 5.6 g (39.9 mmol) of benzoyl chloride in 20 mL THF was introduced over 10 min. After complete addition, the flask was warmed to rt and stirred for an additional hour.

The workup procedure was essentially identical to that described for **13a** giving 10 g of a yellow oil which was resolved by flash chromatography employing hexane: ethyl acetate 2:1 as eluent furnishing 6.3 g (72 %) of a colorless oil.

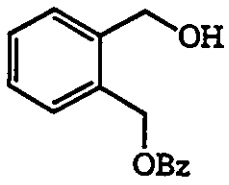


$C_{15}H_{14}O_3$ 242.27

**13b**

**MS** (CI/ISO) : 243 $[M+1]^+$, 225, 163.

**IR** ($CH_2Cl_2$) $\nu_{max}(cm^{-1})$ 3602 (br), 1717 (s), 1108 (m).

**$^1$H-NMR** ($CDCl_3$) δ(ppm) 2.41 (s, 1H); 4.81 (s, 2H); 5.46 (s, 2H); 7.30-7.60 (m, 7H); 8.03 (d, 2H, $J$ = 8.3 Hz).

### 5.7.5 Preparation of 13c

A solution of 2.5 g (18.1 mmol) of *o*-xylenol in 20 mL dry THF was added, dropwise, to an ice cooled, stirred suspension of 800 mg (19.9 mmol) of NaH (60 % dispersion in mineral oil) in 40 mL THF over 5 min under nitrogen atmosphere. After complete addition, the flask was removed from the ice bath and stirred at rt for 2 h until gas evolution ceased. The mixture was again cooled to 0°C and a solution of 2.4 g (19.9 mmol) of pivaloyl chloride in 20 mL THF was introduced over 10 min. After complete addition, the flask was warmed to rt and stirred for an additional hour.

The workup procedure was the same as that described for **13a** giving 3.2 g of a brown oil which was resolved by flash chromatography through a short column of silica gel employing methylene chloride as eluent yielding 2.6 g (65 %) of a colorless oil.

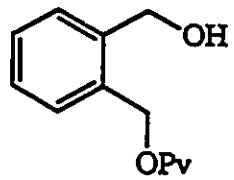


$C_{13}H_{18}O_3$ 222.28

**13c**

**MS** (CI/ISO) : 223 $[M+1]^+$, 205, 121.

**IR** ($CH_2Cl_2$) $\nu_{max}(cm^{-1})$ 3602 (br), 1723 (s), 1152 (m).

**$^1$H-NMR** ($CDCl_3$) δ(ppm) 1.18 (s, 9H); 3.28 (s, 1H); 4.69 (s, 2H); 5.16 (s, 2H); 7.23-7.42 (m, 4H).

### 5.7.6 Preparation of 14a

3.1 g (8.3 mmol) of pyridinium dichromate was added in portions over 5 min to an ice cooled, stirred solution of 1.0 g (5.6 mmol) 2-(acetoxymethyl)benzyl alcohol in 45 mL of dry dichloromethane under nitrogen atmosphere. After complete addition, the mixture was removed from the ice bath and stirred for 12 h at which time tlc analysis (hexane:ethyl acetate 1:1) indicated complete conversion of the starting material. The product mixture was subsequently concentrated on a rotovap at 40 °C, triturated with ether, and filtered, with suction, through 20 g of 70/230 mesh silica gel contained in a scintered glass funnel. Concentration of the solvent yielded 920 mg of a yellow oil which, after further purification via the bisulfite adduct, afforded 790 mg (80 %) of a colorless oil, homogeneous by tlc.

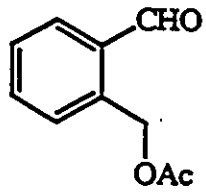


$C_{10}H_{10}O_3$ 178.19

**14a**

**MS** (EI) : 178 $[M]^+$, 136, 119.

**IR** ($CH_2Cl_2$) $\nu_{max}(cm^{-1})$ 1740 (s), 1698 (s), 1037 (m).

**$^1$H-NMR** ($CDCl_3$) δ(ppm) 2.09 (s, 3H); 5.50 (s, 2H);
7.42-7.62 (m, 3H); 7.83 (d, 1H, $J$ = 7.5 Hz);
10.13 (s, 1H).

### 5.7.7 Preparation of 14b

7.0 g (18.6 mmol) of pyridinium dichromate was added in portions over 5 min to an ice cooled, stirred solution of 3.0 g (12.4 mmol) 2-(benzoyloxymethyl)benzyl alcohol in 100 mL of dry dichloromethane under nitrogen atmosphere.

The remainder of the procedure was identical to that described for **14a**, yielding 2.8 g of a yellow oil which, after further purification via the bisulfite adduct, afforded 2.4 g (80 %) of a white solid which crystallized from dichloromethane/hexane.

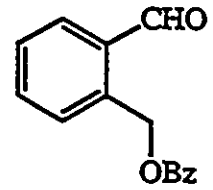


$C_{15}H_{12}O_3$ 240.07

**14b**

| | |
|---|---|
| **MP** | 111-113 °C. |
| **MS** | (EI) : 240 $[M]^+$, 135, 105. |
| **HRMS** | calcd for $C_{15}H_{12}O_3$ 240.0787 found 240.0765. |
| **IR** | ($CH_2Cl_2$) $\nu_{max}(cm^{-1})$ 1721 (s), 1696 (s), 1110 (s). |
| **$^1$H-NMR** | ($CDCl_3$) δ(ppm) 5.80 (s, 2H); 7.39-7.62 (m, 6H); 7.88 (d, 1H, $J$ = 7.0 Hz); 8.07 (d, 2H, $J$ = 8.3 Hz); 10.23 (s, 1H). |

### 5.7.8 Preparation of 14c

3.8 g (10.1 mmol) of pyridinium dichromate was added in portions over 5 min to an ice cooled, stirred solution of 1.5 g (6.6 mmol) 2-(pivaloyloxymethyl)benzyl alcohol in 75 mL of dry dichloromethane under nitrogen atmosphere.

The remainder of the procedure was identical to that described for **14a** yielding 1.8 g of a yellow oil which, after further purification via the bisulfite adduct, afforded 1.1 g (75 %) of a colorless oil.

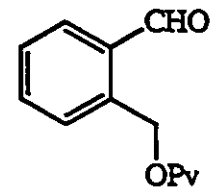


$C_{13}H_{16}O_3$ 220.27

**14c**

**MS** (CI/ISO) : 221 $[M+1]^+$, 135, 119.

**IR** ($CH_2Cl_2$) $\nu_{max}(cm^{-1})$ 1727 (s), 1697 (s), 1149 (m).

**$^1$H-NMR** ($CDCl_3$) δ(ppm) 1.20 (s, 9H); 5.50 (s, 2H);
7.41-7.62 (m, 3H); 7.83 (d, 1H, $J$ = 7.4 Hz);
10.15 (s, 1H).

**5.7.9 Preparation of 16 and 17**

A solution of 235 mg (1.6 mmol) of 2-(methoxymethyl)benzaldehyde and 680 mg (3.0 eq, 4.8 mmol) of dimethyl fumarate in 10 mL of benzene, contained in a quartz test tube, was suspended 10 cm from a medium pressure Hanovia mercury arc lamp and irradiated for 5 h after which time tlc analysis (hexane:ethyl acetate 3:1) indicated complete conversion of the starting materials. Concentration on a rotovap followed by flash chromatography (8 g 230/400 mesh silica gel) employing 3:1 followed by 1:1 hexane:ethyl acetate furnished 62 mg (14 %) of **16** and 31 mg (7 %) of **17**.

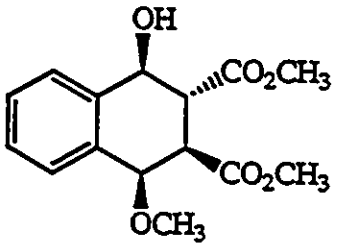


$C_{15}H_{18}O_6$ 294.30

**16**

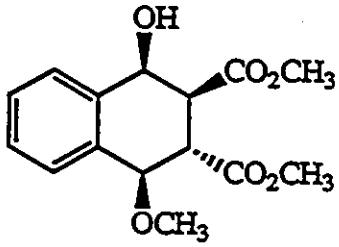


$C_{15}H_{18}O_6$ 294.30

**17**

**MS** (Cl/$Et_2O$) : 295 $[M+1]^+$, 277, 263, 245, 231, 213.

**IR** ($CH_2Cl_2$) $\nu_{max}(cm^{-1})$ 3562 (br), 1725 (s), 1586 (s).

**$^1$H-NMR** ($CDCl_3$) δ(ppm) 16 3.20 (dd, 1H, *J* = 3.0, 10.0 Hz);
3.23 (s, 3H); 3.50 (d, 1H, *J* = 9.5 Hz);
3.65 (dd, 1H, *J* = 6.4, 10.0 Hz); 3.72 (s, 3H);
3.76 (s, 3H); 4.62 (d, 1H, *J* = 3.0 Hz);
4.85 (dd, 1H, *J* = 6.4, 9.5 Hz); 7.20-7.55 (m, 4H).
17 3.20 (dd, 1H, *J* = 4.5, 9.0 Hz); 3.30 (s, 3H);
3.70 (s, 3H); 3.78 (s, 3H); 3.90 (dd, 1H, *J* = 4.0, 9.0 Hz);
4.74 (d, 1H, *J* = 4.5 Hz); 5.05 (dd, 1H, *J* = 4.0, 9.2 Hz);

7.20-7.55 (m, 4H).

**5.7.10 Preparation of 19 and 20**

A solution of 250 mg (1.4 mmol) of 2-(acetoxymethyl)benzaldehyde and 725 mg (3.0 eq, 4.2 mmol) of diethyl fumarate in 10 mL benzene, contained in a quartz test tube, was suspended 10 cm from a medium pressure mercury arc lamp and irradiated until tlc analysis (chloroform:ether 10:1) indicated complete conversion of the aldehyde (7 h). After concentration on a rotovap, the excess diethyl fumarate was removed under high vacuum and the residue resolved by flash chromatography employing chloroform:ether 10:1 as eluent furnishing 382 mg (78 %) of **19** and **20** as a 2:1 mixture of diastereomers.

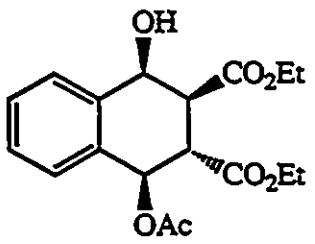


$C_{18}H_{22}O_7$ 350.37

**19**

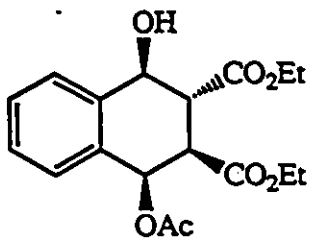


$C_{18}H_{22}O_7$ 350.37

**20**

**MS** (Cl/$Et_2O$) : 244 [M-106]+, 171, 98.

**IR** ($CH_2Cl_2$) $\nu_{max}(cm^{-1})$ 3520 (br), 1732 (s).

**$^1$H-NMR** ($CDCl_3$) δ(ppm) **19** 1.23 (m, 6H); 2.09 (s, 3H); 3.20 (dd, 1H, *J* = 3.1, 13.8 Hz); 3.45 (dd, 1H, *J* = 9.2, 13.8 Hz); 4.15 (m, 4H); 5.06 (d, 1H, *J* = 3.1 Hz); 6.16 (d, 1H, *J* = 9.2 Hz); 7.10-7.65 (m, 4H). **20** 1.23 (m, 6H); 2.09 (s, 3H); 4.15 (m, 4H); 4.78 (d, 1H, *J* = 9.0 Hz); 6.40 (d, 1H, *J* = 3.2 Hz); 7.10-7.65 (m, 4H).

### 5.7.11 Preparation of 21 and 22

A solution of 500 mg (2.1 mmol) of 2-(benzoyloxymethyl)benzaldehyde and 1.1 g (3.0 eq, 6.4 mmol) of diethyl fumarate in 30 mL benzene, contained in a quartz test tube, was suspended 10 cm from a medium pressure mercury arc lamp and irradiated until tlc analysis (chloroform:ether 10:1) indicated complete conversion of the aldehyde (5 h). After concentration on a rotovap, the excess diethyl fumarate was removed under high vacuum and the residue resolved by flash chromatography, employing chloroform:ether 10:1 as eluent, furnishing 625 mg (73 %) of **21** and **22** as a 3:1 mixture of diastereomers.

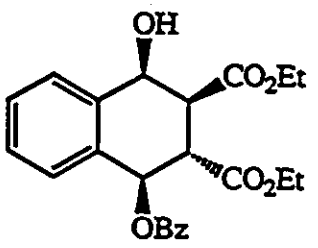


$C_{23}H_{24}O_7$ 412.44

**21**

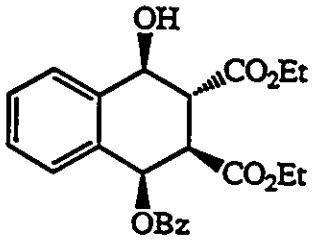


$C_{23}H_{24}O_7$ 412.44

**22**

**MS** (Cl/$Et_2O$): 413 $[M+1]^+$, 395, 291, 273, 245, 201.

**IR** ($CH_2Cl_2$) $\nu_{max}(cm^{-1})$ 3579 (br), 1732 (s), 1186 (m).

**$^1$H-NMR** ($CDCl_3$) δ(ppm) **21** 1.04 (t, 3H, *J* = 7.1 Hz); 1.23 (t, 3H, *J* = 7.2 Hz); 3.35 (dd, 1H, *J* = 3.3, 11.6 Hz); 3.68 (dd, 1H, *J* = 9.1, 11.7 Hz); 4.07 (q, 2H, *J* = 7.1 Hz); 4.15 (q, 2H, *J* = 7.2 Hz); 5.15 (d, 1H, *J* = 3.5 Hz); 6.44 (d, 1H, *J* = 9.2 Hz); 7.20-7.70 (m, 7H); 8.09 (d, 2H, *J* = 8.5 Hz). **22** 1.07 (t, 3H, *J* = 7.2 Hz); 1.32 (t, 3H, *J* = 7.2 Hz); 4.89 (d, 1H, *J* = 9.1 Hz);

6.69 (d, 1H, $J$ = 3.1 Hz); 7.20-7.70 (m, 7H);
7.93 (d, 1H, $J$ = 8.5 Hz).

### 5.7.12 Preparation of 23, 24 and 25

A solution of 500 mg (2.1 mmol) of 2-(benzoyloxymethyl)benzaldehyde and 538 mg (3.0 eq, 6.4 mmol) of freshly distilled methyl acrylate in 30 mL benzene, contained in a quartz test tube, was suspended 10 cm from a medium pressure mercury arc lamp and irradiated until tlc analysis (chloroform:ether 10:1) indicated complete conversion of the aldehyde (5 h). After concentration on a rotovap, the residue was resolved by flash chromatography employing chloroform:ether 10:1 as eluent furnishing 336 mg (50 %) of **23** and 99 mg (15 %) of an equimolar mixture of **24** and **25**.

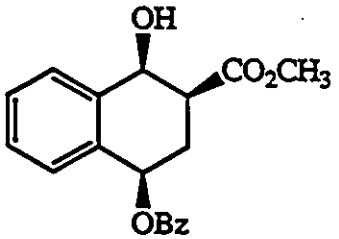


$C_{19}H_{18}O_5$ 326.35

**23**

**MS** (Cl/$Et_2O$) : 327 $[M+1]^+$, 308, 261, 205, 187, 149.

**IR** ($CH_2Cl_2$) $\nu_{max}(cm^{-1})$ 3564 (br), 1720 (s), 1110 (m).

**$^1$H-NMR** ($CDCl_3$) δ(ppm) 2.53 (m, 2H); 3.00 (dt, 1H, $J$ = 3.6, 10.8 Hz);
3.20 (d, 1H, $J$ = 5.9 Hz); 3.67 (s, 3H);
5.04 (dd, 1H, $J$ = 3.6, 5.9 Hz); 6.20 (dd, 1H, $J$ = 6.5, 8.8 Hz);
7.20-7.60 (m, 7H); 8.03 (d, 2H, $J$ = 7.0 Hz).

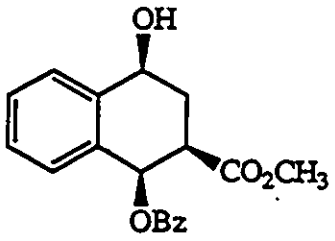


$C_{19}H_{18}O_5$ 326.35

**24**

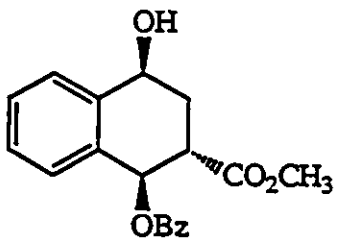


$C_{19}H_{18}O_5$ 326.35

**25**

**MS** (Cl/$Et_2O$) : 327 $[M+1]^+$, 308, 261.

**IR** ($CH_2Cl_2$) $\nu_{max}(cm^{-1})$ 3688 (br), 1732 (s), 1106 (m).

**$^1$H-NMR** ($CDCl_3$) δ(ppm) 2.33 (m, 3H);

**24:** 2.62 (dq, 1H, *J* = 3.1, 5.9, 13.6 Hz);

3.08 (dt, 1H, *J* = 3.4, 12.2 Hz); 3.59 (s, 3H);

4.83 (dd, 1H, *J* = 6.2, 9.9 Hz); 6.61 (d, 1H, *J* = 3.7 Hz);

7.20-7.70 (m, 7H); 8.06 (t, 2H, *J* = 6.8 Hz).

**25:** 3.49 (td, 1H, *J* = 4.9, 9.0, Hz); 3.63 (s, 3H);

4.90 (t, 1H, *J* = 4.3 Hz);

6.52 (d, 1H, *J* = 8.4 Hz); 7.20-7.70 (m, 7H);

7.95 (d, 2H, *J* = 10.4 Hz).

### 5.7.13 Preparation of 26, 27 and 28

A solution of 200 mg (0.9 mmol) of 2-(pivaloyloxymethyl)benzaldehyde and 235 mg (3.0 eq, 2.7 mmol) of freshly distilled methyl acrylate in 30 mL benzene, contained in a quartz test tube, was suspended 10 cm from a medium pressure mercury arc lamp and irradiated until tlc analysis (chloroform:ether 10:1) indicated complete conversion of the aldehyde (4 h). After concentration on a rotovap, the residue was resolved by flash chromatography employing chloroform:ether 10:1 as eluent furnishing 131 mg (47 %) of **26** and 22 mg (8 %) of an equimolar mixture of **27** and **28**.

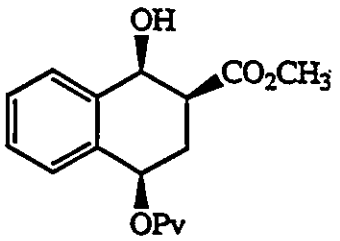


$C_{17}H_{22}O_5$ 306.36

**26**

**$^1$H-NMR** ($CDCl_3$) δ(ppm) 1.24 (s, 9H);
2.27 (dd, 1H, *J* = 10.0, 12.8 Hz);
2.45 (dq, 1H, *J* = 3.1, 6.3, 12.8 Hz);
2.87 (dt, 1H, *J* = 3.1, 12.6 Hz); 3.06 (d, 1H, *J* = 5.3 Hz);
3.74 (s, 3H); 5.02 (dd, 1H, *J* = 4.4, 5.3 Hz);
5.91 (dd, 1H, *J* = 6.5, 10.1 Hz); 7.15-7.40 (m, 4H).

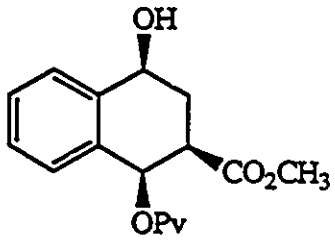


$C_{17}H_{22}O_5$ 306.36

**27**

**$^1$H-NMR** ($CDCl_3$) δ(ppm) 1.10 (s, 9H); 2.23 (m, 1H);
2.52 (dq, 1H, *J* = 2.9, 6.0, 14.1 Hz);
2.96 (dt, 1H, *J* = 3.3, 12.2 Hz); 3.66 (s, 3H);
4.83 (t, 1H, *J* = 5.0 Hz); 6.33 (d, 1H, *J* = 4.0 Hz);
7.10-7.40 (m, 3H); 7.60 (d, 1H, *J* = 7.5 Hz);

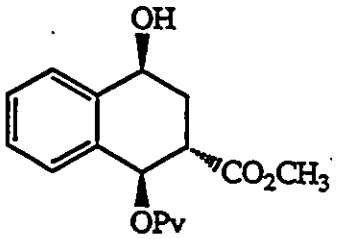


$C_{17}H_{22}O_5$ 306.36

**28**

**$^1$H-NMR** ($CDCl_3$) δ(ppm) 1.21 (s, 9H); 2.13 (m, 1H);
2.36 (m, 1H); 3.31 (td, 1H, *J* = 4.9, 9.7 Hz);
3.65 (s, 3H); 4.75 (m, 1H); 6.20 (d, 1H, *J* = 9.5 Hz);
7.10-7.42 (m, 4H).

**5.7.14 Preparation of 29 and 30**

A solution of 300 mg (1.3 mmol) of 2-(benzoyloxymethyl)benzaldehyde and 376 mg (3.0 eq, 3.8 mmol) of freshly distilled methyl crotonate in 30 mL benzene, contained in a quartz test tube, was suspended 10 cm from a medium pressure mercury arc lamp and irradiated until tlc analysis (chloroform:ether 20:1) indicated complete conversion of the aldehyde (5 h). After concentration on a rotovap, the residue was resolved by flash chromatography employing chloroform:ether 20:1 as eluent furnishing 93 mg (22 %) of **29** and 46 mg (11 %) of **30**.

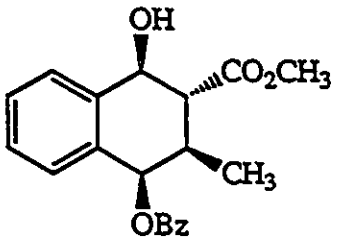


$C_{20}H_{20}O_5$ 340.38

**29**

**MS** (CI/$Et_2O$) : 341 $[M+1]^+$, 323, 275, 219, 201, 169.

**IR** ($CH_2Cl_2$) $\nu_{max}(cm^{-1})$ 3599 (br), 1725 (s), 1729 (s), 1107 (m).

**$^1$H-NMR** ($CDCl_3$) δ(ppm) 1.04 (d, 3H, *J* = 6.8 Hz); 2.38 (dq, 1H, *J* = 3.4, 11.7 Hz); 2.77 (d, 1H, *J* = 8.3 Hz); 3.06 (dd, 1H, *J* = 10.4, 11.9 Hz); 3.77 (s, 3H); 5.06 (t, 1H, *J* = 8.7 Hz); 6.26 (d, 1H, *J* = 3.2 Hz); 6.26 (d, 1H, *J* = 3.2 Hz); 7.20-7.50 (m, 6H); 7.63 (d, 1H, *J* = 7.5 Hz); 7.95 (d, 1H, *J* = 7.0 Hz).

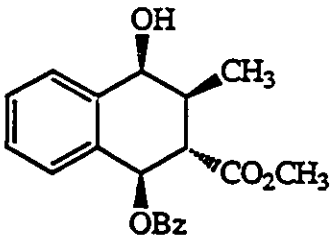


$C_{20}H_{20}O_5$ 340.38

**30**

**MS** (Cl/$Et_2O$) : 341 $[M+1]^+$, 323, 275, 219, 201, 169.

**IR** ($CH_2Cl_2$) $\nu_{max}(cm^{-1})$ 3592 (br), 1723 (s),
1727 (s), 1107 (m).

**$^1$H-NMR** ($CDCl_3$) δ(ppm) 1.17 (d, 3H, $J$ = 6.9 Hz);
1.90 (d, 1H, $J$ = 4.7 Hz); 2.30 (dq, 1H, $J$ = 3.3, 6.9, 12.1 Hz);
3.27 (dd, 1H, $J$ = 9.8, 11.8 Hz); 3.66 (s, 3H);
4.61 (t, 1H, $J$ = 0.9 Hz); 6.51 (d, 1H, $J$ = 9.7 Hz);
7.20-7.49 (m, 6H); 7.53 (d, 1H, $J$ = 6.0 Hz);
8.03 (d, 2H, $J$ = 7.5 Hz).

### 5.7.15 Preparation of 31

A solution of 300 mg (1.3 mmol) of 2-(benzoyloxymethyl)benzaldehyde and 533 mg (3.0 eq, 3.8 mmol) of freshly distilled dimethylacetylene dicarboxylate in 30 mL benzene, contained in a quartz test tube, was suspended 10 cm from a medium pressure mercury arc lamp and irradiated until tlc analysis (chloroform:ether 10:1) indicated complete conversion of the aldehyde (5 h). After concentration on a rotovap, the residue was resolved by flash chromatography employing chloroform followed by chloroform:ether 10:1 as eluents furnishing 242 mg (56 %) of **31**. In addition, 64 mg of unreacted aldehyde was recovered bringing the yield to 71 % with 79 % conversion.

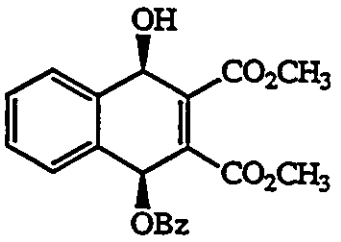


$C_{21}H_{18}O_7$ 382.37

**31**

**MS** (Cl/$Et_2O$) : 365 $[M-17]^+$, 333, 261, 245, 229, 213.

**IR** ($CH_2Cl_2$) $\nu_{max}(cm^{-1})$ 3528 (br), 1728 (s), 1732 (s), 1096 (m).

**$^1$H-NMR** ($CDCl_3$) δ(ppm) 3.47 (d, 1H, $J$ =7.5 Hz); 3.71 (s, 3H); 3.88 (s, 3H); 5.42 (dd, 1H, $J$ = 2.3, 7.4 Hz); 6.85 (d, 1H, $J$ = 2.4 Hz); 7.30-7.60 (m, 7H); 7.98 (d, 2H, $J$ = 7.1 Hz).

### 5.7.16 Preparation of 32

A solution of 200 mg (0.8 mmol) of 2-(benzoyloxymethyl)benzaldehyde and 210 mg (3.0 eq, 2.5 mmol) of freshly distilled methyl propiolate in 30 mL benzene, contained in a quartz test tube, was suspended 10 cm from a medium pressure mercury arc lamp and irradiated until tlc analysis (chloroform:ether 20:1) indicated complete conversion of the aldehyde (6 h). After concentration on a rotovap, the residue was resolved by flash chromatography employing chloroform:ether 20:1 as eluent yielding 54 mg (20 %) of **32** as a yellow oil.

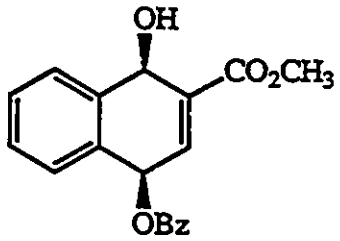


$C_{19}H_{16}O_5$ 324.34

**32**

**MS** (CI/ISO) : 325 $[M+1]^+$, 307, 203.

**IR** ($CH_2Cl_2$) $\nu_{max}(cm^{-1})$ 3548 (br), 1720 (s), 1102 (m).

**$^1$H-NMR** ($CDCl_3$) δ(ppm) 3.85 (s, 3H); 5.48 (t, 1H, *J* = 3.7 Hz); 6.63 (t, 1H, *J* = 3.8 Hz); 7.23 (d, 1H, *J* = 3.8 Hz); 7.30-7.50 (m, 5H); 7.55 (t, 1H, *J* = 7.6 Hz); 7.70 (d, 1H, *J* = 8.0 Hz); 8.05 (d, 2H, *J* = 7.5 Hz).

**5.7.17 Preparation of 37**

A solution of 1.0 g (4.2 mmol) of 2-(benzoyloxymethyl)benzaldehyde in 30 mL benzene, contained in a quartz test tube, was suspended 10 cm from a medium pressure mercury arc lamp and irradiated until tlc analysis (chloroform:ether 10:1) indicated complete conversion of the aldehyde (8 h). After concentration on a rotovap, the residue was resolved by flash chromatography, employing chloroform:ether 10:1 as eluent, furnishing 728 mg (73 %) of **37**.

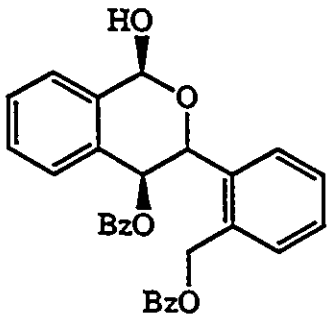


$C_{30}H_{24}O_6$ 480.52

**37**

**MS** (CI/$Et_2O$) : 479 [M-1]+, 463, 445, 341, 323.

**IR** ($CH_2Cl_2$) $\nu_{max}(cm^{-1})$ 3572 (br), 1719 (s), 1103 (m).

**$^1$H-NMR** ($CDCl_3$) δ(ppm) 3.12 (d, 1H, *J* = 4.3 Hz);
5.47 (d, 2H, *J* = 1.3 Hz); 6.01 (d, 1H, *J* = 1.6 Hz);
6.35 (d, 1H, *J* = 1.6 Hz); 6.37 (d, 1H, *J* = 4.9 Hz);
7.15-7.50 (m, 13H); 7.73 (m, 1H); 7.86 (d, 2H, *J* = 7.5 Hz);
8.06 (d, 2H, *J* = 7.5 Hz).

**5.7.18 Preparation of 38 cis and trans**

900 mg (2.4 mmol) of pyridinium dichromate was added, in portions, to an ice cooled, stirred solution of 500 mg (2.1 mmol) of **37** in 15 mL of $CH_2Cl_2$ over the course of 5 min. The reaction mixture was then removed from the ice bath and stirred, under nitrogen atmosphere, for 12 h after which time tlc analysis (Chloroform:ether 20:1) indicated complete conversion of the starting material. The solvent was removed on a rotovap at 40 °C, then triturated with ether and filtered over 3 g (70/230 mesh) silica gel. Concentration of the ether solution gave 415 mg (82 %) of **38c** and **38t** as a 3:1 mixture of diastereomers.

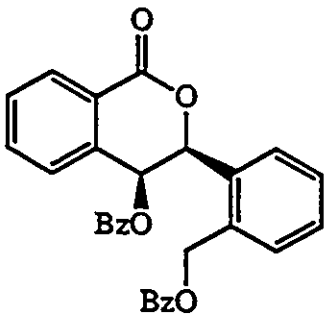


$C_{30}H_{22}O_6$ 478.50

**38c**

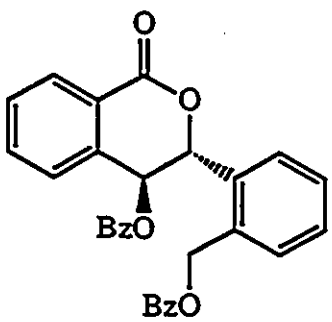


$C_{30}H_{22}O_6$ 478.50

**38t**

**MS** (CI/$Et_2O$) : 479 $[M+1]^+$, 357, 235, 217, 179.

**IR** ($CH_2Cl_2$) $\nu_{max}(cm^{-1})$ 1724 (s), 1099 (m).

**$^1$H-NMR** ($CDCl_3$) δ(ppm) **38c** 5.51 (d, 1H, *J* = 11.7 Hz);
5.60 (d, 1H, *J* = 11.7 Hz); 6.26 (d, 1H, *J* = 6.5 Hz);
6.68 (d, 1H, *J* = 6.5 Hz); 7.85-8.25 (m, 6H)
**38t** 5.36 (d, 1H, *J* = 12.6 Hz); 5.48 (d, 1H, *J* = 12.6 Hz);
6.09 (d, 1H, *J* = 1.7 Hz); 6.41 (d, 1H, *J* = 1.7 Hz);
7.20-7.70 (m, 12H); 7.85-8.25 (m, 6H).

### 5.7.19 Preparation of 13d

A solution of 3.0 g (21.7 mmol) of *o*-xylenol in 40 mL dry THF was added, dropwise, to an ice cooled, stirred suspension of 870 mg (21.7 mmol) of NaH (60 % dispersion in mineral oil) in 30 mL THF over 5 min under nitrogen atmosphere. After complete addition, the flask was removed from the ice bath and stirred at rt for 1 h until gas evolution ceased. The mixture was again cooled to 0°C and a solution of 2.3 g (21.7 mmol) of 3-butenoyl chloride in 20 mL THF was introduced over 10 min. After complete addition, the flask was warmed to rt and stirred for an additional hour.

The workup procedure was essentially identical to that described for **13a** giving 2.8 g of a brown oil which was resolved by flash chromatography, employing hexane: ethyl acetate 2:1 as eluent, furnishing 2.1 g (48 %) of a colorless oil.

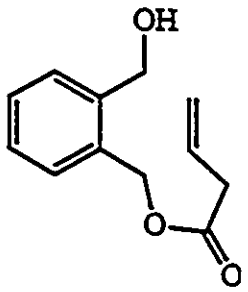


$C_{12}H_{14}O_3$ 206.24

**13d**

**MS** (CI/ISO) : 207 $[M+1]^+$, 189, 163.

**IR** ($CH_2Cl_2$) $\nu_{max}(cm^{-1})$ 3530 (br), 1723 (s).

**$^1$H-NMR** ($CDCl_3$) δ(ppm) 2.35 (t, 1H, *J* = 5.6 Hz);
3.10 (dt, 2H, *J* = 1.4, 7.0 Hz); 4.70 (d, 2H, *J* = 5.2 Hz);
5.11 (dq, 1H, *J* = 1.6, 6.2 Hz); 5.17 (m, 1H);

5.21 (s, 2H); 5.90 (m, 1H); 7.20-7.45 (m, 4H).

### 5.7.20 Preparation of 13e

A solution of 510 mg (3.7 mmol) of *o*-xylenol in 20 mL dry THF was added, dropwise, to an ice cooled, stirred suspension of 150 mg (3.7 mmol) of NaH (60 % dispersion in mineral oil) in 10 mL THF over 5 min under nitrogen atmosphere. After complete addition, the flask was removed from the ice bath and stirred at rt for 1 h until gas evolution ceased. The mixture was again cooled to 0°C and a solution of 675 mg (3.7 mmol) of 2-vinylbenzoyl chloride in 5 mL THF was introduced over 10 min. After complete addition, the flask was warmed to rt and stirred for an additional hour.

The workup procedure was essentially identical to that described for **13a** giving 396 mg (40 %) of a yellow oil.

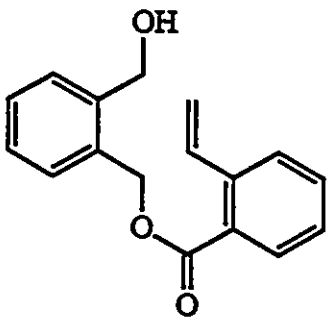


$C_{17}H_{16}O_3$ 268.31

**13e**

**$^1$H-NMR** ($CDCl_3$) δ(ppm) 2.53 (s, 1H); 4.89 (s, 2H); 5.40 (s, 2H); 5.46 (d, 1H, *J* = 11.0 Hz); 5.72 (d, 1H, *J* = 17.1 Hz); 7.20-7.65 (m, 8H); 8.18 (d, 1H, *J* = 7.8 Hz).

### 5.7.21 Preparation of 14d

2.0 g (5.4 mmol) of pyridinium dichromate was added in portions over 5 min to an ice cooled, stirred solution of 745 mg (3.6 mmol) of **13d** in 30 mL of dry dichloromethane under nitrogen atmosphere.

The remainder of the procedure was identical to that described for **14a** yielding 722 mg of crude aldehyde which, after further purification via the bisulfite adduct, afforded 615 mg (84 %) of **14d**.

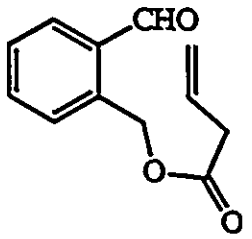


$C_{12}H_{12}O_3$ 204.23

**14d**

**MS** (CI/$Et_2O$) : 205 $[M+1]^+$, 149, 135.

**IR** ($CH_2Cl_2$) $\nu_{max}(cm^{-1})$ 1733 (s), 1698 (s).

**$^1$H-NMR** ($CDCl_3$) δ(ppm) 3.17 (dt, 2H, $J$ = 1.4, 6.9 Hz); 5.18 (dq, 2H, $J$ = 1.4, 13.4 Hz); 5.56 (s, 2H); 5.94 (m, 1H); 7.46-7.64 (m, 3H); 7.85 (d, 1H, $J$ = 7.6 Hz); 10.16 (s, 1H).

### 5.7.22 Preparation of 14e

500 mg (1.3 mmol) of pyridinium dichromate was added in portions over 5 min to an ice cooled, stirred solution of 230 mg (0.9 mmol) of **13d** in 30 mL of dry dichloromethane under nitrogen atmosphere.

The remainder of the procedure was identical to that described for **14a** yielding 212 mg of crude aldehyde which, after further purification via the bisulfite adduct, afforded 155 mg (68 %) of **14e**.

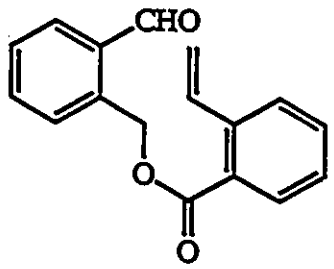


$C_{17}H_{14}O_3$ 266.30

**14e**

**$^1$H-NMR** ($CDCl_3$) δ(ppm) 5.38 (d, 1H, *J* = 10.9 Hz);
5.66 (d, 1H, *J* = 17.3 Hz); 5.83 (s, 2H); 7.20-7.70 (m, 7H);
7.89 (d, 1H, *J* = 7.5 Hz); 8.21 (d, 1H, *J* = 8.3 Hz);
10.13 (s, 1H).

### 5.7.23 Attempted Photocycloaddition of 14d

A solution of 110 mg (0.5 mmol) **14d** in 10 mL benzene (0.05 M) contained in a quartz test tube was suspended 10 cm from a Hanovia medium pressure mercury lamp and irradiated until tlc analysis (hexane:ethyl acetate 2:1) indicated complete conversion of **14d**. Concentration on a rotovap yielded a dark tar whose $^1$H-NMR spectrum showed only broad unresolved signals characteristic of polymeric material. Attempts to purify the material by flash chromatography (230/400 mesh silica gel, hexane:ethyl acetate 2:1) were unsuccessful.

### 5.7.24 Attempted Photocycloaddition of 14e

A solution of 150 mg (0.6 mmol) **14e** in 10 mL benzene (0.06 M) contained in a quartz test tube was suspended 10 cm from a Hanovia medium pressure mercury lamp and irradiated until tlc analysis (hexane:ethyl acetate 5:1) indicated complete conversion of **14e**. Concentration on a rotovap yielded a dark tar whose $^1$H-NMR spectrum showed only broad unresolved signals characteristic of polymeric material. As was the case for **14d**, attempts to purify the crude material by flash chromatography were unsuccessful.

# Chapter 6

## Acyl Cyanides as Carbonyl Heterodienophiles

### 6.1 Photocyclization of o-alkylacetophenones, benzaldehydes and benzoyl cyanides

In this chapter the results obtained from a re-evaluation of the photochemistry of 2-methylbenzoyl cyanide will be discussed. The information garnered during this study led to the strategy proposed in chapter 3 involving the hetero Diels-Alder cycloaddition.

The formation of benzocyclobutenols upon irradiation of

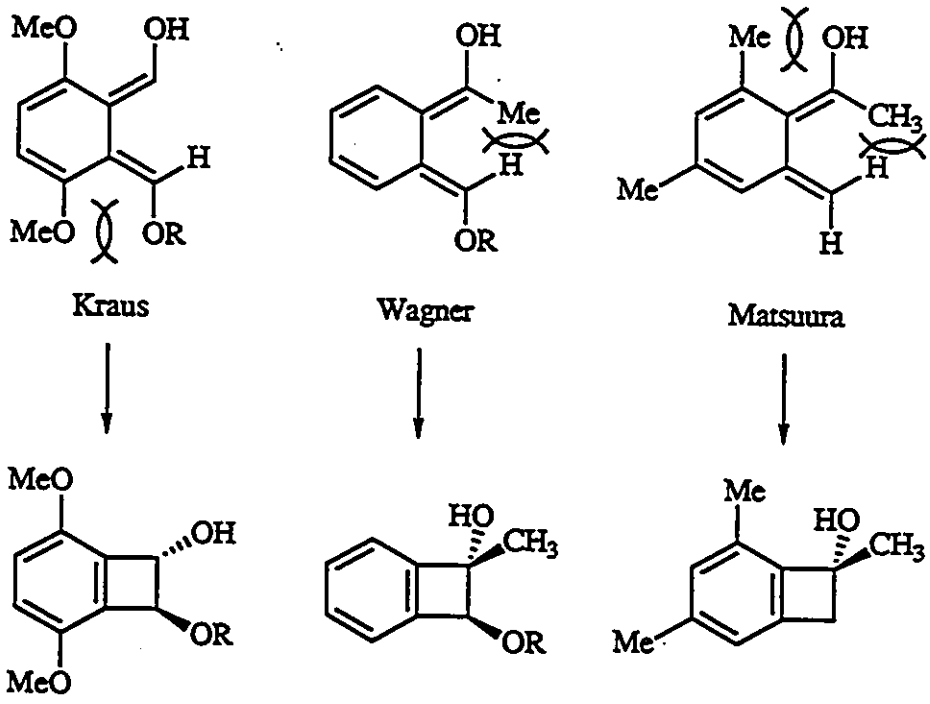


Scheme 6.1

2,4,6-trisubstituted aryl ketones has long puzzled photochemists. Wagner, in a recent publication,[48] concurred with Matsurra's original contention[50] that sterically crowded photoenols (scheme 6.1) favour benzocyclobutenol formation, after observing a similar pattern with various *o*-substituted acetophenones. Earlier mechanistic investigations of the process had led to false conclusions because of the widespread practice of analyzing product mixtures by gas chromatography, a procedure which converted the benzocyclobutenols back to the acetophenones.

In light of these conclusions we proposed that irradiation of 2-methylbenzoyl cyanide (**1a**), whose photoenol **2a** is moderately sterically encumbered as compared to that of 2-methylacetophenone, might lead to the benzocyclobutenone cyanohydrin **4** which, after HCN loss, should yield benzocyclobutenone (scheme 6.2).

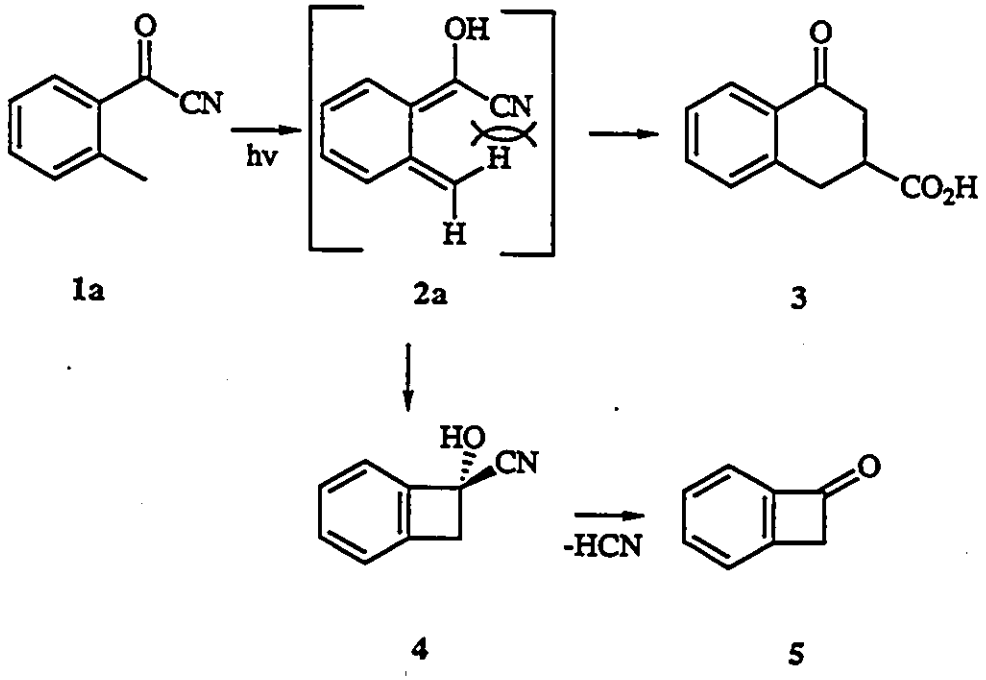


**1a** **2a** **3**

**4** **5**

Scheme 6.2: Proposed electrocyclic ring closure of 2a

Sammes, in an early publication,[58] briefly studied the photochemical behavior of 2-methylbenzoyl cyanide and reported the isolation of tetralone **3** after irradiation of **1a** in the presence of maleic anhydride. Presumably **3** was formed as a result of an initial cycloaddition between the dienol **2a** and maleic anhydride followed by loss of HCN and decarboxylation of the β-ketocarboxylate during hydrolytic workup. The formation of **3** provided evidence for the intermediacy of **2a** and justified a closer examination of the photochemistry of **1a** in the absence of a reactive dienophile.

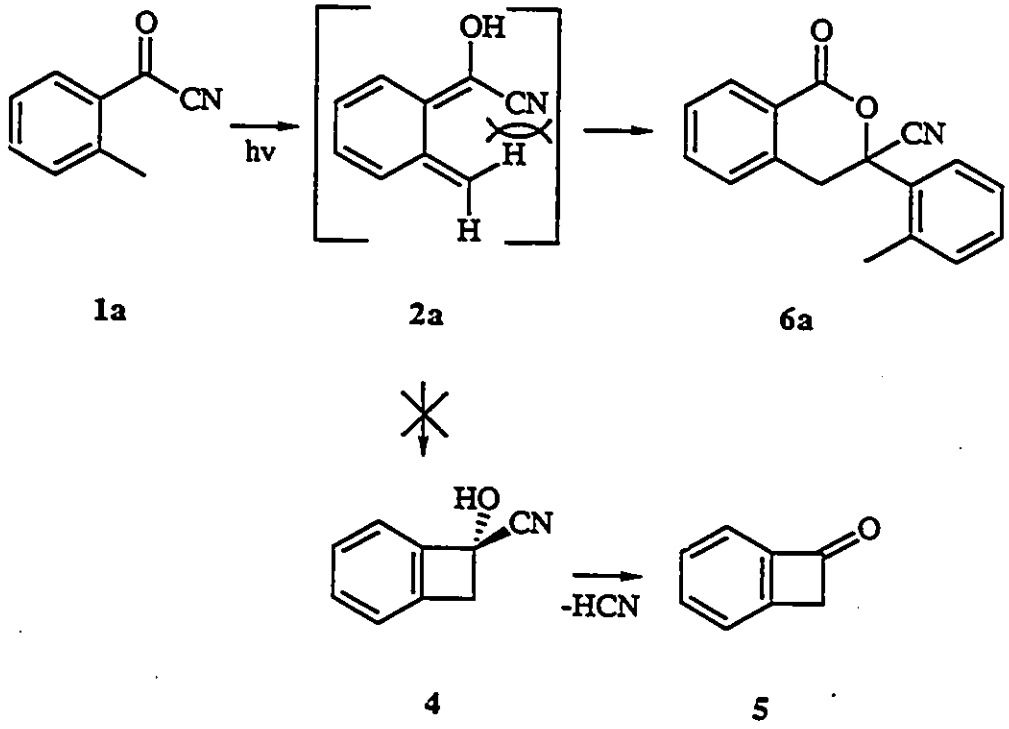


**1a** **2a** **6a**

**4** **5**

Scheme 6.3: Photochemical dimerization of **1a**

As depicted in scheme 6.3, irradiation of acetonitrile solutions of **1a** did not give the expected products **4** or **5**, but afforded the interesting dimer **6a** in 81 % yield. Compound **6a** (mp 126.5-127.5 °C)

gave a prominent molecular ion at m/e 262 $[M-1]^+$ in its EIMS. The $^1$H-NMR spectrum (fig. 6.1), δ(ppm) 2.68 (s, 3H), 3.71 (q, 2H, $J$ = 16.5 Hz), 7.23-7.40 (m, 4H), 7.46-7.70 (m, 3H), 8.16 (d, 1H, $J$ = 7.7 Hz), was informative, particularly the AB system bearing the large geminal coupling constant centered at δ 3.71 ppm. The $^{13}$C-NMR spectrum (fig. 6.2) showed 17 signals that were consistent with the assigned structure.

The formation of compound **6a** is best rationalized if one envisions the *o*-quinodimethane **2a** participating in a [4+2] cycloaddition with the carbonyl group of **1a** acting as a heterodienophile. Sammes, in an early paper, reported similar photochemical transformations in which 2-methylbenzaldehyde had acted as a heterodienophile.[58]

Hetero Diels-Alder reactions have numerous precedents in the literature. Oppolzer[62] and Kametani[63] have demonstrated that imines, nitriles, and aldehydes can serve as dienophiles in both an intermolecular and intramolecular mode. Highly reactive ketones, such as ketomalonates, have received scattered attention in this context;[64] there is also one report where the carbonyl group of an ester participates in a Diels-Alder reaction.[65] Of related interest is the report by Kessar which describes the synthesis of various 3-aryl-3,4-dihydroisocoumarins and protoberberines via the fluorodesilylation of *o*-((trimethylsilyl)methyl)benzoyl chlorides in the presence of aromatic aldehydes and 3,4-dihydroisoquinolium salts.[66] The photochemical dimerization of **1a** described above was without precedent. In fact, examination of the literature revealed no examples in which acyl cyanides had acted as carbonyl heterodienophiles.[67]

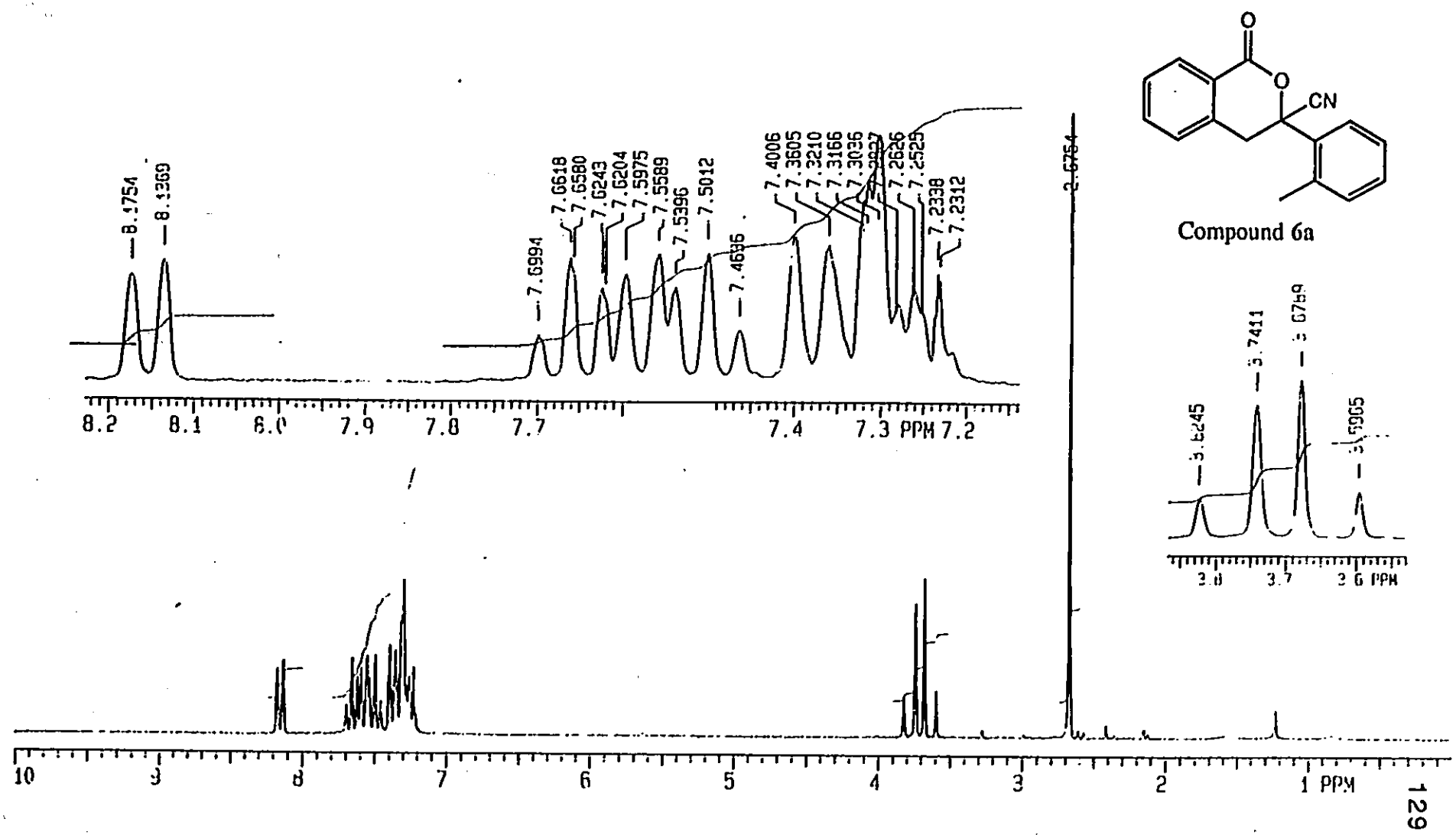


Figure 6.1: $^{1}$H-NMR of compound **6a**.

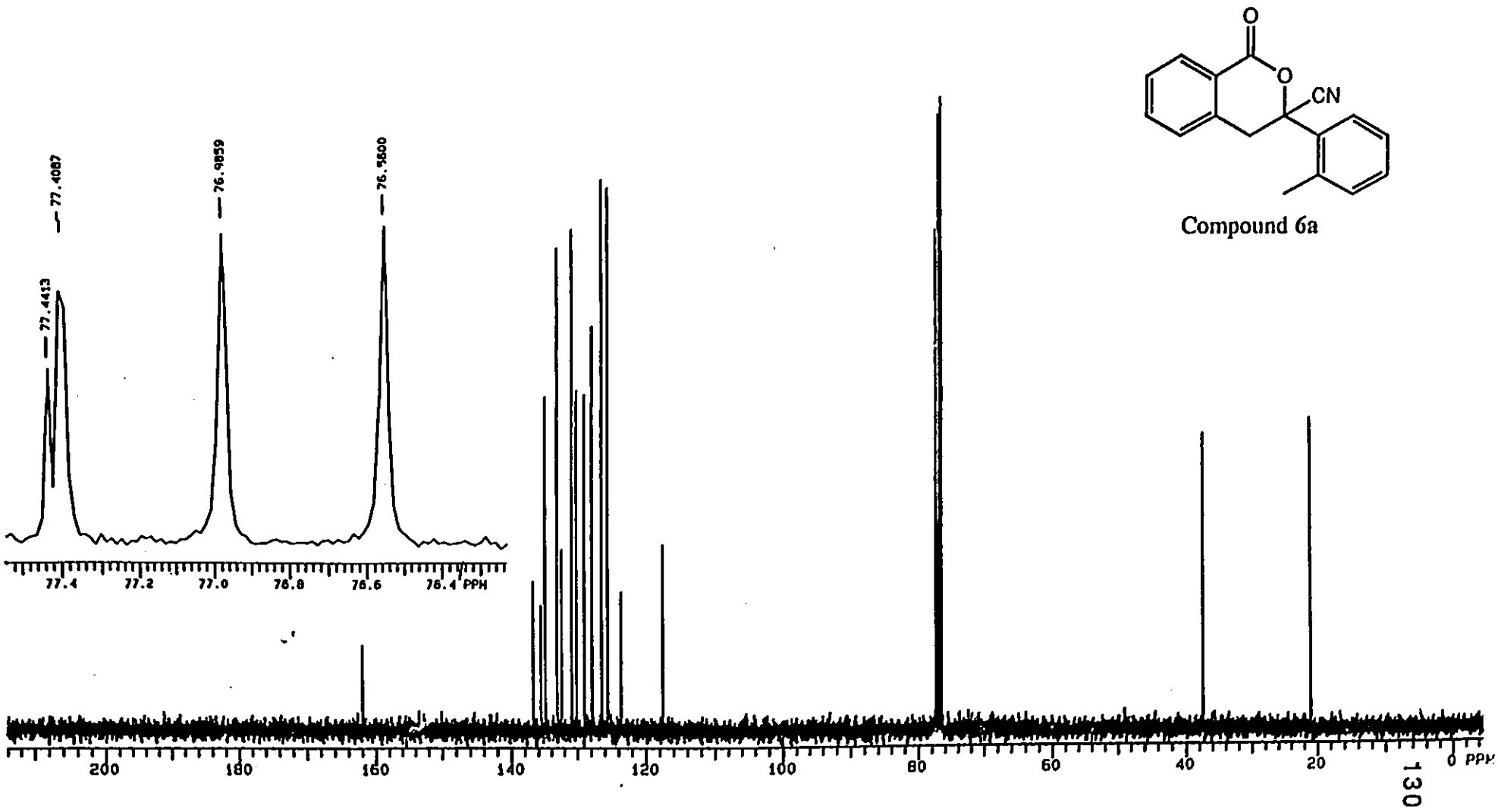


Compound 6a

Figure 6.2: $^{13}$C-NMR of compound 6a.

## 6.2 The synthesis of other aroyl cyanide *o*-QDM precursors

In an effort to explore the generality of this novel transformation, it was decided that several other aroyl cyanides should be prepared and

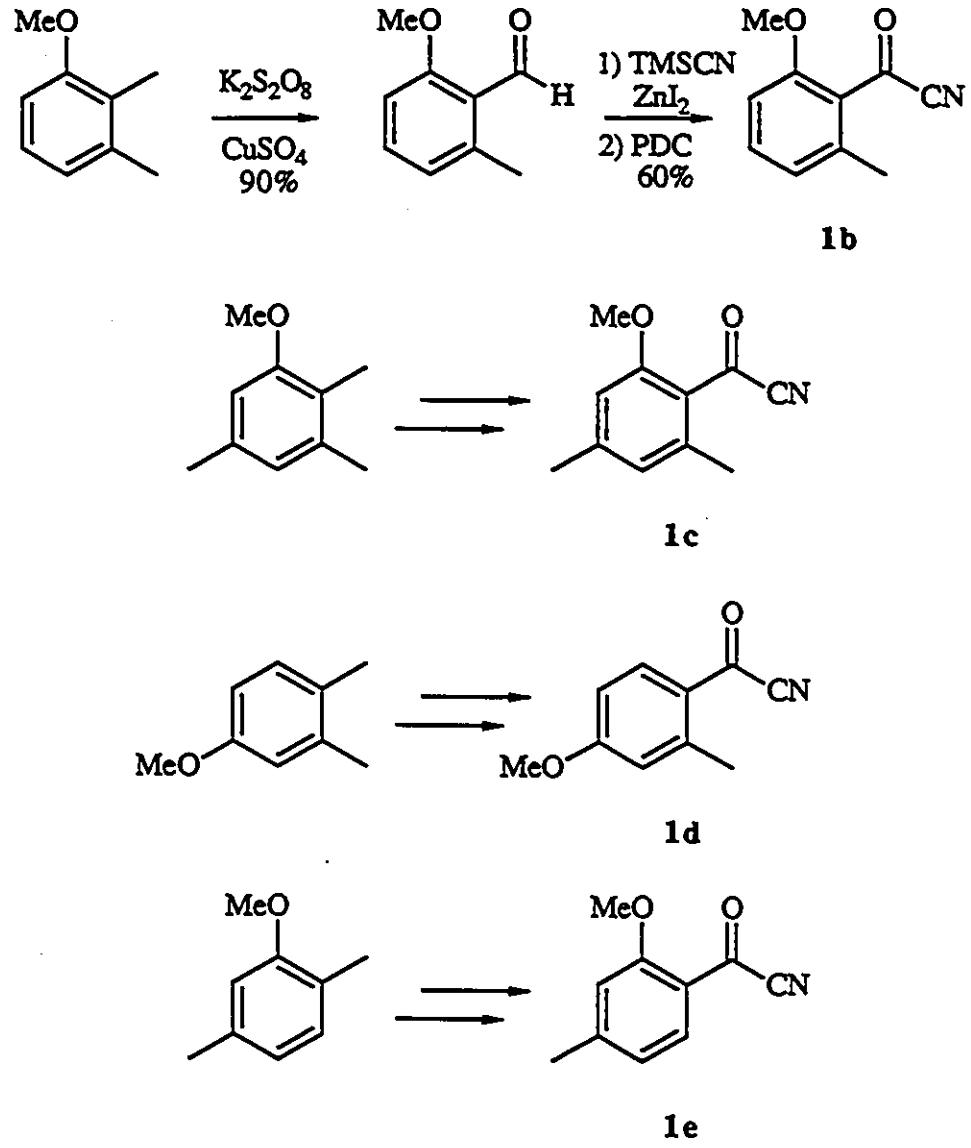


Scheme 6.4: Synthesis of substituted aroyl cyanides **1b-1e**

irradiated in the same manner as **1a**. Scheme 6.4 illustrates the approach taken for the synthesis of aroyl cyanides **1b** through **1e**.

Compound **1b** was prepared in two steps from 2,3-dimethylanisole. The first step involved a regioselective *o*-oxidation to 2-methoxy-6-methylbenzaldehyde, which was accomplished in 90 % yield by refluxing a mixture of the anisole, copper sulfate (1 eq), and potassium persulfate (3 eq) for 15 min in aqueous acetonitrile.[68] The second step involved conversion to the TMS cyanohydrin ($TMSCN/ZnI_2$) followed by in situ oxidation to the aroyl cyanide (PDC).[67] The same methodology was applied, with comparable yields obtained in each case, to the synthesis of aroyl cyanides **1c-1e**.

Compound **1b** (mp 55.3-56.1 $^{o}C$) gave a molecular ion of m/e 175 in its EIMS. The IR spectrum showed two diagnostic absorptions at $\nu_{max}(cm^{-1})$ 2220 (m), ascribed to the cyano function, and 1670 (s), attributed to the carbonyl function. Both the $^{1}H$-NMR (fig. 6.3) and the $^{13}C$-NMR spectra (fig. 6.4) were consistent with the structural assignment.

Compound **1e** (mp 68.2-69.0 $^{o}C$), $^{1}H$-NMR illustrated in figure 6.5, possesses no *o*-alkyl group, and thus was expected to be photochemically inert but capable of undergoing mixed cycloaddition with photoenols such as **2a**.

Aroyl cyanide **1d** (mp 62.0-62.8 $^{o}C$), $^{1}H$-NMR illustrated in figure 6.6, was of some additional interest considering that the similarly substituted aldehyde, due to a lowering of the energy of the $\pi$-$\pi^*$ triplets below that of the n-$\pi^*$ transition, is known to be photochemically unreactive.[54]

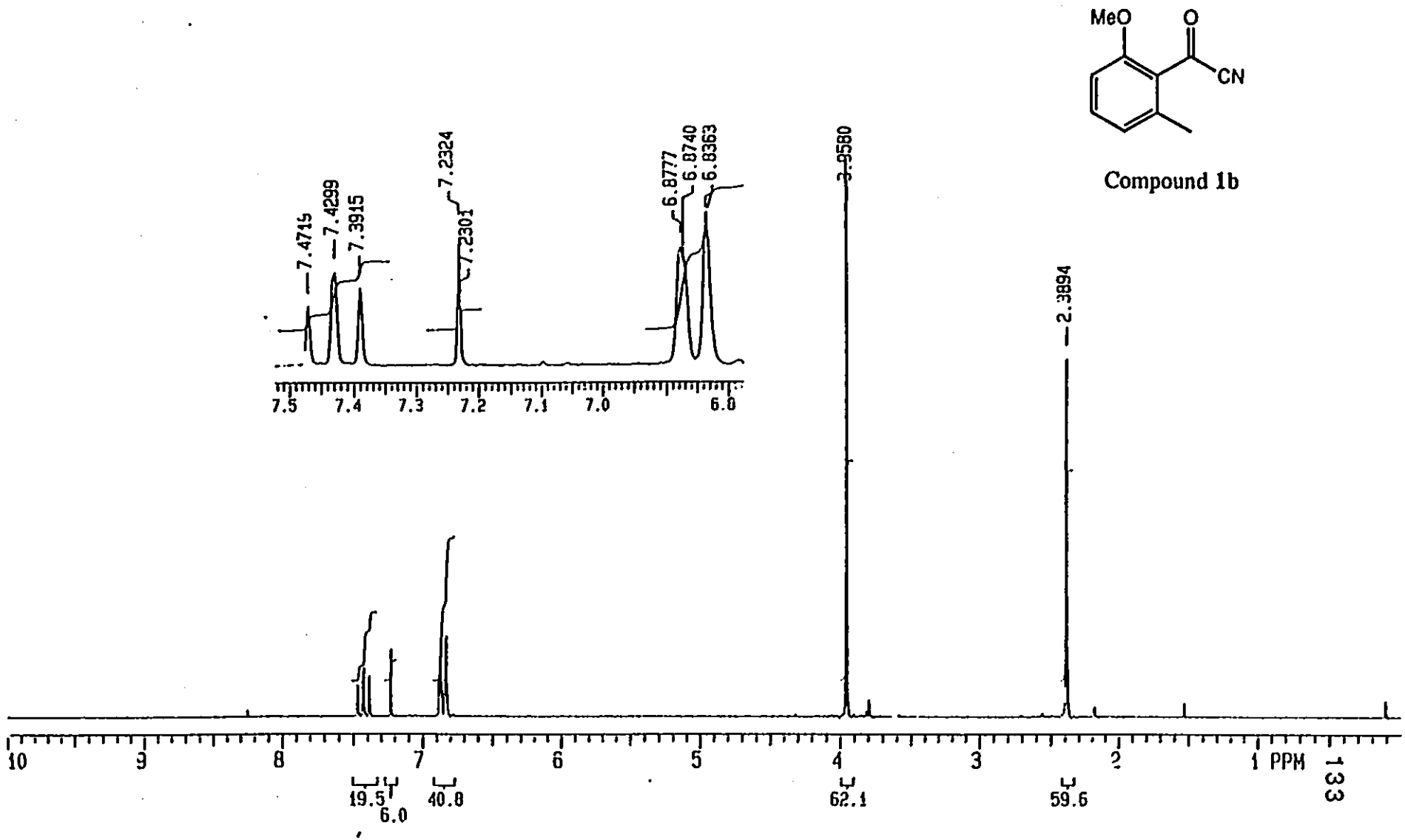


Figure 6.3: $^{1}$H-NMR of compound 1b.

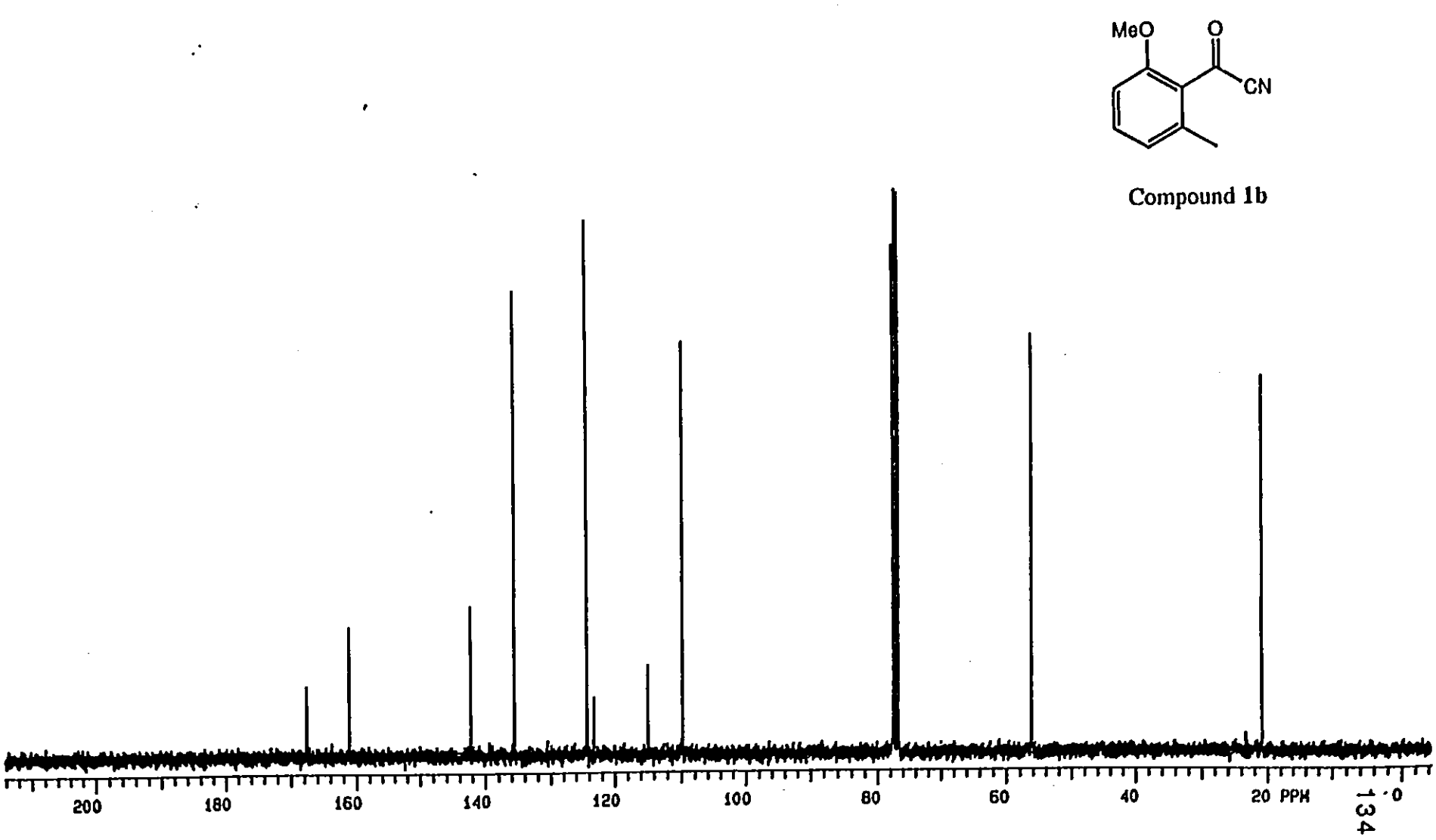


Figure 6.4: $^{13}$C-NMR of compound 1b.

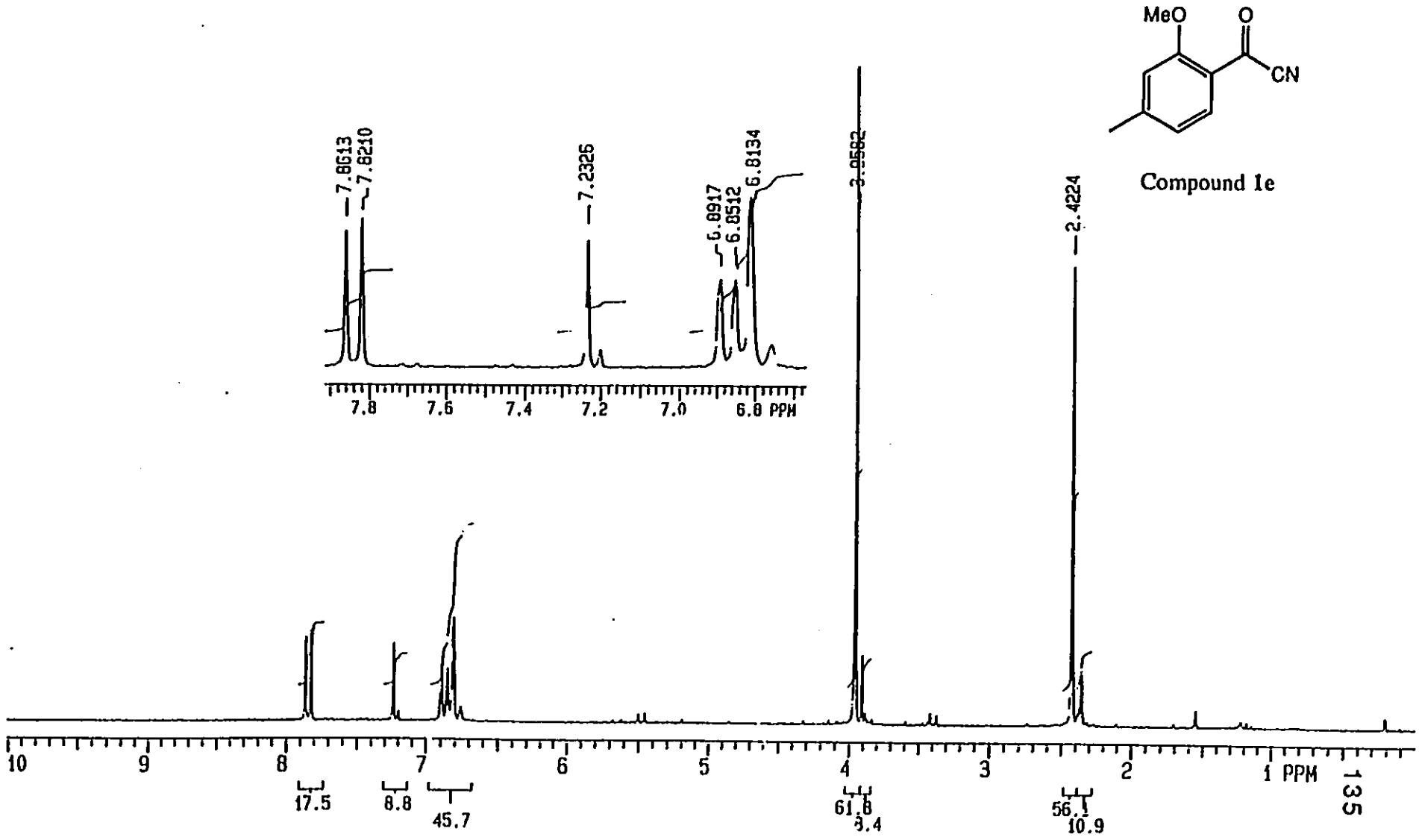


Figure 6.5: $^{1}$H-NMR of compound 1e.

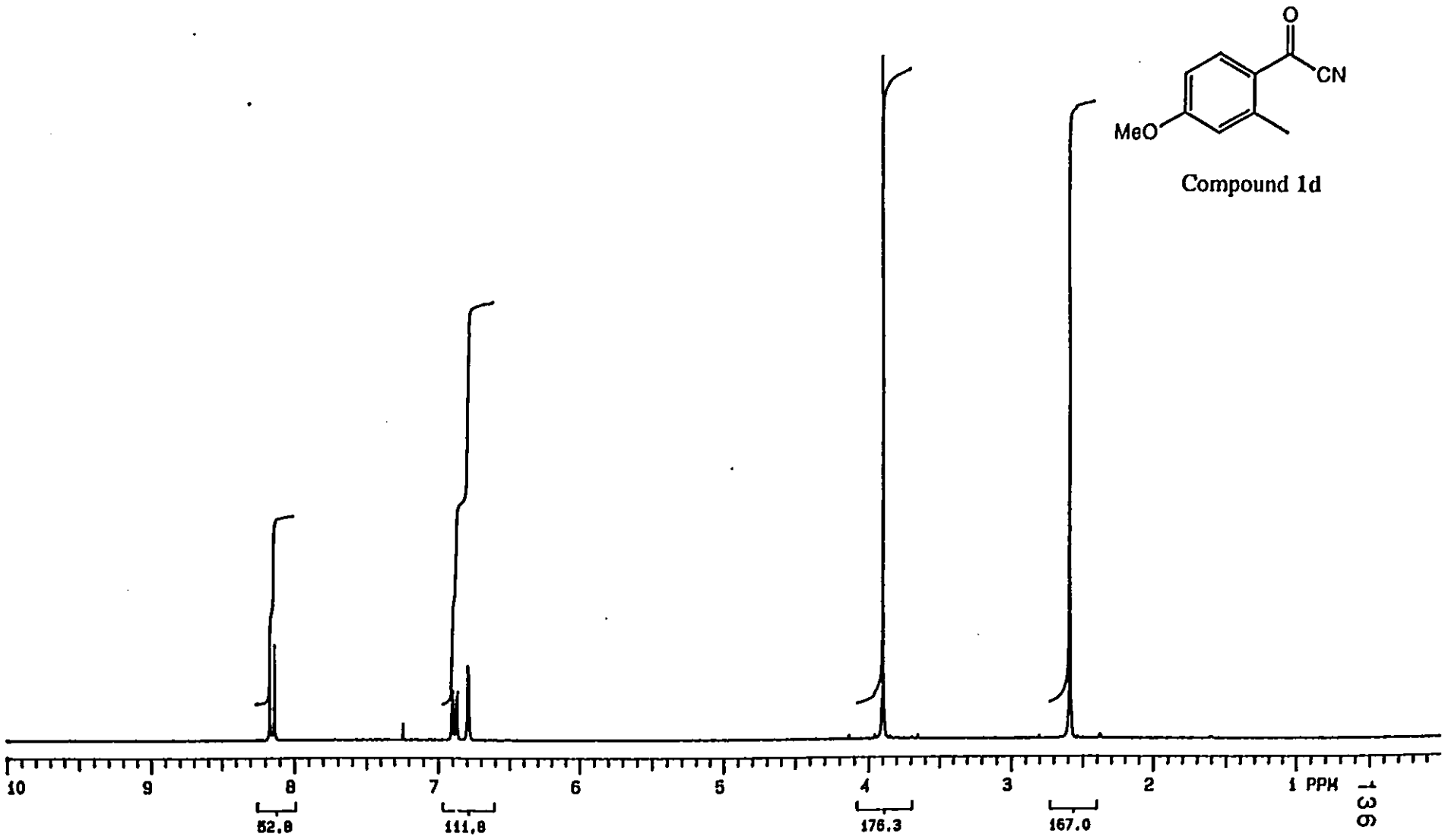


Figure 6.6: $^{1}$H-NMR of compound **1d**.

## 6.3 Preliminary cycloaddition studies

The first substituted aroyl cyanide selected for study was compound **1b** which, when irradiated in acetonitrile solution, furnished the highly substituted dimer **6b** (scheme 6.5) in 90 % yield.

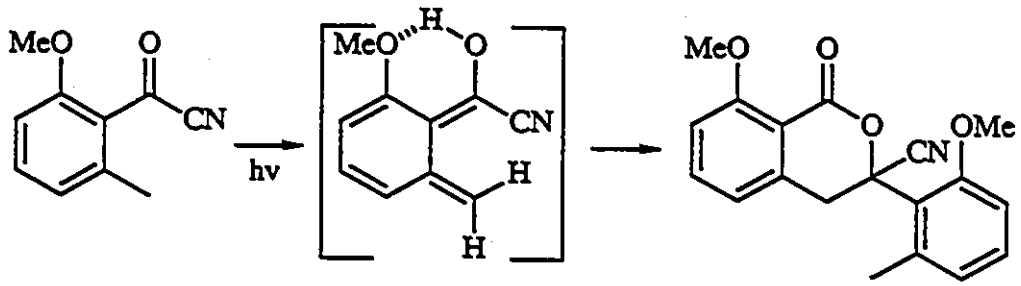


**1b** **2b** **6b**

Scheme 6.5: Photochemical dimerization of **1b**

Compound **6b** readily recrystallized from dichloromethane/hexane yielding colorless crystals (mp 145.3-146.0 °C) which gave, in addition to a prominent $[M-1]^+$ fragment of m/e 322 in the EIMS, an accurate mass determination of 323.1161. The IR spectrum showed a strong absorbance at $\nu_{max}$ 1744 $cm^{-1}$, indicative of the carbonyl function, but curiously, showed no absorbance in the region of 2200 $cm^{-1}$ characteristic of the cyano group. Examination of the IR spectra of other tertiary alkyl cyanides (Aldrich Library of IR Spectra) revealed this to be a consistent pattern. The $^1$H-NMR spectrum (fig. 6.7), was similar to that obtained for **6a**, and exhibited an AB system at $\delta$ 3.57 ppm ($J$ = 16.5 Hz) ascribed to the benzylic methylene hydrogens adjacent to the asymmetric center. The $^{13}$C-NMR spectrum (fig. 6.8)

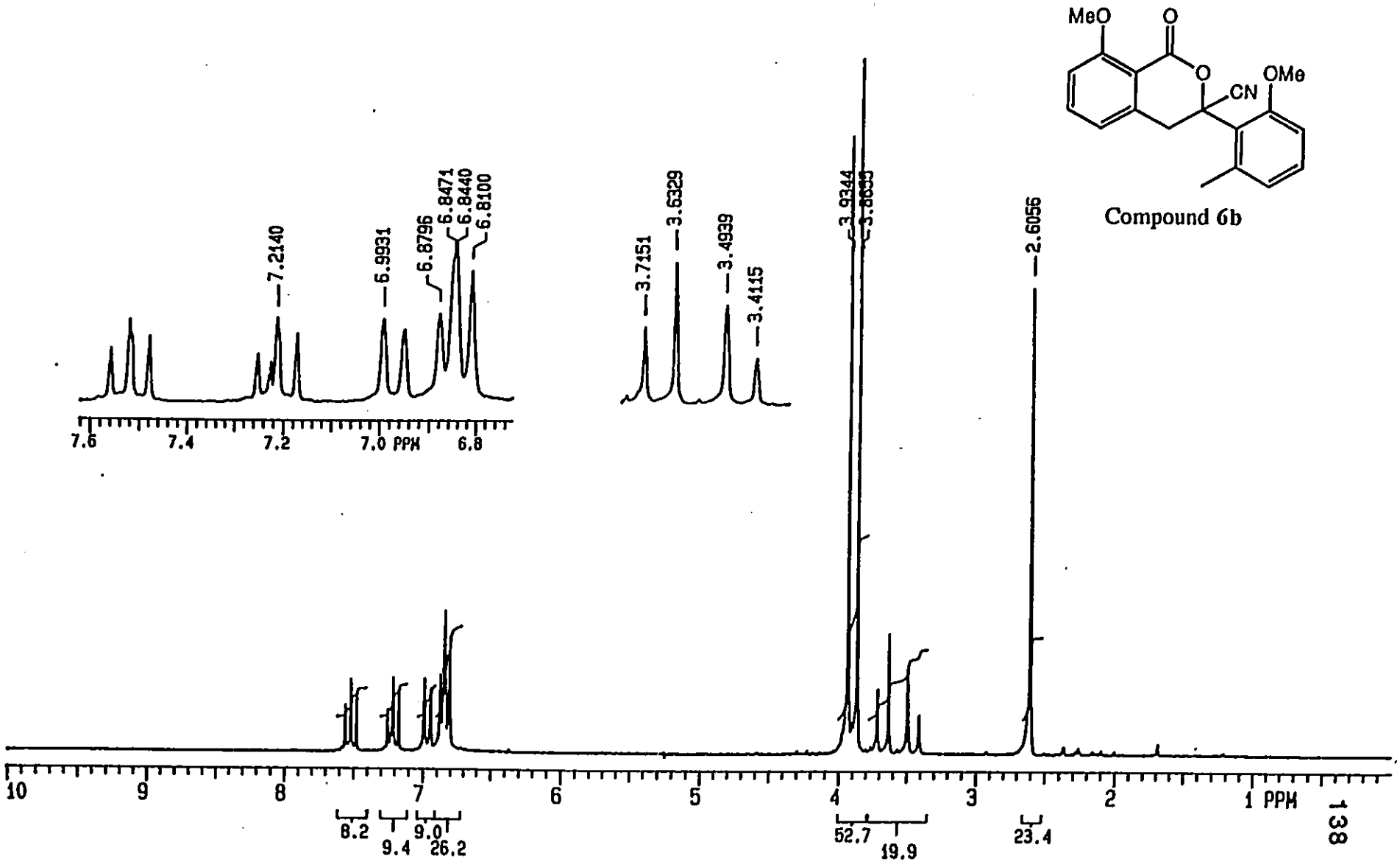


Figure 6.7: $^{1}$H-NMR of compound 6b.

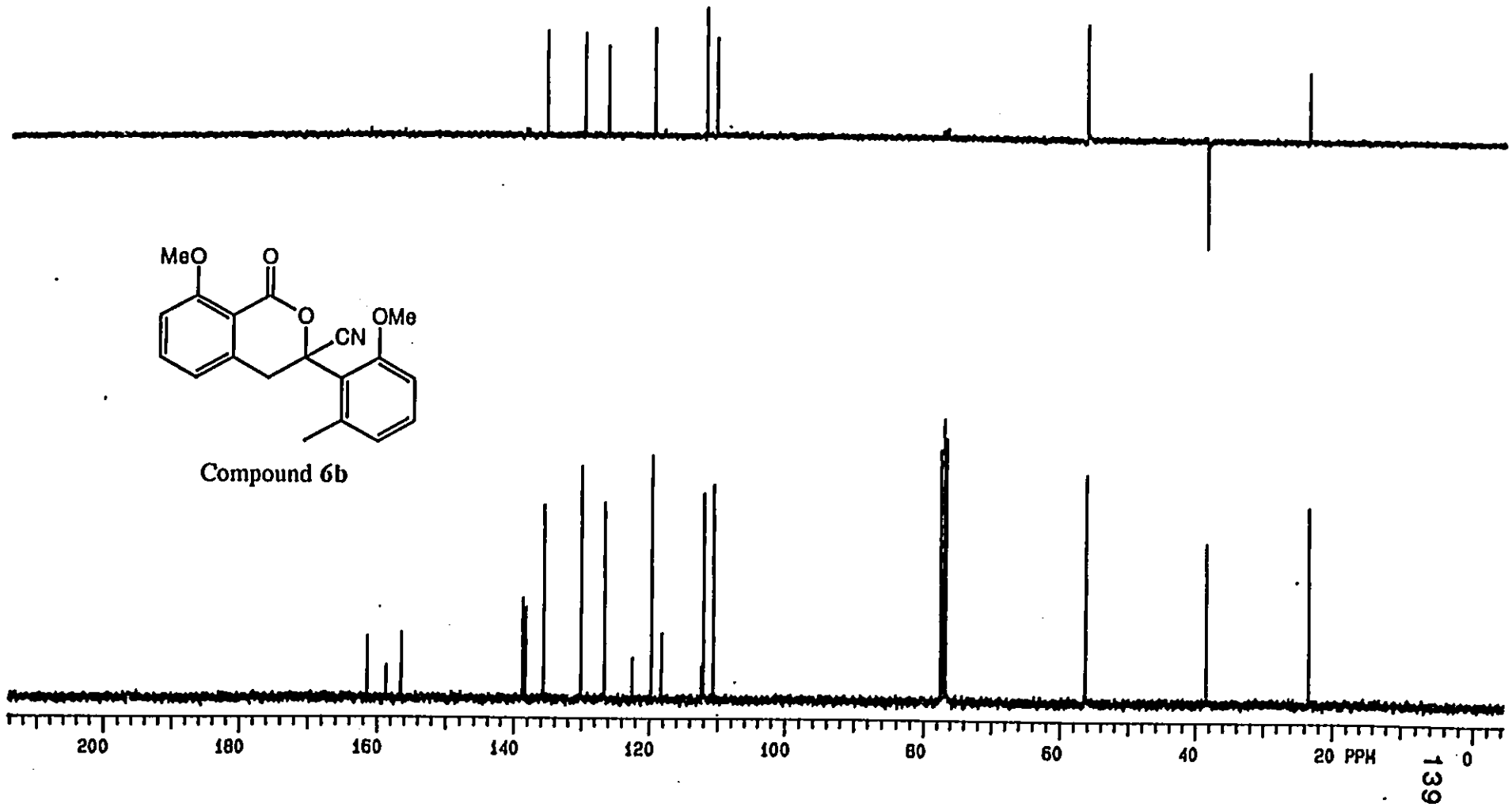


Compound 6b

Figure 6.8: $^{13}$C-NMR of compound 6b.

showed 19 signals with appropriate chemical shifts and multiplicities; the singlet at δ 111.9 ppm was assigned to the cyano carbon.

The highly substituted aroyl cyanide **1c**, was interesting because of its structural similarity to the 2,4,6-trisubstituted aldehydes and

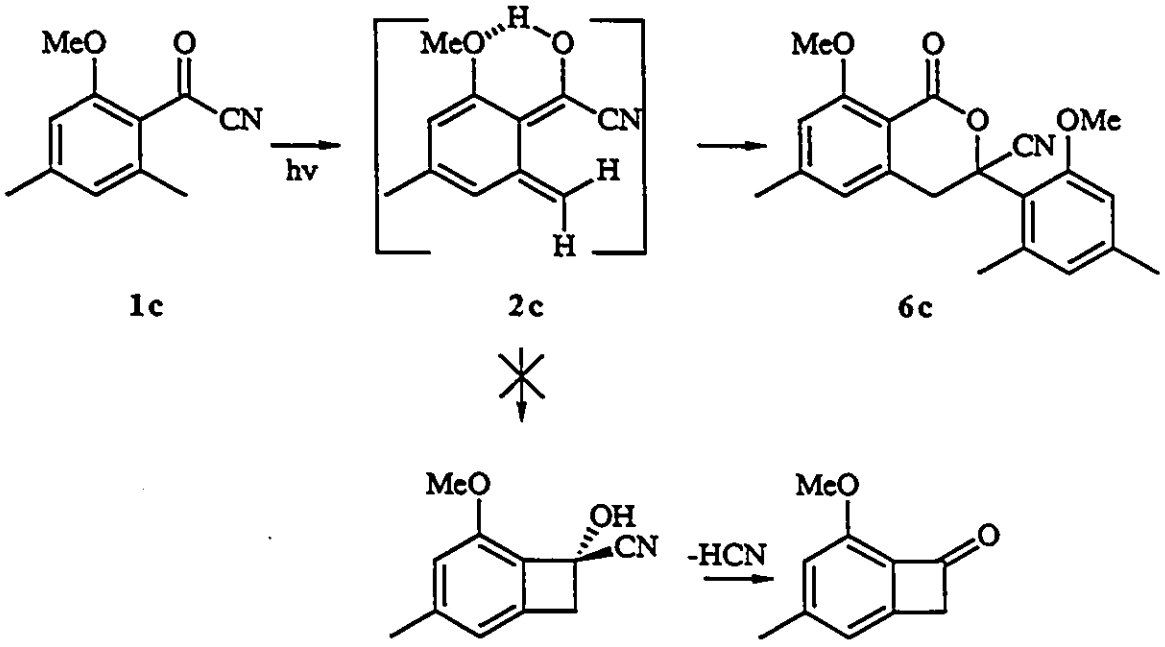


**1c** **2c** **6c**

Scheme 6.6: Photochemical dimerization of **1c**

ketones, studied by Matsuura and others,[50] which are known to form benzocyclobutenols upon irradiation. Compound **1c**, however, upon irradiation of acetonitrile solutions failed to furnish a subtituted benzocyclobutenone, but instead, dimerized affording the densely functionallized 3-cyano-3,4-dihydroisocoumarin **6c** (scheme 6.6) in 50 % yield.

Compound **6c** yielded beautiful colorless crystals (mp 202.5-203.0 °C) on recrystallization from dichloromethane/hexane and in addition to the prominent molecular ion (m/e 351) observed in the EIMS, gave an accurate mass determination of 351.1446. The $^{1}$H-NMR spectrum (fig. 6.9) showed the expected AB quartet centered at δ 3.50 ($J$ = 16.6 Hz) ppm, in addition to 5 singlets at δ 2.28, 2.38, 2.56, 3.85 and 3.93 ppm attributed to the benzylic methyl and methoxy hydrogens. The $^{13}$C-NMR spectrum (fig. 6.10) also exhibited characteristic signals with 3 quartets at δ 21.2, 22.2 and 23.0 ppm, which were ascribed to the benzylic methyl carbons, 2 quartets at δ 56.1 and 56.1 ppm, which were attributed to the methoxy carbons, and two singlets at δ 77.4 and 109.7 ppm, which were assigned to the quaternary benzylic and cyano carbons respectively.

By previous account, compound **1d** was of additional interest because of the photochemical inertness displayed by its aldehydic congener 2-methoxy-6-methylbenzaldehyde. In addition, the tetralones obtained by cycloaddition of carbogenic dienophiles to **2d** (scheme 6.7) would be of potential utility in natural product, particularly steroid, synthesis.[30c] In the event, irradiation of acetonitrile solutions of aroyl cyanide **1d** failed to produce any of the expected dimer **6d**, but instead, afforded only intractable mixtures. While there was some unreacted **1d** present in the product mixture, the accompanying tar suggested that there was some unspecified photoreactivity which may or may not have included the formation of **2d**.

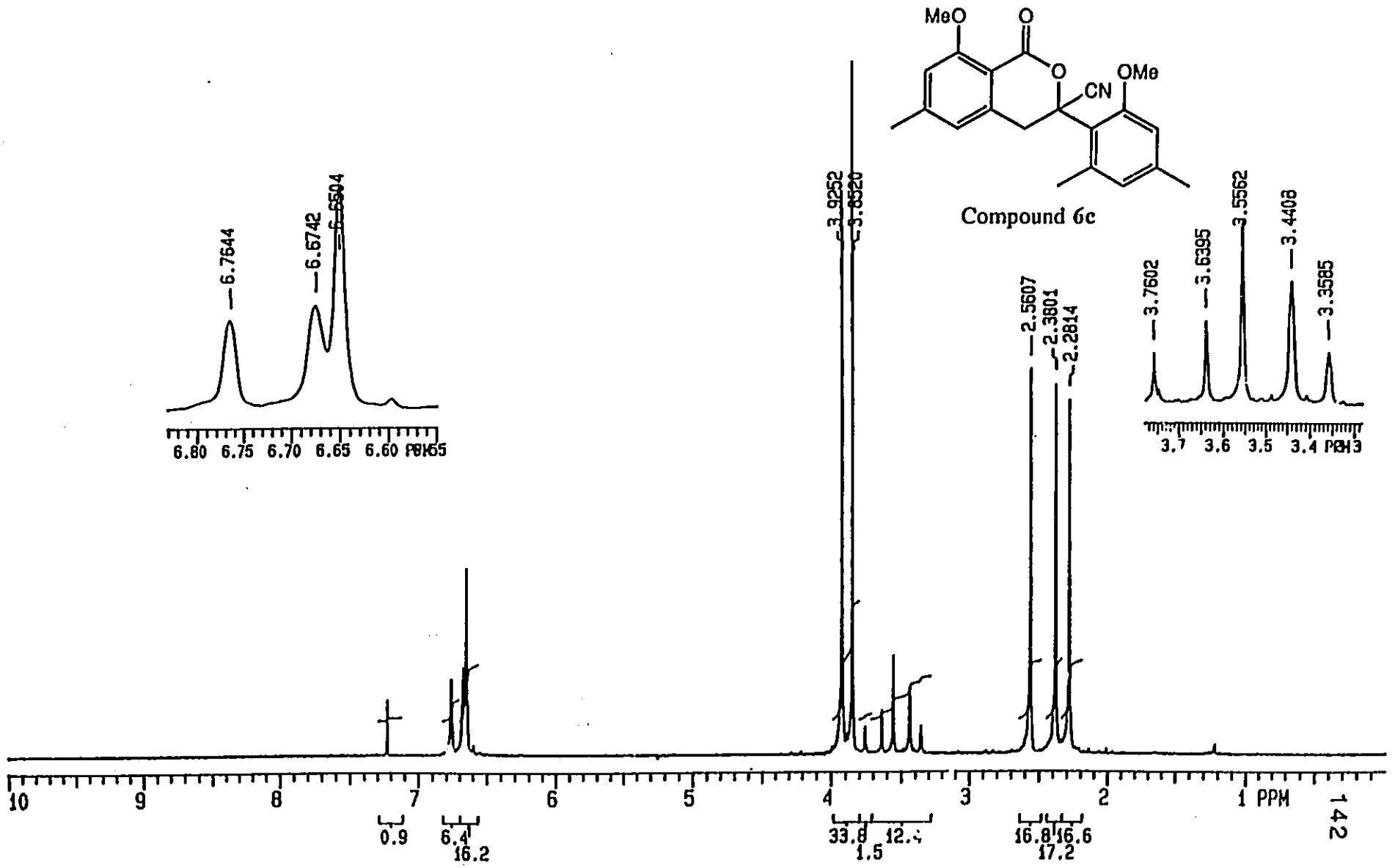


Figure 6.9: $^{1}$H-NMR of compound 6c.

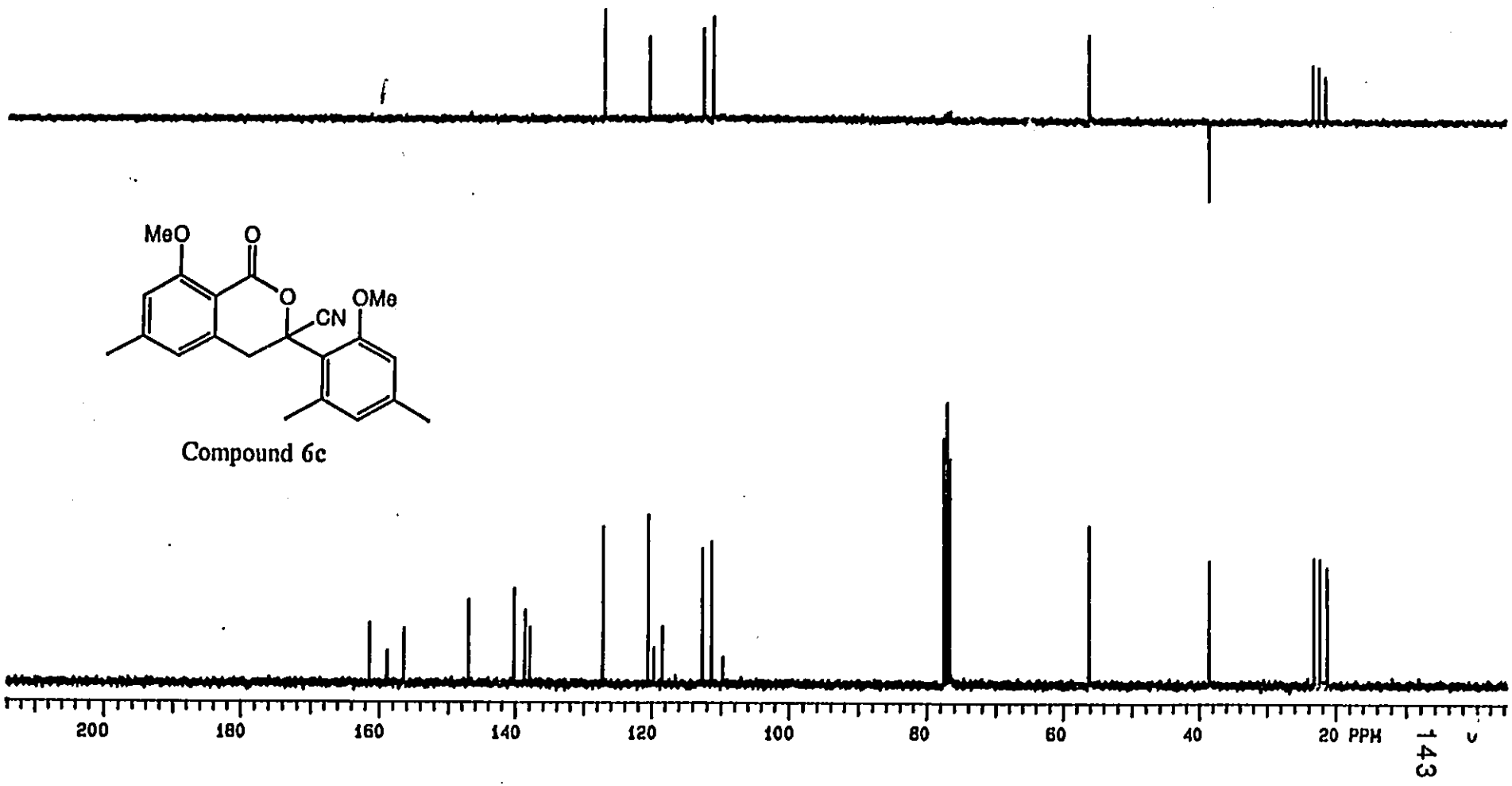


Compound 6c

Figure 6.10: $^{13}$C-NMR of compound 6c.

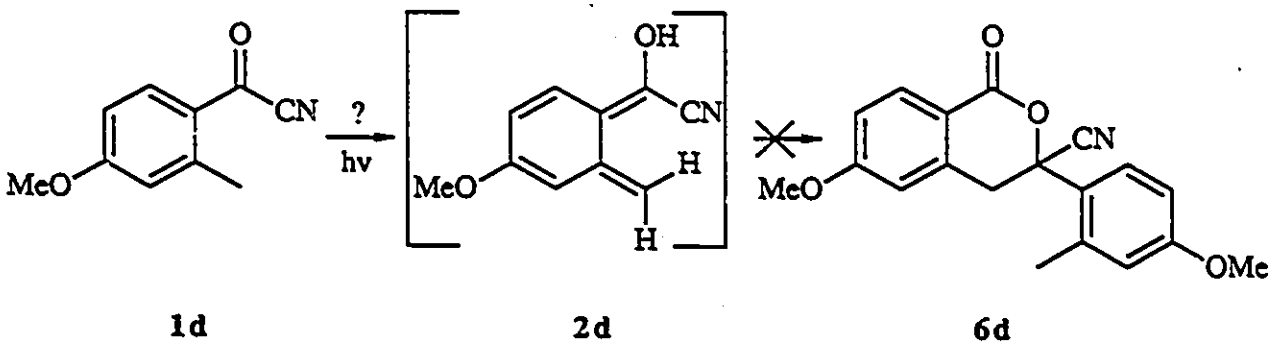


1d 2d 6d

Scheme 6.7: Abortive photochemical dimerization of **1d**

## 6.4 Mixed cycloaddition studies

Obviously, the potential synthetic applications of the adducts obtained from the photoreaction would be expanded considerably if it were possible to carry out mixed cycloadditions to photoenols **2a-2d**.

The prototypical experiment would involve the irradiation of **1a** in the presence of an aroyl cyanide, such as benzoyl cyanide, incapable of undergoing photoenolization. Based on the observations in the preliminary cycloaddition studies, benzoyl cyanide would be expected to compete with **1a**, as a heterodienophile, for the *o*-quinodimethane **2a**. The absence of an *o*-methyl group in benzoyl cyanide should enhance its reactivity, in comparison to **1a**, due to reduced steric hinderance around its carbon-oxygen double bond.

Thus an acetonitrile solution of 2-methylbenzoyl cyanide (**1a**) and 2 eq of benzoyl cyanide was suspended 10 cm from a Hanovia medium pressure mercury lamp and irradiated for 6h. Flash chromatography (5:1 hexane:ethyl acetate) of the crude product mixture afforded the mixed adduct **7a** (scheme 6.8) in 75 % yield.

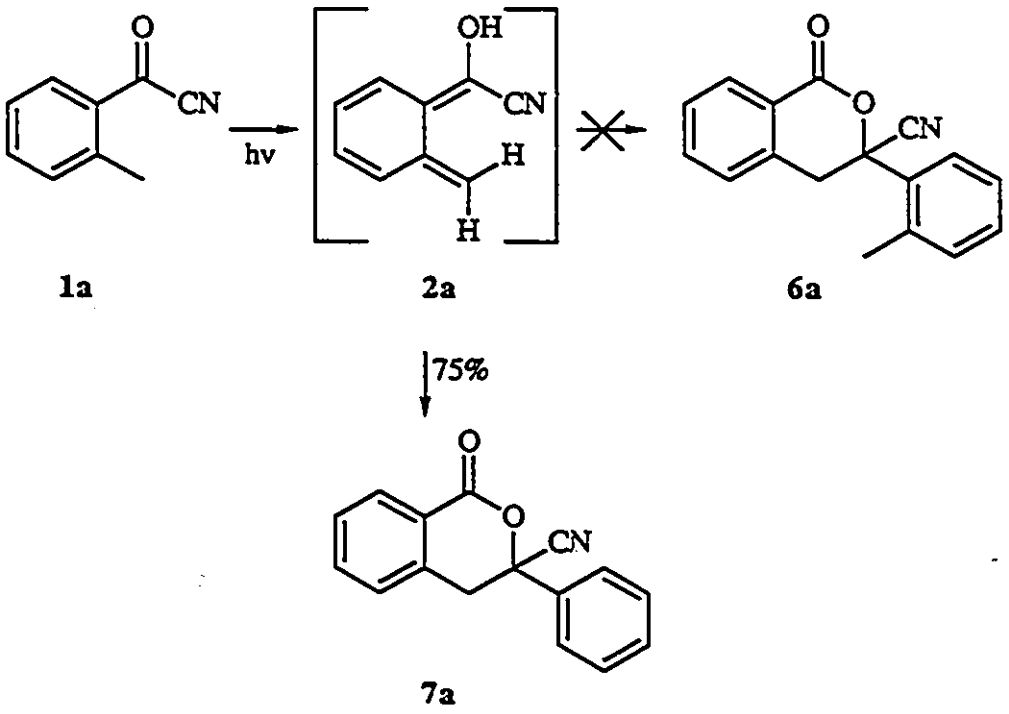


Scheme 6.8: Photoenolization of **1a** in the presence of benzoyl cyanide

Compound **7a** was obtained as colorless plates (mp 144.6-146.1 $^{o}$C) on recrystallization from ether/hexane. The $^{1}$H-NMR spectrum (fig. 6.11) was similar to that observed for **6a**, exhibiting a pronounced AB quartet centered at δ 3.54 ($J$ = 16.7 Hz) ppm arising from the benzylic methylene protons. A major discriminating factor, with respect to **6a**, was the conspicuous absence of any signals corresponding to a benzylic methyl group. The $^{13}$C-NMR spectrum (fig. 6.12) consisted of 14 signals, the most notable being peaks at δ 40.3 ppm, attributed to the benzylic methylene carbon, at δ 78.2 ppm, ascribed to the benzylic quaternary center, and at δ 117.8 ppm, assigned to the cyano carbon.

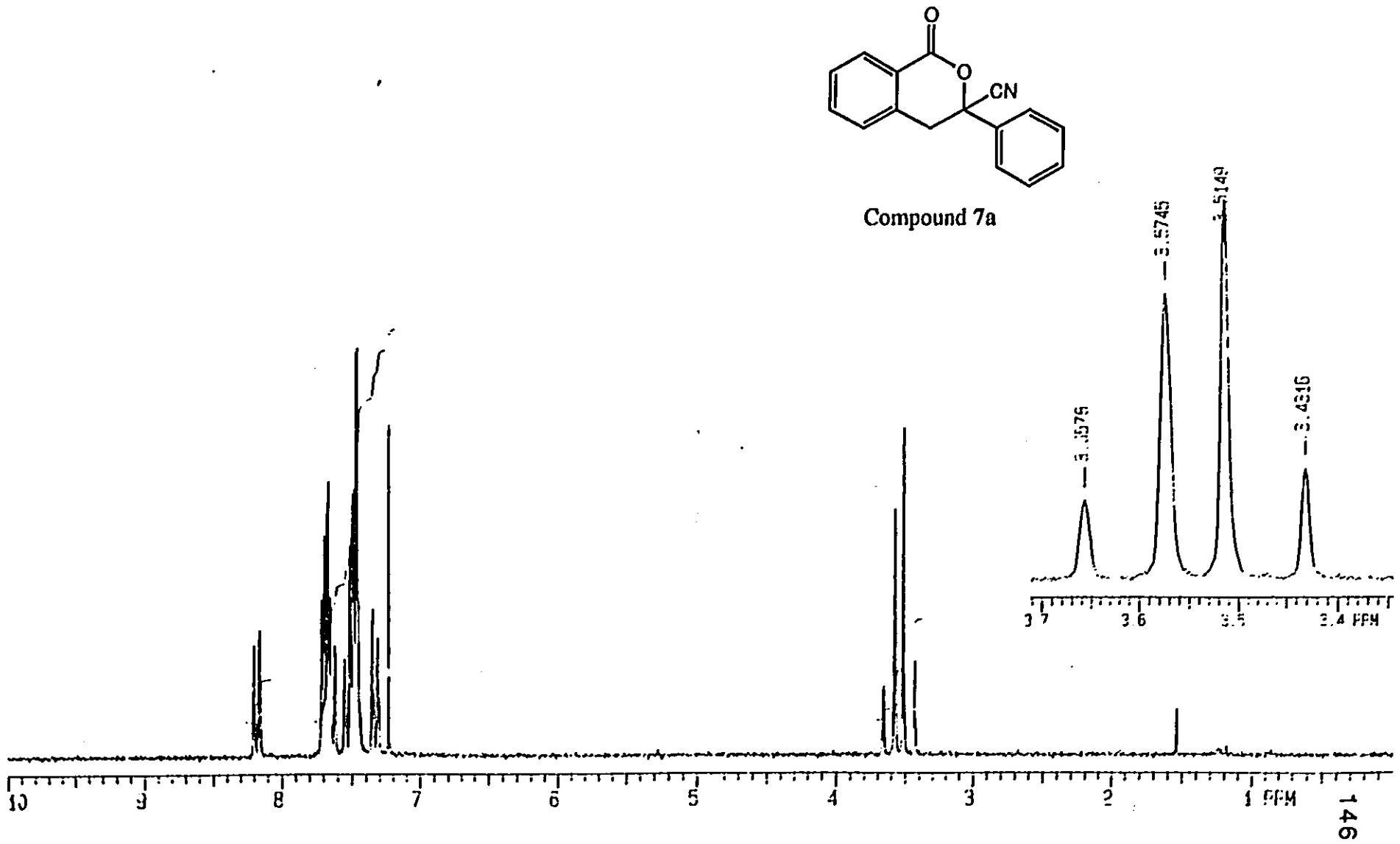


Figure 6.11: $^{1}$H-NMR of compound **7a**.

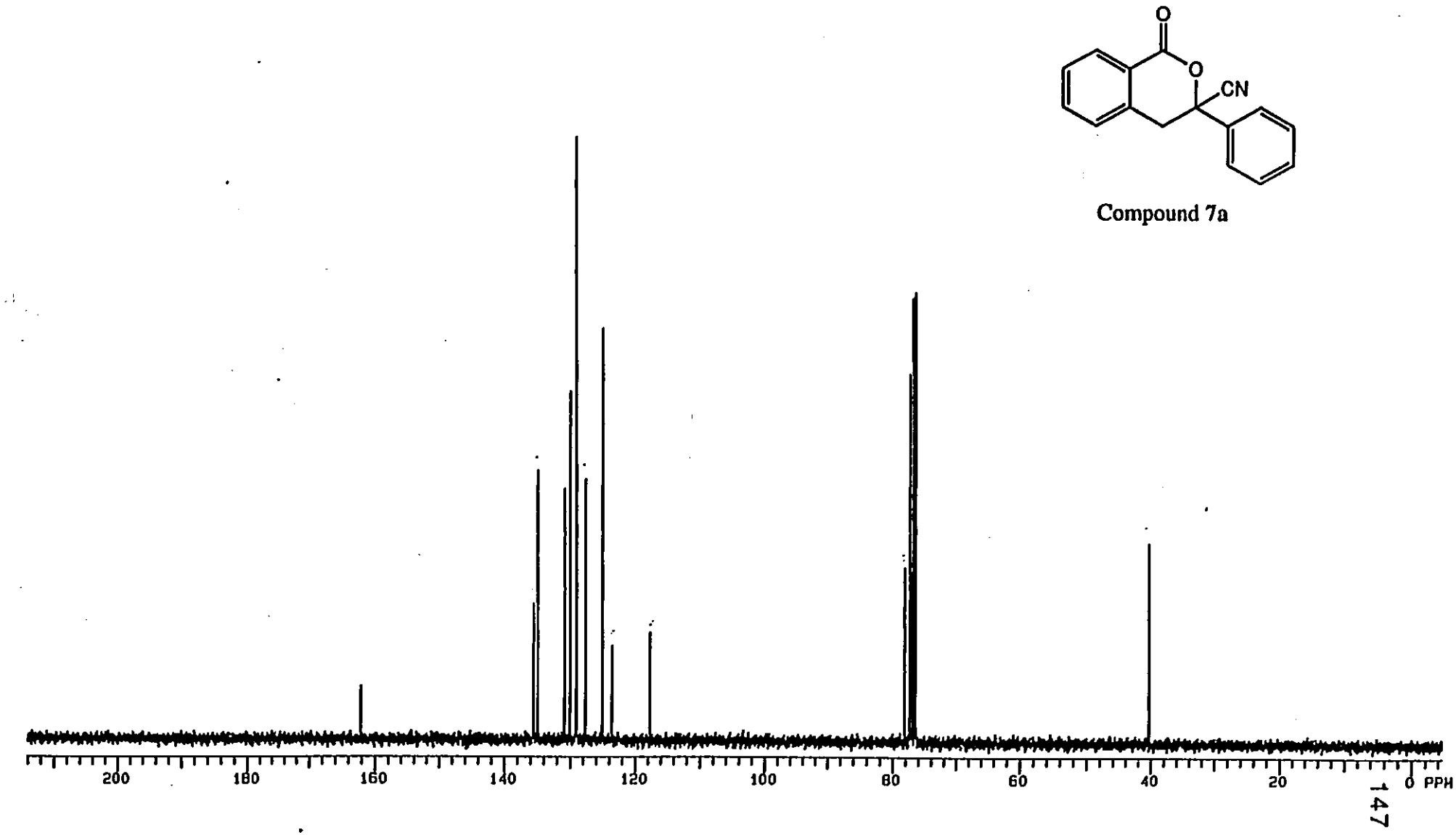


Figure 6.12: $^{13}$C-NMR of compound **7a**.

The exclusive formation of the mixed adduct **7a** confirmed the prediction that benzoyl cyanide, being less sterically encumbered than 2-methylbenzoyl cyanide **1a**, should be a better competitor for **2a**. In light of this observation it seemed likely that the same preference should be operative, perhaps to a greater extent, with compound **1b** which is 2,6-disubstituted.

Irradiation of an acetonitrile solution of **1b** and 2 eq of benzoyl cyanide lead to the exclusive formation of the mixed adduct **7b** in 88 % yield (scheme 6.9).

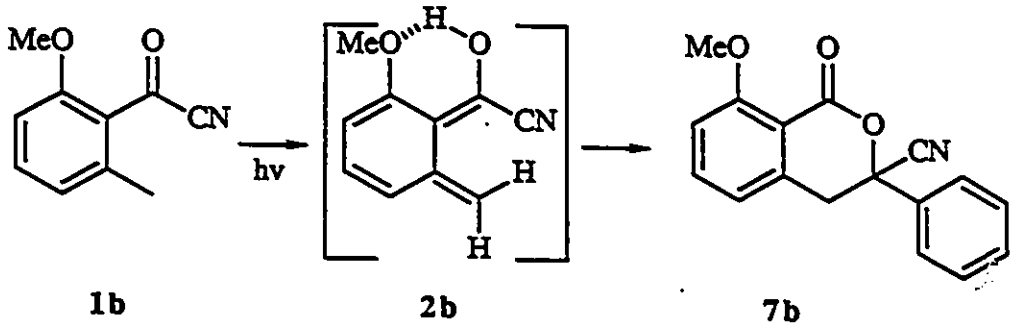


**1b** **2b** **7b**

Scheme 6.9: Photoenolization of **1b** in the presence of benzoyl cyanide

Compound **7b** (mp 146.0-147.0 °C) exhibited the expected molecular ion (m/e 279) in its EIMS. Both the $^{1}$H-NMR and the $^{13}$C-NMR spectra showed signals consistent with the structural assignment particularly the AB system centered at δ 3.39 ($J$ = 16.4 Hz) ppm in the former, and the signals at δ 41.2 (t, benzylic methylene), 77.5 (s, benzylic quaternary) and 112.0 (s, cyano carbon) ppm in the latter.

The aroyl cyanide **1c** was also found to undergo mixed cycloaddition (scheme 6.10) with benzoyl cyanide to form adduct **7c** (mp 166.0-167.0 °C) in 78 % yield.

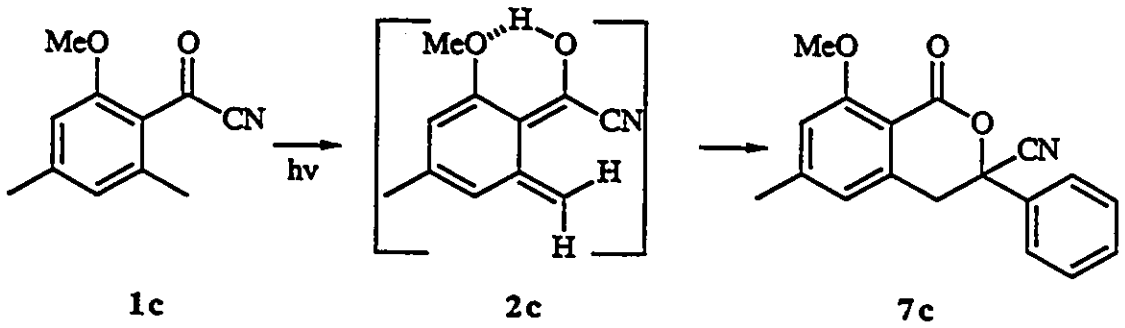


**1c** **2c** **7c**

Scheme 6.10: Photoenolization of **1c** in the presence of benzoyl cyanide

The preceding examples demonstrated that employing a less sterically encumbered aroyl cyanide as the heterodienophile in Diels-Alder reactions with acyl cyanide derived *o*-quinodimethanes, such as **2a**, leads to mixed cycloadducts. Based on these observations one would predict that irradiation of an acetonitrile solution of **1b** and **1e** would lead to the mixed adduct **7d** (scheme 6.11). The experimental results confirmed the expectations as irradiation of an equimolar mixture of **1b** and **1e** afforded the mixed adduct **7d** in 95 % yield.

Compound **7d** (mp 176.5-177.5 °C) was readily discriminated from the structurally similar dimer **6b** by examination of the proton and carbon NMR spectra. The $^1$H-NMR spectrum (fig. 6.13), in addition to

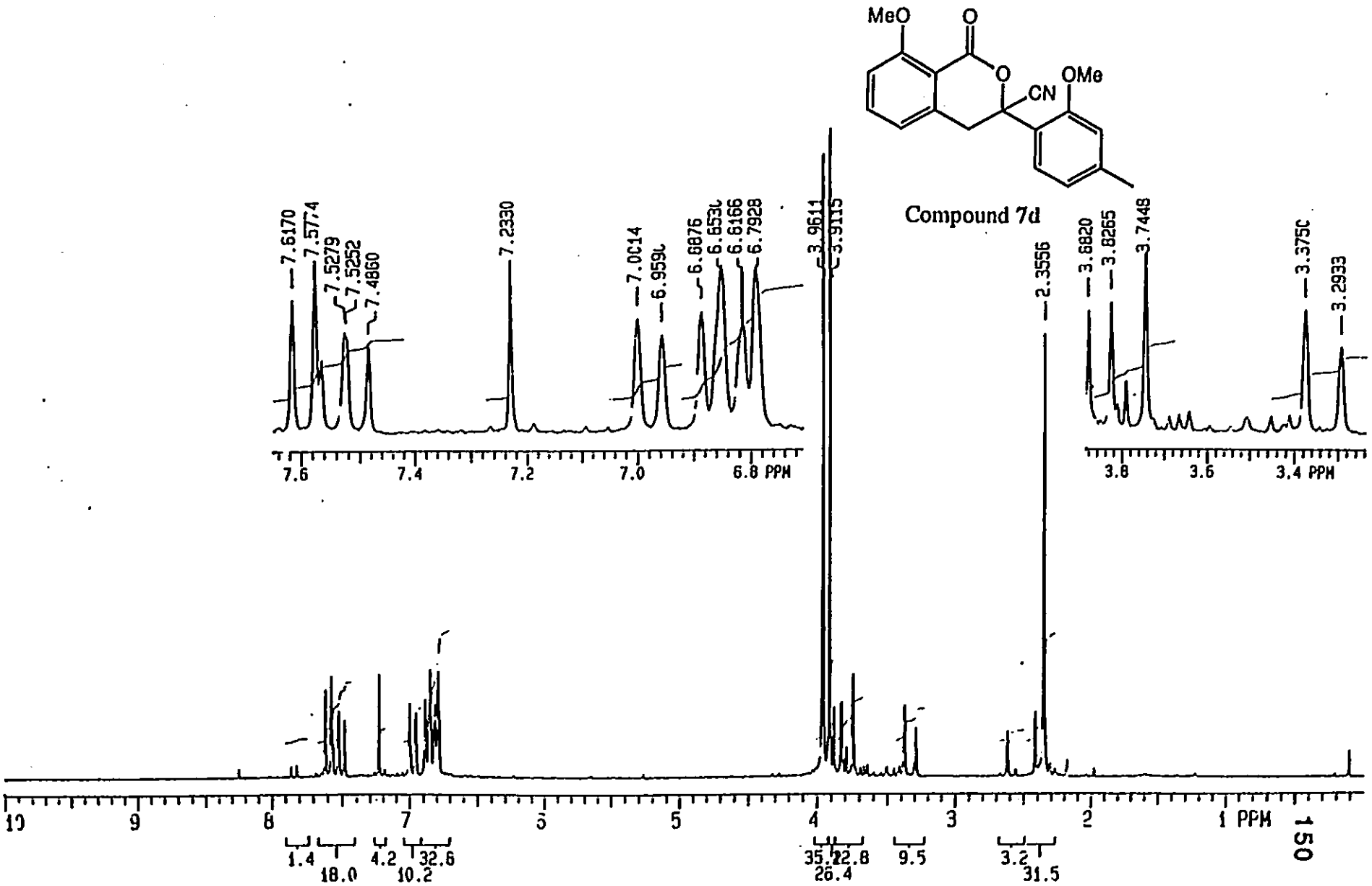


Figure 6.13: $^{1}$H-NMR of compound **7d**.

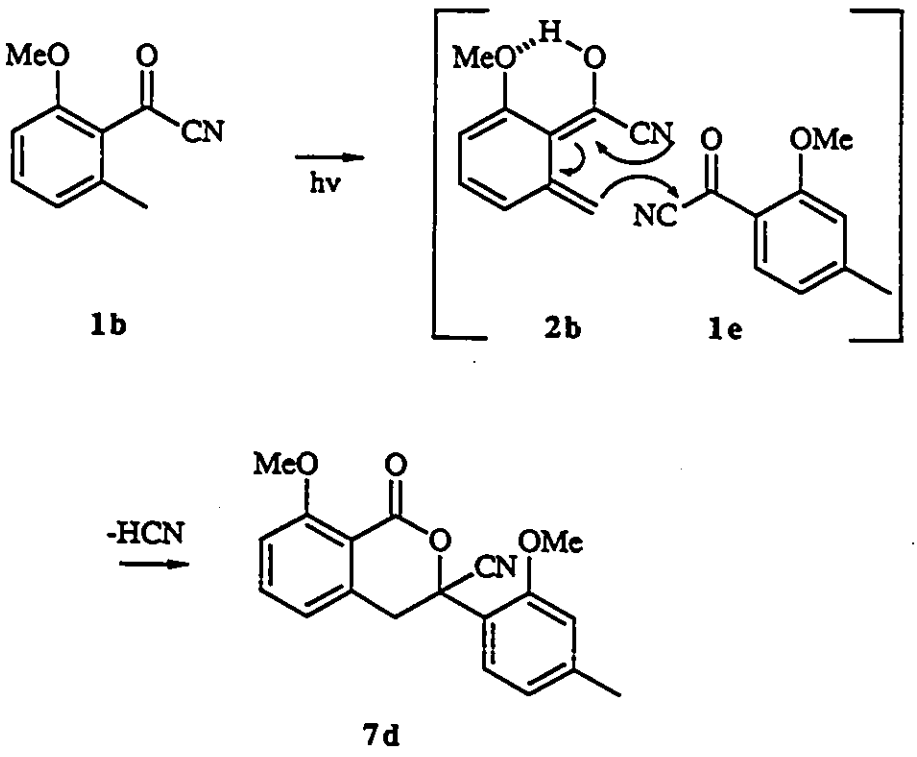


Scheme 6.11: Photoenolization of **1b** in the presence of **1e**

the signals at δ 3.91 and 3.96 ppm ascribed to the methoxy protons, showed characteristic signals at δ 2.36 (methyl hydrogens) and δ 3.56 ppm, the latter as an AB quartet with $J$ = 16.3 Hz assigned to the benzylic methylene hydrogens. The $^{13}$C-NMR spectrum (fig. 6.14) exhibited 19 signals, all consistent with the structural assignment. The most notable resonances occurred at δ 21.5 ppm (methyl carbon), the triplet at δ 38.2 ppm (benzylic methylene carbon), the singlet at δ 77.4 ppm (benzylic quaternary), and the singlet at δ 112.3 ppm (cyano carbon). All differed significantly from the corresponding signals for **6b**.

The final experiment in this section involved extension of the cycloaddition to alkyl carbonyl cyanide heterodienophiles. Indeed,

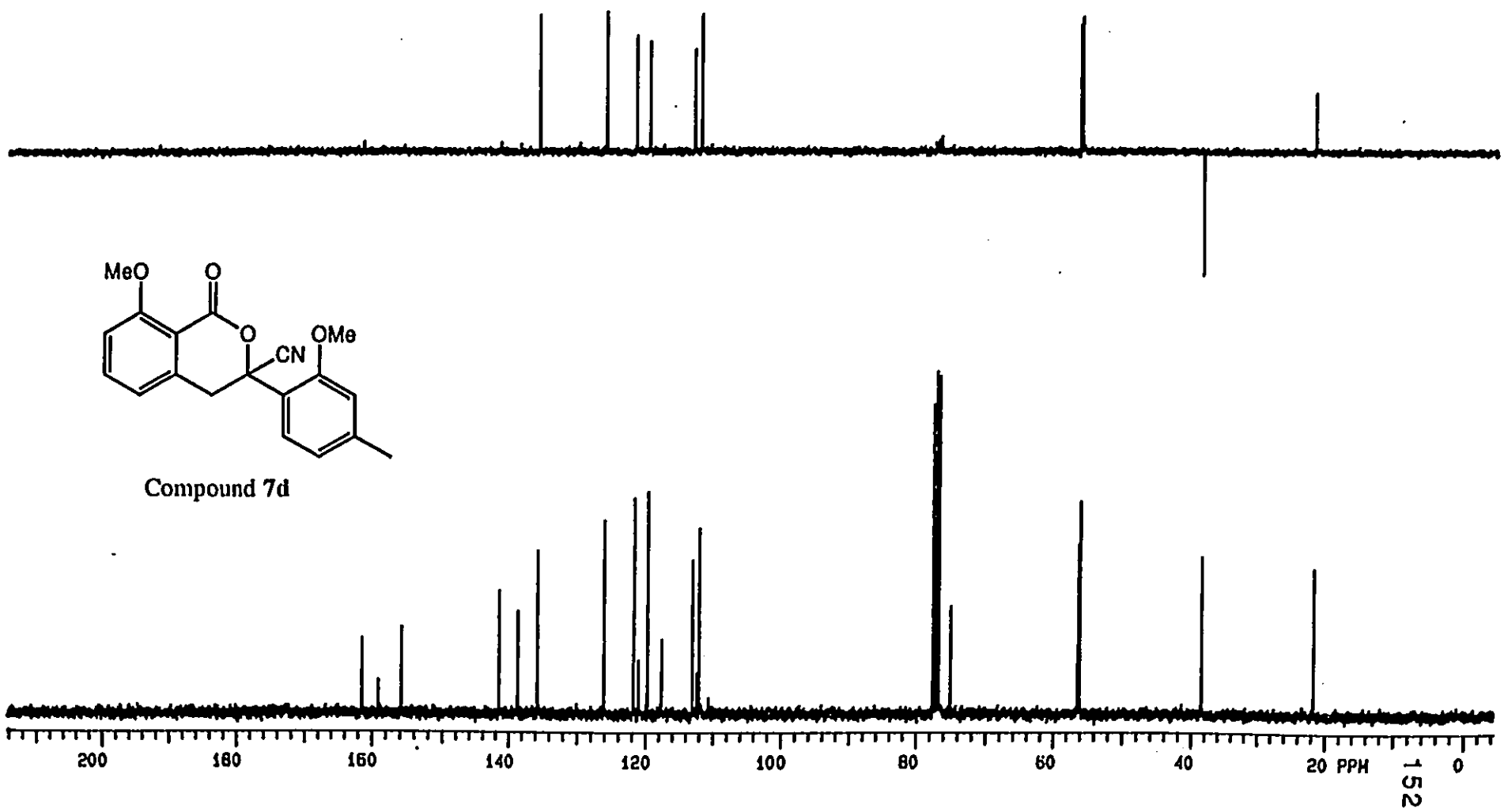


Compound **7d**

Figure 6.14: $^{13}$C-NMR of compound **7d**.

irradiation of an acetonitrile solution of **1a** and 2 eq of acetyl cyanide furnished, after flash chromatography, the adduct **7e** in 50 % yield (scheme 6.12).

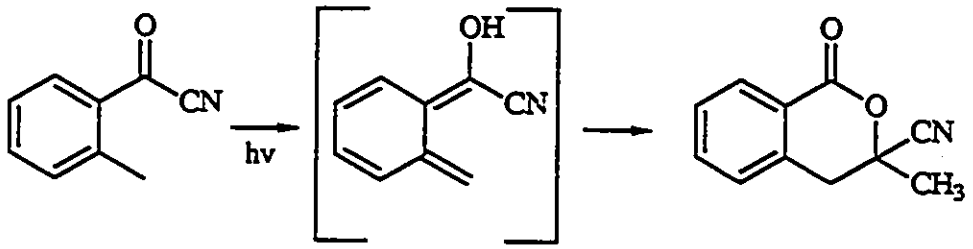


**1a** **2a** **7e**

Scheme 6.12: Photocycloaddition of 2a and acetyl cyanide

The infrared spectrum of cycloadduct **7e** (mp 98.0-100.0 °C) exhibited a diagnostic absorption at $\nu_{max}$ 1746 $cm^{-1}$ and, in keeping with all of the other cycloadducts in this class, showed no absorbance near $\nu_{max}$ 2220 $cm^{-1}$, the region corresponding to the cyano function. The proton and carbon NMR spectra (figures 6.15 and 6.16) were consistent with the assigned structure. The $^1$H-NMR spectrum in particular, showed the expected AB quartet centered at δ 3.29 ($J$ = 16.6 Hz) ppm, as well as a pronounced singlet at δ 1.94 ppm arising from the methyl hydrogens. The $^{13}$C-NMR spectrum showed the now familiar signals at δ 38.3 (t), 77.4 (s) and 118.5 (s) ppm attributed to the benzylic methylene, benzylic quaternary, and cyano carbons respectively.

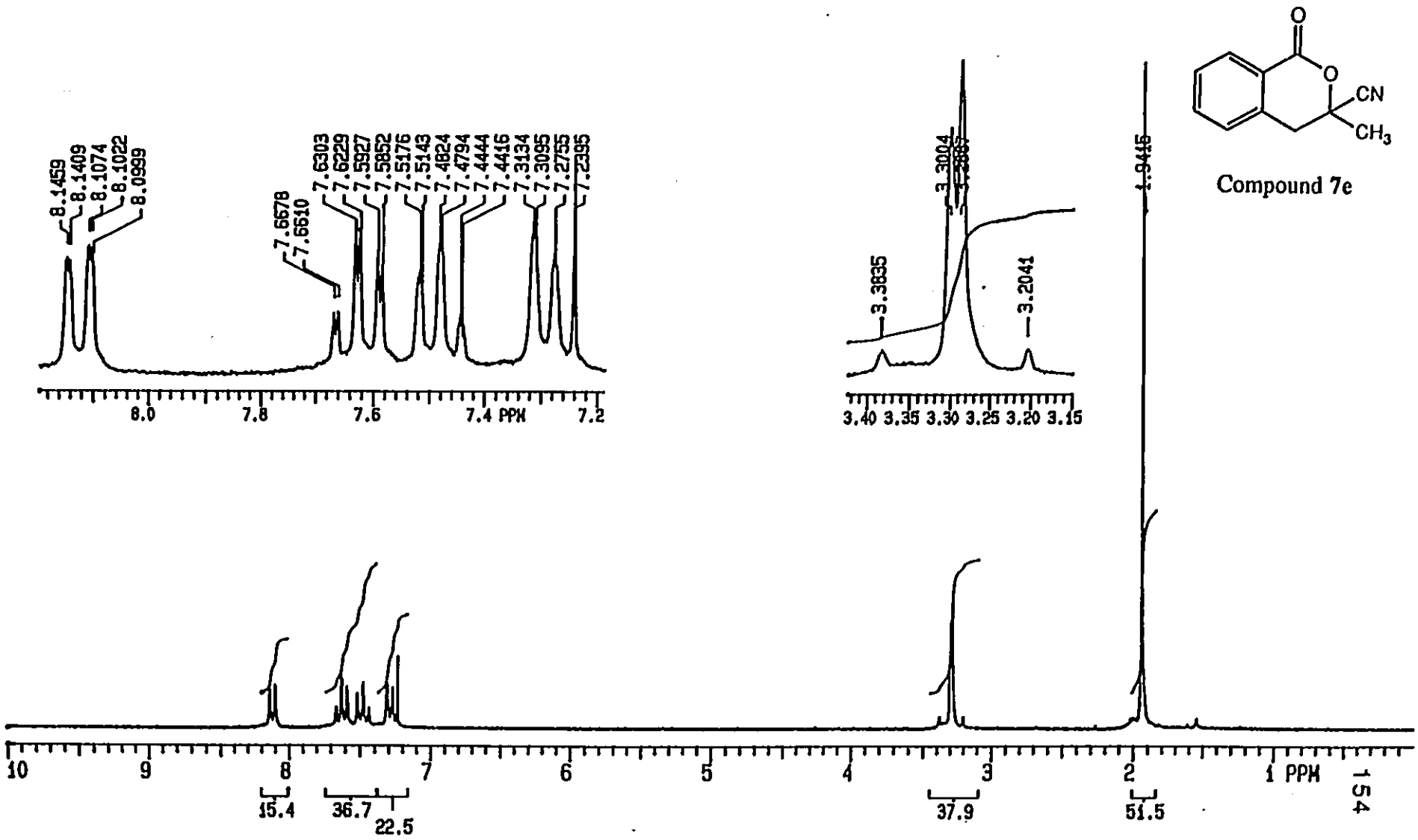


Figure 6.15: $^{1}$H-NMR of compound **7e**.

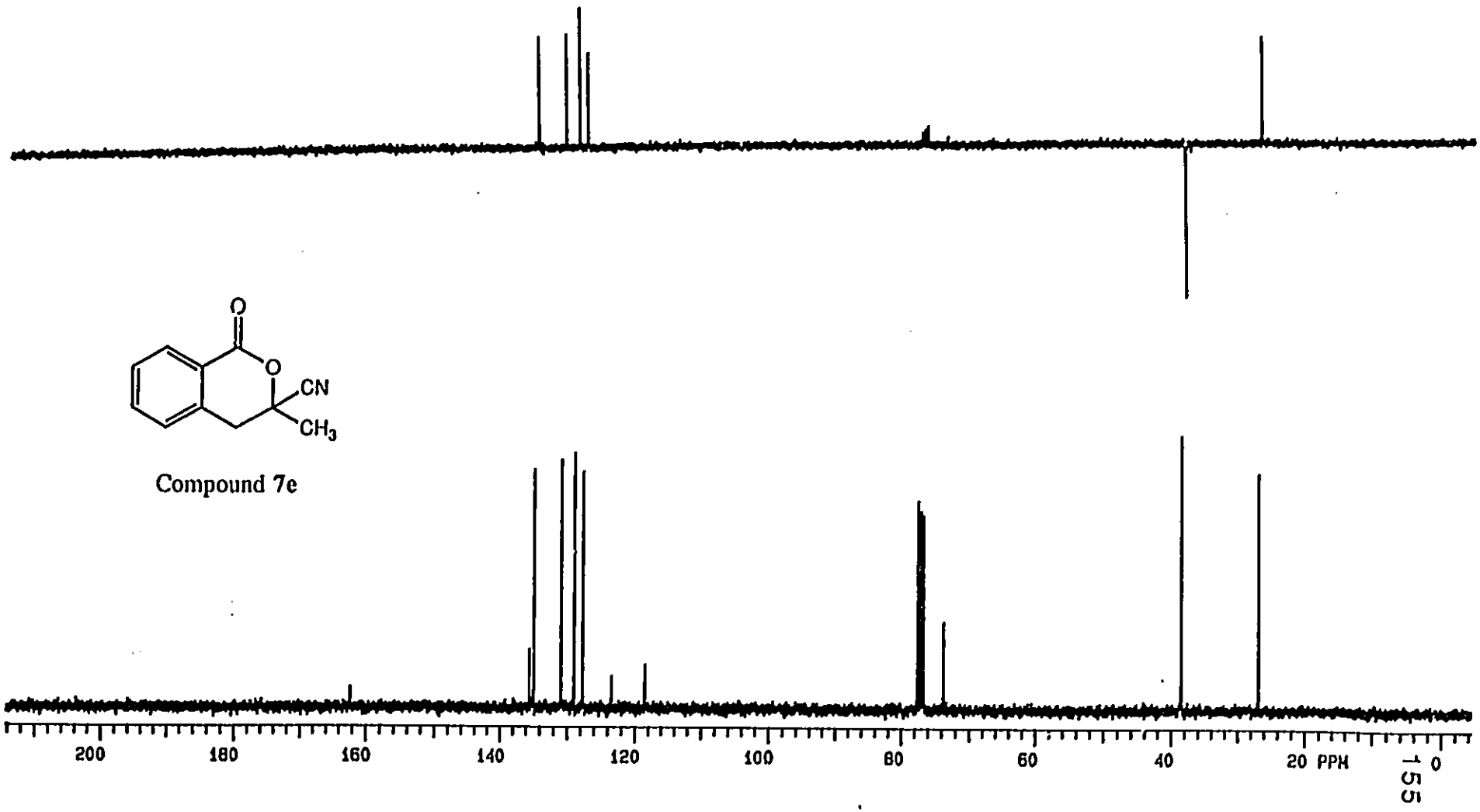


Figure 6.16: $^{13}$C-NMR of compound 7e.

## 6.5 Cycloaddition with thermally generated *o*-quinodimethanes

The previous sections have firmly established the facility with which aromatic and alkyl acyl cyanides act as heterodienophiles in Diels-Alder reactions with photochemically generated *o*-quinodimethanes. As was described in chapter 3, *o*-quinodimethanes can also be generated by thermal processes such as extrusion reactions. In the interest of further substantiating the proposed pericyclic [4+2] mechanism, and diversifying the synthetic potential of the acyl cyanide cycloaddition, attention was next directed to studying the facility of these compounds to act as heterodienophiles with thermally generated *o*-quinodimethanes.

Recalling the cycloaddition of photochemically generated **2a** and benzoyl cyanide described in the previous section, one can envision the mechanism as a concerted [4+2] cycloaddition between the E-*o*-quinodimethane and benzoyl cyanide (scheme 6.13). Alternatively, it is also possible that the process may occur in a stepwise fashion proceeding first to a zwitterionic intermediate, then, undergoing ring closure and HCN loss, forming the final product **7a**.

In an effort to discriminate between these two processes, some means of assessing the degree to which the cationic moiety of the zwitterionic intermediate undergoes free rotation would be desirable. This information could be aquired if an E,E-α,α'-disubstituted-*o*-quinodimethane was employed in a cycloaddition with benzoyl cyanide,

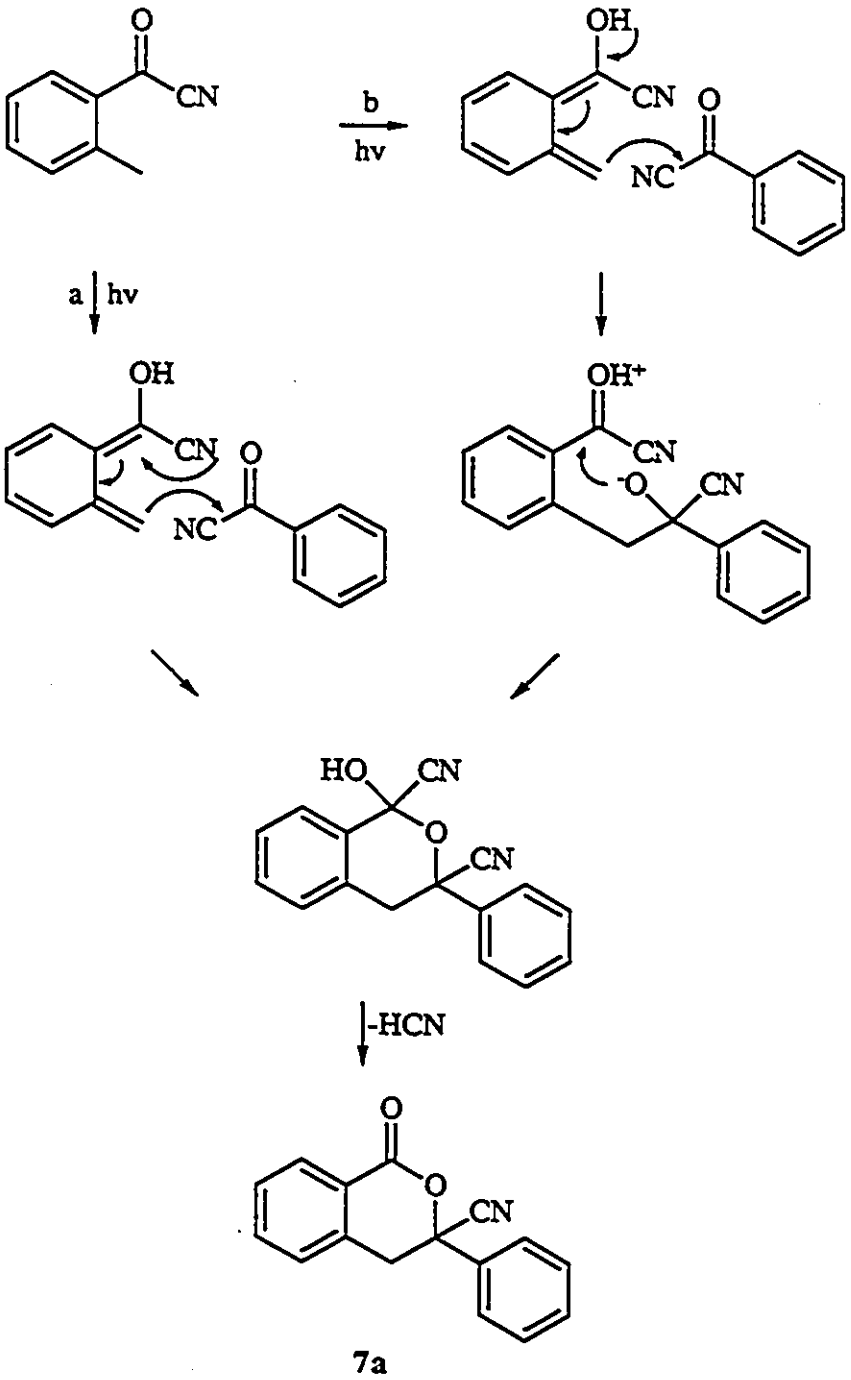


7a

Scheme 6.13: Proposed mechanistic pathways leading to 7a:
a) Concerted mechanism b) Stepwise mechanism

followed by determination of the diastereomer distribution of the cycloadducts. Charlton and Durst[56] have described the use of *cis*-1-

methoxy-3-phenyl-1,3-dihydrobenzo[c]thiophene 2,2-dioxide (8a) (scheme 6.14) as an *o*-quinodimethane precursor. Sulfone **8a**, when heated to reflux in benzene or cyclohexane solution , extrudes $SO_2$ suprafacially forming the α,α'-disubstituted-E,E-*o*-quinodimethane **9a**. Cycloaddition of **9a** with benzoyl cyanide should, if a concerted mechanism were operative, lead to two diastereomeric adducts with the endo adduct, due to secondary orbital interactions between **9a** and the cyano π-orbitals, predominating. In addition, the phenyl and methoxy groups would be expected to possess a syn relationship in both cycloadducts.

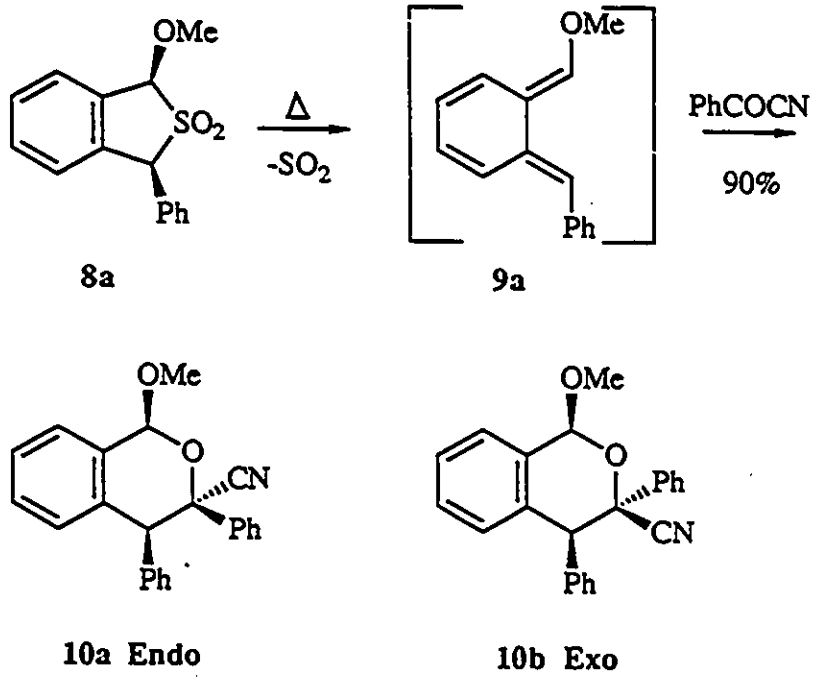


Scheme 6.14: Cycloaddition of **9a** with benzoyl cyanide

As depicted in scheme 6.14, thermolysis of a cyclohexane solution of **8a** and 2 eq of benzoyl cyanide afforded a 3:1 ratio of adducts **10a** (endo) and **10b** (exo) in 90 % yield.

Compound **10a** (mp 237.2-238.4 °C) readily recrystallized from dichloromethane/hexane, yielding colorless crystals, and gave a prominent molecular ion in its CIMS at m/e 342. The $^{1}$H-NMR spectrum (fig. 6.17) , in addition to the downfield signals arising from the aryl hydrogens, showed singlets at δ 3.83 ppm, ascribed to the methoxy protons, δ 4.36 ppm, attributed to the southern benzylic hydrogen, and δ 6.23 ppm, assigned to the acetal proton. The $^{13}$C-NMR spectrum (fig. 6.18) exhibited 19 signals representing 23 carbons, as expected considering the symmetry present in the pair of monosubstituted benzene appendages. Key signals included two methine carbons at δ 54.8 and 101.0 ppm, assigned to the southern and northern benzylic carbons, and peaks at δ 57.4 ppm, attributed to the methoxy carbon, and at δ 76.6 and 119.4 ppm, due to the benzylic quaternary and cyano carbons respectively. The syn relationship between the benzylic methoxy and phenyl moieties was unambiguously established by means of an X-ray structure determination[69] which is illustrated in figure 6.19. The ORTEP diagram clearly shows the *cis* relationship of the phenyl appendages, and the syn positioning of the methoxy and benzylic aryl groups, confirming that the endo isomer had predominated in the cycloaddition.

Compound **10b** (mp 123.5-124.8 °C) was tentatively assigned the structure indicated in scheme 6.14. Adduct **10b** gave a less prominent molecular ion in its CIMS (m/e 342), but exhibited a larger fragment at m/e 315 (-HCN) suggesting an anti relationship between the benzylic hydrogen and the cyano group. The $^{1}$H-NMR spectrum (fig. 6.20) was similar to that of **10a**, but showed upfield shifts for both the acetal and methoxy hydrogens. The *cis*-phenyl rings of compound **10a** (fig.

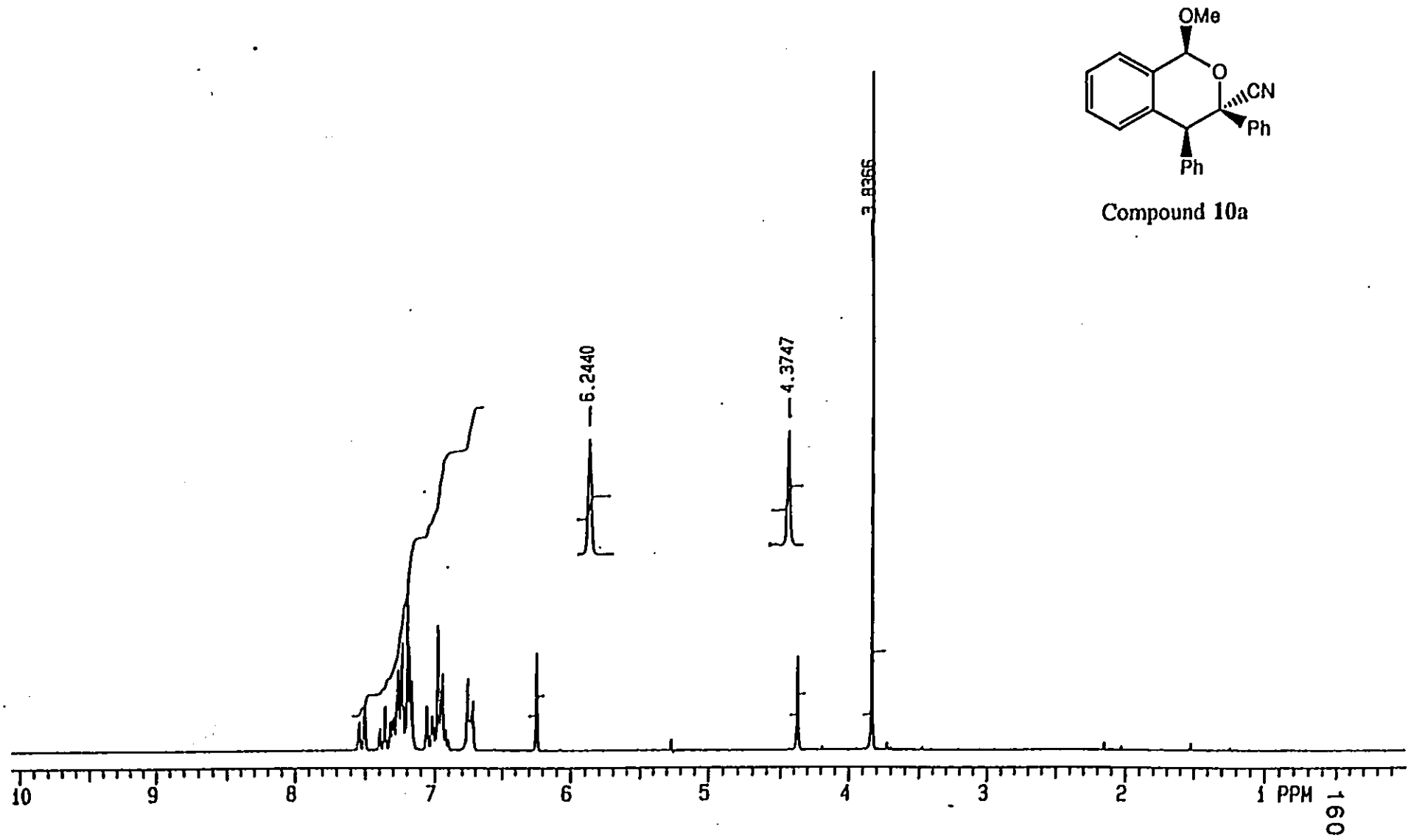


Figure 6.17: $^{1}$H-NMR of compound **10a**.

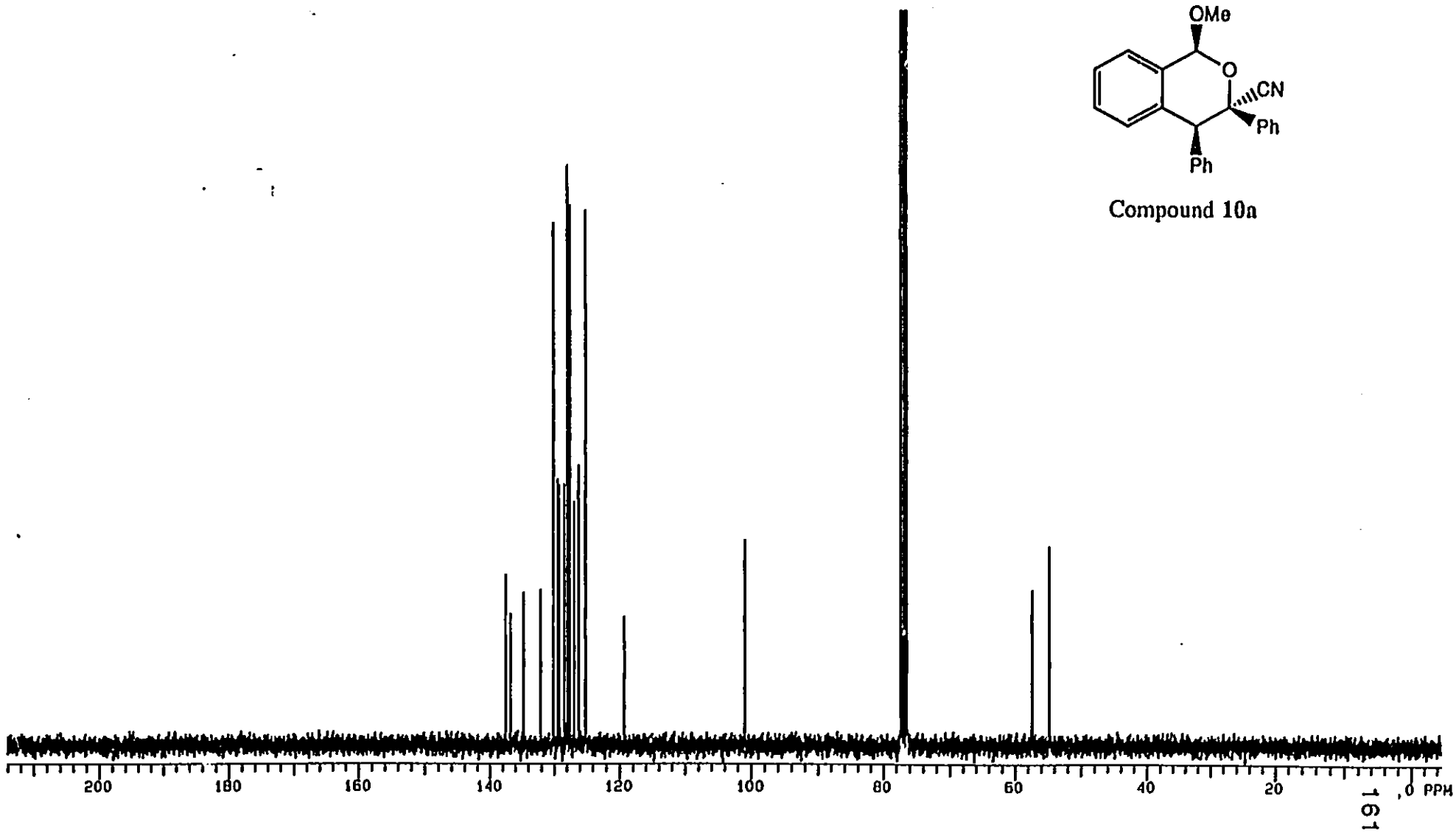


Figure 6.18: $^{13}$C-NMR of compound **10a**.

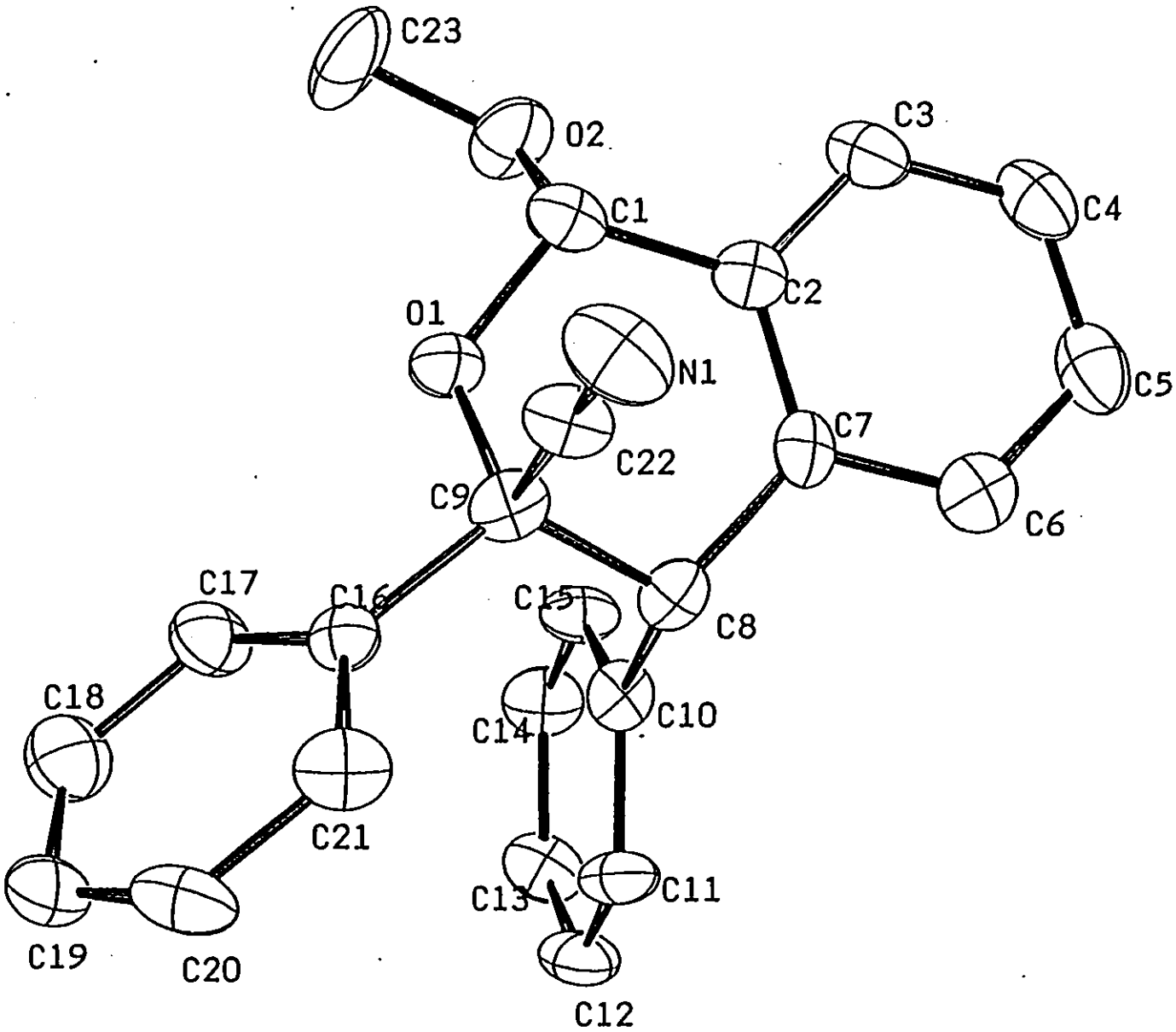


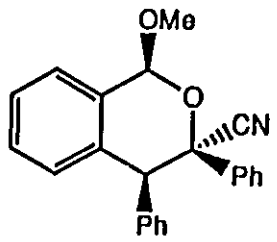


Compound **10a**

Figure 6.19: ORTEP diagram of compound **10a**.

6.19) are positioned such that the methoxy and the acetal hydrogens are deshielded. The upfield shifts of the methoxy and acetal hydrogens observed for **10b** would be expected if the phenyl rings were trans and could freely rotate. The $^{13}$C-NMR spectrum (fig. 6.21) also showed signals analogous to those present for **10a**, all in agreement with the assigned structure.

The exclusive formation of only two diastereomers (**10a** and **10b**) clearly supports the concerted mechanism. Had the stepwise mechanism been in operation, two additional diastereomers (1,4-trans) would have accompanied **10a** and **10b**.

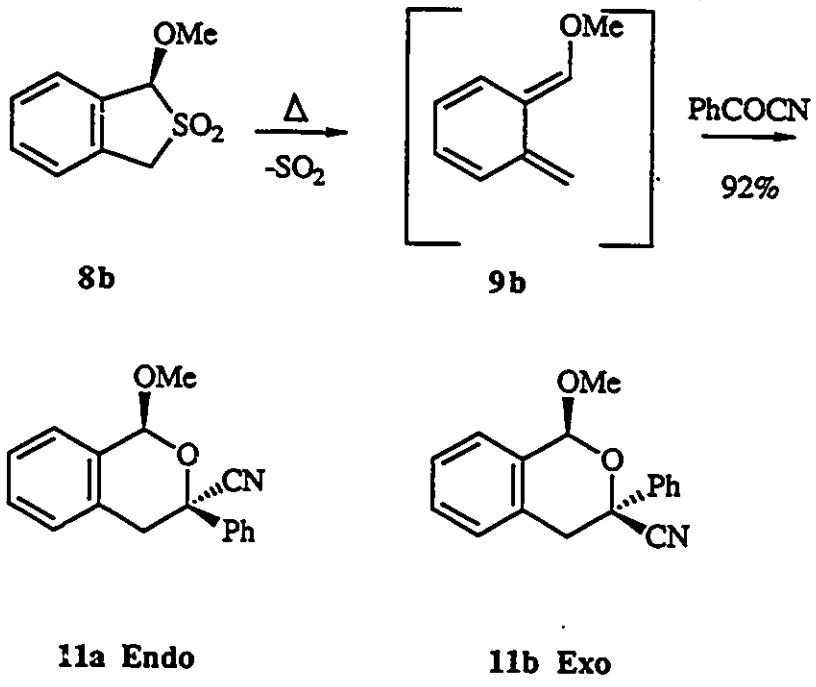


Scheme 6.15: Cycloaddition of **9b** with benzoyl cyanide

The *o*-quinodimethane obtained by thermolysis of 1-methoxy-1,3-dihydrobenzo[c]thiophene 2,2-dioxide **8b** (scheme 6.15) has also been

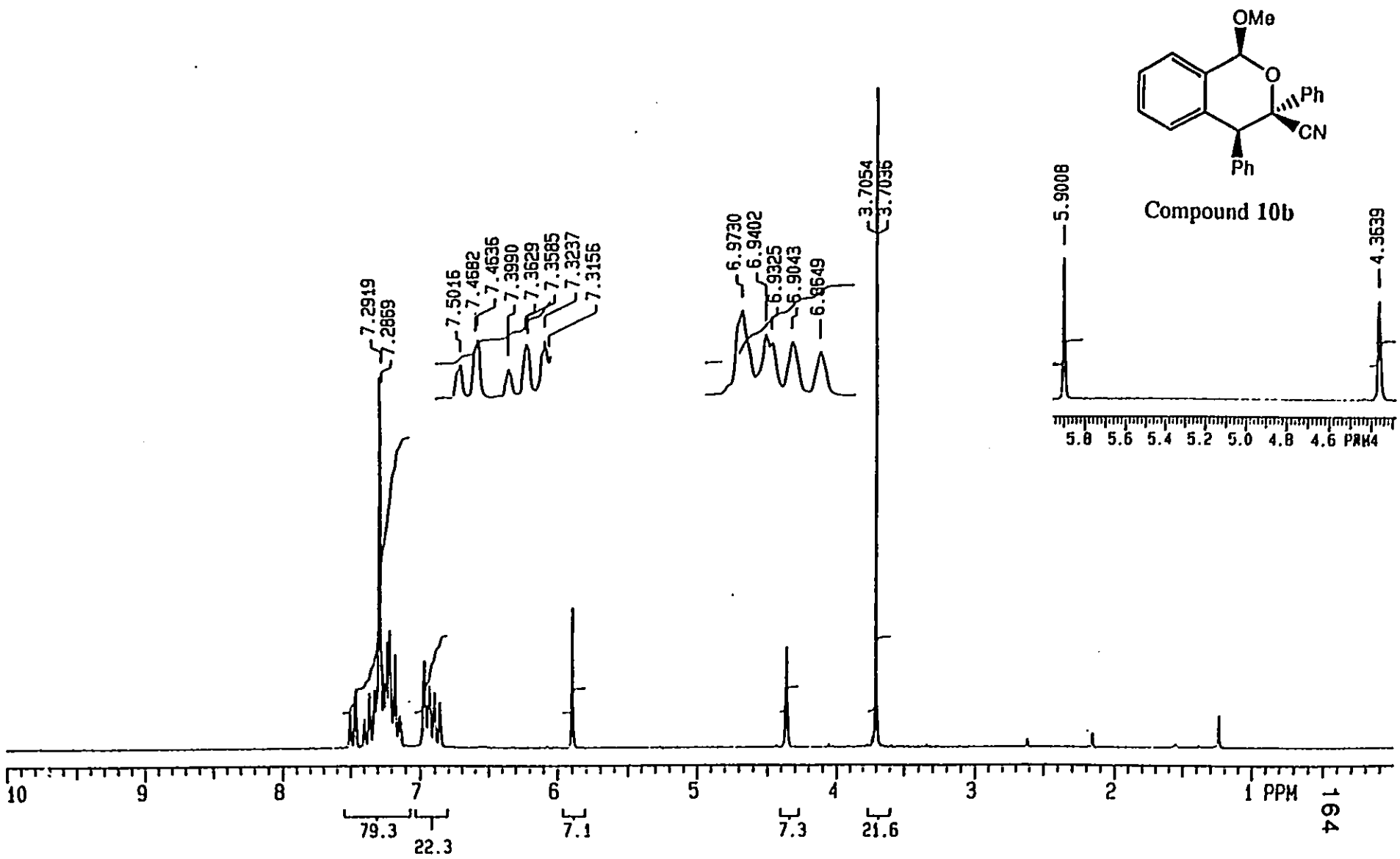


Figure 6.20: $^{1}$H-NMR of compound 10b.

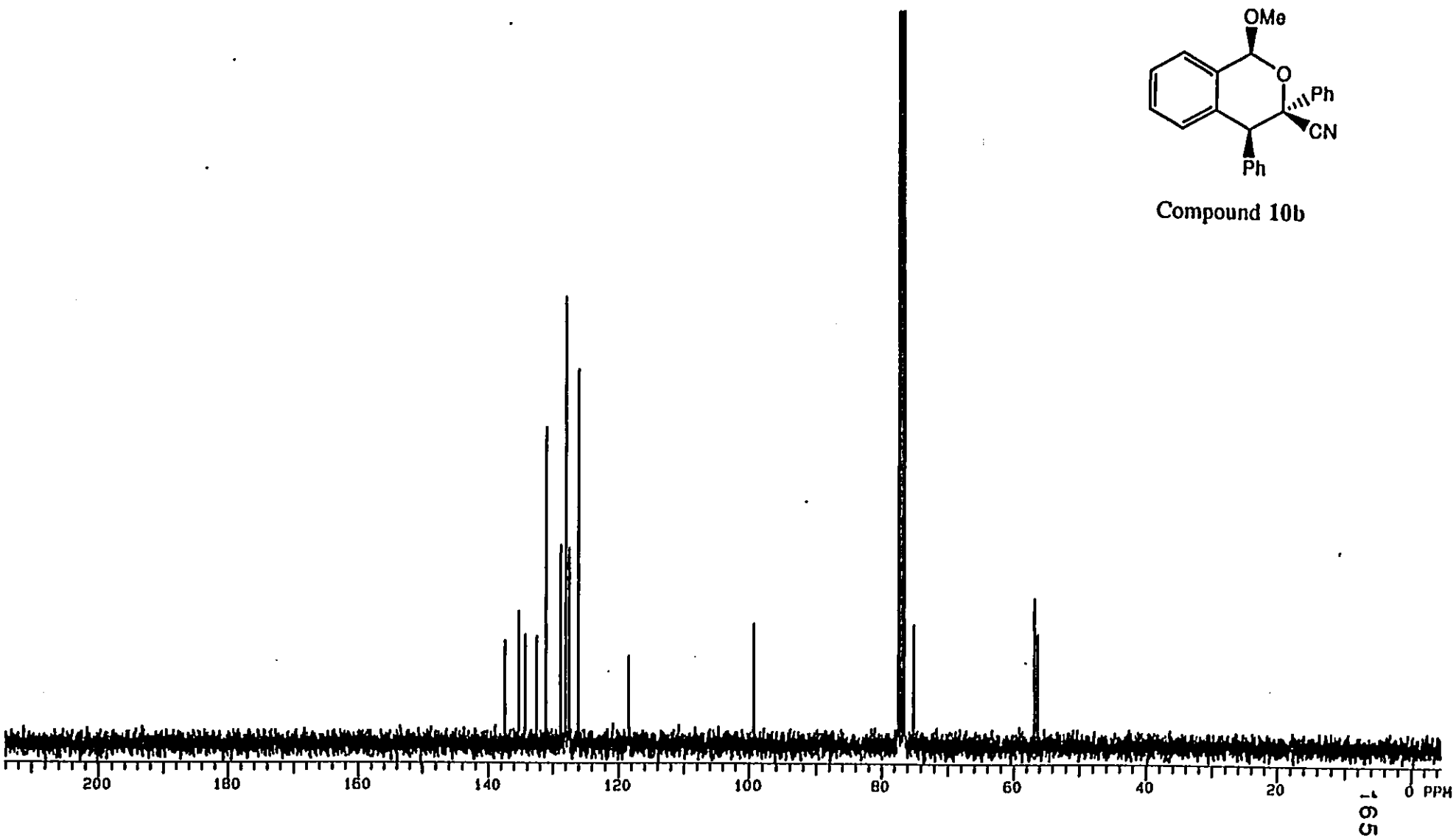


Compound 10b

Figure 6.21: $^{13}$C-NMR of compound 10b.

studied by Charlton and Durst.[56] Though less useful from a mechanistic viewpoint, **8b** was efficiently trapped by benzoyl cyanide affording a 3:1 ratio of the diastereomeric adducts **11a** and **11b** in 92 % yield.

Compounds **11a** (mp 80.1-82.6 °C), the endo adduct, and **11b** (mp 91.8-92.6 °C), the exo product, both presented spectral data (CIMS, IR, $^1$H-NMR) in accord with the structural assignments. The $^1$H-NMR spectrum of **11a** is illustrated in figure 6.22.

Acetyl cyanide, which was successfully reacted with photoenol **2a**, was found to react with the thermally generated *o*-quinodimethane **9b** furnishing a 2:1 ratio of the adducts (unseparated) **12a** and **12b** in 70 % yield after flash chromatography. The diastereomeric pair was identified readily by examination of the $^1$H-NMR spectrum which showed a pair of AB quartets centered at δ 3.10 ($J$ = 16.1 Hz) and 3.06 ($J$ = 15.6 Hz) ppm, ascribed to the benzylic methylene hydrogens, two singlets at δ 3.54 and 3.65 ppm, arising from the methoxy protons, and two singlets at δ 1.76 and 1.79 ppm, attributed to the methyl hydrogens.

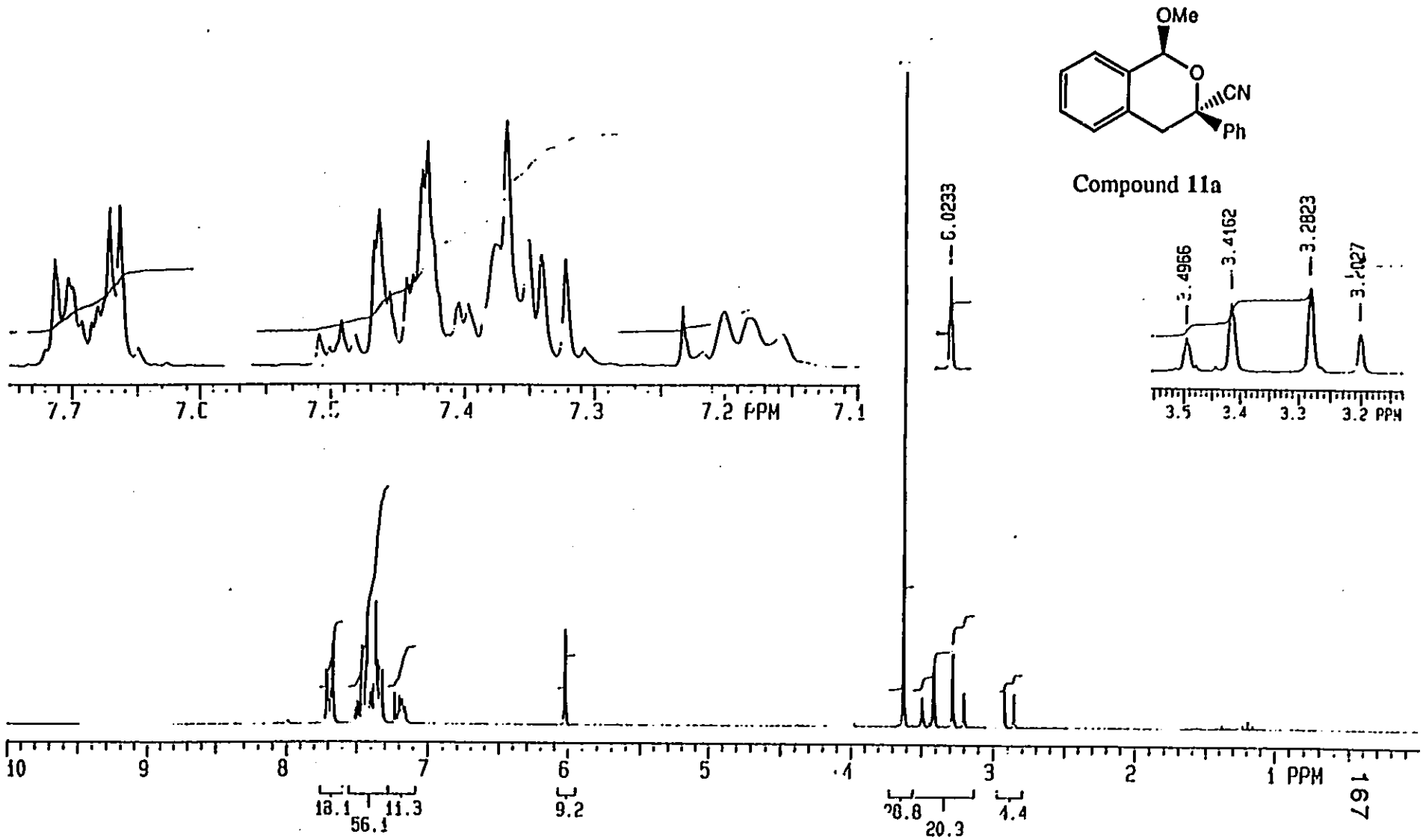


Figure 6.22: $^{1}$H-NMR of compound 11a.

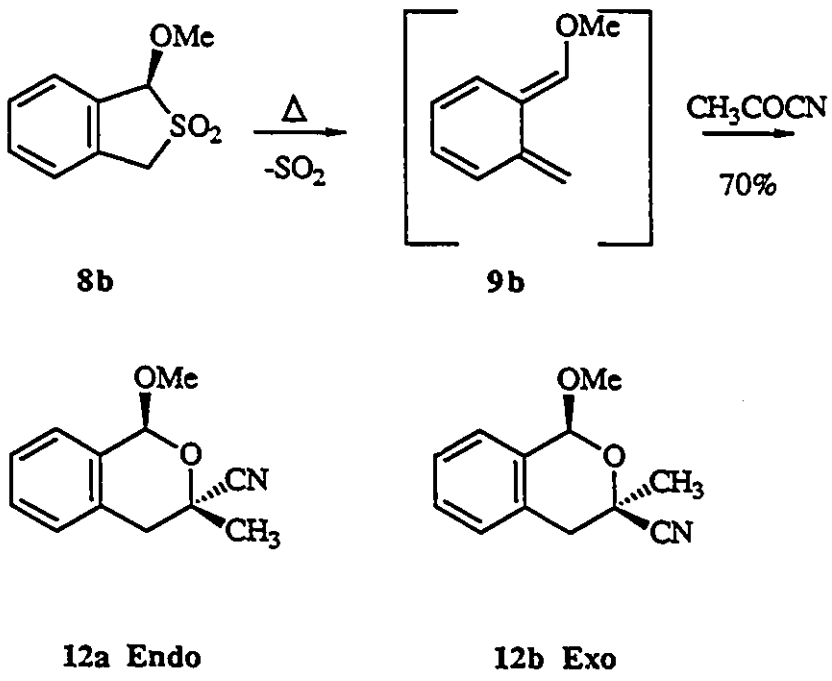


Scheme 6.16: Cycloaddition of **9b** with acetyl cyanide

## 6.6 Relative reactivity and competition experiments

The next set of experiments was designed to assess the relative reactivity of the aroyl cyanides, compared to other hetero and carbogenic dienophiles, in cycloadditions with thermally generated *o*-quinodimethanes. Typically, the regime involved thermolysis of a toluene solution of 1-methoxy-1,3-dihydrobenzo[c]thiophene 2,2-dioxide (**8b**), 1 eq of benzoyl cyanide, and 1 eq of a competitive dienophile and then assessing the product ratio by $^1$H-NMR, or by a combination of GC and GC-MS.

Competitions involving reactive dienophiles such as dimethyl fumarate led, not unexpectedly, to the exclusive formation of tetralins, as assessed by GC-MS.

Two competition experiments involving heterodienophiles were undertaken with benzaldehyde and phenylglyoxal. Thermolysis of a toluene solution of 1-methoxy-1,3-dihydrobenzo[c]thiophene 2,2-dioxide in the presence of one eq each of benzoyl cyanide and benzaldehyde led to the exclusive formation of the cyano adducts **11a** and **11b**, as determined by examination of the crude $^1$H-NMR spectrum. Prior to the competition experiment with phenylglyoxal, it was necessary to determine if the α-ketoaldehyde was capable of reacting with **9b**.

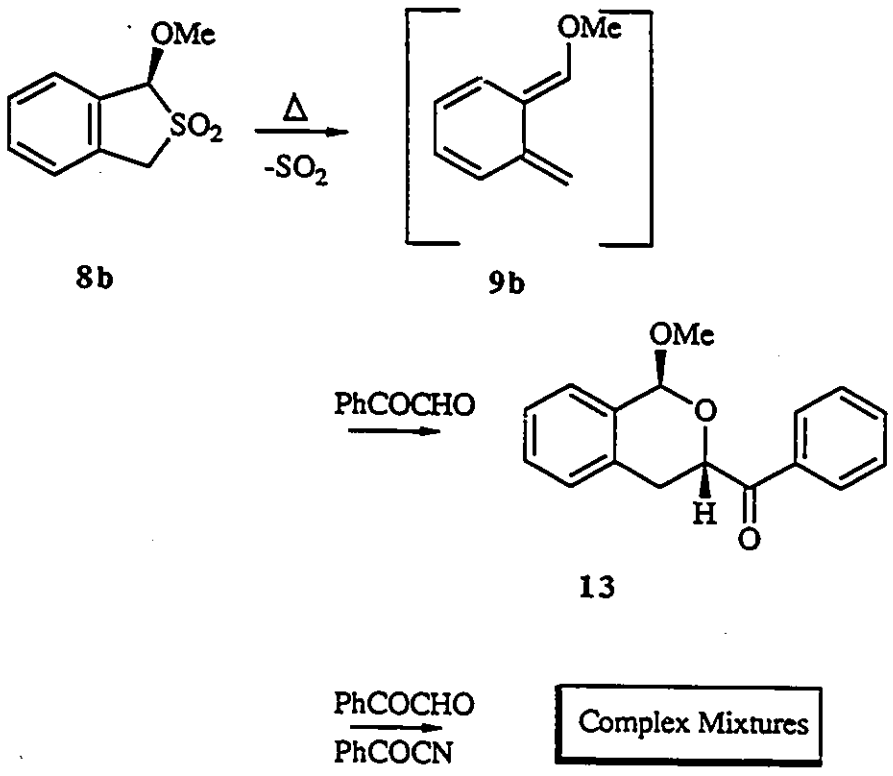


Scheme 6.17: Competition between phenylglyoxal and benzoyl cyanide

Indeed, thermolysis of a toluene solution of phenylglyoxal and **8b** led to the isolation of compound **13** in 28 % yield, after flash

chromatography. Thermolysis of a toluene solution of **8b** in the presence of 1 eq each of benzoyl cyanide and phenylglyoxal, however, led to complex mixtures of products with none of the adducts **11a**, **11b** or **13** being detected by GCMS.

The next series of experiments, as depicted in scheme 6.18, was undertaken to assess the effect of *o*-substitution on the reactivity of the aroyl cyanides as heterodienophiles.

Reflux of a toluene solution of **8b** and **1a** (1.5 eq) gave the adduct **14** (two diastereomers) in 42 % yield, after flash chromatography. The CIMS of the diastereomeric pair (**14a** and **14b**) exhibited a prominent $[M+1]^+$ ion (m/e 280), as well as a major fragment (m/e 253) corresponding to a loss of HCN. The $^1$H-NMR spectrum of the mixture (fig. 6.23) also supported the structural assignment showing two pronounced AB quartets centered at δ 3.52 ($J$ = 15.9 Hz) and 3.50 ($J$ = 15.8 Hz) ppm, ascribed to the benzylic methylene protons, four singlets at δ 2.68, 2.70, 3.60, and 3.76 ppm, attributed to the methyl and methoxy hydrogens, and two additional singlets at δ 5.78 and 6.11 ppm, assigned to the acetal protons.

In view of the modest yield recorded for the cycloaddition of **9b** and aroyl cyanide **1a**, it was expected that **1b**, being 2,6-disubstituted, would afford marginal results at best. This proved to be the case as reflux of a toluene solution of **8b** and **1b** led to the recovery of unreacted **1b**, accompanied by polymeric tar. Presumably, in contrast to the photochemical reactions, the presence of two *o*-substituents was sufficient to preclude cycloaddition.

Compound **1e**, possessing only a single ortho substituent, was expected to afford results similar to **1a**, however, reflux of a toluene

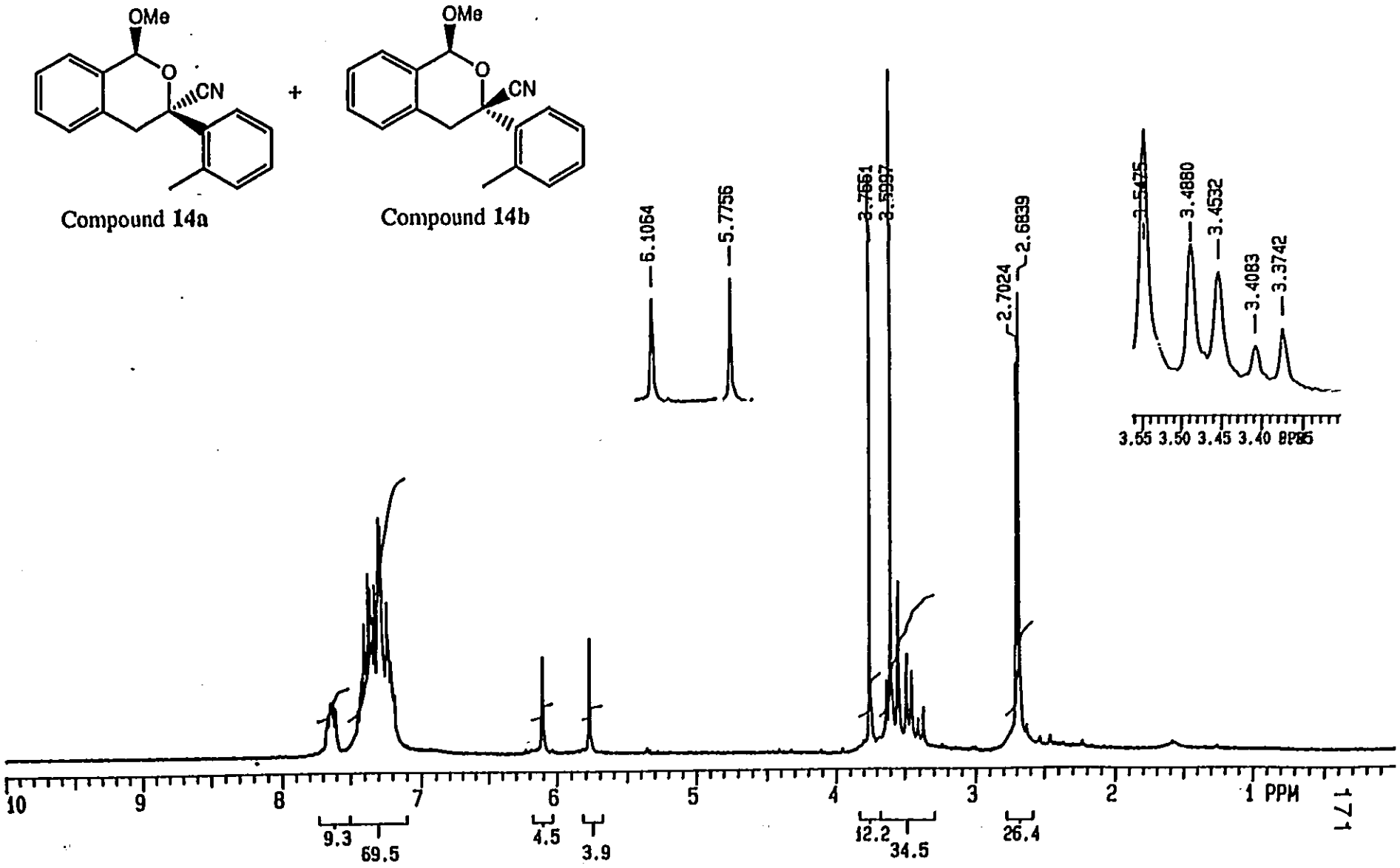


Figure 6.23: $^{1}$H-NMR of compounds **14a** and **14b**.

solution of **8b** and **1e** lead to the isolation of only minute quantities of adduct **15**.

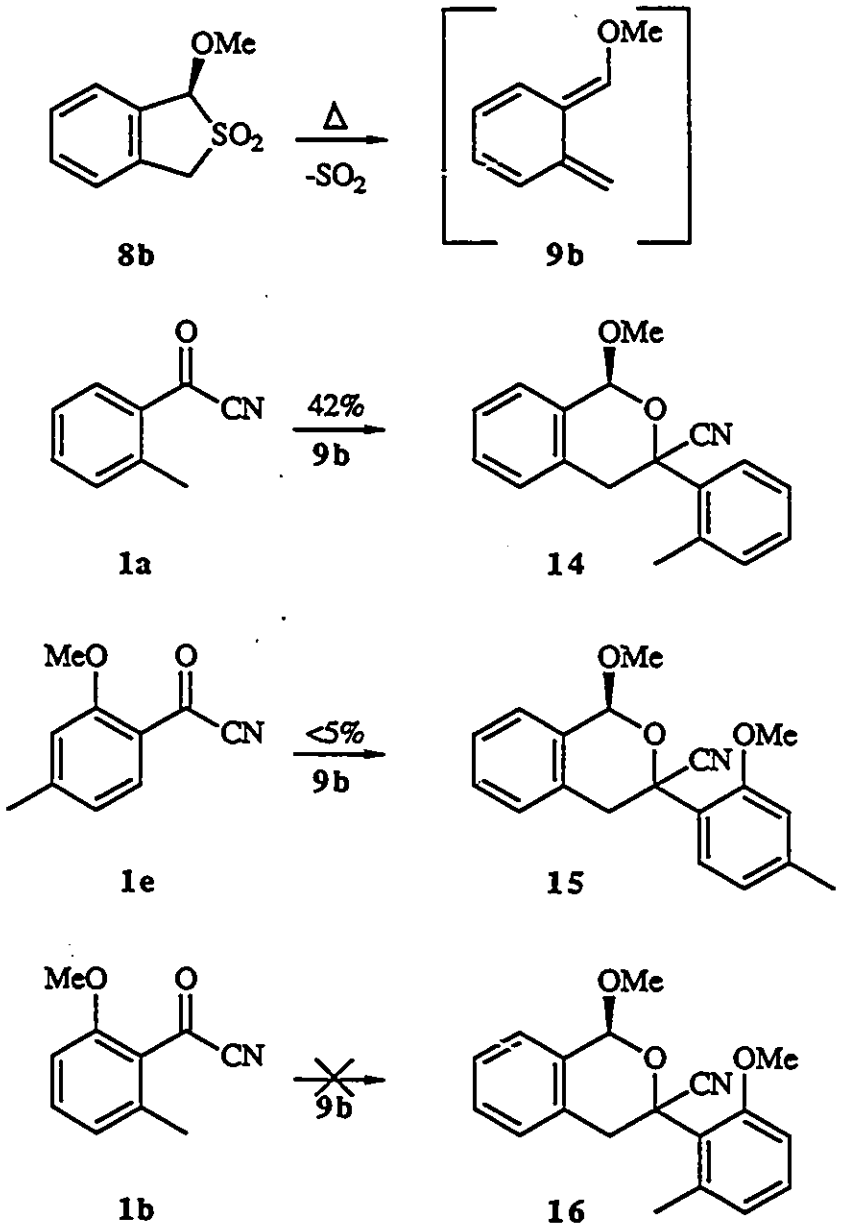


Scheme 6.18: Effect of *o*-substitution on heterodienophile reactivity

This apparent incongruity may be explained if one considers the known acid sensitivity of intermediate **9b**.[70] Aroyl cyanide **1e**, possessing electron donating groups in both the ortho and para positions, may have hydrolysed to the extent that significant acid impurity accumulated, quenching **9b** to give *o*-tolualdehyde, and thereby precluding cycloaddition.

The last set of experiments in this section involved a return to the photochemically generated *o*-quinodimethane **2a**.

Kessar[66] has reported that the *o*-((trimethylsilyl)methyl)benzoyl derivative **17**, upon fluorodesilylation in the absence of a dienophile, affords **18**. The mechanism proposed involved a

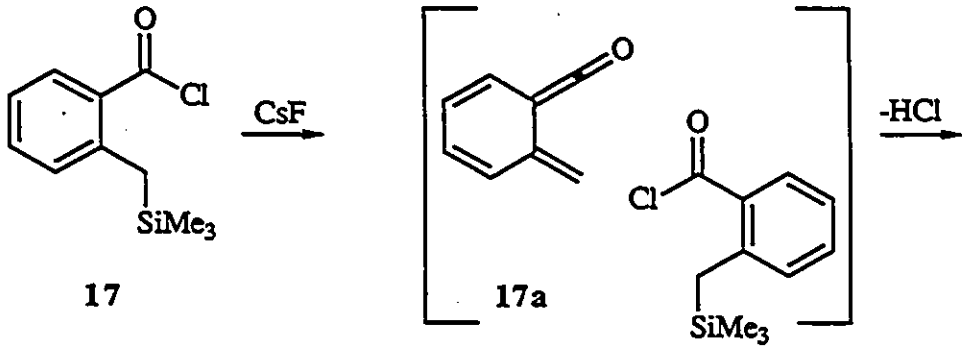


**17** **17a**

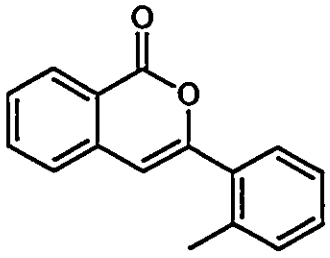


**18**

Scheme 6.19: Kessar's dimerization sequence

hetero Diels-Alder reaction between ketene **17a** and unreacted **17**, followed by HCl loss and desilylation giving **18**. Alternatively, **17** may be attacked by the benzylic anion preceding **17a**, followed by intramolecular cyclization.

Given the comparable reactivity of benzoyl cyanide and chloride as acylating agents, it seemed a reasonable extension that the latter should also undergo cycloaddition with **2a**. Irradiation of an acetonitrile solution of **1a** and benzoyl chloride, however, slowly produced only the **1a** dimer. The low apparent quantum efficiency observed for the dimerization was likely a result of acidic impurities which are known to catalyse photoenol reketonization.

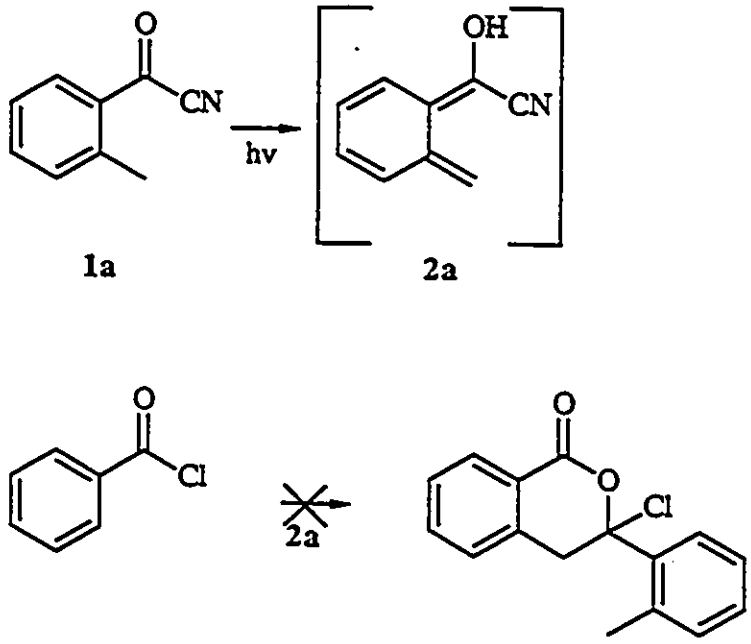


Scheme 6.20: Attempted Cycloaddition of 2a and benzoyl cyanide

The same reaction conditions were applied with three other acylating reagents as well (scheme 6.21). In each case, examination of

the $^1$H-NMR spectra of the crude reaction mixtures suggested that only the dimer **6a** had formed, and that no mixed cycloadditions had occurred. Closer examination of the $^1$H-NMR spectrum of the benzoyl

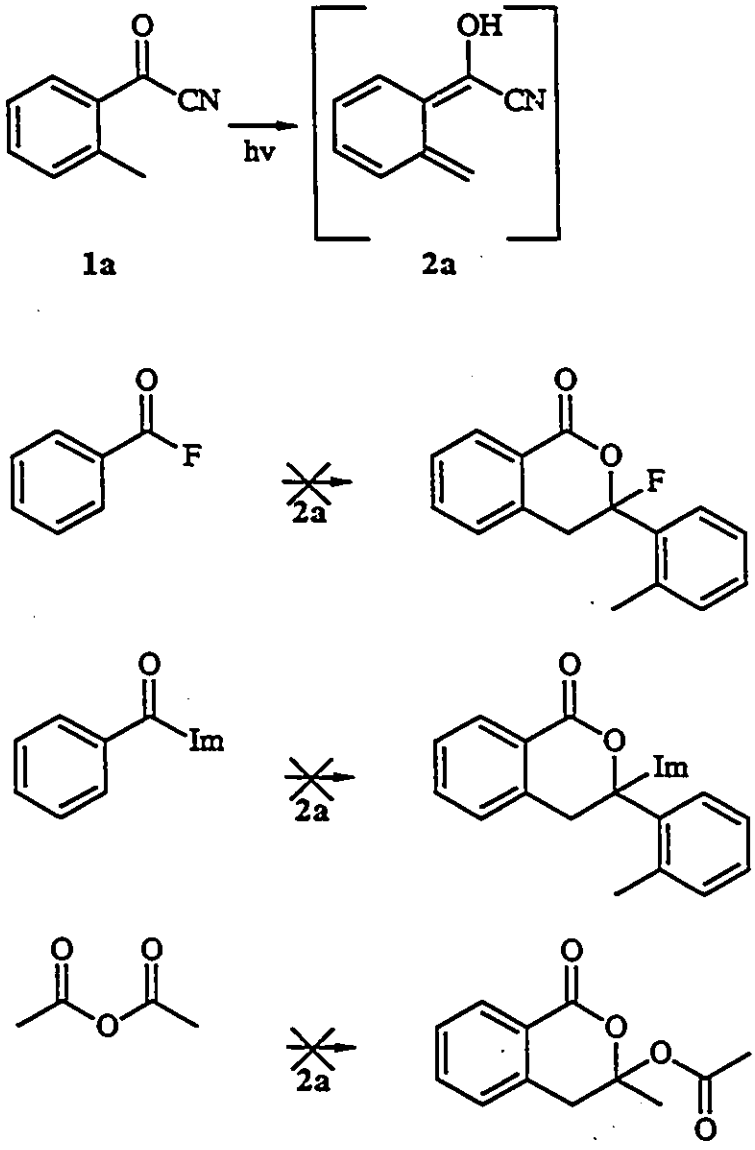


Scheme 6.21: Attempted cycloaddition of 2a with benzoyl fluoride, benzoyl imidazole and acetic anhydride

fluoride run, however, revealed a small AB quartet adjacent to the AB system arising from **6a** (fig. 6.24) indicating that competitive cycloaddition (< 10%) to the aroyl fluoride may have occurred. It was also of note that in each case the dimerization had proceeded to completion, likely because of the reduced capacity for the latter three acylating agents to produce acidic by-products.

## 6.7 Sulfur dioxide trapping experiments

The use of 1,3-dihydrobenzo[c]thiophene 2,2-dioxides as *o*-quinodimethane precursors (vide infra) has been well documented in the literature. The 1-hydroxy derivatives, in particular, are readily obtained by irradiation of *o*-alkyl aldehydes and ketones in the presence of $SO_2$.[55,71]

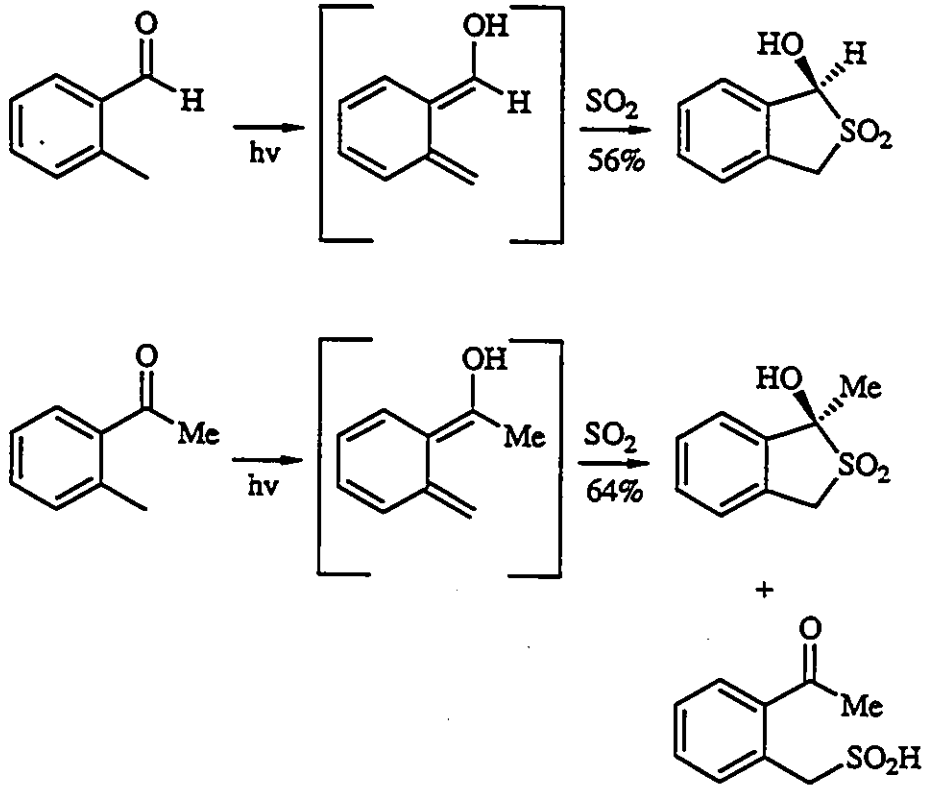


Scheme 6.22: Charlton and Durst's α-oxygenated benzothiophenedioxides

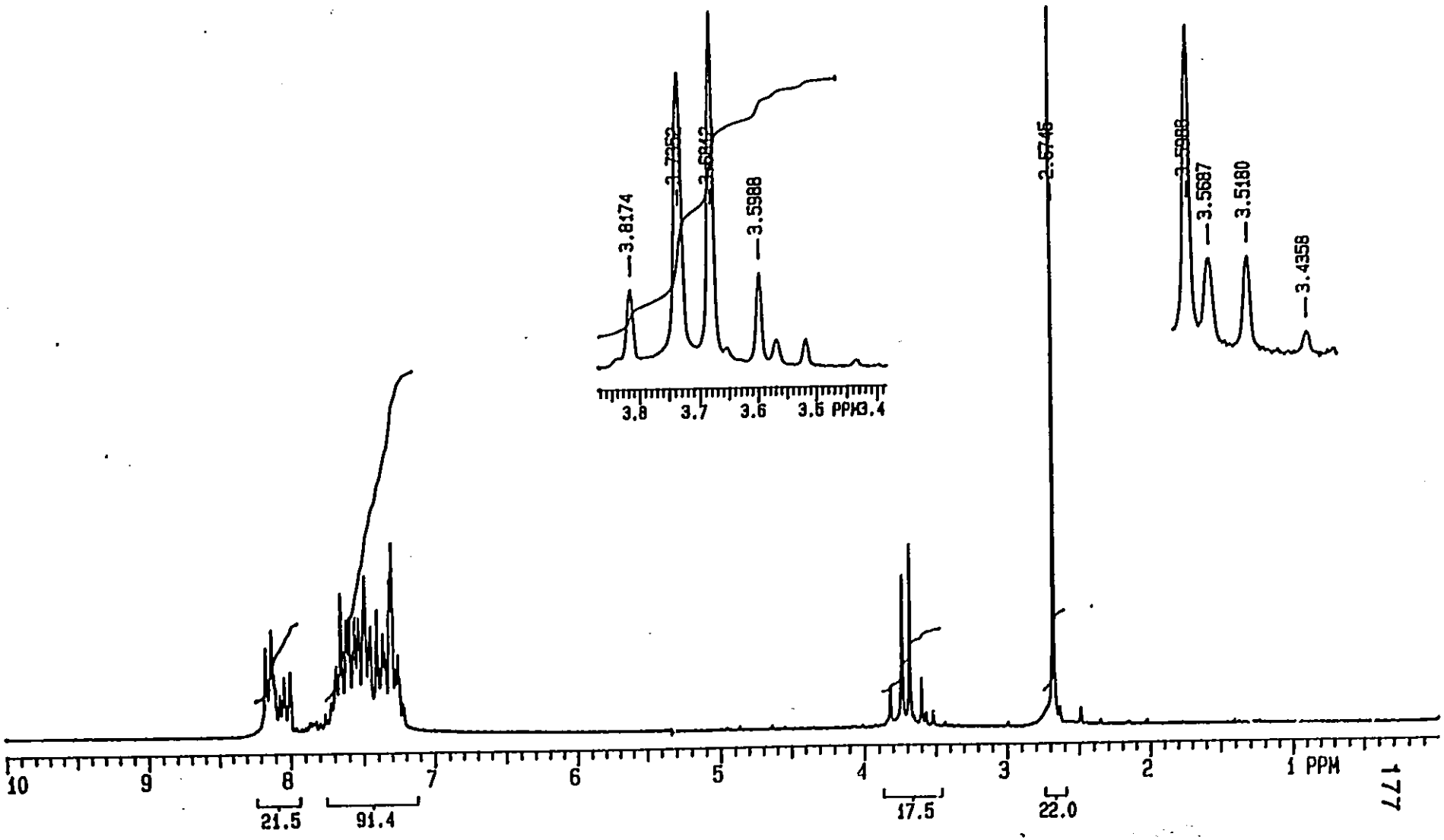


Figure 6.24: $^{1}$H-NMR of cycloaddition of 2a and benzoyl fluoride.

The parallel between the above examples and photoenol **2a** was obvious and in the event, irradiation of a $SO_2$ saturated benzene solution of **1a** resulted in the deposition of a light brown precipitate, whose analytical and spectral properties indicated structure **19a**.

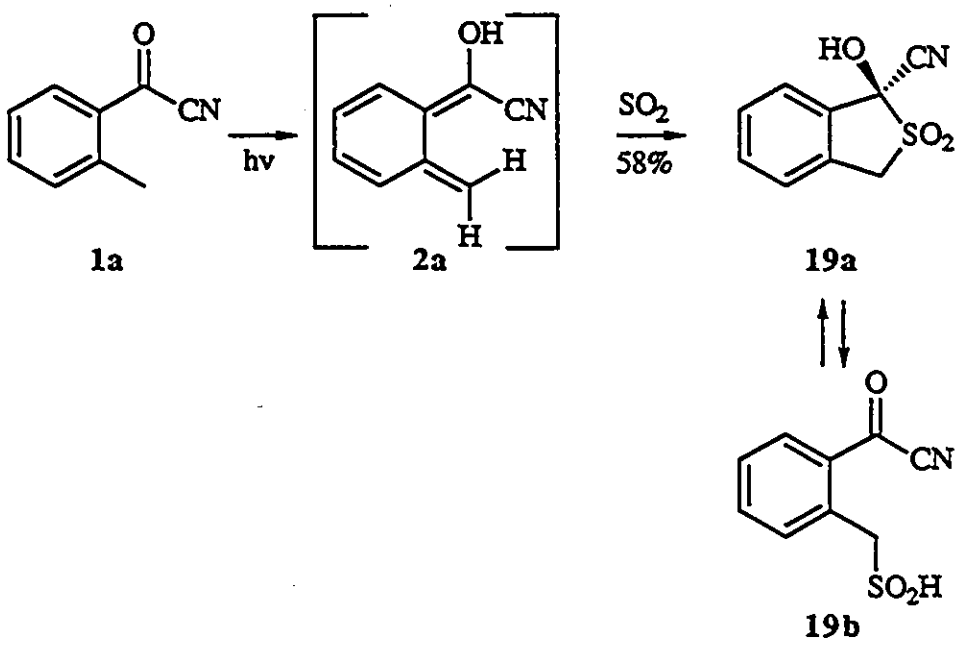


**1a** **2a** **19a** **19b**

Scheme 6.23: Irradiation of **1a** in the presence of $SO_2$

Sulfone **19a** [mp 137-138 °C (dec)] gave no molecular ion by EI or CIMS but exhibited a prominent fragment (m/e 145) corresponding to a loss of $SO_2$. The $^1$H-NMR spectrum (fig. 6.25a) showed a pronounced AB quartet centered at δ 4.71 ($J$ = 16.0 Hz) ppm, assigned to the benzylic methylene hydrogens, in addition to characteristic signals in the aromatic region. There was also an additional singlet observed at δ 4.47 ppm, and closer examination of an expansion of the aromatic region (fig. 6.25b) revealed a subordinate sequence of signals at δ 7.60 (d, 1H,

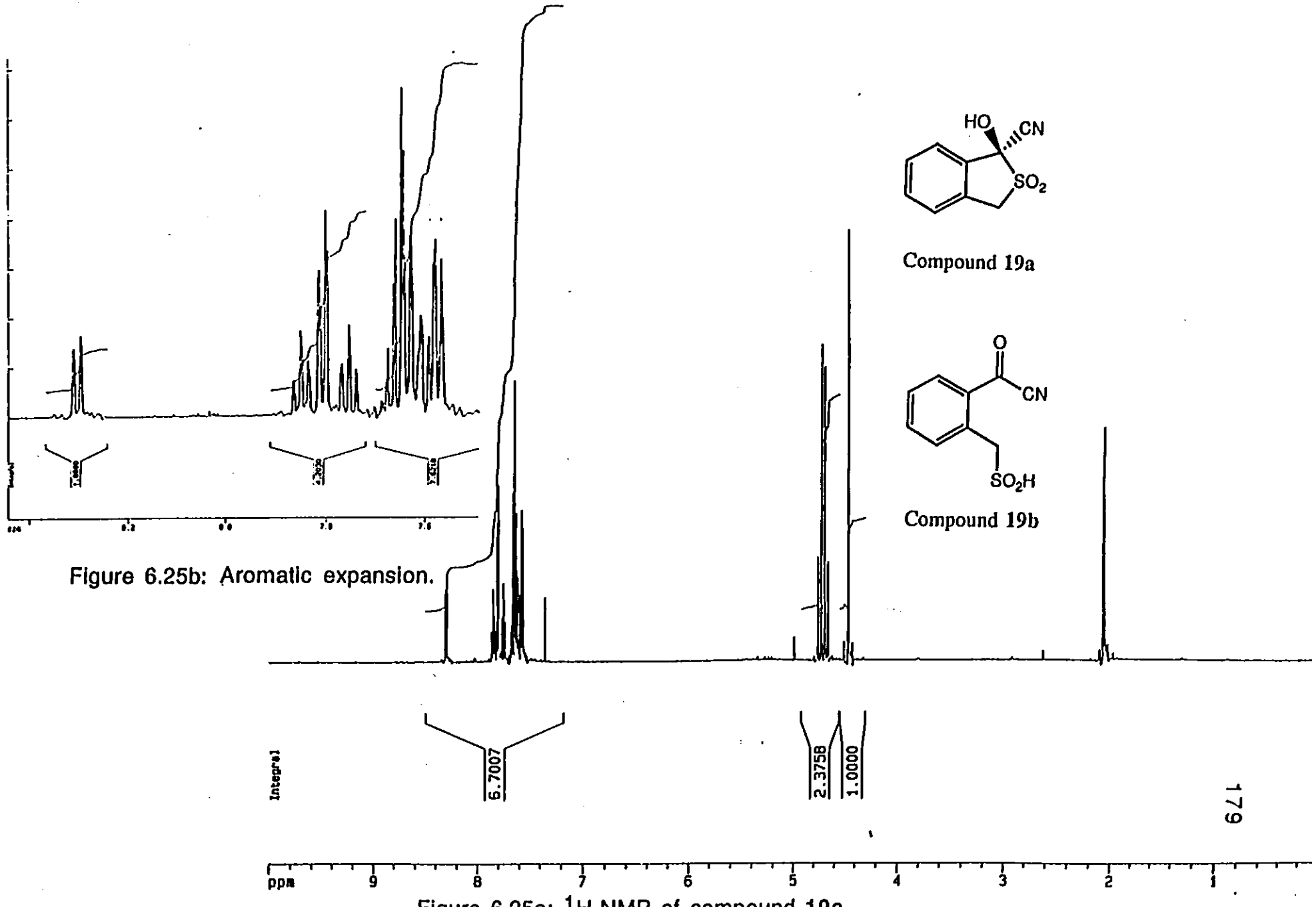


Figure 6.25b: Aromatic expansion.

Figure 6.25a: $^{1}$H-NMR of compound 19a.

$J$ = 8.8 Hz), 7.76 (t, 1H, $J$ = 7.5 Hz), 7.86 (t, 1H, $J$ = 8.8 Hz) and 8.30 (d, 1H, $J$ = 7.5 Hz) ppm, indicating that the ring opened isomer **19b** may be present, in chloroform-*d* solution, in a ratio of (**19a:19b**) 2:1.

Aroyl cyanide **1b** was also irradiated under similar conditions furnishing the sulfone cyanohydrin **20** in 50 % yield.

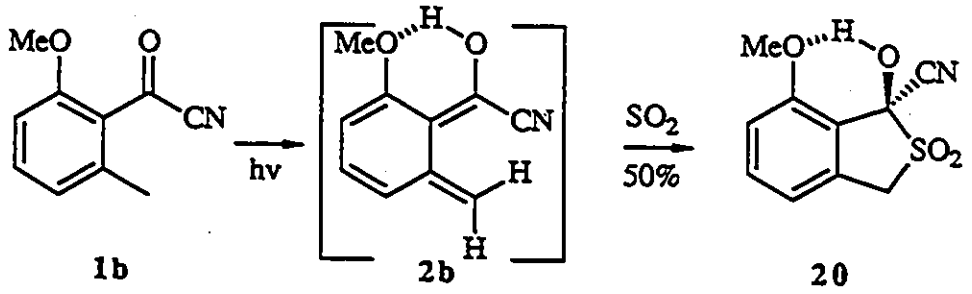


**1b** **2b** **20**

Scheme 6.24: Irradiation of **1b** in the presence of $SO_2$

Not surprisingly compound **20** also failed to produce a molecular ion by EI or CIMS exhibiting instead, a pronounced fragment (m/e 175) corresponding to a loss of $SO_2$. The $^1$H-NMR spectrum was similar to that of **19**, also showing an AB quartet centered at δ 4.26 ($J$ = 16.0 Hz) ppm. Two additional singlets at δ 2.70, and 3.62 ppm were assigned to the hydroxyl and the methoxy protons respectively. Examination of the aromatic region revealed only one series of characteristic signals at δ 6.71 (d, 1H, $J$ = 7.6 Hz), 6.82 (d, 1H, $J$ = 8.6 Hz) and 7.22 (t, 1H, $J$ = 7.9 Hz) ppm, indicating that none of the ring opened isomer contributed. It is likely that intramolecular H-bonding, depicted in scheme 6.24, shifts the equilibrium between the two isomers in favour of the bicyclic structure.

The usefulness of benzothiophenedioxides as convenient *o*-quinodimethane precursors, particularly in reactions with photoactive dienophiles such as dimethyl maleate, which isomerize upon irradiation, has been well demonstrated in the literature.[30] In this context, it was expected that sulfones **19** and **20** would provide a thermal route to the *o*-QDMs **2a** and **2b**, for cycloadditions with photosensitive dienophiles.

Encouragingly, when sulfone **19** was heated to its melting point (137-138 °C) in a capillary tube, gas evolution ($SO_2$ extrusion) was clearly visible during decomposition. Thus it was reasoned that thermolysis of a toluene or xylene solution of **19** and dimethyl fumarate should afford **21** after cycloaddition and HCN loss from the unstable tetralone cyanohydrin.

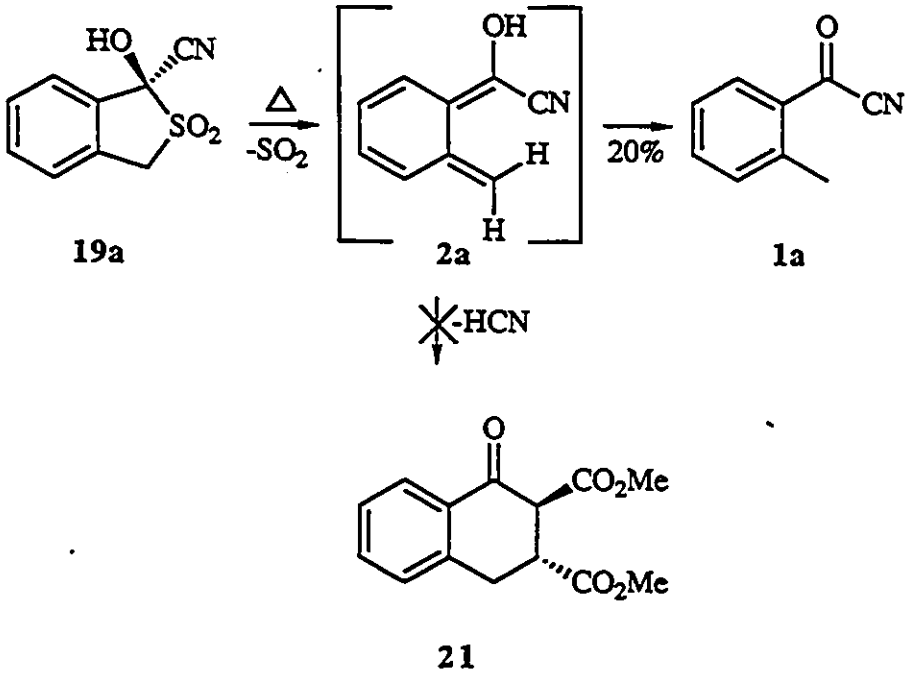


**19a** **2a** **1a** **21**

Scheme 6.25: Thermolysis of **19** in the presence of dimethyl fumarate

The projected formation of **2a** was based on the principles regarding torquoselectivity developed by Houk et al,[35] which predicted the outward rotation of the more electron rich hydroxyl function, and the inward rotation of the electron withdrawing cyano moiety.

Unfortunately, reflux of toluene or xylene solutions of **19** and dimethyl fumarate did not yield the expected cycloaddition product **21**, but instead, produced complex mixtures accompanied by **1a** (10-20 %); even thermolyses attempted in the presence of the acid scavenger $ZnO_2$ proved fruitless. Presumably, **1a** may have formed by intramolecular 1,5-hydrogen transfer in the minor *o*-QDM **2a'** or by intermolecular proton transfer in the major *o*-QDM **2a**.

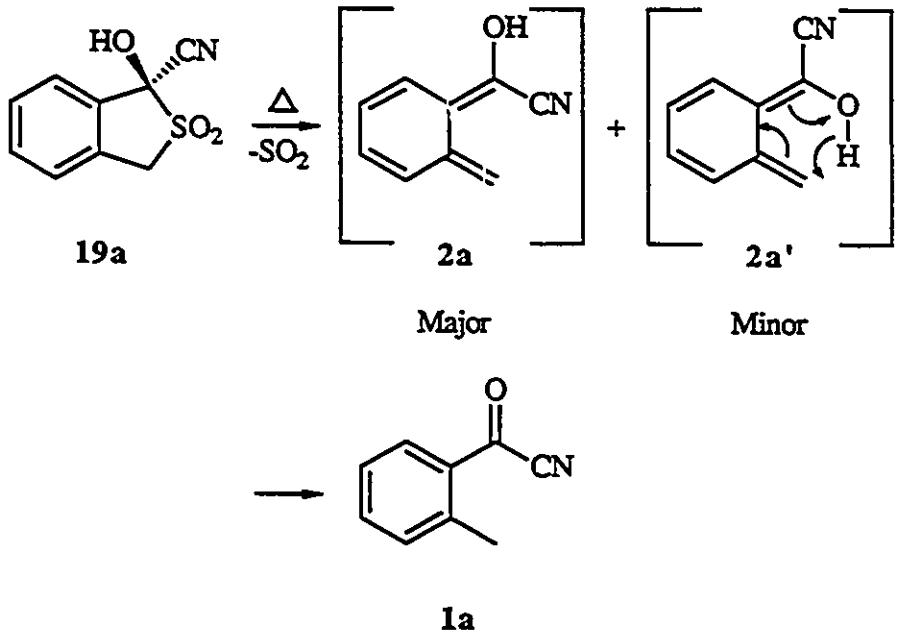


**1a**

Scheme 6.26: Alternative paths leading to **1a**.

Considering the proposed mechanisms of decomposition of *o*-QDMs **2a** and **2a'** it appeared likely that exploitation of **19** or **20** as *o*-QDM precursors would be possible only after protection of the hydroxyl function. Dissapointingly, time constraints permitted the investigation of only a single method of hydroxyl protection. As indicated in scheme 6.27, attempts to protect **19** as the methyl ether **22**, employing the methodology described by Charlton and Durst,[32] were unsuccessful, leading instead, to the methyl carboxylate **23**. The structure of **23**

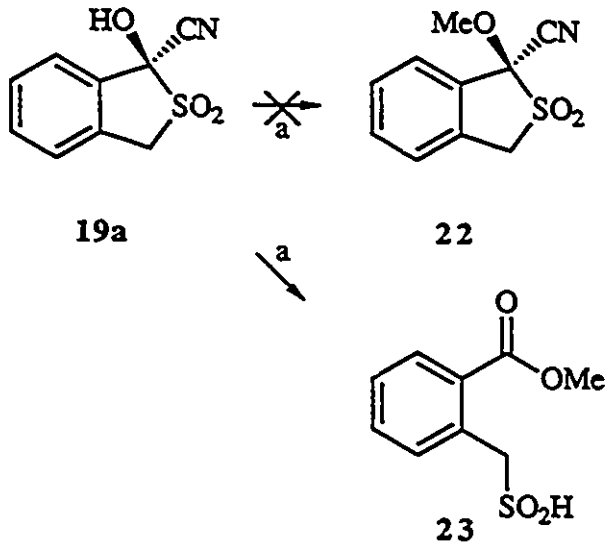


Scheme 6.27: Abortive hydroxyl protection of **19a**.
a) $MeOH/CH_2Cl_2$ TsOH.

followed from the $[M+1]^+$ ion obtained in the CIMS, the infrared [1706, 1281, 1074 $cm^{-1}$] absorptions, and the $^1H$-NMR data [δ (ppm) 3.51 (s, 3H); 4.04 (s, 2H); 5.46 (s, 1H); 7.00-7.28 (m, 3H); 7.61 (d, 1H, $J$ = 8.4 Hz).

## 6.8 Conclusions

The experimental observations described in this chapter clearly demonstrate the propensity of aroyl cyanides to participate in hetero Diels-Alder cycloadditions with photochemically and thermally generated *o*-quinodimethanes.

While the irradiation of *o*-methylaroyl cyanides failed to produce benzocyclobutenones or their cyanohydrins, the E-photoenols produced were shown to undergo efficient homocycloaddition (dimerization with loss of HCN) and heterocycloaddition (with less sterically encumbered, photochemically inert aroyl cyanides) yielding a diverse array of highly functionalized 3,4-dihydro-3-cyano-isocoumarins.

## 6.9 Experimental section

**General:** The general experimental considerations described in chapter 5 are applicable here as well with the exception of the 500 MHz $^1$H-NMR spectra, which were aquired employing a 500 MHz Bruker AMX-500 instrument, and the elemental analysis, which was performed at the Guelph Chemical Laboratories.

### 6.10.1 2-Methylbenzoyl cyanide (1a)[58]

A mixture of 20 g (0.13 mol) 2-methylbenzoyl chloride, 6.3 g (0.13 mol) sodium cyanide, and 0.1 g (0.36 mmol) tetrabutylammonium chloride in 140 mL of 5:1 dichloromethane-water was vigorously stirred at rt for 12 h after which time IR analysis indicated complete reaction. After filtration of the solids the organic phase was separated, dried over magnesium sulphate and concentrated in vacuo giving 19.6 g of a yellow oil. Vacuum distillation furnished 11.3 g (60 %) of a colorless liquid (bp 75-80°C/10 mm) which solidified on refrigeration.

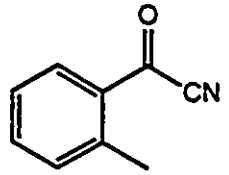


$C_9H_7NO$ 145.16

**1a**

**MS** (EI) 145 $[M]^+$, 118.0, 90.

**IR** ($CH_2Cl_2$) $\nu_{max}(cm^{-1})$ 2222 (m), 1680 (s).

**$^1$H-NMR** ($CDCl_3$) δ(ppm) 2.61 (s, 3H); 7.35 (d, 1H, $J$ = 7.5 Hz); 7.44 (t, 1H, $J$ = 7.5 Hz); 7.60 (t, 1H, $J$ = 7.4 Hz); 8.20 (d, 1H, $J$ = 7.8 Hz).

### 6.10.2 2-Methoxy-6-methylbenzoyl cyanide (1b)

To an ice cooled stirred solution of 5.0 g (33.3 mmol) 2-methoxy-6-methylbenzaldehyde and 100 mg zinc iodide (0.3 mmol) in 75 mL dichloromethane was added 3.6 g (4.9 mL, 36.7 mmol) of trimethylsilyl cyanide via syringe under nitrogen atmosphere. The mixture was allowed to warm to rt and tlc analysis (hexane:ethyl acetate 3:1) indicated complete conversion after 1 h. The solvent was removed on a rotovap at 40 °C and the concentrate passed through 20 g 70-230 mesh silica gel with 150 mL dichloromethane. The dichloromethane solution of the TMS cyanohydrin was transferred to a 250 mL round bottomed flask, cooled to 0 °C under nitrogen atmosphere and 18.8 g (50.0 mmol) of pyridinium dichromate was introduced, with efficient stirring, over 5 min. The mixture was stirred at rt for 12 h after which time the solvent was removed on a rotovap at 20 °C. The residue was triturated with ether and filtered through 20 g 70-230 mesh silica gel. Concentration of the ether solution produced 4.2 g of crude **1b** which furnished 3.5 g (60 %) of purified **1b** as yellow needles after flash chromatography (230-400 mesh silica gel, 3:1 hexane:ethyl acetate) and recrystallization (dichloromethane-hexane).

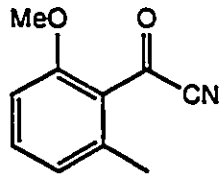


$C_{10}H_9NO_2$ 175.19

**1b**

**MP** 55.3-56.1 °C.

**MS** (EI) 175 $[M]^+$, 160, 148.

**HRMS** calcd for $C_{10}H_9NO_2$ 175.0633 found 175.0635.

**IR** ($CH_2Cl_2$) $\nu_{max}(cm^{-1})$ 2220 (m), 1670 (s).

**$^1$H-NMR** ($CDCl_3$) δ(ppm) 2.39 (s, 3H); 3.96 (s, 3H); 6.86 (d, 1H, $J$ = 7.5 Hz); 6.87 (d, 1H, $J$ = 8.3 Hz); 7.43 (t, 1H, $J$ = 8.4 Hz).

**$^{13}$C NMR** ($CDCl_3$) δ 20.7 (q); 56.1 (q); 109.7 (d); 114.8 (s); 123.2 (s); 124.2 (d); 135.5 (d); 142.2 (s); 161.1 (s); 167.6 (s).

### 6.10.3 2-Methoxy-4,6-dimethylbenzoyl cyanide (1c)

A solution of 5.0 g (33.3 mmol) 2-methoxy-4,6-dimethylbenzaldehyde in 75 mL dichloromethane was similarly treated as described for **1b**. Concentration of the product mixture followed by trituration with ether and filtration through a silica gel plug gave 5.6 g of a tan brown solid. The crude aroyl cyanide was readily crystallized from dichloromethane-hexane furnishing 4.6 g (79 %) of pure **1c** as yellow crystals.

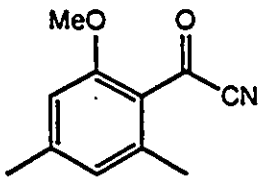


$C_{11}H_{11}NO_2$ 189.21

**1c**

**MP** 71.8-72.5 °C.

**MS** (EI) 189 $[M]^+$, 174, 162.

**HRMS** calcd for $C_{11}H_{11}NO_2$ 189.0790 found 189.0802.

**IR** ($CH_2Cl_2$) $\nu_{max}(cm^{-1})$ 2219 (m), 1608 (s).

**$^1$H-NMR** ($CDCl_3$) δ(ppm) 2.34 (s, 3H); 2.35 (s, 3H); 3.93 (s, 3H); 6.65 (s, 1H); 6.66 (s, 1H).

**$^{13}$C NMR** ($CDCl_3$) δ(ppm) 21.0 (q); 22.2 (q); 55.9 (q); 110.4 (d); 115.0 (s); 120.6 (s); 125.4 (d); 142.6 (s); 147.5 (s); 161.5 (s); 166.8 (s).

### 6.10.4 2-Methyl-4-methoxybenzoyl cyanide (1d)

A solution of 5.0 g (33.3 mmol) 2-methyl-4-methoxybenzaldehyde in 75 mL dichloromethane was similarly treated as described for **1b**. Concentration of the product mixture followed by trituration with ether and filtration through a silica gel plug gave 5.1 g of a yellow solid. The crude aroyl cyanide crystallized from ether-hexane furnishing 4.5 g (78 %) of pure **1d** as colorless needles.

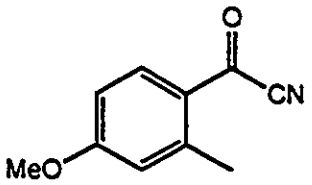


$C_{10}H_9NO_2$ 175.19

**1d**

**MP** 62.0-62.8 °C.

**MS** (EI) 175 $[M]^+$, 163, 148.

**HRMS** calcd for $C_{10}H_9NO_2$ 175.0633 found 175.0648.

**IR** ($CH_2Cl_2$) $\nu_{max}(cm^{-1})$ 2219 (m), 1667 (s).

**$^1$H-NMR** ($CDCl_3$) δ(ppm) 2.59 (s, 3H); 3.90 (s, 3H);
6.79 (d, 1H, $J$ = 2.0 Hz); 6.88 (dd, 1H, $J$ = 2.0, 8.8 Hz);
8.15 (d, 1H, $J$ = 8.8 Hz).

**$^{13}$C NMR** ($CDCl_3$) δ(ppm) 22.4 (q); 55.7 (q); 111.7 (d);
113.6 (s); 118.5 (d); 124.9 (s); 138.2 (d);
146.0 (s); 165.2 (s); 166.6 (s).

### 6.10.5 2-Methoxy-4-methylbenzoyl cyanide (1e)

A solution of 5.0 g (33.3 mmol) 2-methoxy-4-methylbenzaldehyde in 75 mL dichloromethane was similarly treated as described for **1b**. Silica gel chromatography (230-400 mesh, 5:1 hexane:ethyl acetate) gave 3.8 g (65 %) **1e** as a yellow oil, which solidified on storage at 0°C, and readily recrystallized from dichloromethane/hexane.

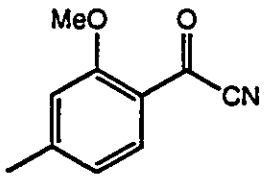


$C_{10}H_9NO_2$ 175.19

**1e**

**MP** 68.2-69.0 °C.

**MS** (EI) 175 [M]+, 158, 149.

**HRMS** calcd for $C_{10}H_9NO_2$ 175.0633 found 175.0643.

**IR** ($CH_2Cl_2$) $\nu_{max}(cm^{-1})$ 2221 (m), 1608 (s).

**$^1$H-NMR** ($CDCl_3$) δ(ppm) 2.42 (s, 3H); 3.96 (s, 3H); 6.81 (s, 1H); 6.87 (d, 1H, $J$ = 8.1 Hz); 7.84 (d, 1H, $J$ = 8.1 Hz).

**$^{13}$C NMR** ($CDCl_3$) δ(ppm) 22.5 (q); 55.9 (q); 112.9 (d); 114.3 (s); 120.2 (s); 122.1 (d); 132.6 (d); 150.5 (s); 161.3 (s); 164.7 (s).

### 6.10.6 3,4-Dihydro-3-cyano-3-(2-methylphenyl)-1H-2-benzopyran-1-one (6a)

A solution of 300 mg (2.1 mmol) 2-methylbenzoyl cyanide in 2.0 mL of acetonitrile (1.0 M) contained in a quartz test tube, was suspended 10 cm from a Hanovia medium pressure mercury lamp and irradiated until tlc analysis indicated complete conversion of the starting material (5-6 h). Concentration of the solvent on a rotovap at 40 °C followed by flash chromatography (230-400 mesh silica gel, 5:1 hexane:ethyl acetate) of the crude adduct gave 220 mg (81 %) of a white

solid which recrystallized from dichloromethane-hexane giving colorless needles.

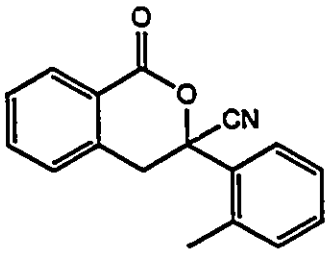


$C_{17}H_{13}NO_2$ 263.09

**6a**

**MP** 126.5-127.5 °C.

**MS** (EI) 262 $[M-1]^+$, 245, 218.

**HRMS** calcd for $C_{17}H_{13}NO_2$ 263.0946 found 263.0935.

**IR** ($CH_2Cl_2$) $\nu_{max}(cm^{-1})$ 1747 (s).

**$^1$H-NMR** ($CDCl_3$) δ(ppm) 2.68 (s, 3H); 3.64 (d, 1H, $J$ = 16.5 Hz); 3.78 (d, 1H, $J$ = 16.5 Hz); 7.23-7.40 (m, 4H); 7.46-7.70 (m, 3H); 8.16 (d, 1H, $J$ = 7.7 Hz).

**$^{13}$C NMR** ($CDCl_3$) δ(ppm) 20.9 (q); 37.4 (t); 77.4 (s); 117.5 (s); 123.7 (s); 125.6 (d); 126.4 (d); 127.9 (d); 129.0 (d); 130.2 (d); 130.8 (d); 132,4 (s); 133.1 (d); 135.0 (d); 135.6 (s); 136.8 (s); 162.0 (s).

### 6.10.7 3,4-Dihydro-3-cyano-8-methoxy-3-(2-methoxy-6-methylphenyl)-1H-2-benzopyran-1-one (6b)

A solution of 300 mg (1.7 mmol) 2-methoxy-6-methylbenzoyl cyanide in 2.0 mL of acetonitrile contained in a quartz test tube, was irradiated as described for **6a** until tlc analysis (hexane:ethyl acetate 2:1) indicated complete conversion of the starting material (12 h).

Concentration of the solvent on a rotovap at 40 °C followed by flash chromatography (230-400 mesh silica gel, dichloromethane) of the crude adduct gave 249 mg (90 %) of a white solid, which crystallized from dichloromethane-hexane yielding colorless crystals

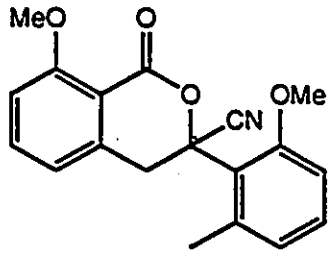


$C_{19}H_{17}NO_4$ 323.12

**6b**

| | |
|---|---|
| **MP** | 145.3-146.0 °C. |
| **MS** | (EI) 322 $[M-1]^+$, 278, 263. |
| **HRMS** | calcd for $C_{19}H_{17}NO_4$ 323.1158 found 323.1161. |
| **IR** | ($CH_2Cl_2$) $\nu_{max}(cm^{-1})$ 1744 (s). |
| **$^1$H-NMR** | ($CDCl_3$) δ(ppm) 2.61 (s, 3H); 3.45 (d, 1H, $J$ = 16.5 Hz); 3.67 (d, 1H, $J$ = 16.5 Hz); 3.87 (s, 3H); 3.94 (s, 3H); 6.85 (m, 3H); 6.98 (d, 1H, $J$ = 8.5 Hz); 7.22 (dd, 1H, $J$ = 7.8, 5.4 Hz); 7.53 (dd, 1H, $J$ = 7.8, 8.3 Hz). |
| **$^{13}$C NMR** | ($CDCl_3$) δ(ppm) 23.2 (q); 38.2 (t); 56.1 (q); 56.2 (q); 77.0 (s); 110.5 (d); 111.9 (s); 112.3 (d); 118.2 (s); 119.6 (d); 122.4 (s); 126.4 (d); 130.0 (d); 135.6 (d); 138.2 (s); 138.7 (s); 156.4 (s); 158.6 (s); 161.4 (s). |

### 6.10.8 3,4-Dihydro-3-cyano-8-methoxy-6-methyl-3-(2-methoxy-4,6-dimethylphenyl)-1H-2-benzopyran-1-one (6c)

A solution of 300 mg (1.6 mmol) 2-methoxy-4,6-dimethylbenzoyl cyanide in 2.0 mL of acetonitrile was irradiated as above until tlc analysis indicated complete conversion of the starting material (16 h). Concentration of the solvent at 40 °C followed by flash chromatography (230-400 mesh silica gel, hexane:ethyl acetate 2:1) gave 140 mg (50 %) of a white solid, which crystallized from dichloromethane-hexane yielding colorless crystals.

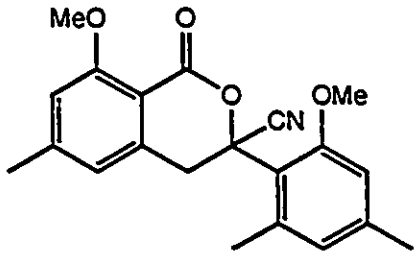


$C_{21}H_{21}NO_4$ 351.15

**6c**

**MP** 202.5-203.0 °C.

**MS** (EI) 351 $[M]^+$, 350, 306.

**HRMS** calcd for $C_{21}H_{21}NO_4$ 351.1471 found 351.1446.

**IR** ($CH_2Cl_2$) $\nu_{max}(cm^{-1})$ 1741 (s).

**$^1$H-NMR** ($CDCl_3$) δ(ppm) 2.28 (s, 3H); 2.38 (s, 3H); 2.56 (s, 3H); 3.40, 3.60 (d, 1H, $J$ = 16.6 Hz); 3.85 (s, 3H); 3.93 (s, 3H); 6.65 (s, 2H); 6.67 (s, 1H); 6.76 (s, 1H).

**$^{13}$C NMR** ($CDCl_3$) d(ppm) 21.2 (q); 22.2 (q); 23.0 (q); 38.4 (t); 56.1 (q); 56.1 (q); 77.4 (s); 109.7 (s); 111.3 (d); 112.6 (d); 118.4 (s); 119.7 (s); 120.5 (d); 127.2 (d); 137.9 (s); 138.6 (s); 140.1 (s); 147.0 (s); 156.4 (s);

158.9 (s); 161.4 (s).

**6.10.9 3,4-Dihydro-3-cyano-3-phenyl-1H-2-benzopyran-1-one (7a).**

A solution of 300 mg (2.1 mmol) 2-methylbenzoyl cyanide and 550 mg (4.1 mmol) of benzoyl cyanide in 2.0 mL of acetonitrile was irradiated as described above for 6 h. Concentration of the solvent on a rotovap at 40 °C followed by flash chromatography (230-400 mesh silica gel, 5:1 hexane:ethyl acetate) of the crude adduct gave 385 mg (75 %) of a white solid, which crystallized from ether-hexane yielding colorless plates.

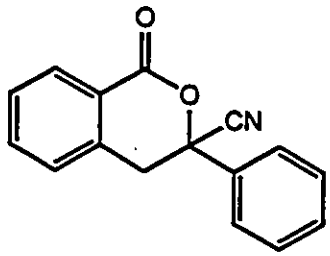


$C_{16}H_{11}NO_2$ 249.08

7a

**MP** 144.6-146.1 °C.

**MS** (EI) 249 $[M]^+$, 203, 190.

**HRMS** calcd for $C_{16}H_{11}NO_2$ 249.0790 found 249.0809.

**IR** ($CH_2Cl_2$) $\nu_{max}(cm^{-1})$ 1748 (s).

**$^1$H-NMR** ($CDCl_3$) δ(ppm) 3.47, 3.62 (d, 1H, $J$ = 16.7 Hz); 7.34 (d, 1H, $J$ = 7.5 Hz);7.45-7.55 (m, 4H); 7.61-7.71 (m, 3H); 8.19 (d, 1H, $J$ = 7.7 Hz).

**$^{13}$C NMR** ($CDCl_3$) δ(ppm) 40.3 (t); 78.2 (s); 117.8 (s); 123.6 (s); 125.1 (d); 127.7 (d); 129.0 (d); 129.2 (d); 130.1 (d);

130.9 (d); 135.0 (d); 135.5 (s); 135.7 (s); 162.2 (s).

### 6.10.10 3,4-Dihydro-3-cyano-3-phenyl-8-methyl-1H-2-benzopyran-1-one (7b)

A solution of 300 mg (1.7 mmol) 2-methoxy-6-methylbenzoyl cyanide and 450 mg (3.4 mmol) benzoyl cyanide in 2.0 mL of acetonitrile was irradiated as above for 6 h. Concentration of the solvent followed by flash chromatography (230-400 mesh silica gel, hexane:ethyl acetate 3:1) of the crude adduct gave 420 mg (88 %) of a white solid.

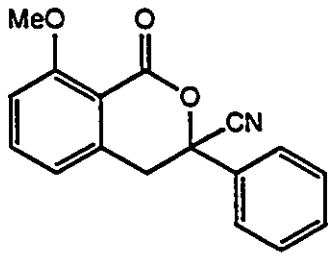


$C_{17}H_{13}NO_3$ 279.09

**7b**

**MP** 146.0-147.0 °C.

**MS** (EI) 279 $[M]^+$, 249, 220.

**HRMS** calcd for $C_{17}H_{13}NO_3$ 279.0895 found 279.0888.

**IR** ($CH_2Cl_2$) $\nu_{max}(cm^{-1})$ 1748 (s).

**$^1$H-NMR** ($CDCl_3$) δ(ppm) 3.39, 3.74 (d, 1H, $J$ = 16.4 Hz); 3.98 (s, 3H); 6.87 (d, 1H, $J$ = 7.6 Hz); 7.02 (d, 1H, $J$ = 8.6 Hz); 7.40-7.50 (m, 3H); 7.57 (t, 1H, $J$ = 7.6 Hz); 7.65-7.75 (m, 2H).

**$^{13}$C NMR** ($CDCl_3$) δ(ppm) 41.2 (t); 56.3 (q); 77.5 (s); 112.0 (s); 112.3 (d); 117.8 (s); 119.5 (d); 125.1 (d); 129.1 (d); 130.0 (d); 135.7 (s); 135.9 (d); 138.0 (s); 158.8 (s); 161.6 (s).

**6.10.11 3,4-Dihydro-3-cyano-8-methoxy-6-methyl-3-phenyl-1H-2-benzopyran-1-one (7c)**

A solution of 300 mg (1.6 mmol) 2-methoxy-4,6-dimethyibenzoyl cyanide and 420 mg (3.2 mmol) benzoyl cyanide in 2.0 mL of acetonitrile was irradiated as above for 6 h. Concentration of the solvent followed by flash chromatography (230-400 mesh silica gel, 5:1 hexane:ethyl acetate) gave 363 mg (78 %) of a white solid.

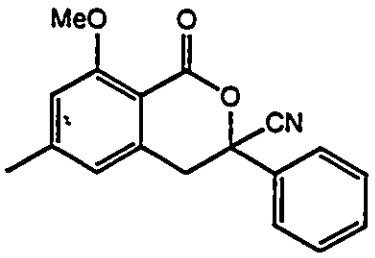


$C_{18}H_{15}NO_3$ 293.11

**7c**

**MP** 166.0-167.0 °C.

**MS** (EI) 293 $[M]^+$, 263, 247.

**HRMS** calcd for $C_{18}H_{15}NO_3$ 293.1052 found 293.1055.

**IR** ($CH_2Cl_2$) $\nu_{max}(cm^{-1})$ 1746 (s).

**$^1$H-NMR** ($CDCl_3$) δ(ppm) 2.41 (s, 3H); 3.33 (d, 1H, $J$ = 16.1 Hz); 3.49 (d, 1H, $J$ = 16.1 Hz); 3.97 (s, 3H); 6.69 (s, 1H); 6.82 (s, 1H); 7.50 (m, 3H); 7.70 (m, 2H).

**$^{13}$C NMR** ($CDCl_3$) δ(ppm) 22.2 (q); 41.2 (t); 56.2 (q); 77.4 (s); 109.4 (s); 112.9 (d); 117.9 (s); 120.4 (d); 125.1 (d); 129.0 (d); 129.9 (d); 135.8 (s); 137.8 (s); 147.6 (s); 159.0 (s); 161.7 (s).

### 6.10.12 3,4-Dihydro-3-cyano-8-methoxy-3-(2-methoxy-4-methylphenyl)-1H-2-benzopyran-1-one (7d)

A solution of 300 mg (1.7 mmol) 2-methoxy-6-methylbenzoyl cyanide and 300 mg (1.7 mmol) 2-methoxy-4-methylbenzoyl cyanide in 2.0 mL of acetonitrile contained in a quartz test tube was irradiated for 6 h after which time tlc analysis indicated complete conversion of the starting materials. Concentration of the solvent at 40°C followed by flash chromatography (230-400 mesh silica gel, 2:1 hexane:ethyl acetate) of the crude adduct gave 526 mg (95 %) of a yellow solid.

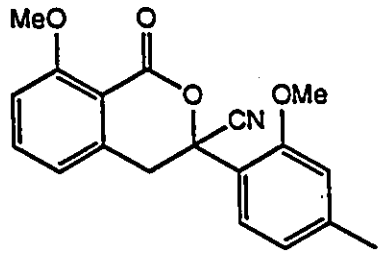


$C_{19}H_{17}NO_4$ 323.12

**7d**

**MP** 176.5-177.5 °C.

**MS** (EI) 323 $[M]^+$, 293, 278.

**HRMS** calcd for $C_{19}H_{17}NO_4$ 323.1158 found 323.1161.

**IR** ($CH_2Cl_2$) $\nu_{max}(cm^{-1})$ 1745 (s).

**$^1$H-NMR** ($CDCl_3$) δ(ppm) 2.36 (s, 3H); 3.33, 3.79 (d, 1H, $J$ = 16.3 Hz); 3.91 (s, 3H); 3.96 (s, 3H); 6.84 (m, 3H); 6.98 (d, 1H, $J$ = 8.5 Hz); 7.53 (dd, 1H, $J$ = 7.8, 7.6 Hz); 7.60 (d, 1H, $J$ = 7.9 Hz).

**$^{13}$C NMR** ($CDCl_3$) δ(ppm) 21.5 (q); 38.2 (t); 55.9 (q); 56.2 (q); 77.4 (s); 111.9 (d); 112.3 (s); 112.9 (d); 117.6 (s); 119.7 (d); 121.0 (s); 121.7 (d); 126.1 (d); 135.7 (d);

138.5 (s): 141.5 (s); 155.8 (s); 159.1 (s); 161.4 (s).

### 6.10.13 3,4-Dihydro-3-cyano-3-methyl-1H-2-benzopyran-1-one (7e)

A solution of 300 mg (2.1 mmol) 2-methylbenzoyl cyanide and 285 mg (4.1 mmol) acetyl cyanide in 2.0 mL of acetonitrile was irradiated as described above until tlc analysis indicated complete conversion of the starting material (12 h). Concentration of the solvent followed by flash chromatography (230-400 mesh silica gel, 3:1 hexane:ethyl acetate) gave 192 mg (50 %) of a white solid.

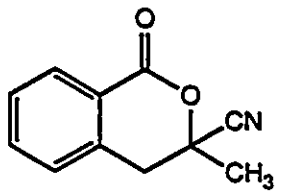


$C_{11}H_9NO_2$ 187.06

**7e**

**MP** 98.0-100.0 °C.

**MS** (EI) 187 $[M]^+$, 172, 144.

**HRMS** calcd for $C_{11}H_9NO_2$ 187.0633 found 187.0646.

**IR** ($CH_2Cl_2$) $\nu_{max}(cm^{-1})$ 1746 (s).

**$^1$H-NMR** ($CDCl_3$) δ(ppm) 1.94 (s, 3H); 3.25, 3.34 (d, 1H, $J$ = 16.6 Hz); 7.29 (d, 1H, $J$ = 6.8 Hz); 7.48 (t, 1H, $J$ = 6.4 Hz); 7.63 (dt, 1H, $J$ = 1.4, 7.5 Hz); 8.12 (dd, 1H, $J$ = 1.4, 7.5 Hz).

**$^{13}$C NMR** ($CDCl_3$) δ(ppm) 26.6 (q); 38.3 (t); 77.4 (s); 118.5 (s); 123.3 (s); 127.6 (d); 128.9 (d); 130.8 (d); 134.8 (d); 135.4 (s); 162.3 (s).

### 6.10.14 Preparation of compounds 10a and 10b

A solution of 235 mg (0.9 mmol) of *cis*-1-methoxy-3-phenyl-1,3-dihydrobenzo[c]thiophene 2,2-dioxide and 240 mg (1.8 mmol) of benzoyl cyanide in 8 mL of cyclohexane was heated to reflux under nitrogen atmosphere until tlc analysis (dichloromethane: hexane 2:1) indicated complete conversion of the starting materials (6 h). Concentration on a rotovap followed by flash chromatography (230-400 mesh silica gel) furnished **10a** and **10b** (3:1 ratio) in 90 % yield.

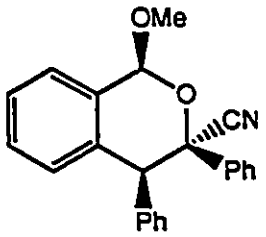


$C_{23}H_{19}NO_2$ 341.41

**10a**

**MP** 237.2-238.4 °C.

**MS** (CI/$Et_2O$) 342 $[M+1]^+$, 315, 310, 179.

**IR** ($CH_2Cl_2$) $\nu_{max}(cm^{-1})$ 1069 (s), 1015 (s).

**$^1$H-NMR** ($CDCl_3$) δ(ppm) 3.83 (s, 3H); 4.36 (s, 1H); 6.23 (s, 1H); 6.73 (dd, 2H, *J* = 1.7, 7.5 Hz); 6.90-7.00 (m, 3H); 7.03 (d, 1H, *J* = 8.1 Hz); 7.15-7.27 (m, 6H); 7.37 (d, 1H, *J* = 7.4 Hz); 7.51 (d, 1H, *J* = 7.7 Hz).

**$^{13}$C NMR** ($CDCl_3$) d(ppm) 54.8 (d); 57.4 (q); 76.6 (s); 101.0 (d); 119.4 (s); 125.1 (d); 126.2 (d); 126.9 (d); 127.6 (d); 127.9 (d); 128.0 (d); 128.5 (d); 129.2 (d); 129.6 (d); 130.2 (d); 132.2 (s); 134.8 (s); 136.8 (s); 137.5 (s).

**X-Ray Structure Data:**

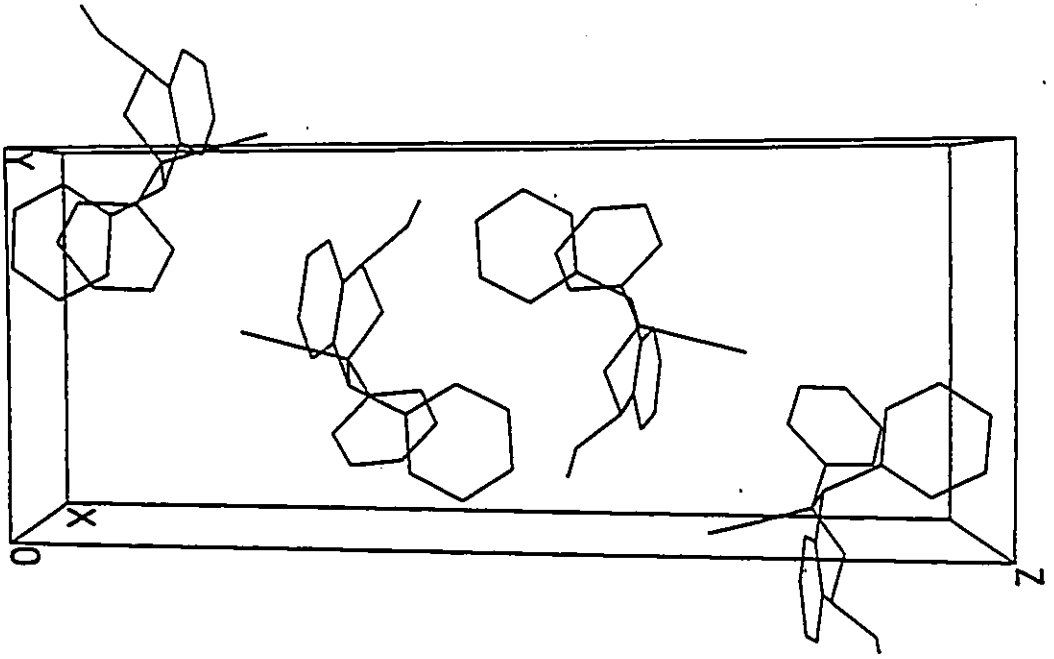


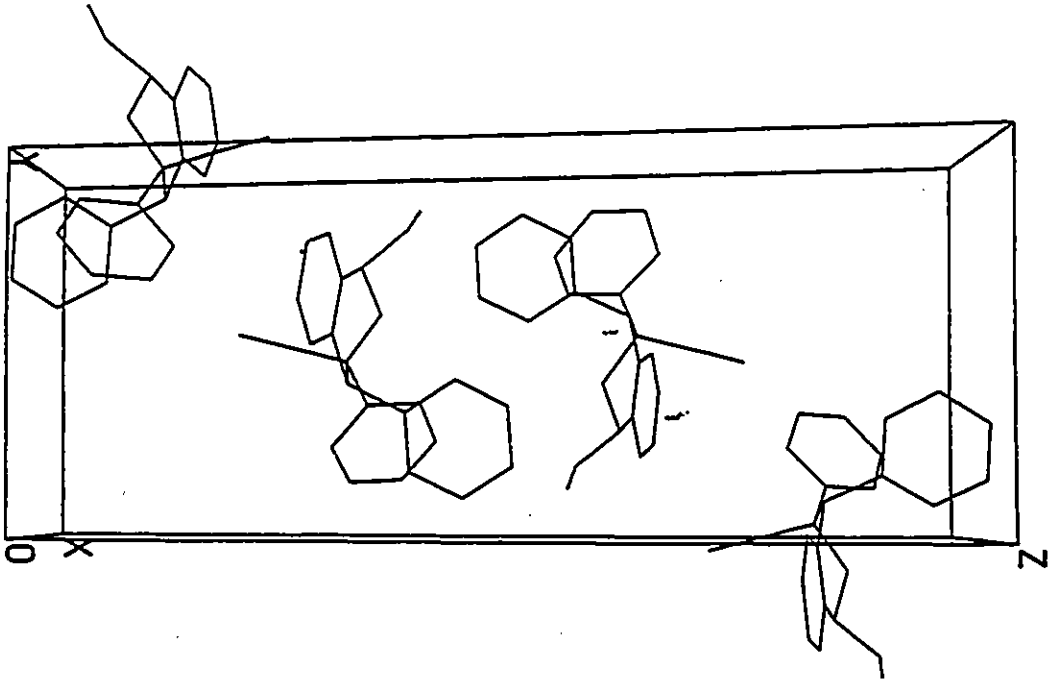

Space Group and Cell Dimensions  Monoclinic,  P 21/n
a  8.4809(14)  b  9.2811(17)  c  22.940(5)
beta 100.528(15)
Volume  1775.3(6)A**3

Empirical formula : O2 N C23 H19

Cell dimensions were obtained from 24 reflections with 2Theta angle in the range 40.00 - 50.00 degrees.

Crystal dimensions : 0.20 X 0.20 X 0.20 mm

FW = 341.41  Z = 4  F(000) = 720.26

Dcalc 1.277Mg.m-3, mu 0.09mm-1, lambda 0.70930A, 2Theta(max) 49.9

The intensity data were collected on a Nonius diffractometer, using the theta/2theta scan mode.
The h,k,l ranges are :--  -10 9,  0 11,  0 27
No. of reflections measured  3338
No. of unique reflections  3115
No. of reflections with Inet > 2.5sigma(Inet)  2315
No correction was made for absorption

The last least squares cycle was calculated with
45 atoms, 311 parameters and 2312 out of 3115 reflections.
Weights based on counting-statistics were used.

The residuals are as follows :--
For significant reflections,  RF 0.085, Rw 0.058 GoF 10.45
For all reflections,  RF 0.126, Rw 0.058.
where RF = Sum(Fo-Fc)/Sum(Fo),
Rw = Sqrt[Sum(w(Fo-Fc)**2)/Sum(wFo**2)] and
GoF = Sqrt[Sum(w(Fo-Fc)**2)/(No. of reflns - No. of params.)]
The maximum shift/sigma ratio was 0.258.

In the last D-map, the deepest hole was -0.400e/A**3,
and the highest peak 0.410e/A**3.

Secondary ext. coeff. = 1.976234  sigma = 0.025286

Table . Distances(A) to the least-squares planes.

Plane no. 1

Equation of the plane :- 2.437(16)X + 0.508(19)Y + 22.772(6)Z = 2.594(11)

Distances(A) to the plane from the atoms in the plane.

| | | | |
|---|---|---|---|
| C2 | -0.012(6) | C3 | 0.005(6) |
| C4 | 0.005(6) | C5 | -0.006(6) |
| C6 | -0.003(6) | C7 | 0.011(6) |

Chi squared for this plane 10.953

Plane no. 2

Equation of the plane : 8.287(4)X + 0.158(19)Y + 0.69(4)Z = 2.850(5)

Distances(A) to the plane from the atoms in the plane.

| | | | |
|---|---|---|---|
| C10 | 0.003(6) | C11 | 0.000(6) |
| C12 | -0.005(6) | C13 | 0.007(6) |
| C14 | -0.003(6) | C15 | -0.002(6) |

Chi squared for this plane 2.611

Plane no. 3

Equation of the plane :- 5.887(12)X + 5.789(15)Y + 11.01(4)Z = 0.445(8)

Distances(A) to the plane from the atoms in the plane.

| | | | |
|---|---|---|---|
| C16 | 0.008(5) | C17 | -0.013(6) |
| C18 | 0.010(6) | C19 | -0.003(6) |
| C20 | -0.001(6) | C21 | -0.003(6) |

Chi squared for this plane 10.093

Dihedral angle between planes A and B

| A | B | Angle(deg) |
|---|---|---|
| 1 | 2 | 94.42(16) |
| 1 | 3 | 54.76(17) |
| 2 | 3 | 126.26(16) |

Table of Bond Distances in Angstroms

| | | | |
|---|---|---|---|
| O1-C1 | 1.452(5) | C11-H11a | 1.03(3) |
| O1-C9 | 1.427(5) | C12-C13 | 1.398(7) |
| O2-C1 | 1.394(5) | C12-H12 | 0.92(4) |
| O2-C23 | 1.440(6) | C13-C14 | 1.390(7) |
| N1-C22 | 1.133(6) | C13-H13 | 1.06(4) |
| C1-C2 | 1.500(6) | C14-C15 | 1.394(6) |
| C1-H1 | 1.06(3) | C14-H14 | 1.07(4) |
| C2-C3 | 1.382(6) | C15-H15 | 0.98(5) |
| C2-C7 | 1.409(6) | C16-C17 | 1.375(6) |
| C3-C4 | 1.369(7) | C16-C21 | 1.396(6) |
| C3-H3 | 1.08(4) | C17-C18 | 1.379(7) |
| C4-C5 | 1.404(7) | C17-H17 | 0.89(4) |
| C4-H4 | 0.93(4) | C18-C19 | 1.376(7) |
| C5-C6 | 1.376(7) | C18-H18 | 1.06(4) |
| C5-H5 | 1.19(3) | C19-C20 | 1.375(7) |
| C6-C7 | 1.383(7) | C19-H19 | 1.07(4) |
| C6-H6 | 0.91(4) | C20-C21 | 1.394(7) |
| C7-C8 | 1.515(6) | C20-H20 | 0.85(4) |
| C8-C9 | 1.561(6) | C21-H21 | 1.01(4) |
| C8-C10 | 1.512(6) | C23-H23A | 0.94(4) |
| C8-H8 | 1.16(3) | C23-H23B | 1.04(4) |
| C9-C16 | 1.531(6) | C23-H23C | 0.91(6) |
| C9-C22 | 1.502(6) | H11-C11b | 1.03(3) |
| C10-C11 | 1.391(6) | | |
| C10-C15 | 1.400(6) | | |
| C11-C12 | 1.393(7) | | |

Table of Bond Angles in Degree

| | | | |
|---|---|---|---|
| C1-O1-C9 | 114.1(3) | C12-C11-H11a | 120.9(18) |
| C1-O2-C23 | 110.6(4) | C11-C12-C13 | 121.0(4) |
| O1-C1-O2 | 105.7(3) | C11-C12-H12 | 123(3) |
| O1-C1-C2 | 113.0(3) | C13-C12-H12 | 115(3) |
| O1-C1-H1 | 106.4(18) | C12-C13-C14 | 118.7(4) |
| O2-C1-C2 | 109.3(4) | C12-C13-H13 | 119.6(24) |
| O2-C1-H1 | 106.9(18) | C14-C13-H13 | 121.7(24) |
| C2-C1-H1 | 115.0(18) | C13-C14-C15 | 119.8(4) |
| C1-C2-C3 | 119.1(4) | C13-C14-H14 | 119.1(20) |
| C1-C2-C7 | 121.1(4) | C15-C14-H14 | 121.1(21) |
| C3-C2-C7 | 119.6(4) | C10-C15-C14 | 122.1(4) |
| C2-C3-C4 | 120.9(5) | C10-C15-H15 | 117(3) |
| C2-C3-H3 | 112.6(22) | C14-C15-H15 | 120(3) |
| C4-C3-H3 | 124.7(22) | C9-C16-C17 | 122.2(4) |
| C3-C4-C5 | 120.3(4) | C9-C16-C21 | 117.6(4) |
| C3-C4-H4 | 126.4(23) | C17-C16-C21 | 120.2(4) |
| C5-C4-H4 | 113.3(23) | C16-C17-C18 | 119.7(4) |
| C4-C5-C6 | 118.7(4) | C16-C17-H17 | 113(3) |
| C4-C5-H5 | 121.2(16) | C18-C17-H17 | 125(3) |
| C6-C5-H5 | 120.1(16) | C17-C18-C19 | 121.5(4) |
| C5-C6-C7 | 121.9(4) | C17-C18-H18 | 118.5(23) |
| C5-C6-H6 | 121.4(24) | C19-C18-H18 | 119.8(23) |
| C7-C6-H6 | 115.9(24) | C18-C19-C20 | 118.5(4) |
| C2-C7-C6 | 118.6(4) | C18-C19-H19 | 114.1(21) |
| C2-C7-C8 | 121.2(4) | C20-C19-H19 | 124.9(21) |
| C6-C7-C8 | 120.1(4) | C19-C20-C21 | 121.6(4) |
| C7-C8-C9 | 108.4(4) | C19-C20-H20 | 117(3) |
| C7-C8-C10 | 112.1(3) | C21-C20-H20 | 120(3) |
| C7-C8-H8 | 104.6(17) | C16-C21-C20 | 118.4(4) |
| C9-C8-C10 | 111.8(4) | C16-C21-H21 | 121.2(23) |
| C9-C8-H8 | 105.8(17) | C20-C21-H21 | 120.3(23) |
| C10-C8-H8 | 113.6(17) | N1-C22-C9 | 179.6(4) |
| O1-C9-C8 | 110.0(3) | O2-C23-H23A | 104.3(24) |
| O1-C9-C16 | 106.5(3) | O2-C23-H23B | 109.1(21) |
| O1-C9-C22 | 109.5(3) | O2-C23-H23C | 111(4) |
| C8-C9-C16 | 113.8(4) | H23A-C23-H23B | 93(3) |
| C8-C9-C22 | 107.6(4) | H23A-C23-H23C | 102(4) |
| C16-C9-C22 | 109.4(4) | H23B-C23-H23C | 129(4) |
| C8-C10-C11 | 119.6(4) | | |
| C8-C10-C15 | 122.8(4) | | |
| C11-C10-C15 | 117.5(4) | | |
| C10-C11-C12 | 121.0(4) | | |
| C10-C11-H11a | 117.4(18) | | |

Table of Atomic Parameters x,y,z and Biso.
E.S.Ds. refer to the last digit printed.

| | x | y | z | Biso |
|---|---|---|---|---|
| O1 | 0.1393(4) | 0.08467 | 0.11836(13) | 2.45(16) |
| O2 | 0.2267(4) | 0.2994 (3) | 0.08925(14) | 3.44(18) |
| N1 | 0.1777(5) | 0.0314 (4) | 0.26657(18) | 3.72(23) |
| C1 | 0.2446(6) | 0.2057 (5) | 0.13751(20) | 2.44(24) |
| C2 | 0.4174(5) | 0.1629 (5) | 0.15445(19) | 2.05(22) |
| C3 | 0.5332(5) | 0.2692 (5) | 0.16523(20) | 2.78(25) |
| C4 | 0.6916(6) | 0.2347 (6) | 0.18294(21) | 3.3 ( 3) |
| C5 | 0.7390(6) | 0.0900 (6) | 0.19078(20) | 3.2 ( 3) |
| C6 | 0.6232(6) | -0.0154 (5) | 0.18084(19) | 2.6 ( 3) |
| C7 | 0.4623(5) | 0.0173 (5) | 0.16352(19) | 2.04(24) |
| C8 | 0.3397(5) | -0.1025 (5) | 0.15047(18) | 1.98(22) |
| C9 | 0.1716(5) | -0.0400 (5) | 0.15500(19) | 2.10(22) |
| C10 | 0.3401(5) | -0.1719 (5) | 0.09086(18) | 1.91(23) |
| C11 | 0.3428(6) | -0.3213 (5) | 0.08635(21) | 2.7 ( 3) |
| C12 | 0.3481(6) | -0.3883 (5) | 0.03237(22) | 3.1 ( 3) |
| C13 | 0.3522(6) | -0.3072 (5) | -0.01870(20) | 3.0 ( 3) |
| C14 | 0.3478(6) | -0.1578 (5) | -0.01501(20) | 2.9 ( 3) |
| C15 | 0.3422(6) | -0.0920 (5) | 0.03922(19) | 2.5 ( 3) |
| C16 | 0.0329(5) | -0.1447 (5) | 0.13484(19) | 1.93(22) |
| C17 | -0.0607(6) | -0.1379 (5) | 0.07927(21) | 3.1 ( 3) |
| C18 | -0.1866(6) | -0.2327 (5) | 0.06396(21) | 3.6 ( 3) |
| C19 | -0.2171(6) | -0.3389 (5) | 0.10226(22) | 3.4 ( 3) |
| C20 | -0.1217(6) | -0.3465 (5) | 0.15748(22) | 3.5 ( 3) |
| C21 | 0.0051(6) | -0.2510 (5) | 0.17485(19) | 2.7 ( 3) |
| C22 | 0.1750(6) | 0.0012 (5) | 0.21856(19) | 2.29(24) |
| C23 | 0.0689(6) | 0.3623 (6) | 0.0785 ( 3) | 5.9 ( 4) |
| H1 | 0.197 (4) | 0.259 (4) | 0.1711 (14) | 2.2 ( 9) |
| H3 | 0.489 (5) | 0.373 (4) | 0.1478 (18) | 5.9 (13) |
| H4 | 0.777 (4) | 0.299 (4) | 0.1903 (16) | 4.3 (12) |
| H5 | 0.876 (4) | 0.058 (4) | 0.2063 (14) | 2.3 (10) |
| H6 | 0.650 (4) | -0.111 (4) | 0.1790 (16) | 4.4 (12) |
| H8 | 0.372 (4) | -0.181 (4) | 0.1899 (15) | 2.7 (10) |
| H11 | 0.322 (4) | 0.620 (3) | 0.1224 (14) | 1.5 ( 9) |
| H12 | 0.345 (5) | -0.486 (5) | 0.0270 (18) | 6.1 (13) |
| H13 | 0.356 (5) | -0.361 (5) | -0.0592 (19) | 7.1 (14) |
| H14 | 0.346 (4) | -0.096 (4) | -0.0542 (16) | 4.7 (12) |
| H15 | 0.352 (6) | 0.013 (5) | 0.0434 (20) | 9.6 (17) |
| H17 | -0.044 (5) | -0.059 (4) | 0.0591 (18) | 6.1 (14) |
| H18 | -0.253 (5) | -0.229 (5) | 0.0202 (17) | 6.2 (14) |
| H19 | -0.333 (5) | -0.387 (4) | 0.0904 (17) | 5.3 (13) |
| H20 | -0.136 (5) | -0.417 (4) | 0.1795 (17) | 5.4 (13) |
| H21 | 0.079 (4) | -0.264 (4) | 0.2143 (16) | 5.0 (12) |
| H23A | 0.064 (5) | 0.413 (4) | 0.0427 (16) | 4.9 (12) |
| H23B | -0.014 (4) | 0.285 (4) | 0.0593 (16) | 4.6 (12) |
| H23C | 0.059 (7) | 0.433 (6) | 0.1050 (25) | 15.9 (24) |

Biso is the Mean of the Principal Axes of the Thermal Ellipsoid

Table of u(i,j) or U values *100.
E.S.Ds. refer to the last digit printed

| | u11(U) | u22 | u33 | u12 | u13 | u23 |
|---|---|---|---|---|---|---|
| O1 | 3.26(21) | 2.22(19) | 3.81(22) | -0.09(18) | 0.58(18) | 0.32(17) |
| O2 | 4.20(24) | 3.35(23) | 5.6 ( 3) | 0.27(20) | 1.10(21) | 1.95(19) |
| N1 | 5.4 ( 3) | 4.7 ( 3) | 4.5 ( 3) | -1.5 ( 3) | 1.9 ( 3) | -0.8 ( 3) |
| C1 | 4.0 ( 3) | 2.6 ( 3) | 2.8 ( 3) | -0.3 ( 3) | 1.1 ( 3) | -0.2 ( 3) |
| C2 | 3.3 ( 3) | 3.2 ( 3) | 1.5 ( 3) | -0.1 ( 3) | 1.12(24) | -0.59(25) |
| C3 | 3.4 ( 3) | 3.8 ( 3) | 3.5 ( 3) | -0.7 ( 3) | 0.9 ( 3) | -0.5 ( 3) |
| C4 | 3.8 ( 3) | 4.9 ( 4) | 3.9 ( 3) | -1.5 ( 3) | 1.3 ( 3) | -0.9 ( 3) |
| C5 | 3.1 ( 3) | 5.7 ( 4) | 3.5 ( 3) | -0.2 ( 3) | 0.7 ( 3) | -1.6 ( 3) |
| C6 | 4.2 ( 3) | 4.1 ( 3) | 1.8 ( 3) | 0.4 ( 3) | 0.8 ( 3) | -0.7 ( 3) |
| C7 | 2.9 ( 3) | 3.5 ( 3) | 1.4 ( 3) | 0.0 ( 3) | 0.53(24) | -0.40(24) |
| C8 | 3.2 ( 3) | 3.0 ( 3) | 1.4 ( 3) | 0.3 ( 3) | 0.79(24) | 0.62(24) |
| C9 | 3.5 ( 3) | 2.6 ( 3) | 2.0 ( 3) | 0.2 ( 3) | 0.9 ( 3) | 0.81(25) |
| C10 | 3.3 ( 3) | 2.6 ( 3) | 1.4 ( 3) | 0.1 ( 3) | 0.70(24) | 0.22(24) |
| C11 | 3.6 ( 3) | 2.3 ( 3) | 4.6 ( 4) | -0.1 ( 3) | 1.7 ( 3) | 0.3 ( 3) |
| C12 | 4.4 ( 4) | 2.4 ( 3) | 5.6 ( 4) | -0.2 ( 3) | 1.9 ( 3) | -1.1 ( 3) |
| C13 | 4.7 ( 4) | 3.7 ( 3) | 3.2 ( 3) | -0.6 ( 3) | 1.6 ( 3) | -1.1 ( 3) |
| C14 | 5.1 ( 4) | 3.4 ( 3) | 2.8 ( 3) | -0.4 ( 3) | 1.7 ( 3) | 0.3 ( 3) |
| C15 | 4.6 ( 3) | 2.8 ( 3) | 2.2 ( 3) | -0.2 ( 3) | 1.2 ( 3) | -0.2 ( 3) |
| C16 | 2.7 ( 3) | 2.5 ( 3) | 2.3 ( 3) | 0.2 ( 3) | 0.90(24) | 0.07(24) |
| C17 | 4.8 ( 4) | 3.2 ( 3) | 3.4 ( 3) | -0.4 ( 3) | -0.1 ( 3) | -0.2 ( 3) |
| C18 | 5.0 ( 4) | 4.1 ( 4) | 4.0 ( 4) | -0.5 ( 3) | -0.4 ( 3) | -0.4 ( 3) |
| C19 | 3.4 ( 3) | 3.5 ( 3) | 5.9 ( 4) | -0.2 ( 3) | 0.7 ( 3) | -1.2 ( 3) |
| C20 | 6.0 ( 4) | 2.5 ( 3) | 5.3 ( 4) | -0.8 ( 3) | 2.3 ( 3) | -0.4 ( 3) |
| C21 | 4.5 ( 3) | 3.4 ( 3) | 2.4 ( 3) | -0.2 ( 3) | 1.0 ( 3) | 0.3 ( 3) |
| C22 | 3.9 ( 3) | 3.0 ( 3) | 2.0 ( 3) | -0.5 ( 3) | 1.2 ( 3) | 0.06(25) |
| C23 | 3.9 ( 4) | 4.8 ( 4) | 13.2 ( 6) | 1.1 ( 4) | -0.1 ( 4) | 4.5 ( 4) |

Anisotropic Temperature Factors are of the form
Temp=-2*Pi*Pi*(h*h*u11*astar*astar+---+2*h*k*u12*astar*bstar+---)

| | | | | | | | | | |
|---|---|---|---|---|---|---|---|---|---|
| C9 | O1 | C1 | O2 | 163.9( 4) | C9 | O1 | C1 | C2 | 44.4( 3) |
| C9 | O1 | C1 | H1 | -82.7( 17) | C1 | O1 | C9 | C8 | -65.9( 3) |
| C1 | O1 | C9 | C16 | 170.3( 4) | C1 | O1 | C9 | C22 | 52.2( 3) |
| C23 | O2 | C1 | O1 | 68.2( 3) | C23 | O2 | C1 | C2 | -169.8( 5) |
| C23 | O2 | C1 | H1 | -44.8( 17) | C1 | O2 | C23 | H23A | -172.8( 22) |
| C1 | O2 | C23 | H23B | -74.1( 20) | C1 | O2 | C23 | H23C | 76.6( 34) |
| O1 | C1 | C2 | C3 | 170.7( 5) | O1 | C1 | C2 | C7 | -13.8( 2) |
| O2 | C1 | C2 | C3 | 53.3( 3) | O2 | C1 | C2 | C7 | -131.2( 5) |
| H1 | C1 | C2 | C3 | -66.9( 17) | H1 | C1 | C2 | C7 | 108.7( 17) |
| C1 | C2 | C3 | C4 | 177.5( 5) | C1 | C2 | C3 | H3 | -16.9( 20) |
| C7 | C2 | C3 | C4 | 1.9( 3) | C7 | C2 | C3 | H3 | 167.4( 21) |
| C1 | C2 | C7 | C6 | -178.1( 5) | C1 | C2 | C7 | C8 | 6.3( 2) |
| C3 | C2 | C7 | C6 | -2.5( 3) | C3 | C2 | C7 | C8 | -178.2( 5) |
| C2 | C3 | C4 | C5 | -0.4( 3) | C2 | C3 | C4 | H4 | 178.5( 22) |
| H3 | C3 | C4 | C5 | -164.0( 21) | H3 | C3 | C4 | H4 | 14.8( 29) |
| C3 | C4 | C5 | C6 | -0.6( 3) | C3 | C4 | C5 | H5 | -179.8( 16) |
| H4 | C4 | C5 | C6 | -179.6( 22) | H4 | C4 | C5 | H5 | 1.2( 26) |
| C4 | C5 | C6 | C7 | -0.1( 3) | C4 | C5 | C6 | H6 | 169.1( 23) |
| H5 | C5 | C6 | C7 | 179.1( 16) | H5 | C5 | C6 | H6 | -11.7( 27) |
| C5 | C6 | C7 | C2 | 1.6( 3) | C5 | C6 | C7 | C8 | 177.3( 5) |
| H6 | C6 | C7 | C2 | -168.1( 23) | H6 | C6 | C7 | C8 | 7.6( 22) |
| C2 | C7 | C8 | C9 | -24.8( 2) | C2 | C7 | C8 | C10 | 99.1( 4) |
| C2 | C7 | C8 | H8 | -137.4( 16) | C6 | C7 | C8 | C9 | 159.6( 5) |
| C6 | C7 | C8 | C10 | -76.5( 4) | C6 | C7 | C8 | H8 | 47.0( 16) |
| C7 | C8 | C9 | O1 | 53.0( 3) | C7 | C8 | C9 | C16 | 172.4( 5) |
| C7 | C8 | C9 | C22 | -66.2( 3) | C10 | C8 | C9 | O1 | -71.1( 3) |
| C10 | C8 | C9 | C16 | 48.3( 3) | C10 | C8 | C9 | C22 | 169.7( 5) |
| H8 | C8 | C9 | O1 | 164.8( 16) | H8 | C8 | C9 | C16 | -75.9( 16) |
| H8 | C8 | C9 | C22 | 45.6( 16) | C7 | C8 | C10 | C11 | 132.1( 5) |
| C7 | C8 | C10 | C15 | -46.0( 3) | C9 | C8 | C10 | C11 | -105.9( 4) |
| C9 | C8 | C10 | C15 | 76.0( 4) | H8 | C8 | C10 | C11 | 13.8( 16) |
| H8 | C8 | C10 | C15 | -164.3( 17) | O1 | C9 | C16 | C17 | 22.4( 2) |
| O1 | C9 | C16 | C21 | -158.6( 5) | C8 | C9 | C16 | C17 | -98.9( 4) |
| C8 | C9 | C16 | C21 | 80.1( 4) | C22 | C9 | C16 | C17 | 140.6( 5) |
| C22 | C9 | C16 | C21 | -40.4( 3) | O1 | C9 | C22 | N1 | 174.7( 6) |
| C8 | C9 | C22 | N1 | -65.8( 4) | C16 | C9 | C22 | N1 | 58.4( 4) |
| C8 | C10 | C11 | C12 | -178.1( 5) | C15 | C10 | C11 | C12 | 0.2( 3) |
| C8 | C10 | C15 | C14 | 177.9( 5) | C8 | C10 | C15 | H15 | 4.7( 26) |
| C11 | C10 | C15 | C14 | -0.3( 3) | C11 | C10 | C15 | H15 | -173.5( 27) |
| C10 | C11 | C12 | C13 | 0.6( 2) | C10 | C11 | C12 | H12 | -177.0( 25) |
| C11 | C12 | C13 | C14 | -1.2( 3) | C11 | C12 | C13 | H13 | -179.8( 23) |
| H12 | C12 | C13 | C14 | 176.5( 25) | H12 | C12 | C13 | H13 | -2.0( 33) |
| C12 | C13 | C14 | C15 | 1.1( 3) | C12 | C13 | C14 | H14 | -177.3( 20) |
| H13 | C13 | C14 | C15 | 179.6( 23) | H13 | C13 | C14 | H14 | 1.2( 29) |
| C13 | C14 | C15 | C10 | -0.3( 2) | C13 | C14 | C15 | H15 | 172.7( 27) |
| H14 | C14 | C15 | C10 | 178.0( 20) | H14 | C14 | C15 | H15 | -9.0( 32) |
| C9 | C16 | C17 | C18 | -178.4( 5) | C9 | C16 | C17 | H17 | -9.9( 24) |
| C21 | C16 | C17 | C18 | 2.6( 3) | C21 | C16 | C17 | H17 | 171.1( 25) |
| C9 | C16 | C21 | C20 | 179.4( 5) | C9 | C16 | C21 | H21 | -5.1( 20) |
| C17 | C16 | C21 | C20 | -1.6( 3) | C17 | C16 | C21 | H21 | 173.9( 21) |
| C16 | C17 | C18 | C19 | -2.8( 3) | C16 | C17 | C18 | H18 | -176.8( 22) |
| H17 | C17 | C18 | C19 | -169.8( 25) | H17 | C17 | C18 | H18 | 16.2( 32) |
| C17 | C18 | C19 | C20 | 1.9( 3) | C17 | C18 | C19 | H19 | 164.9( 21) |
| H18 | C18 | C19 | C20 | 175.8( 22) | H18 | C18 | C19 | H19 | -21.2( 29) |
| C18 | C19 | C20 | C21 | -0.9( 3) | C18 | C19 | C20 | H20 | -174.4( 26) |
| H19 | C19 | C20 | C21 | -161.9( 21) | H19 | C19 | C20 | H20 | 24.5( 32) |
| C19 | C20 | C21 | C16 | 0.7( 3) | C19 | C20 | C21 | H21 | -174.8( 21) |

| | | | | |
|---|---|---|---|---|
| H20 | C20 | C21 | C16 | 174.1( 26) |
| O2 | C23 | H23A | H23B | 110.7( 27) |
| H23B | C23 | H23A | H23B | 0.0( 24) |
| H23C | C23 | H23A | H23B | -132.2( 50) |
| O2 | C23 | H23B | H23A | -106.4( 27) |
| H23C | C23 | H23B | H23A | 109.8( 47) |
| H23A | C23 | H23C | H23A | 0.0( 28) |
| C23 | H23A | H23B | C23 | 0.0( 5) |
| C23 | H23A | H23C | C23 | 0.0( 5) |

| | | | | |
|---|---|---|---|---|
| H20 | C20 | C21 | H21 | -1.4( 32) |
| O2 | C23 | H23A | H23C | -117.1( 32) |
| H23B | C23 | H23A | H23C | 132.2( 42) |
| H23C | C23 | H23A | H23C | 0.0( 41) |
| H23A | C23 | H23B | H23A | 0.0( 27) |
| O2 | C23 | H23C | H23A | 111.5( 38) |
| H23B | C23 | H23C | H23A | -105.6( 47) |
| H23C | H23A | H23B | C23 | -28.0( 25) |
| H23B | H23A | H23C | C23 | 33.5( 28) |

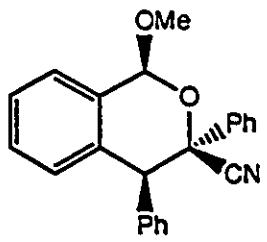


$C_{23}H_{19}NO_2$ 341.41

**10b**

**MP** 123.5-124.8 °C.

**MS** (CI/$Et_2O$) 342 $[M+1]^+$, 315, 310.

**IR** ($CH_2Cl_2$) $\nu_{max}(cm^{-1})$ 1029 (s), 1009 (s).

**$^1$H-NMR** ($CDCl_3$) δ(ppm) 3.70 (s, 3H); 4.36 (s, 1H); 5.90 (s, 1H); 6.88 (d, 1H, *J* = 7.9 Hz); 6.96 (d, 2H, *J* = 6.6 Hz); 7.13-7.34 (m, 9H); 7.38 (d, 1H, *J* = 8.1 Hz); 7.48 (d, 1H, *J* = 6.7 Hz).

**$^{13}$C NMR** ($CDCl_3$) δ(ppm) 56.3 (q); 56.8 (d); 75.1 (s); 99.3 (d); 118.5 (s); 126.1 (d); 127.5 (d); 127.6 (d); 128.0 (d); 128.0 (d); 128.1 (d); 128.8 (d); 128.9 (d); 131.1 (d); 132.5 (s); 134.3 (s); 135.3 (s); 137.5 (s).

### 6.10.15 Preparation of compounds 11a and 11b

A solution of 135 mg (0.7 mmol) of 1-methoxy-1,3-dihydrobenzo[c]thiophene 2,2-dioxide and 180 mg (1.4 mmol) of benzoyl cyanide in 8 mL of toluene was heated to reflux under nitrogen atmosphere until tlc analysis (dichloromethane: hexane 2:1) indicated complete conversion of the starting materials (2 h). Concentration (in vacuo) followed by flash chromatography (230-400 mesh silica gel) furnished **11a** and **11b** (3:1 ratio) in 92 % yield.

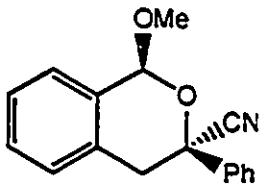


$C_{17}H_{15}NO_2$ 265.31

**11a**

**MP** 80.1-82.6 °C.

**MS** (CI/$Et_2O$) 266 $[M+1]^+$, 234, 207, 149.

**IR** ($CH_2Cl_2$) $\nu_{max}(cm^{-1})$ 1015 (s).

**$^1$H-NMR** ($CDCl_3$) δ(ppm) 3.36 (q, 2H, $J$ = 16.0 Hz); 3.64 (s, 3H); 6.04 (s, 1H); 7.15-7.24 (m, 1H); 7.30-7.51 (m, 6H); 7.69 (dd, 2H, $J$ = 1.6, 8.2 Hz).

**$^{13}$C NMR** ($CDCl_3$) δ(ppm) 40.8 (t); 55.9 (q); 75.0 (s); 100.6 (d); 119.1 (s); 125.0 (d); 126.3 (d); 127.8 (d); 128.0 (d); 128.9 (d); 129.2 (d); 131.0 (s); 132.7 (s); 138.7 (s).

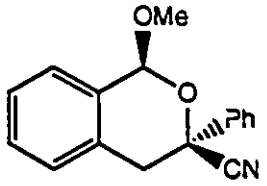


$C_{17}H_{15}NO_2$ 265.31

**11b**

**MP** 91.8-92.6 °C.

**MS** (CI/$Et_2O$) 266 $[M+1]^+$, 234, 207.

**IR** ($CH_2Cl_2$) $\nu_{max}(cm^{-1})$ 1012 (s).

**$^1$H-NMR** ($CDCl_3$) δ(ppm) 3.32 (q, 2H, $J$ = 16.4 Hz); 3.70 (s, 3H); 5.81 (s, 1H); 7.11-7.18 (m, 1H); 7.30-7.49 (m, 6H); 7.65 (dd, 2H, $J$ = 2.4, 8.2 Hz).

### 6.10.16 Preparation of compounds 12a and 12b

A solution of 145 mg (0.7 mmol) of 1-methoxy-1,3-dihydrobenzo[c]thiophene 2,2-dioxide and 101 mg (1.5 mmol) of acetyl cyanide in 3 mL of toluene was heated to reflux under nitrogen atmosphere until tlc analysis (dichloromethane: hexane 2:1) indicated complete conversion of the starting materials (2 h). Concentration (in vacuo) followed by flash chromatography (230-400 mesh silica gel) furnished **12a** and **12b** (2:1 ratio) in 70 % yield.

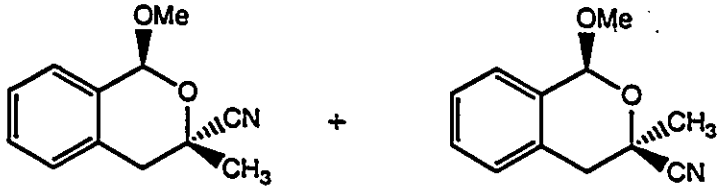


$C_{12}H_{13}NO_2$ 203.24 **12a**

$C_{12}H_{13}NO_2$ 203.24 **12b**

**MS** (EI) 202 $[M-1]^+$, 188, 172, 154, 144.

**IR** ($CH_2Cl_2$) $\nu_{max}(cm^{-1})$ 1087 (s),1016 (s).

**$^1$H-NMR** ($CDCl_3$) δ(ppm) **12a** 1.79 (s, 3H); 3.10 (q, 2H, $J$ = 16.1 Hz); 3.54 (s, 3H); 5.80 (s, 1H); 7.08-7.20 (m, 1H); 7.21-7.36 (m, 3H); **12b** 1.76 (s, 3H); 3.06 (q, 2H, $J$ = 15.6 Hz); 3.65 (s, 3H); 5.57 (s, 1H); 7.08-7.20 (m, 1H); 7.21-7.36 (m, 3H).

### 6.10.17 Competition between dimethyl fumarate and benzoyl cyanide

A solution of 100 mg (0.5 mmol) of 1-methoxy-1,3-dihydrobenzo[c]thiophene 2,2-dioxide, 73 mg (0.5 mmol) dimethyl fumarate and 66 mg (0.5 mmol) of benzoyl cyanide in 5 mL toluene was heated to reflux for 4 h. Concentration in vacuo yielded 251 mg of crude material. Capillary GC analysis showed no **11a** or **11b** was present and the GC-MS showed a molecular ion at m/e 278 corresponding to the tetralin derived from dimethyl fumarate.

### 6.10.18) Competition between benzaldehyde and benzoyl cyanide

A solution of 100 mg (0.5 mmol) of 1-methoxy-1,3-dihydrobenzo[c]thiophene 2,2-dioxide, 54 mg (0.5 mmol) benzaldehyde and 66 mg (0.5 mmol) of benzoyl cyanide in 5 mL toluene was heated to reflux for 4 h. Concentration in vacuo yielded 227 mg of crude material which was identified, by $^1$H-NMR, as a mixture of benzaldehyde, **11a** and **11b**.

### 6.10.19 Preparation of 13

A solution of 100 mg (0.5 mmol) of 1-methoxy-1,3-dihydrobenzo[c]thiophene 2,2-dioxide and 92 mg (0.6 mmol) of phenyl glyoxal in 5 mL of toluene was heated to reflux under nitrogen atmosphere for 4 h. Concentration in vacuo followed by flash chromatography (230-400 mesh silica gel, 5:1 hexane:ethyl acetate) afforded 38 mg (28 %) of **13**.

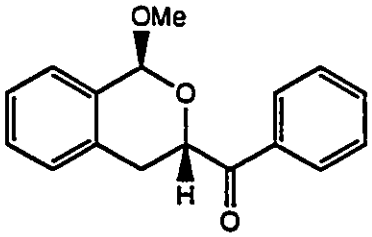


$C_{17}H_{16}O_3$ 268.31

**13**

**MS** (CI/ISO) 269 $[M+1]^+$, 237, 163, 131, 105.

**IR** ($CH_2Cl_2$) $\nu_{max}(cm^{-1})$ 1696 (s).

**$^1$H-NMR** ($CDCl_3$) δ(ppm) 3.03 (ddd, 2H, $J$ = 3.2, 11.4, 16.7 Hz); 3.63 (s, 3H); 5.53 (dd, 1H, $J$ = 3.2, 11.4 Hz); 5.66 (s, 1H); 7.10-7.65 (m, 7H); 8.03 (d, 2H, $J$ = 8.4 Hz).

### 6.10.20) Competition between phenylglyoxal and benzoyl cyanide

A solution of 50 mg (0.3 mmol) of 1-methoxy-1,3-dihydrobenzo[c]thiophene 2,2-dioxide, 34 mg (0.3 mmol) phenylglyoxal and 33 mg (0.3 mmol) of benzoyl cyanide in 5 mL toluene was heated to reflux for 4 h. Concentration in vacuo yielded 78 mg of crude material. Capillary GC analysis showed a large number of products, none of which had retention times corresponding to **11a**, **11b** or **13**. Examination of the $^1$H-NMR spectrum revealed broad unresolved signals suggesting that a polymeric mixture had formed.

### 6.10.21 Preparation of 14a and 14b

A solution of 100 mg (0.5 mmol) of 1-methoxy-1,3-dihydrobenzo[c]thiophene 2,2-dioxide and 100 mg (0.7 mmol) of 2-

methylbenzoyl cyanide in 5 mL of toluene was heated to reflux under nitrogen atmosphere until tlc analysis (hexane:ethyl acetate 5:1) indicated complete conversion of the starting materials (2 h). Concentration of the product mixture followed by flash chromatography yielded 59 mg (42 %) of **14a** and **14b** as a 9:8 mixture of isomers.

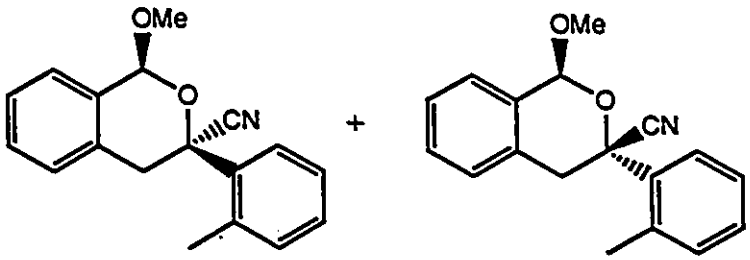


$C_{18}H_{17}NO_2$ 279.34 $C_{18}H_{17}NO_2$ 279.34

**14a** **14b**

**MS** (CI/ISO) 280 $[M+1]^+$, 253, 248, 221.

**IR** ($CH_2Cl_2$) $\nu_{max}(cm^{-1})$ 1009 (s), 1085 (m).

**$^1$H-NMR** ($CDCl_3$) δ(ppm) **14a** 2.68 (s, 3H); 3.52 (q, 2H, $J$ = 15.9 Hz); 3.60 (s, 3H); 6.11 (s, 1H); 7.10-7.50 (m, 7H); 7.65 (m, 1H); **14b** 2.70 (s, 3H); 3.50 (q, 2H, $J$ = 15.8 Hz); 3.76 (s, 3H); 5.78 (s, 1H); 7.10-7.50 (m, 7H); 7.65 (m, 1H).

### 6.10.22 Attempted preparation of 15

A solution of 100 mg (0.5 mmol) of 1-methoxy-1,3-dihydrobenzo[c]thiophene 2,2-dioxide and 90 mg (0.5 mmol) of 2-methoxy-4-methylbenzoyl cyanide in 5 mL of toluene was heated to reflux under nitrogen atmosphere until tlc analysis (hexane:ethyl acetate 3:1) indicated complete conversion of the starting materials (2 h). Concentration of the product mixture followed by flash

chromatography yielded unreacted aroyl cyanide, and polymeric by-products.

### 6.10.23 Attempted preparation of 16

A solution of 100 mg (0.5 mmol) of 1-methoxy-1,3-dihydrobenzo[c]thiophene 2,2-dioxide and 90 mg (0.5 mmol) of 2-methoxy-6-methylbenzoyl cyanide in 5 mL of toluene was heated to reflux under nitrogen atmosphere until tlc analysis (hexane:ethyl acetate 3:1) indicated complete conversion of the starting materials (2 h). Concentration (in vacuo) followed by flash chromatography (230-400 mesh silica gel) yielded unreacted 2-methoxy-6-methylbenzoyl cyanide accompanied by polymeric by-products.

### 6.10.24 Competitive photocycloadditions

To six test tubes (A-F), each charged with 100 mg (0.7 mmol) of 2-methylbenzoyl cyanide in 2.0 mL of acetonitrile, was added: A] 97 mg (0.7 mmol) benzoyl chloride; B] 86 mg (0.7 mmol) benzoyl fluoride; C] 119 mg (0.7 mmol) benzoyl imidazole; D] 94 mg (0.7 mmol)methyl benzoate; F] 70 mg (0.7 mmol) acetic anhydride. The tubes were suspended 10 cm from the lamp and irradiated for 12 h. After irradiation the product mixtures were concentrated on a rotovap and identified by $^1$H-NMR spectroscopy. Reaction completion was estimated by comparing the integrations of the methyl signal at d 2.62 ppm (2-methylbenzoyl cyanide), and the AB quartet at d 3.71 (dimer 6a). The results were as follows:

A] 10 % homo-, 0 % hetero-cycloaddition.

B] 90% homo-, 10% hetero-cycloaddition.*

C] 100 % homo-cycloaddition.

D] 100 % homo-cycloaddition.

E] 100 % homo-cycloaddition.

F] 100 % homo-cycloaddition.

* As judged by the appearance of a second AB system at d 3.54 (q, 2H, *J* = 16.4 Hz), 10 % the size of the quartet at d 3.71 ppm (dimer 6a).

### 6.10.25 1-Hydroxy-1-cyano-1,3-dihydrobenzo[c]thiophene 2,2-Dioxide (19)

A solution of 300 mg (2.1 mmol) 2-methylbenzoyl cyanide in 30 mL of benzene (10% $SO_2$), contained in a quartz test tube, was suspended 10 cm from a Hanovia medium pressure mercury lamp and irradiated until tlc analysis (hexane:ethyl acetate 3:1) indicated complete conversion of the aroyl cyanide (4 h). The product, which precipitated from benzene solution, was isolated by filtration giving 250 mg (58 %) of a yellow solid.

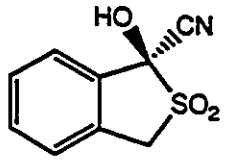


$C_9H_7NO_3S$ 209.22

**19a**

**MP** 137-138 °C (dec).

**MS** (EI) 145 $[M-64]^+$, 118, 90.

**EA** calc: C(51.67 %) H(3.37 %) N(6.70 %) S(15.33 %).
found: C(51.49 %) H(3.64 %) N(6.64 %) S(15.43 %).

**IR** ($CH_2Cl_2$) $\nu_{max}(cm^{-1})$ 1241 (m), 1032 (m).

**$^1$H-NMR** 500 MHz ($CDCl_3$) δ(ppm) 4.71 (q, 2H, *J* = 16.0 Hz);
7.58 (d, 1H, *J* = 6.3 Hz); 7.64 (t, 1H, *J* = 7.3 Hz);
7.65 (t, 1H, *J* = 8.3 Hz); 7.81 (d, 1H, *J* = 7.5 Hz).

**$^{13}$C NMR** ($CDCl_3$) δ(ppm) 53.1 (t); 70.0 (s); 114.1 (s); 126.9 (d);
127.5 (d); 130.2 (d) ; 131.6 (s); 132.5 (d); 134.1 (s).

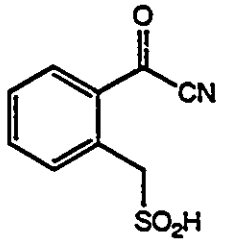


$C_9H_7NO_3S$ 209.22

**19b**

**IR** ($CH_2Cl_2$) $\nu_{max}(cm^{-1})$ 1661 (m).

**$^1$H-NMR** 500 MHz ($CDCl_3$) δ(ppm) 4.47 (s, 2H);
7.60 (d, 1H, *J* = 8.8 Hz); 7.76 (t, 1H, *J* = 7.5 Hz);
7.86 (t, 1H, *J* = 8.8 Hz); 8.30 (d, 1H, *J* = 7.5 Hz).

### 6.10.26 1-Hydroxy-1-cyano-1,3-dihydro-7-methoxy-benzo[c]thiophene 2,2-Dioxide (20)

A solution of 200 mg (1.1 mmol) 2-methoxy-6-methylbenzoyl cyanide in 25 mL of benzene (saturated with $SO_2$), contained in a quartz test tube, was suspended 10 cm from a Hanovia medium pressure

mercury lamp and irradiated until tlc analysis (hexane:ethyl acetate 3:1) indicated complete conversion of the aroyl cyanide (4 h). Concentration of the crude material on a rotovap followed by flash chromatography yielded 137 mg (50 %) of **20**, as a light green oil.

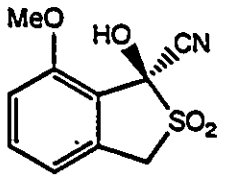


$C_{10}H_9NO_4S$ 239.25

**20**

**MS** (EI) 175 $[M-64]^+$, 148, 129.

**IR** ($CH_2Cl_2$) $\nu_{max}(cm^{-1})$ 3500 (br), 2216 (w), 1295 (s), 1036 (s).

**$^1$H-NMR** ($CDCl_3$) δ(ppm) 2.70 (s, 1H); 3.62 (s, 3H); 4.26 (q, 2H, *J* = 16.0 Hz); 6.71 (d, 1H, *J* = 7.6 Hz); 6.82 (d, 1H, *J* = 8.6 Hz); 7.22 (t, 1H, *J* = 7.9 Hz).

### 6.10.27 Thermolysis of 19 in the presence of dimethyl fumarate

Trace $ZnO_2$ (ca. 5 mg) was added to a stirred solution of 50 mg (0.2 mmol) 1-Hydroxy-1-cyano-1,3-dihydrobenzo[c]thiophene 2,2-Dioxide (**19**) and 70 mg (0.4 mmol) of dimethyl fumarate in 5 mL *o*-xylene. The mixture was then heated to reflux under nitrogen atmosphere for 12 h. The blackened mixture was cooled to rt, filtered through celite, and the xylene evaporated under high vacuum. The $^1$H-

NMR spectrum of the crude material showed only broad unresolved peaks. The mixture was subsequently passed through a silica gel plug (3:1 hexane:ethyl acetate). Evaporation of the solvent gave approximately 6 mg (16 %) 2-methylbenzoyl cyanide.

### 6.10.28 Attempted conversion of 19 to the methyl ether 22.

A trace of TsOH (ca. 5 mg) was added to a stirred solution of 50 mg (0.2 mmol) 1-Hydroxy-1-cyano-1,3-dihydrobenzo[c]thiophene 2,2-Dioxide (19) in 16 mL of 50 % MeOH in $CH_2Cl_2$ and the mixture heated to reflux. After 12 h the solvent was evaporated giving 53 mg of crude material whose spectral characteristics indicated structure **23**.

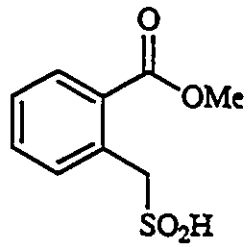


$C_9H_{10}O_4S$ 214.24

**23**

**MS** (CI/ISO) 215 $[M+1]^+$, 197, 181, 165.

**IR** ($CH_2Cl_2$) $\nu_{max}(cm^{-1})$ 1706 (s), 1281 (s), 1074 (s).

**$^1$H-NMR** ($CDCl_3$) δ(ppm) 3.51 (s, 3H); 4.04 (s, 2H); 5.46 (s, 1H); 7.00-7.28 (m, 3H); 7.61 (d, 1H, $J$ = 8.4 Hz).

# Chapter 7

# Acyl Cyanides as Carbonyl Heterodienophiles: Synthetic Applications of the Cycloadducts

## 7.1 Introduction

In chapter 6, an account was given which described the capacity of aroyl cyanides to participate in hetero Diels-Alder reactions with electron rich *o*-quinodimethanes. In this chapter, the results obtained from an investigation of the synthetic potential of the cycloadducts will be presented, as well as attempts to construct the tetracyclic carbon skeleton of defucogilvocarcin M via the intermolecular Diels-Alder approach described in chapter 3.

The generalized strategy for exploitation of the cycloadducts as synthetic intermediates is depicted in scheme 7.1.

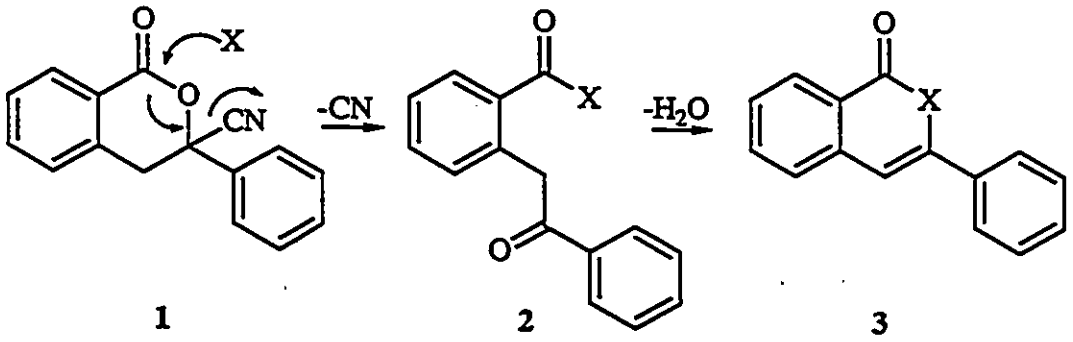


Scheme 7.1: General synthetic strategy involving a tandem addition cyclization sequence via nucleophile X.

Presumably, cycloadduct **1** should be susceptible to nucleophilic attack at its carbonyl center leading, after CN loss, to the dicarbonyl compound **2**. Subsequently, it should be possible to effect cyclization of **2** to the bicyclic structure **3**.

## 7.2 An isoquinolone synthesis

The isoquinolone (1-oxo-1,2-dihydroisoquinoline) ring system is a structural component of several medicinally important alkaloids;[72] these compounds have proven to be useful synthetic intermediates as well, with applications to the synthesis of indenoisoquinolines,[73] protoberberines[74] and dibenzoquinolizine derivatives.[75]

Classical isoquinolone synthetic methodology has included the treatment of isocoumarins with substituted amines,[76] conversions of homophthalic acids and anhydrides,[77] and the reaction of dilithiated *N*,2-dimethyl benzamides with *N*,*N*-dimethylcarboxamides.[78]

A recently published isoquinolone synthesis[79] involved an intramolecular Wittig olefination of several substituted *N*-acyl-*N*-methyl-*o*-triphenylphosphoniomethylbenzamide bromides (scheme 7.2).

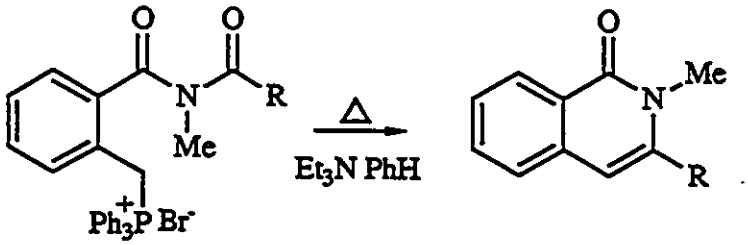


**4** **5**

Scheme 7.2: Couture's isoquinolone synthesis

Recalling the general strategy described in the introduction, the proposed approach to isoquinolones employing the cycloadducts should be intuitively obvious. In principle, as depicted in scheme 7.3, nucleophilic attack of an appropriately substituted amine should produce a ketoamide capable of cyclizing to the isoquinolone ring system. In practise, this proved to

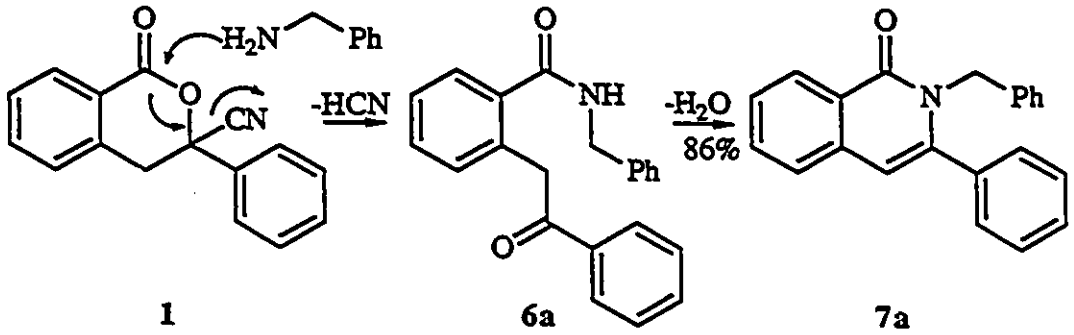


Scheme 7.3: Addition-elimination sequence leading to isoquinolone 7a

be the case as reflux of a cyclohexane solution of 3,4-dihydro-3-cyano-3-phenyl-1H-2-benzopyran-1-one (1) and benzyl amine (1.2 eq) for 15 h cleanly afforded the ketoamide **6a** [IR ($CH_2Cl_2$) $\nu_{max}(cm^{-1})$ 1646 (s)] in quantitative yield. Cyclization to the isoquinolone was accomplished efficiently in 86 % yield by refluxing in 50 % aqueous acetic acid for 3h. Isoquinolone **7a** was readily identified on the basis of its spectral properties, for example, the EIMS showed a prominent fragment at m/e 310 $[M-1]^+$, giving an accurate mass determination of 311.1287 (calcd for $C_{22}H_{17}NO$ 311.1310), and the IR spectrum showed a strong absorbance at $\nu_{max}$ 1652 $cm^{-1}$, consistent with the conjugated amide functionality. The $^1H$ and $^{13}C$-NMR spectra (figures 7.1 and 7.2) also supported the structural assignment; the former showed, in addition to

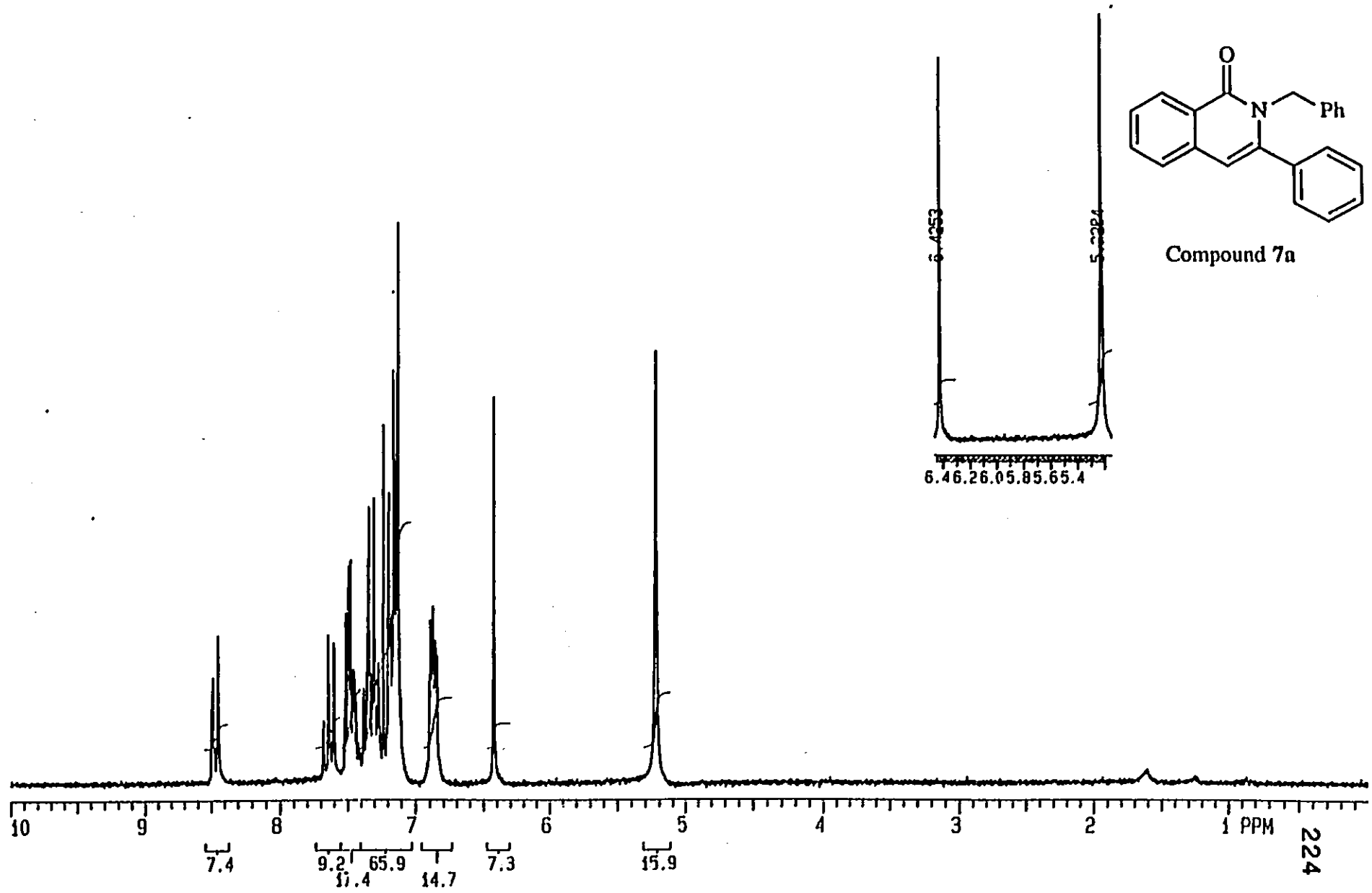


Figure 7.1: $^{1}$H-NMR of compound 7a.

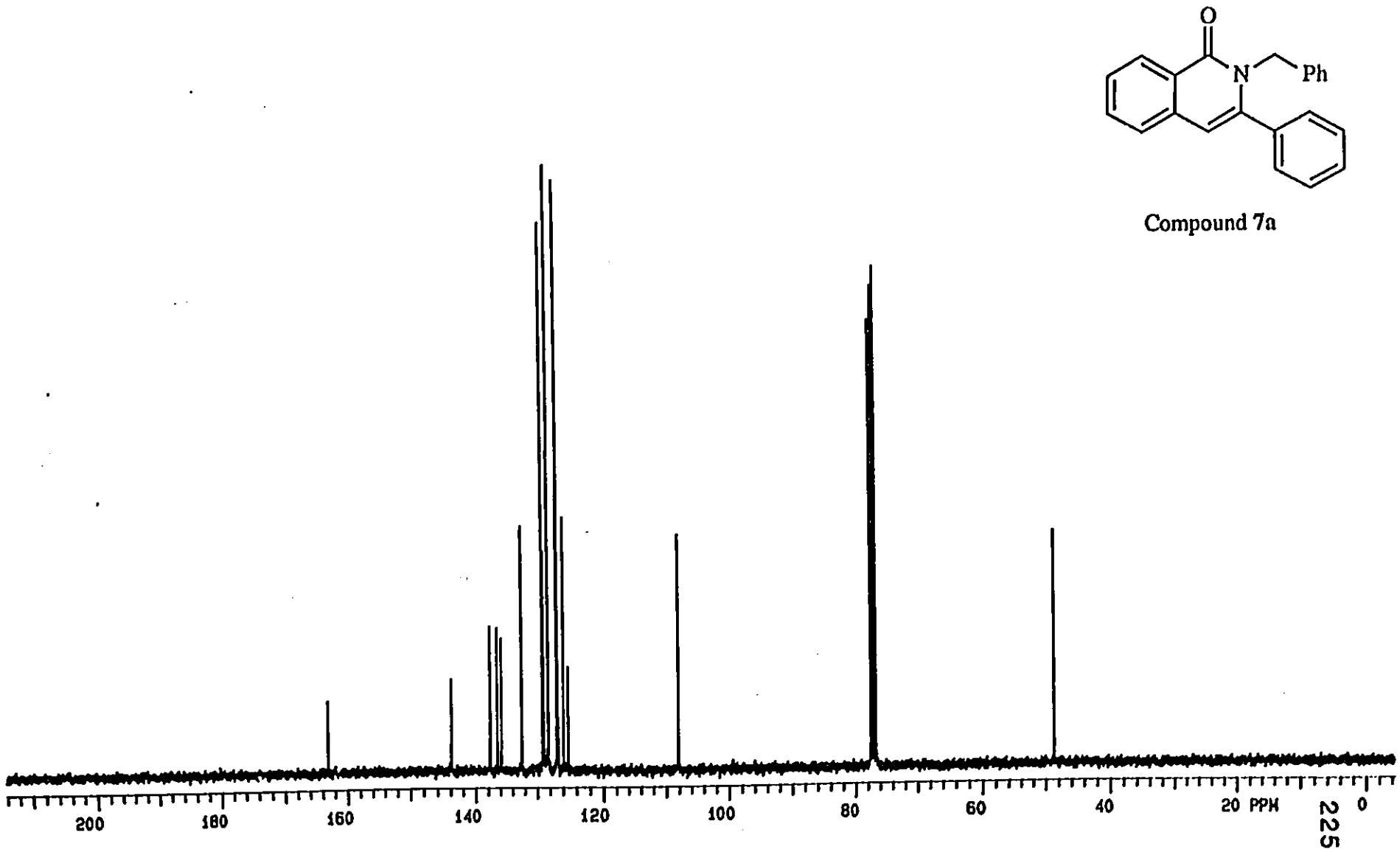


Figure 7.2: $^{13}$C-NMR of compound 7a.

the aromatic hydrogen resonances, two key signals at δ 5.23 (s, 2H) ppm, assigned to the benzylic protons, and δ 6.43 (s, 1H) ppm, attributed to the benzylic methinyl hydrogen; the latter exhibited 18 signals, as expected given the degree of symmetry present, with key assignments including the triplet at δ 48.5 ppm, arising from the benzylic methylene carbon, and the singlet at δ 163.1 ppm, derived from the amide carbonyl.

The synthetic sequence was applicable employing alkyl amines as well, as was demonstrated by the reaction of n-butyl amine with cycloadduct **1** (scheme 7.4).

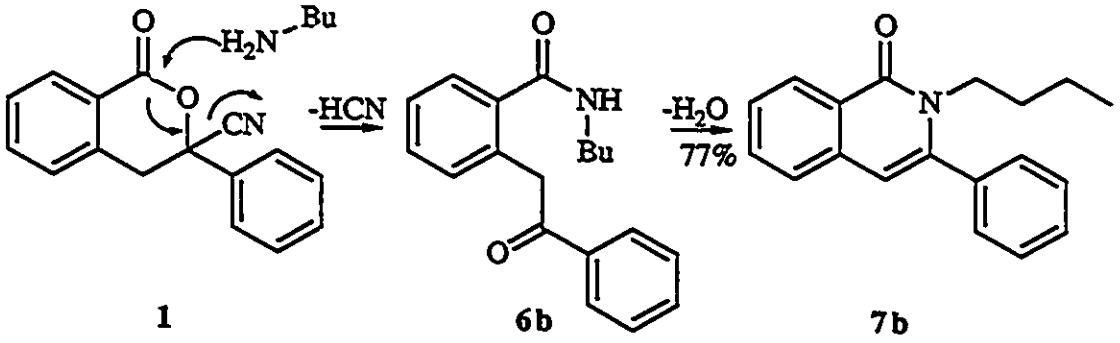


Scheme 7.4: Addition-elimination sequence leading to isoquinolone **7b**

Compound **7b** was obtained in 77 % isolated yield. The IR spectrum, as was the case for isoquinolone **7a**, showed a strong absorbance at $\nu_{max}$ 1648 $cm^{-1}$, confirming the conjugated amide functionality. Both the $^{1}H$ and $^{13}C$-NMR spectra were consistent with the structural assignment.

Two additional examples of the methodology were studied (scheme 7.6) starting with the alkyl cycloadduct **6**. Reflux of a

cyclohexane solution of 3,4-dihydro-3-cyano-3-methyl-1H-2-benzopyran-1-one (8) and benzyl amine (1.2 eq) for 15 h, followed by a 3 h reflux of the ketoamide intermediate in 50 % aqueous acetic acid, furnished isoquinolone **9a** in 57 % yield. Similar treatment of adduct **8**, utilizing n-butyl amine, afforded isoquinolone **9b** in 85 % yield, after flash chromatography. Both compounds were characterized readily on the basis of Mass, IR, $^{1}$H-NMR and $^{13}$C-NMR spectral data.

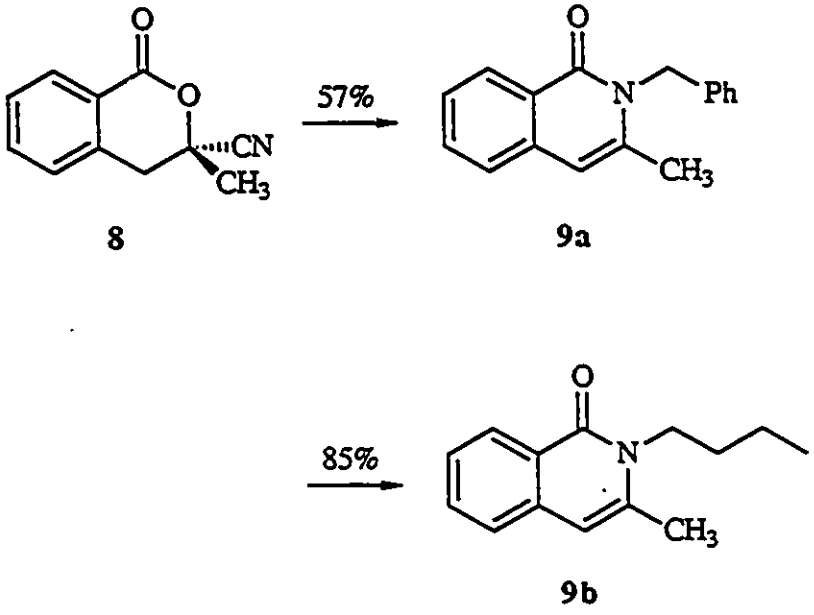


Scheme 7.5: Synthesis of isoquinolones **9a** and **9b**

The success of the preceding examples was encouraging and suggested that the approach taken could constitute a highly versatile isoquinolone synthesis. As illustrated in scheme 7.6, employing various aroyl cyanides, both as *o*-QDM precursors and as heterodienophiles,

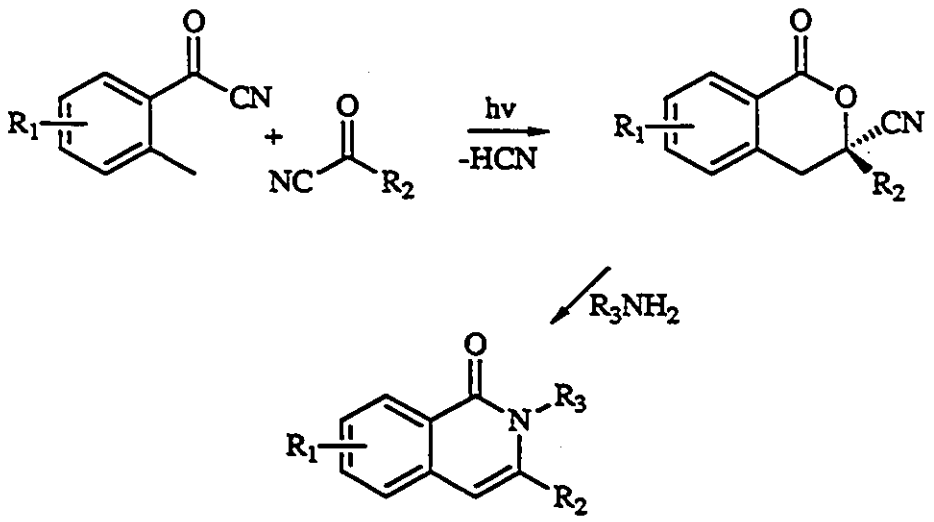


Scheme 7.6: Versatile isoquinolone synthesis

together with an alkyl or aryl amine, should provide a facile entry to a large number of substituted isoquinolones.

## 7.3 An isocoumarin synthesis

In an effort to extend further the synthetic utility of the cycloadducts, the potential for an isocoumarin preparation was briefly investigated. The cycloadducts **1** and **8** are essentially masked isocoumarins which, it may be envisioned, have undergone addition of HCN across the 3,4-double bond. It follows that the isocoumarin ring system should be accessible by base catalysed elimination of HCN. Initial attempts employing DBU or DBN, known to efficiently catalyse dehydrohalogenation,[80] gave unsatisfactory results with both **1** and **8**.

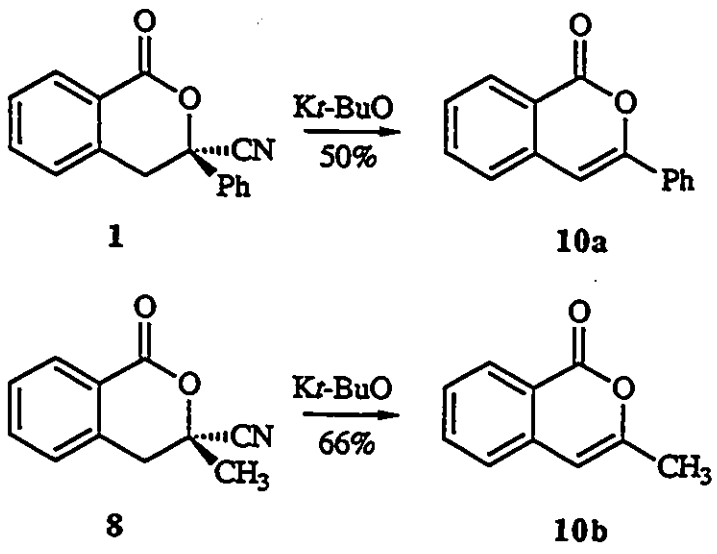


Scheme 7.7: Synthesis of isocoumarins **10a** and **10b**

Potassium *t*-butoxide proved to be the reagent of choice as treatment of an ice cooled THF solution of compound **1** (scheme 7.7) with 1.5 equivalents of the base yielded the known isocoumarin **10a** in 50 % yield. Similarly, isocoumarin **10b** was prepared from **8** in 66 % yield.

Both **10a** and **10b** exhibited spectral characteristics consistent with those found in the literature.[81,82]

## 7.4 Synthesis of naphthols and naphthoquinones

Recalling the general strategy depicted in scheme 7.1, substitution of X for a carbon nucleophile (scheme 7.8) should result, after CN loss, in the formation of an acetophenone intermediate capable of undergoing cyclization to the naphthol. Thus the naphthol **13a** was prepared, by

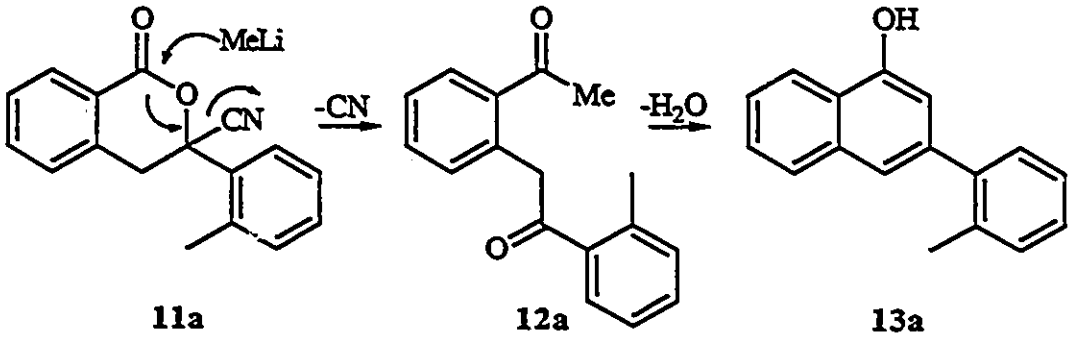


Scheme 7.8: Synthesis of naphthol **13a** via MeLi

treatment of a THF solution (cooled to -78°C under nitrogen atm.) of 3,4-dihydro-3-cyano-3-(2-methylphenyl)-1H-2-benzopyran-1-one (**11a**) with 2.2 eq of MeLi (1.4 M ether solution), in 60 % yield after acidic workup and flash chromatography; none of the acetophenone intermediate **12a** was isolated from the product mixture.

The naphthol **13a**, $M^+$= 234 (EIMS), showed a broad absorbance at $\nu_{max}$ 3577 $cm^{-1}$ in the infrared. Both the $^1$H-NMR and the $^{13}$C-NMR spectra were in support of the structural assignment; the former (fig.

7.3) exhibited key signals at δ 2.30 (s, 3H) ppm, assigned to the methyl hydrogens, δ 5.53 (s, 1H) ppm, ascribed to the hydroxyl proton, and δ 6.78 (s, 1H) and 7.36 (s, 1H) ppm, attributed to the isolated aromatic hydrogens; the latter exhibited 17 signals, the most notable being the peak at δ 20.5 ppm, arising from the methyl carbon.

Scheme 7.9 illustrates the results obtained from attempts to extend

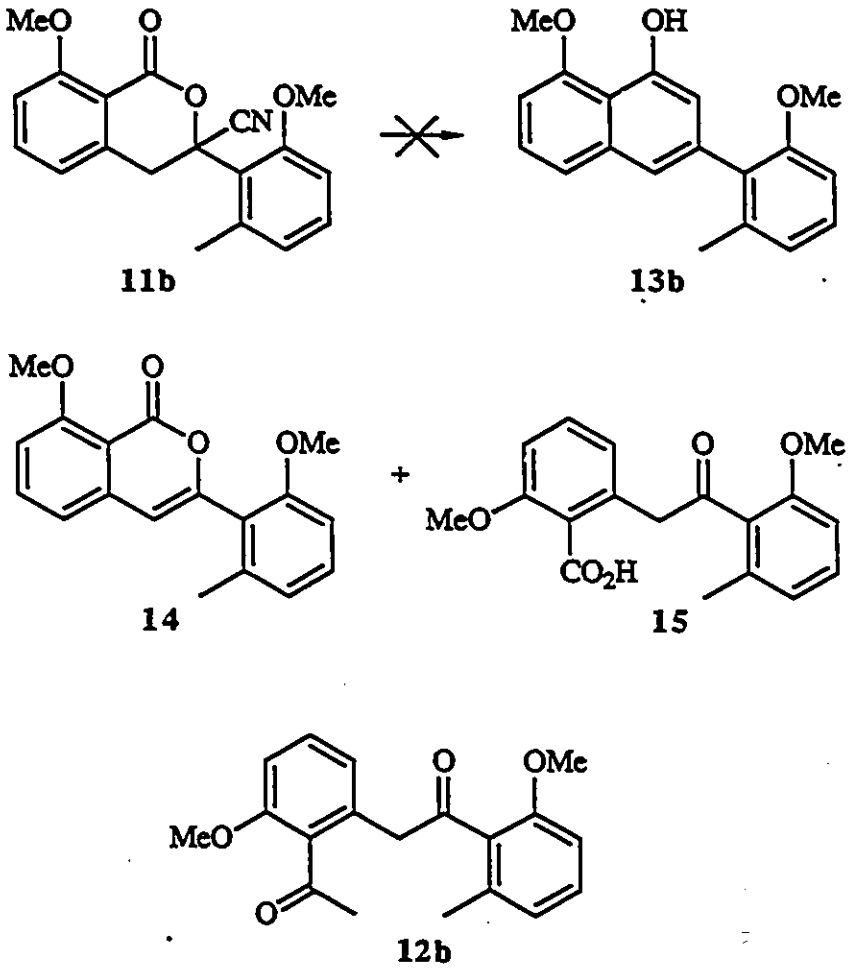


Scheme 7.9: Abortive synthesis of naphthol **13b**

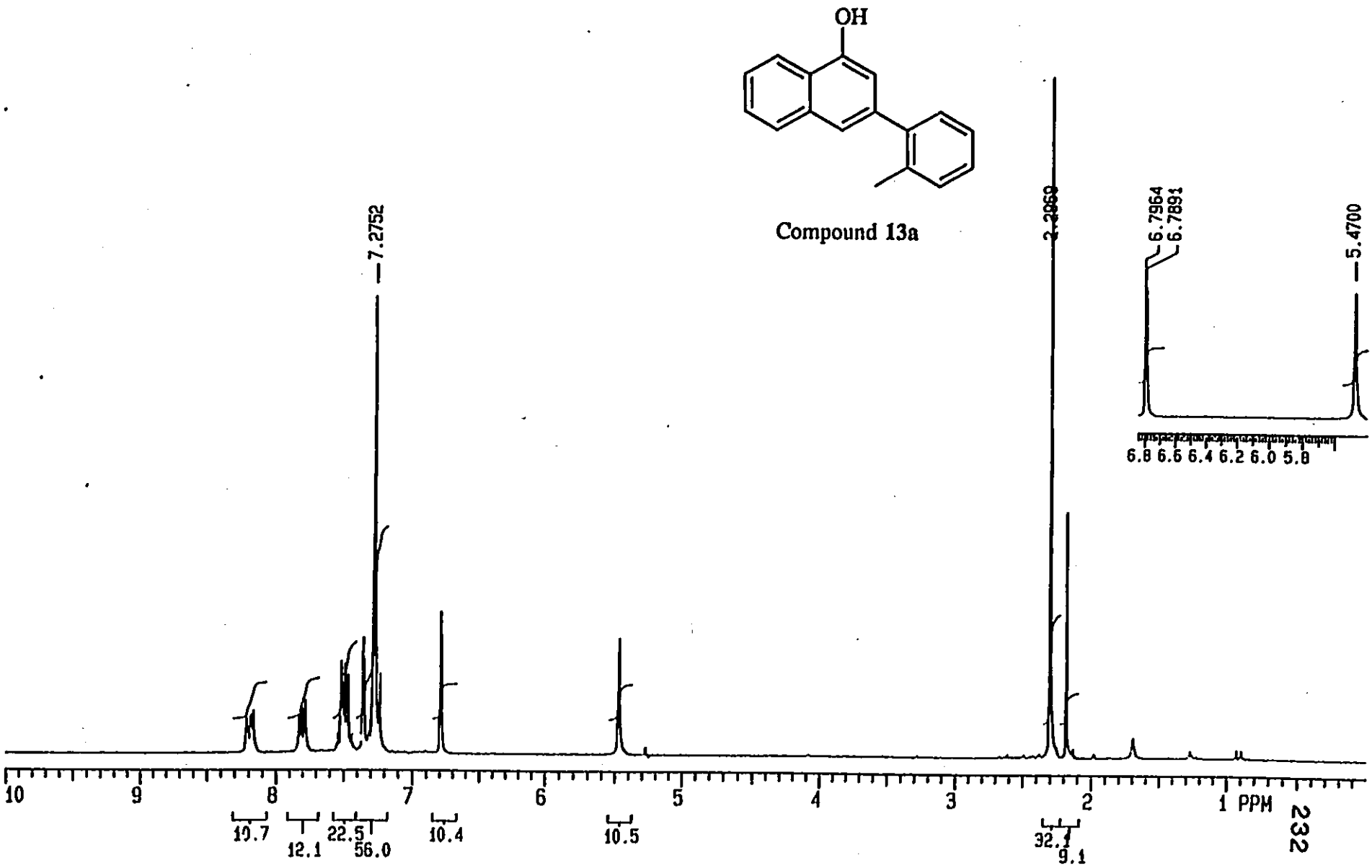


Figure 7.3: $^{1}$H-NMR of compound 13a.

the methodology to adduct **11b**. Treatment of a THF solution of **11b** with 2.2 eq of MeLi (at -78°C) failed to produce any of the anticipated naphthol (**13b**), but rather, afforded compounds tentatively identified as acetophenone **12b**, isocoumarin **14** and carboxylate **15**; all attempts to cyclize **12b** led to complex mixtures. Presumably, compound **14** arose from β elimination of the cyano moiety, and **15** from hydrolysis of **14** on workup. The isolation of **12b** as the major product suggests that the steric encumberance inherent in the 2,6-disubstituted aryl ketone was sufficient to preclude cyclization.

The most important reaction in this category, in terms of the defucogilvocarcin M synthesis, involved the formation of naphthol **13c** from cycloadduct **11c**.

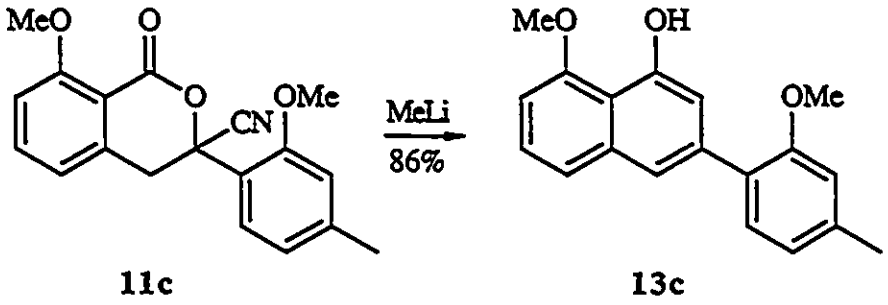


**11c** **13c**

Scheme 7.10: Synthesis of naphthol **13c**

Treatment of a THF solution (-78°C) of **11c** with 2.2 eq of MeLi furnished naphthol **13c** in 86 % yield, after flash chromatography. The facile conversion of both **11a** and **11c** to naphthols **13a** and **13c**, respectively, and the failure to reproduce the result with adduct **11b**

supported the postulate that it was the steric hinderance in **11b** which inhibited its cyclization.

Naphthol **13c** was identified readily on the basis of its spectrometric characteristics. The EIMS, for example, exhibited a prominent molecular ion at m/e 294 [M+] and the IR spectrum showed a characteristically broad absorbance at $\nu_{max}$ 3404 $cm^{-1}$ due to the phenolic function. The $^1$H-NMR spectrum (fig. 7.4) was similarly informative exhibiting, in addition to the aromatic hydrogen resonances, a singlet at δ 2.40 ppm, assigned to the methyl hydrogens, and two singlets at δ 3.80 and 4.04 ppm, both ascribed to the methoxy protons. The $^{13}$C-NMR spectrum, illustrated in figure 7.5, gave 19 signals the most notable of which included a trio of quartets at δ 21.5, 55.5, and 56.1 ppm, assigned to the benzylic methyl, and to the methoxy carbons, respectively.

Both naphthols **13a** and **13c** were efficiently converted to the naphthoquinones by treatment of aqueous acetonitrile solutions with 2.2 eq of [bis(trifluoroacetoxy)iodo]benzene (Btfl).[83]

Naphthoquinone **16a** [$M^+$ = 248] formed in 83 % yield as a brilliant yellow oil. The IR spectrum showed a strong absorbance at $\nu_{max}$ 1654 $cm^{-1}$ consistent with the quinone functionality while the $^1$H-NMR spectrum gave peaks at δ 2.21 (s, 3H), 6.90 (s, 1H), 7.12-7.33 (m, 4H), 7.74 (m, 2H), and 8.11 (m, 2H) ppm.

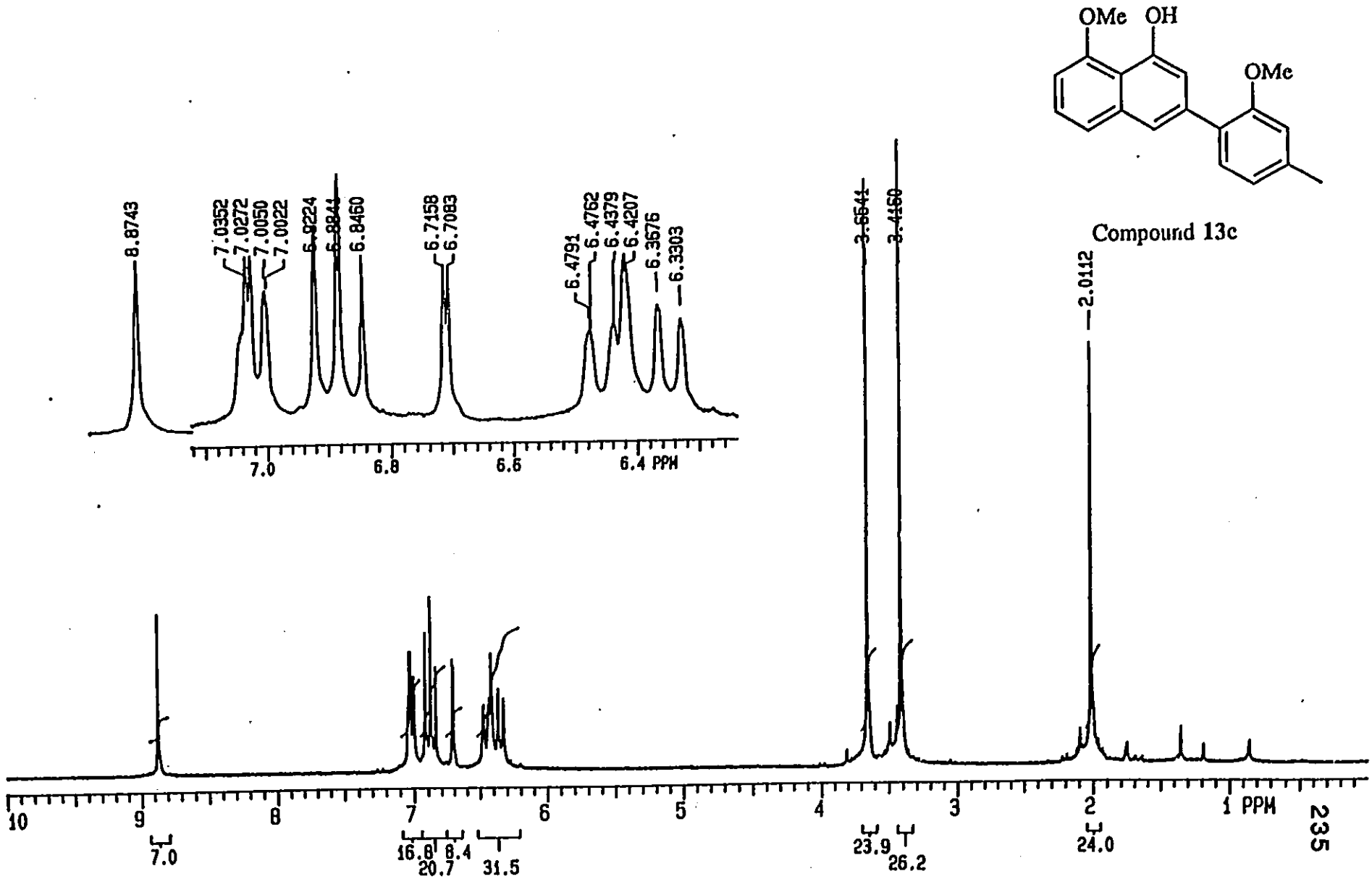


Figure 7.4: $^{1}$H-NMR of compound 13c.

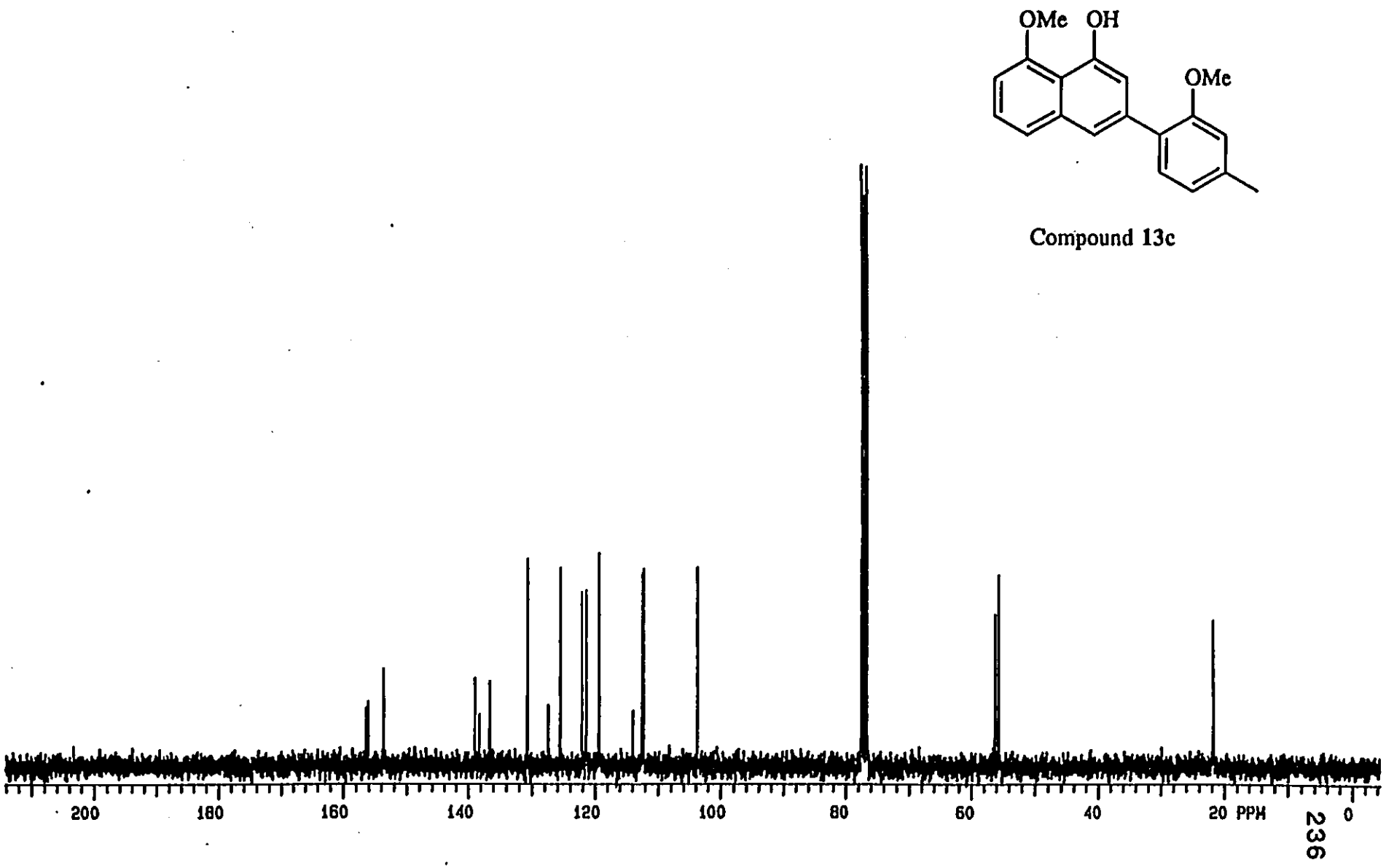


Figure 7.5: $^{13}$C-NMR of compound **13c**.

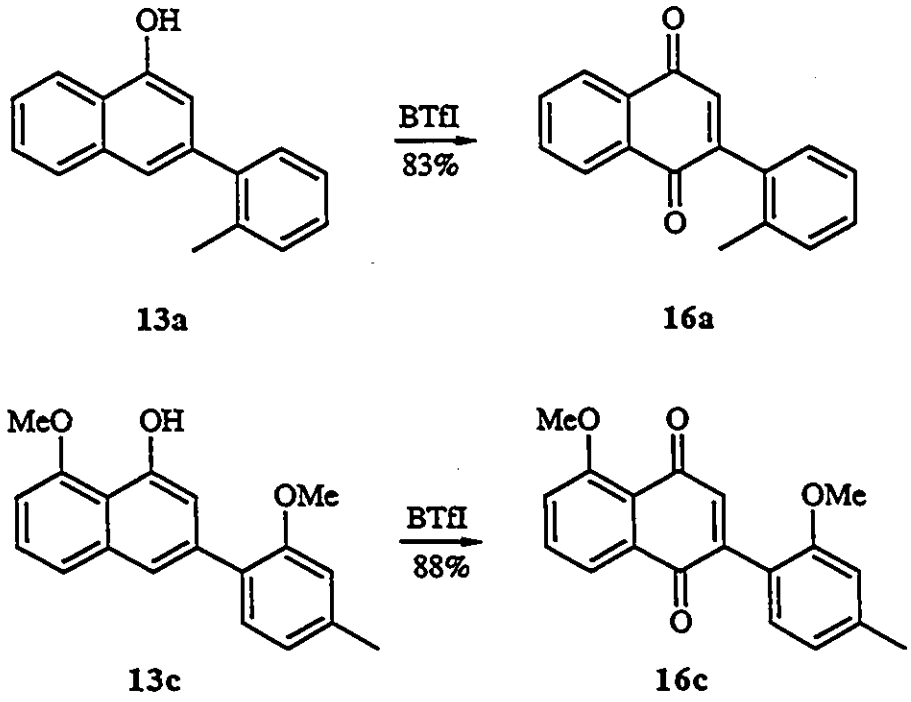


Scheme 7.11: Preparation of naphthoquinones **16a** and **16c**

Compound **16c**, an orange oil, also formed in excellent yield (88 %). The EIMS showed the expected molecular ion at m/e 308 while the IR spectrum exhibited a strong absorbance at $\nu_{max}$ 1656 $cm^{-1}$, consistent with the quinone functionality. The $^{1}$H-NMR spectrum (fig. 7.6), in addition to the aromatic proton resonances, showed key signals at δ 2.38, 3.74 and 3.99 ppm, assigned to the methyl and methoxy hydrogens, and a pair of singlets at δ 6.77 and 6.92 ppm, attributed to the quinone and to the isolated aromatic protons, respectively. The $^{13}$C-NMR spectrum (fig. 7.7) exhibited characteristic signals which included a trio of quartets at δ 21.8, 55.7 and 56.5 ppm, assigned to the methyl and methoxy carbons, a doublet at δ 112.2 ppm,

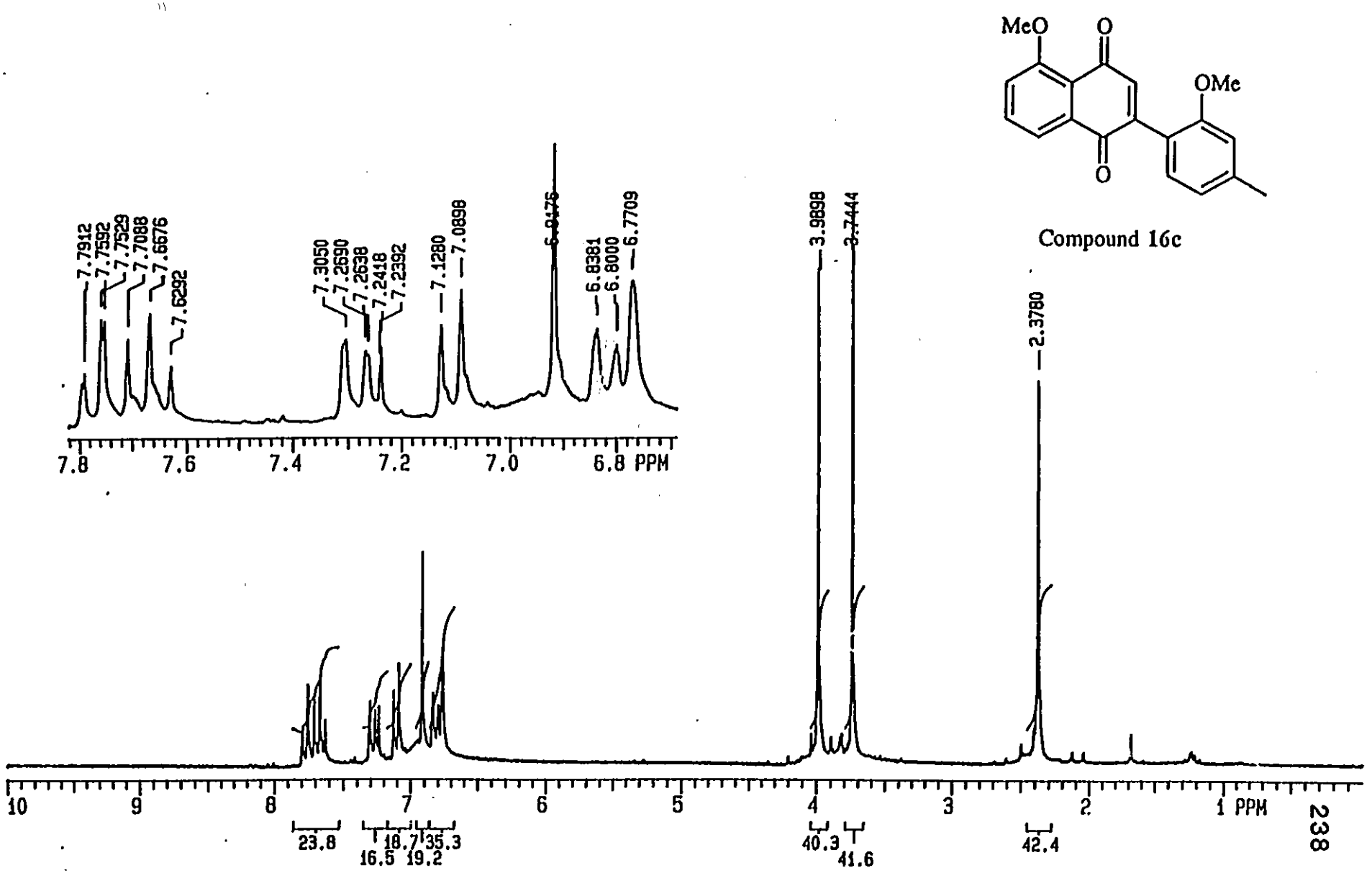


Figure 7.6: $^{1}$H-NMR of compound 16c.

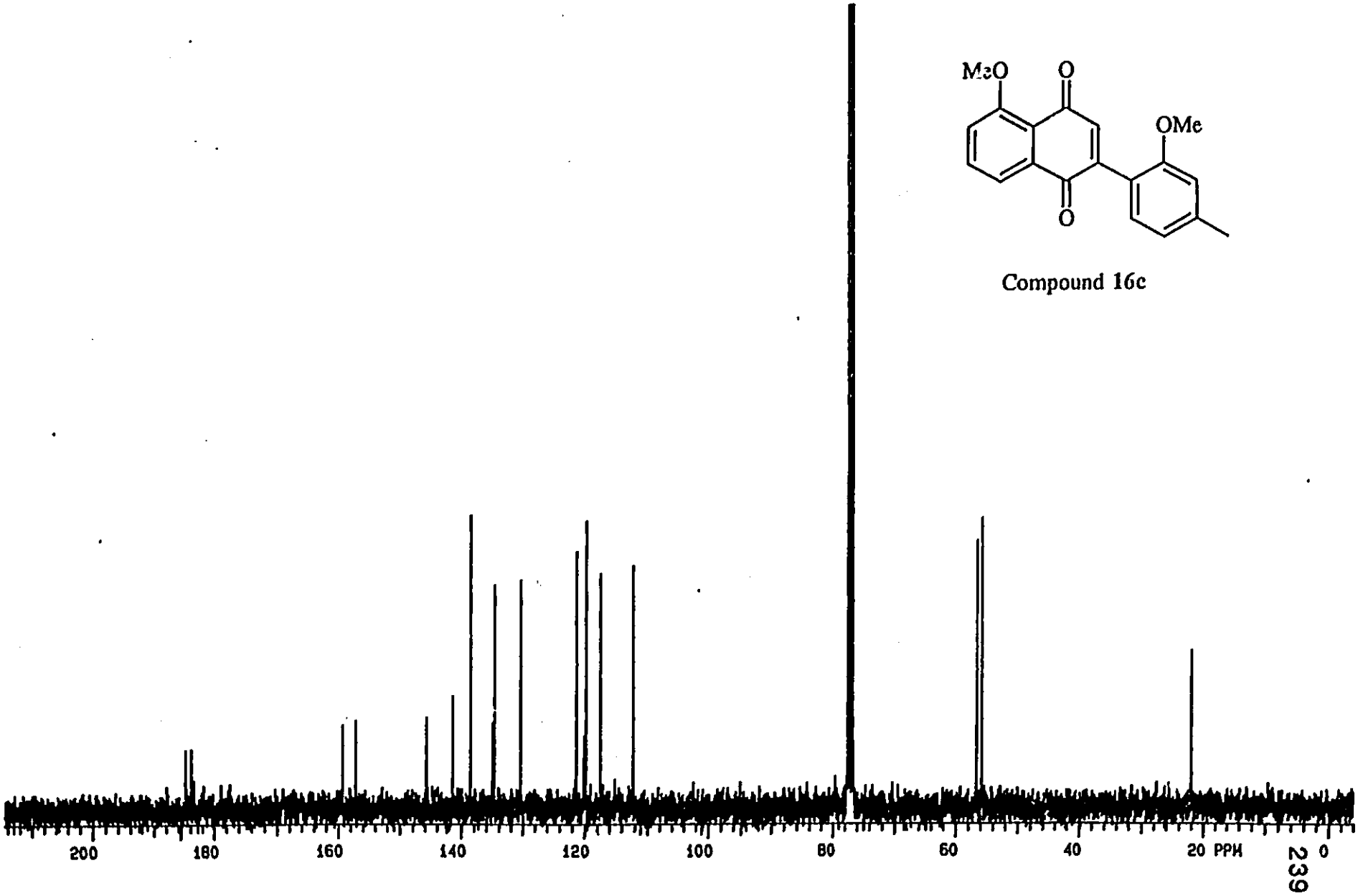


Figure 7.7: $^{13}$C-NMR of compound **16c**.

ascribed to the quinone a carbon, and three singlets at δ 77.2, 183.9, and 184.8 ppm, attributed to the quinone quaternary α carbon and carbonyl carbons, respectively.

## 7.5 Attempted cyclization of naphthoquinone 16a

In keeping with the synthetic methodology proposed for the synthesis of the benzonaphthopyranone ring system in chapter three (scheme 3.5: path a), attention was next directed at effecting electrocyclization of the naphthoquinone **16a**, via base treatment.

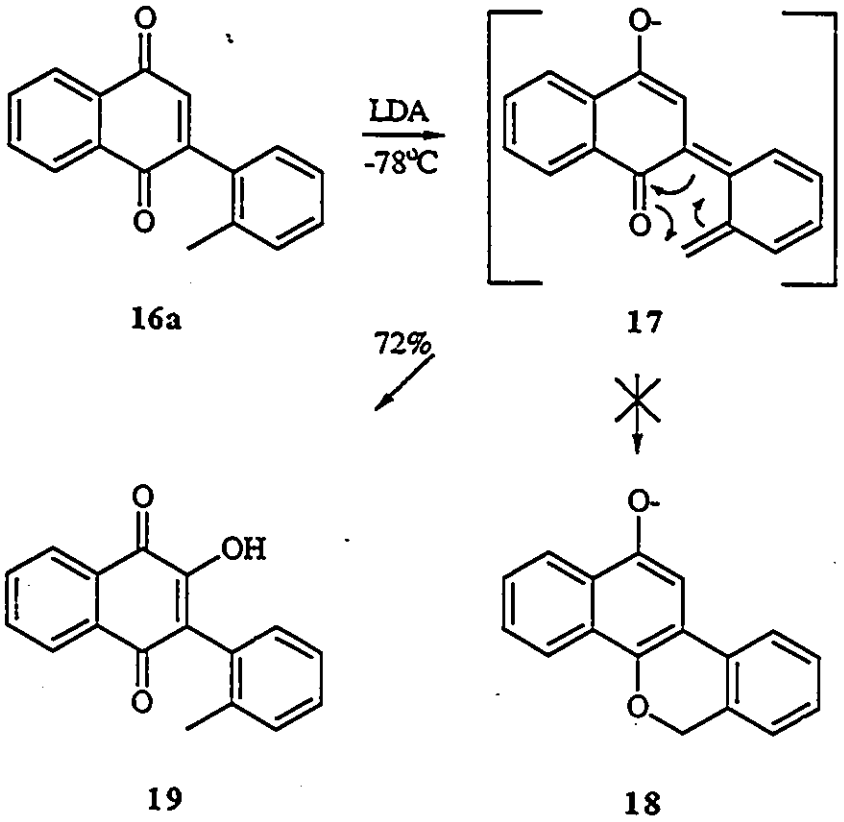


Scheme 7.12: Attempted cyclization of naphthoquinone **16a**

As illustrated in scheme 7.12, treatment of a THF solution of naphthoquinone **16a** with 2.2 eq of LDA, followed by quenching with 10 % aqueous HCl, failed to furnish the desired benzonaphthopyran **18**, but rather, afforded the hydroxyquinone **19** in 72 % yield. Treatment of **16a** with other bases, such as K*t*-BuO, produced the same brightly coloured solutions (yellow to red); repeatedly producing hydroxyquinone **19** on workup. Scheme 7.13 illustrates a possible mechanism for the formation of **19**.

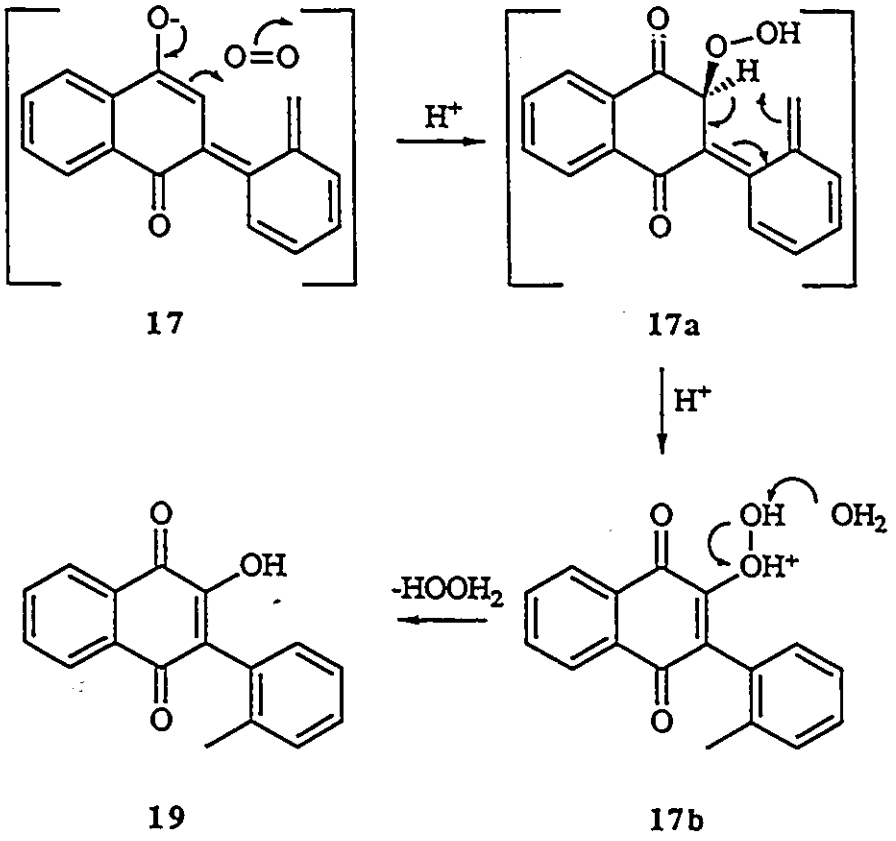


Scheme 7.13: Postulated mechanistic sequence leading to **19**

The reaction of intermediate **17** with dissolved oxygen should lead to the hydroperoxide **17a**. Intermediate **17a** could then undergo a

1,5-hydrogen shift affording **17b**, which, under the acidic conditions, should readily decompose to the hydroxyquinone **19**.

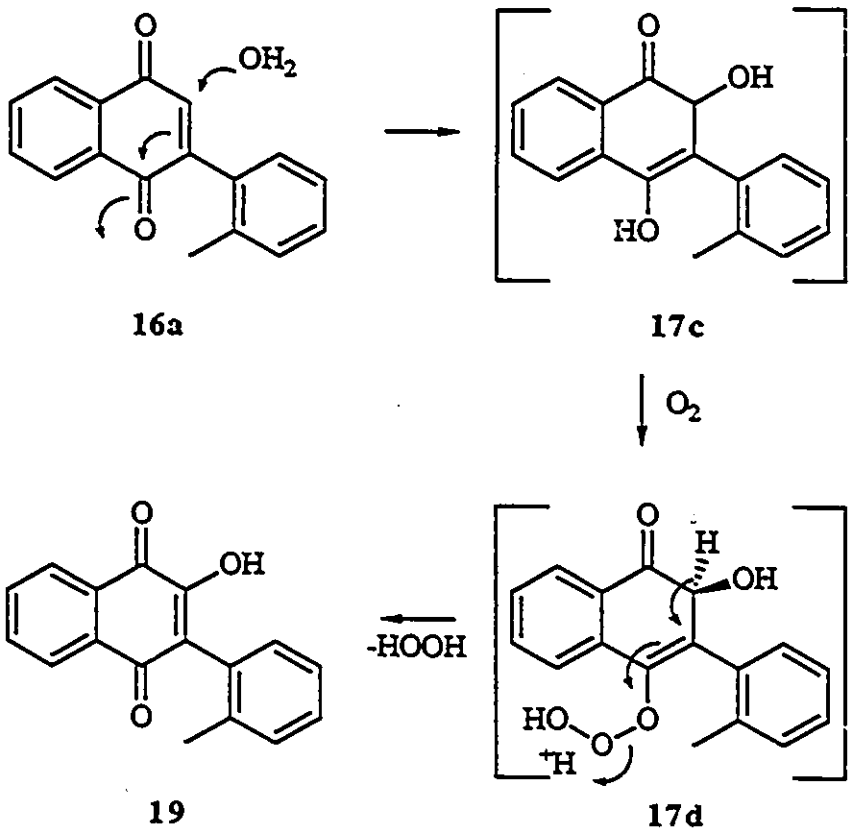


**16a** **17c**

**19** **17d**

Scheme 7.14: Alternative mechanism leading to **19**

An alternative sequence (scheme 7.14) would involve a 1,4 addition of $H_2O$ to **16a**, followed by in situ oxidation of the semiquinone intermediate **17d**. Similar 1,4 additions of nucleophiles to quinones have been well documented in the literature.[84]

Several abortive attempts to effect the cyclization under acidic conditions were also undertaken. For example, while treatment of a dichloromethane solution of **16a** with excess $BF_3$-etherate yielded

highly coloured solutions, only starting material was isolated upon workup.

## 7.6 Photochemical behavior of naphthoquinone 16a

Before proceeding with naphthoquinone **16c**, a brief investigation of the photochemical behavior of compound **16a** was undertaken. Examination of the literature revealed no previous studies of the photochemistry of **16a**, however, two relevant examples were found dealing with the photocyclization of *N*-(*o*-tolyl)phthalimide[85] (scheme 7.15) and α-(*o*-tolyl)acetophenone.[86a]

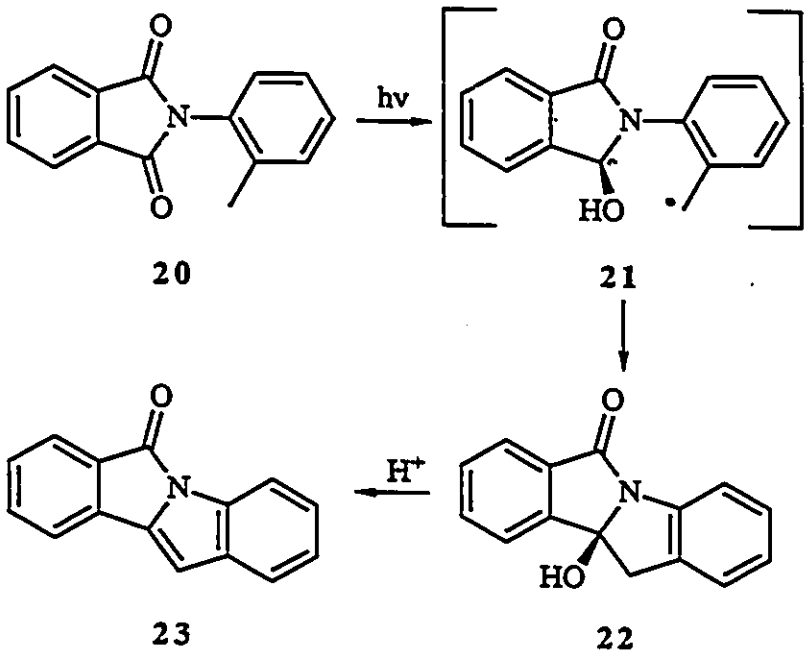


Scheme 7.15: Kanaoka's *N*-(*o*-tolyl)phthalimide photocyclization

As depicted in scheme 7.15, irradiation of the *N*-(*o*-tolyl)phthalimide **20** resulted, via intramolecular H-abstraction, in the

formation of the 1,5 biradical **21** which subsequently cyclized to the tetracyclic tertiary alcohol **22**. Acid catalysed elimination furnished the 6H-isoindolo[2,1a]indol-6-one **23** in good yield.

Given the *N*-(*o*-tolyl)phthalimide and a-(*o*-tolyl)acetophenone photocyclization precedents, it was postulated that an analogous cyclization should be possible with naphthoquinone **16a**. Scheme 7.16 illustrates the product obtained when **16a** was irradiated in acetonitrile solution.

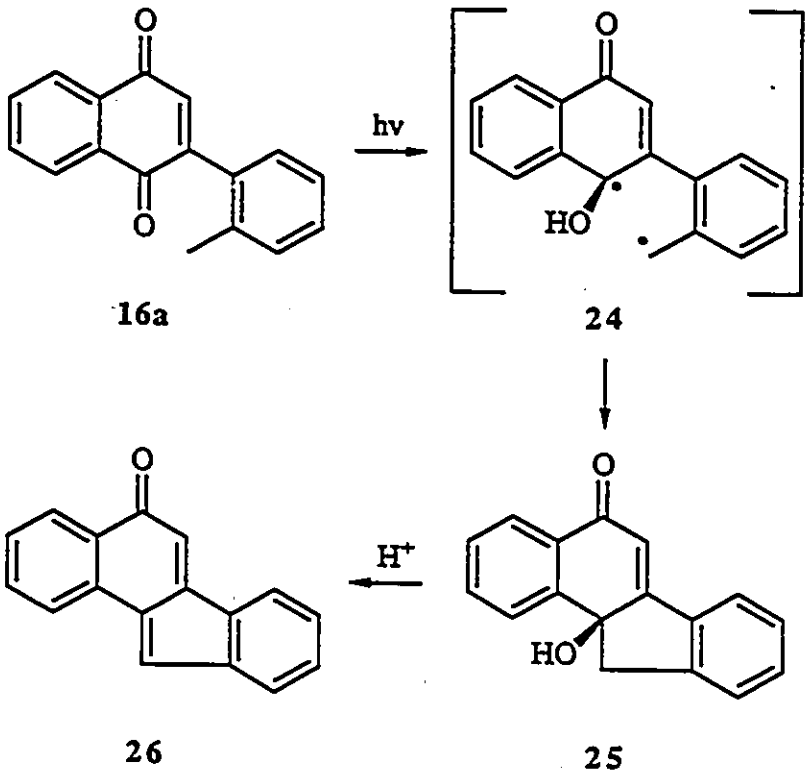


Scheme 7.16: Photocyclization of naphthoquinone **16a**

Compound **25** displayed a prominent molecular ion (m/e 248) in its EIMS, as well as a fragment corresponding to a loss of $H_2O$ (m/e 230). The IR spectrum of **25** also supported the structural assignment exhibiting two diagnostic absorbances at $\nu_{max}$ 3315 and 1683 $cm^{-1}$, which verified the presence of the carbonyl and hydroxyl groups. The most notable signals present in the $^1H$-NMR spectrum (fig. 7.8) included an AB quartet centered at $\delta$ 3.53 ($J$ = 15.9 Hz) ppm (benzylic methylene), and a singlet at $\delta$ 6.63 ppm (quinone aH).

Presumably, irradiation of **16a** lead to the biradical **24**, which subsequently underwent cyclization to the tertiary alcohol **25**. The reaction places naphthoquinone **16a** in same photochemical category as *N*-(*o*-tolyl)phthalimide and a-(*o*-tolyl)acetophenone, introducing some interesting possibilities for the synthesis of novel DNA intercalating agents from naphthoquinone precursors.

Finally, treatment of a dichloromethane solution of **25** with TsOH gave the highly coloured quinone methide **26** [calcd for $C_{17}H_{12}O_2$ 248.0837 found 248.0864], consolidating the analogy with the *N*-(*o*-tolyl)phthalimide system. Only a single report of compound **25** was found in the literature. Schaden[86b] reported isolating minute quantities of 5*H*-benzo[a]fluoren-5-one (**25**), a side product of the pyrolysis of chrysene-6,12-dione; details regarding the properties of **25** were not given.

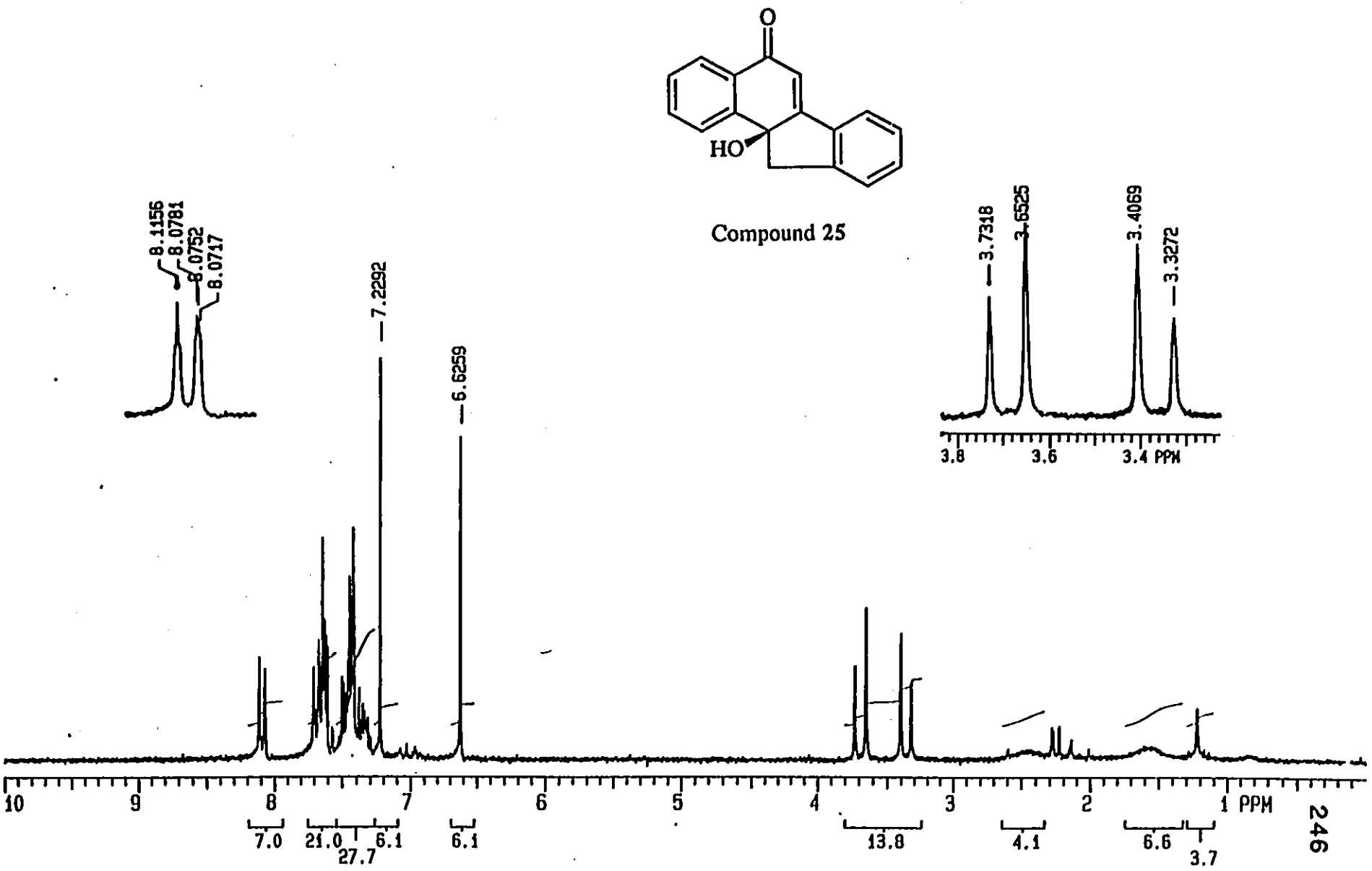


Figure 7.8: $^{1}$H-NMR of compound **25**.

## 7.7 Attempted synthesis of the defucogilvocarcin M ring system by anionic carbamoyl transfer

In section 3.2.1 a two part strategy for the synthesis of defucogilvocarcin M was proposed.

The first part invoked the possibility of applying an intermolecular Diels-Alder cycloaddition to construct the naphthalene component of the system. The work described in chapter six laid the foundation for the intermolecular cycloaddition, while the methodology described in section 7.4 addressed the problem of converting the cycloadducts to 3-aryl naphthols and naphthoquinones (scheme 7.17).

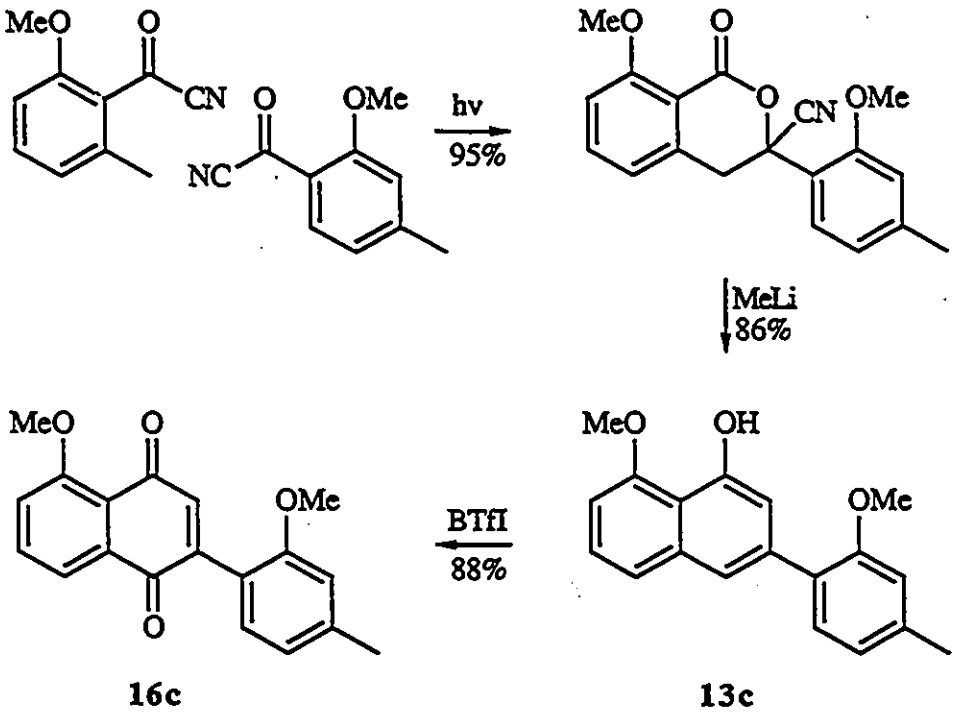


**16c** **13c**

Scheme 7.17: Synthesis of intermediates **13c** and **16c**

The second part, to be described in this section, proposed to form the C ring by remote metalation, followed by ring to ring carbamoyl transfer, and lactonization. Snieckus has published some interesting work in this area; the most relevant of which described the synthesis of the dibenzo[b,d]pyranone **28**.[87]

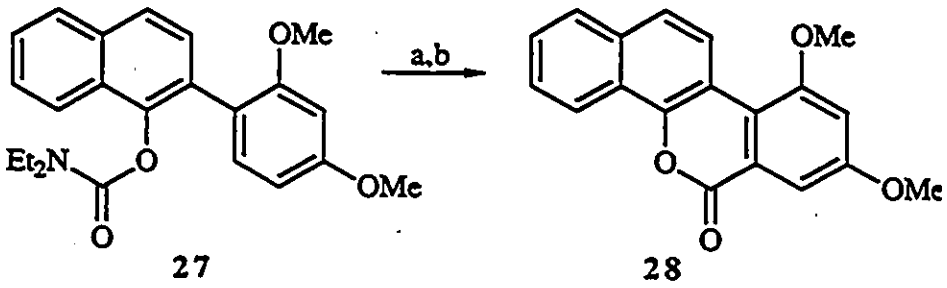


Scheme 7.18: Snieckus' dibenzo[c,d]pyranone synthesis
a) LDA/THF rf (63%) b) AcOH rf (95%)

Remote metallation of **27**, driven by a complex induced proximity effect,[88] leads to intramolecular carbamoyl transfer (facilitated by the nucleofugacity of the phenolate anion), and then, on acid treatment, to the lactone **28**.

It was expected that the same methodology should be applicable to the synthesis of defucogilvocarcin M starting from hydroquinone **29**.

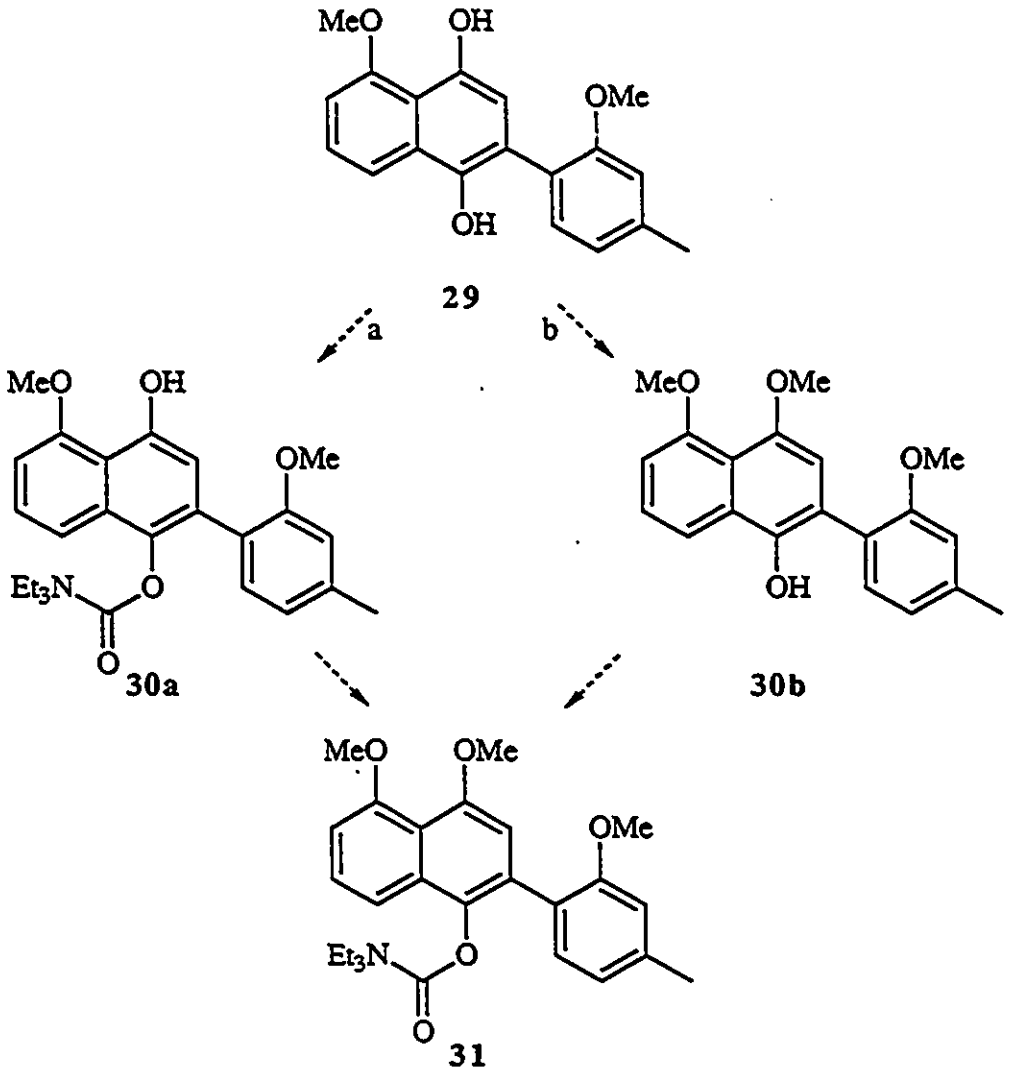


Scheme 7.19: Alternative pathways leading to **31**

As depicted in scheme 7.19, hydroquinone **29** could possibly be converted to the benzonaphthopyranone precursor **31** via two pathways denoted a and b. Pathway a would involve, first, a regioselective carbamate formation (**30a**), whereas, pathway b would begin with a regioselective *o*-methylation (**30b**).

**Pathway a**

Hydroquinone **29** was readily prepared by dropwise addition of a saturated aqueous solution of $Na_2S_2O_4$ to a stirred THF solution of quinone **16c**. Reaction completion was judged by tlc, and by the disappearance of the brilliant orange colour of the quinone **16c**. After separation of the phases and drying of the THF solution, **29** was converted to the mono-oxyanion, by treatment with one eq of NaH at 0°C, then quenched with one equivalent of diethyl carbamoyl chloride.

Unfortunately, extractive workup and flash chromatography failed to produce the desired monocarbamate **30a**, but rather afforded the dicarbamate **32** in 23 % yield. Several additional attempts were made and in each case, only **16c** and **32** were isolated.

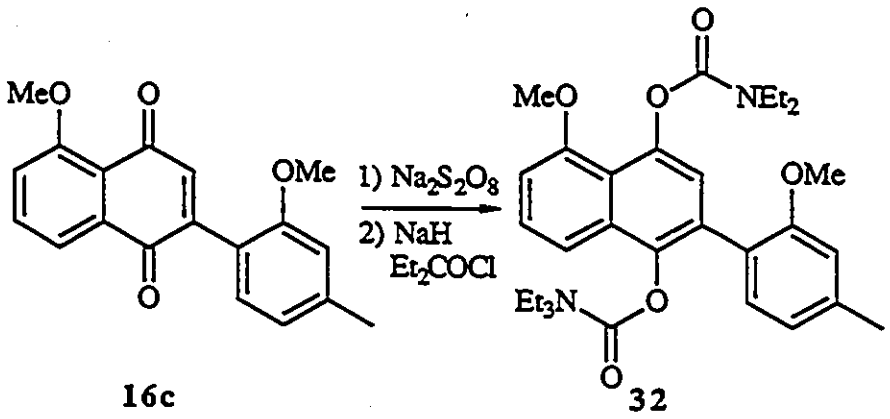


**16c** **32**

The dicarbamate structure **32** followed from the 508 molecular ion observed in the EIMS and the integration ratio of the N-ethyl vs the methoxy signals in the proton NMR.

Remote metallation of **32** was not attempted since it was anticipated that under the vigourous conditions required (LDA/THF

reflux) *o*-metallation in the naphthalene ring rather than remote metallation would occur preferentially.

## 7.8 Conclusions

In this chapter the cycloadducts described in chapter 6 were demonstrated to be useful synthetic intermediates with applications to the synthesis of isoquinolones, isocoumarins, naphthols, and naphthoquinones. In section 7.7, an anionic carbamoyl transfer strategy was developed, which involved two alternative pathways to the key intermediate **31**. Unfortunately time limitations permitted only the investigation of path a, which yielded the dicarbamate **32**.

## 7.9 Experimental section

**General:** The same general experimental considerations which were described in chapters 5 and 6 may be applied to the following procedures a well.

**1-Oxo-3-phenyl-2-phenylmethyl-1,2-dihydroisoquinoline (7a).**

A solution of 200 mg (0.8 mmol) 3,4-dihydro-3-cyano-3-phenyl-1H-2-benzopyran-1-one and 130 mg (1.2 mmol) benzylamine in 10 mL cyclohexane was heated to reflux for 15 h after which time tlc analysis indicated complete conversion of the starting materials. The solvent was removed on a rotovap, the concentrate dissolved in 10 mL 50 % aqueous acetic acid, and the mixture heated to reflux for an additional 3h. After cooling to rt, the product mixture was diluted with 20 mL of water and extracted with three 15 ml portions of dichloromethane. The combined organic phases was dried over $MgSO_4$, filtered, and concentrated giving a yellow oil, which after flash chromatography (230-400 mesh silica gel, 3:1 hexane:ethyl acetate), furnished 217 mg (86 %) of purified **7a**.

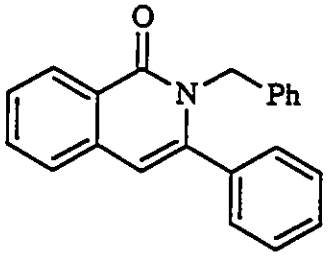


$C_{22}H_{17}NO$ 311.13

**7a**

| | |
|---|---|
| **MS** | (EI) m/e 310 $[M-1]^+$, 232, 205. |
| **HRMS** | calcd for $C_{22}H_{17}NO$ 311.1310 found 311.1287. |
| **IR** | ($CH_2Cl_2$) $\nu_{max}(cm^{-1})$ 1652 (s). |
| **$^1$H-NMR** | ($CDCl_3$) δ(ppm) 5.23 (s, 2H); 6.43 (s, 1H); 6.88 (m, 2H); 7.14-7.70 (m, 11H); 8.48 (d, 1H, $J$ = 8.0 Hz). |
| **$^{13}$C NMR** | ($CDCl_3$) δ(ppm) 48.5 (t); 108.0 (d); 125.2 (s); 125.8 (d); |

126.7 (d); 126.8 (d); 126.9 (d); 128.2 (d); 128.2 (d); 128.3 (d); 128.8 (d); 129.1 (d); 132.5 (d); 135.8 (s); 136.4 (s); 137.6 (s); 143.8 (s); 163.1 (s).

**2-Butyl-1-oxo-3-phenyl-1,2-dihydroisoquinoline (7b)**

A solution of 275 mg (1.1 mmol) 3,4-dihydro-3-cyano-3-phenyl-1H-2-benzopyran-1-one and 120 mg (1.7 mmol) n-butylamine in 15 mL cyclohexane was treated as described for **7a**. Flash chromatography (230-400 mesh silica gel, 3:1 hexane:ethyl acetate) gave 236 mg (77 %) of purified **7b**:

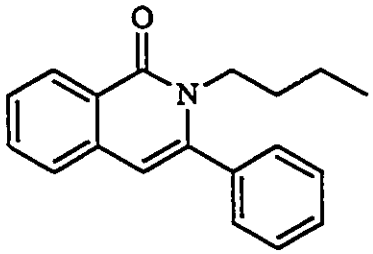

$C_{19}H_{19}NO$ 277.14

**7b**

**MS** (EI) m/e 277 $[M]^+$, 260, 234, 221.

**HRMS** calcd for $C_{19}H_{19}NO$ 277.1426 found 277.1446.

**IR** ($CH_2Cl_2$) $\nu_{max}(cm^{-1})$ 1648 (s).

**$^1$H-NMR** ($CDCl_3$) δ(ppm) 0.70 (t, 3H, $J$ = 7.4 Hz); 1.11 (m, 2H); 1.52 (m, 2H); 3.92 (t, 2H, $J$ = 7.7 Hz); 6.37 (s, 1H); 7.40 (m, 7H); 7.60 (t, 1H, $J$ = 7.4 Hz).

**$^{13}$C NMR** ($CDCl_3$) δ(ppm) 13.4 (q); 19.9 (t); 30.7 (t); 45.3 (t); 107.7 (d); 125.2 (s); 125.6 (d); 126.5 (d); 127.9 (d); 128.3 (d); 128.8 (d); 129.0 (d); 132.2 (d); 136.2 (s);

136.2 (s); 143.6 (s); 162.7 (s).

**1-Oxo-3-methyl-2-phenylmethyl-1,2-dihydroisoquinoline (7c)**

A solution of 217 mg (1.2 mmol) 3,4-dihydro-3-cyano-3-methyl-1H-2-benzopyran-1-one and 200 mg (1.8 mmol) benzylamine in 15 mL cyclohexane was treated as described for **7a**. Flash chromatography (230-400 mesh silica gel, 4:1 hexane:ethyl acetate) gave 165 mg (57 %) of purified **7c**:

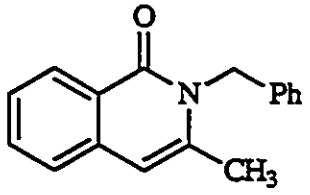


$C_{17}H_{15}NO$ 249.12

**7c**

**MS** (EI) m/e 249 $[M]^+$, 232, 172, 158.

**HRMS** calcd for $C_{17}H_{15}NO$ 249.1154 found 249.1161.

**IR** ($CH_2Cl_2$) $\nu_{max}(cm^{-1})$ 1657 (s).

**$^1$H-NMR** ($CDCl_3$) δ(ppm) 2.30 (s, 3H); 5.40 (s, 2H); 6.34 (s, 1H); 7.13 (d, 2H, $J$ = 7.6 Hz); 7.23 (m, 3H); 7.41 (m, 2H); 7.59 (t, 1H, $J$ = 7.5 Hz); 8.41 (d, 1H, $J$ = 8.1 Hz).

**$^{13}$C NMR** ($CDCl_3$) δ(ppm) 20.6 (q); 47.0 (t); 106.1 (d); 124.4 (s); 125.0 (d); 125.9 (d); 126.3 (d); 127.1 (d); 128.2 (d); 128.7 (d); 132.3 (d); 136.8 (s); 137.2 (s); 139.5 (s); 163.4 (s).

**2-Butyl-1-oxo-3-methyl-1,2-dihydroisoquinoline (7d)**

A solution of 289 mg (1.5 mmol) 3,4-dihydro-3-cyano-3-methyl-1H-2-benzopyran-1-one and 210 mg (2.3 mmol) n-butylamine in 15 mL cyclohexane was treated as described for **7a**. Flash chromatography (230-400 mesh silica gel, 4:1 hexane:ethyl acetate) gave 281 mg (85 %) of purified **7d**:

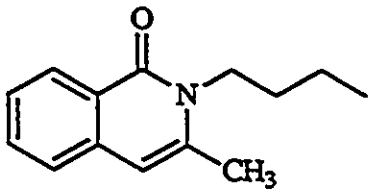


$C_{14}H_{17}NO$ 215.13

**7d**

**MS** (EI) m/e 215 $[M]^+$, 198, 186, 173.

**HRMS** calcd for $C_{14}H_{17}NO$ 215.1310 found 215.1298.

**IR** ($CH_2Cl_2$) $\nu_{max}(cm^{-1})$ 1651 (s)

**$^1$H-NMR** ($CDCl_3$) δ(ppm) 0.92 (t, 3H, *J* = 7.2 Hz); 1.41 (m, 2H); 1.64 (m, 2H); 2.35 (s, 3H); 4.01 (t, 2H, *J* = 7.7 Hz); 6.25 (s, 1H); 7.33 (m, 2H); 7.50 (t, 1H, *J* = 8.3 Hz); 8.31 (d, 1H, *J* = 8.1 Hz).

**$^{13}$C NMR** ($CDCl_3$) δ(ppm) 13.7 (q); 20.3 (q); 20.4 (t); 30.9 (t); 44.1 (t); 105.9 (d); 124.5 (s); 124.8 (d); 125.7 (d); 127.8 (d); 132.0 (d); 136.6 (s); 138.9 (s); 162.9 (s).

**3-Phenyl-1H-2-benzopyran-1-one (10a)**

To a stirred solution of 100 mg (0.4 mmol) 3,4-dihydro-3-cyano-3-phenyl-1H-2-benzopyran-1-one in 15 mL of dry THF, cooled to 0°C,

was added 70 mg (0.6 mmol) of potassium *t*-butoxide under nitrogen atmosphere. The mixture was warmed to rt and stirred for 15 h after which time TLC analysis indicated complete conversion of the starting material. The reaction was quenched by dropwise addition of 6.0 mL 10 % aqueous HCL followed by extraction with three 15 mL aliquots of dichloromethane. After drying over $MgSO_4$ and concentrating the solvent, the crude isocoumarin was resolved by flash chromatography (230-400 mesh silica gel, 4:1 hexane:ethyl acetate) furnishing 45 mg (50 %) of purified **10a**, mp 89-90 °C, which exhibited spectral characteristics consistent with the literature values[81].

**3-Methyl-1H-2-benzopyran-1-one (10b)**

A stirred solution of 100 mg (0.5 mmol) 3,4-dihydro-3-cyano-3-methyl-1H-2-benzopyran-1-one in 15 mL dry THF was treated as described above and gave, after flash chromatography (230-400 mesh silica gel, dichloromethane), 57 mg (66 %) of purified **10b**, mp 74 °C, which exhibited spectral characteristics consistent with the literature values[82].

**3-(2-Methylphenyl)-naphthol (13a).**

To a stirred THF solution of 600 mg (2.3 mmol) 3,4-dihydro-3-cyano-3-(2-methylphenyl)-1H-2-benzopyran-1-one, cooled to -78°C under nitrogen atmosphere, was added 1.8 mL (2.5 mmol) MeLi (1.4 M in ether) via syringe. The mixture was maintained at -78°C for 30 min before a second 1.8 mL aliquot of MeLi was administered. The reaction mixture was then warmed to rt over 30 min and left stirring overnight (15 h). The yellow solution was quenched by dropwise addition of 10 %

aqueous HCl and the resulting phases separated. The aqueous layer was extracted with ether and the combined organic phases partitioned over brine. The resulting ether solution was dried over $MgSO_4$ and concentrated on a rotovap giving 412 mg of a brown oil. Flash chromatography (230-400 mesh silica gel, 1:2 hexane:dichloromethane) furnished 320 mg (60 %) of **13a** as a yellow oil.

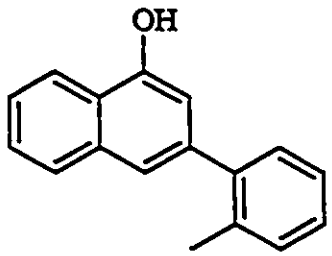


$C_{17}H_{14}O$ 234.10

**13a**

**MS** (EI) m/e 234 $[M]^+$, 215, 202.

**HRMS** calcd for $C_{17}H_{14}O$ 234.1045 found 234.1043.

**IR** ($CH_2Cl_2$) $\nu_{max}(cm^{-1})$ 3577 (br).

**$^1$H-NMR** ($CDCl_3$) δ(ppm) 2.30 (s, 3H); 5.53 (s, 1H); 6.78 (s, 1H); 7.28 (s, 4H); 7.36 (s, 1H); 7.50 (m, 2H); 7.82 (m, 1H); 8.20 (m, 1H).

**$^{13}$C NMR** ($CDCl_3$) δ(ppm) 20.5 (q); 110.5 (d); 120.6 (d); 121.5 (d); 123.3 (s); 125.1 (d); 125.7 (d); 126.7 (d); 127.3 (d); 127.7 (d); 129.8 (d); 130.3 (d); 134.5 (s); 135.5 (s); 139.7 (s); 141.7 (s); 151.0 (s).

**8-Methoxy-3-(2-methoxy-6-methylphenyl)-naphthol (13b)**

750 mg (2.3 mmol) of 3,4-Dihydro-3-cyano-8-methoxy-3-(2-methoxy-6-methylphenyl)-1H-2-benzopyran-1-one was treated as was described above giving 822 mg of a brown oil. Thin layer chromatography (hexane:ethyl acetate 1:1) indicated three products were present (rf 0.1, 0.5 and 0.8). The product mixture was redissolved in ether and extracted with 5 % aqueous $NaHCO_3$. The aqueous phase was acidified and extracted into ethyl acetate. Analysis of each of the base soluble and insoluble components by tlc indicated three separate products tentatively identified as **12b** (430 mg, 60 %), **14** and **15** (168 mg, 23 %).

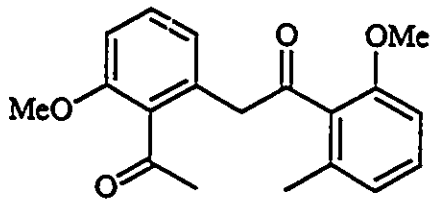


$C_{19}H_{20}O_4$ 312.36

**12b**

**$^1$H-NMR** ($CDCl_3$) δ(ppm) 2.12 (s, 3H); 2.46 (s, 3H); 3.81 (s, 3H); 3.82 (s, 3H); 4.18 (s, 2H); 6.73 (d, 1H, *J* = 8.4 Hz); 6.75 (d, 1H, *J* = 7.7 Hz); 6.79 (d, 1H, *J* = 8.6 Hz); 6.84 (d, 1H, *J* = 8.6 Hz); 7.19 (t, 1H, *J* = 8.0 Hz); 7.27 (t, 1H, *J* = 8.3 Hz).

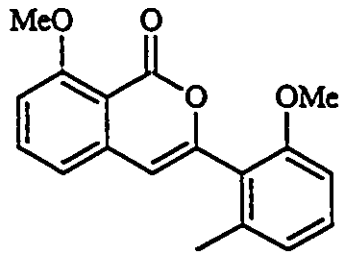


$C_{18}H_{16}O_4$ 296.32

**14**

**$^1$H-NMR** ($CDCl_3$) δ(ppm) 2.28 (s, 3H); 3.74 (s, 3H); 4.00 (s, 3H);
6.39 (s, 1H); 6.76 (d, 1H, *J* = 8.4 Hz); 6.83 (d, 1H, *J* = 7.6 Hz);
6.94 (d, 1H, *J* = 8.4 Hz); 6.96 (d, 1H, *J* = 7.8 Hz);
7.25 (t, 1H, *J* = 8.0 Hz); 7.60 (t, 1H, *J* = 8.2 Hz).

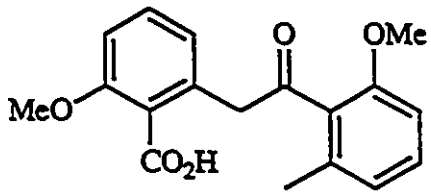


$C_{18}H_{18}O_5$ 314.34

**15**

**$^1$H-NMR** ($CDCl_3$) δ(ppm) 2.19 (s, 3H); 3.83 (s, 3H); 3.93 (s, 3H);
4.45 (s, 2H); 6.75 (t, 2H, *J* = 7.5 Hz); 6.90 (d, 1H, *J* = 7.5 Hz);
6.92 (d, 1H, *J* = 8.3 Hz); 7.20 (t, 1H, *J* = 7.9 Hz);
7.39 (t, 1H, *J* = 8.0 Hz).

**8-Methoxy-3-(2-methoxy-4-methylphenyl)-naphthol (13c)**

100 mg (0.3 mmol) of 3,4-Dihydro-3-cyano-8-methoxy-3-(2-methoxy-4-methylphenyl)-1H-2-benzopyran-1-one was treated as was described above giving 108 mg of a brown oil. Flash chromatography (230-400 mesh silica gel, 3:1 hexane:ethyl acetate) furnished 78 mg (86 %) of **13c** as a yellow oil.

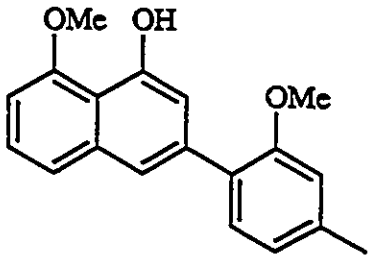


$C_{19}H_{18}O_3$ 294.13

**13c**

**MS** (EI) m/e 294 $[M]^+$, 267, 234.

**HRMS** calcd for $C_{19}H_{18}O_3$ 294.1256 found 294.1274.

**IR** ($CH_2Cl_2$) $\nu_{max}(cm^{-1})$ 3404 (Br).

**$^1$H-NMR** ($CDCl_3$) δ(ppm) 2.40 (s, 3H); 3.80 (s, 3H); 4.04 (s, 3H); 6.73 (d, 1H, $J$ = 7.7 Hz); 6.81 (s, 1H); 6.85 (d, 1H, $J$ = 8.4 Hz); 7.10 (d, 1H, $J$ = 1.5 Hz); 7.27 (t, 2H, $J$ = 7.6 Hz); 7.40 (d, 1H, $J$ = 6.2 Hz); 7.42 (d, 1H, $J$ = 1.6 Hz); 9.27 (s, 1H).

**$^{13}$C NMR** ($CDCl_3$) δ(ppm) 21.5 (q); 55.5 (q); 56.1 (q); 103.7 (d); 112.2 (d); 112.4 (d); 113.9 (s); 119.3 (d); 121.4 (d); 122.1 (d); 125.5 (d); 127.4 (s); 130.7 (d); 136.6 (s); 138.2 (s); 138.9 (s); 153.6 (s); 156.0 (s); 156.4 (s).

**2-(2-methylphenyl)-1,4-naphthoquinone (16a)**

810 mg (1.9 mmol) of iodobenzene bis(trifluoroacetate) was added, in portions, over 5 min to an ice cooled, stirred solution of 200 mg (0.9 mmol) 3-(2-methylphenyl)-naphthol (**13a**) in 30 mL of 2:1 acetonitrile:water. The mixture was stirred for an additional 30 min at 0°C after which time tlc analysis (dichloromethane:hexane 3:1) indicated complete conversion of the starting materials. The reaction mixture was then warmed to rt, diluted with 30 mL water, and extracted with two 20 mL portions of ether. The combined organic phases were dried over MgSO4, and concentrated (rotovap) giving 342 mg of a yellow oil. Flash chromatography (5 g 230-400 mesh silica gel) furnished 177 mg (83 %) of purified 2-(2-methylphenyl)-1,4-naphthoquinone (**16a**), as a brilliant yellow oil.

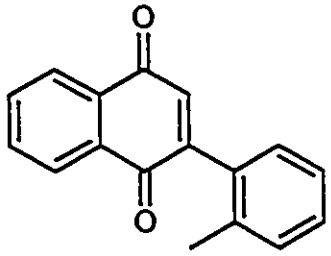

$C_{17}H_{12}O_2$ 248.08

**16a**

| | |
|---|---|
| **MS** | (EI) m/e 248 $[M]^+$, 247, 231, 219, 191. |
| **HRMS** | calcd for $C_{17}H_{12}O_2$ 248.0874 found 248.0825. |
| **IR** | ($CH_2Cl_2$) $\nu_{max}(cm^{-1})$ 1654 (s). |
| **$^1$H-NMR** | ($CDCl_3$) δ(ppm) 2.21 (s, 3H); 6.90 (s, 1H); 7.12-7.33 (m, 4H); 7.74 (m, 2H); 8.11 (m, 2H). |

**2-(2-methoxy-4-methylphenyl)-5-methoxy-1,4-naphthoquinone (16c)**

965 mg (2.2 mmol) of iodobenzene bis(trifluoroacetate) was added, in portions, over 5 min to an ice cooled, stirred solution of 300 mg (1.0 mmol) 8-methoxy-3-(2-methoxy-4-methylphenyl)-naphthol (**13c**) in 30 mL of 2:1 acetonitrile:water. The reaction mixture was treated as described above furnishing 276 mg (88 %) of 2-(2-methoxy-4-methylphenyl)-5-methoxy-1,4-naphthoquinone (**16c**) as an orange oil.

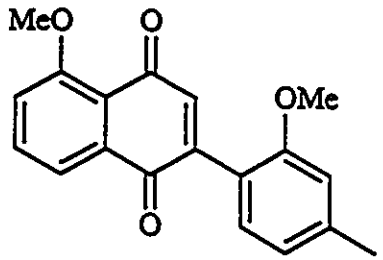


$C_{19}H_{16}O_4$ 308.10

**16c**

**MS** (EI) m/e 308 $[M]^+$, 277, 249, 204, 149.

**HRMS** calcd for $C_{19}H_{16}O_4$ 308.1049 found 308.1044.

**IR** ($CH_2Cl_2$) $\nu_{max}(cm^{-1})$ 1656 (s).

**$^1$H-NMR** ($CDCl_3$) δ(ppm) 2.38 (s, 3H); 3.74 (s, 3H); 3.99 (s, 3H); 6.77 (s, 1H); 6.82 (d, 1H, *J* = 7.6 Hz); 6.92 (s, 1H); 7.12 (d, 1H, *J* = 7.6 Hz); 7.28 (d, 1H, *J* = 8.2 Hz); 7.67 (t, 1H, *J* = 7.7 Hz); 7.78 (d, 1H, *J* = 7.7 Hz).

**$^{13}$C NMR** ($CDCl_3$) δ(ppm) 21.8 (q); 55.7 (q); 56.5 (q); 77.2 (s); 112.2 (d); 117.4 (d); 119.7 (d); 120.1 (s); 121.3 (d); 130.3 (d); 134.7 (d); 135.0 (s); 138.5 (d); 141.4 (s);

145.7 (s); 157.1 (s); 159.3 (s); 183.9 (s); 184.8 (s).

**Attempted cyclization of 2-(2-methylphenyl)-1,4-naphthoquinone to pyran 18**

A solution of 110 mL (0.8 mmol) of diisopropylamine and 3.4 mL of nBuLi (0.8 mmol, 2.4 M hexane sclution) in 10 mL dry THF (-78°C) was transferred, via cannula, to a stirred solution of 100 mg (0.4 mmol) 2-(2-methylphenyl)-1,4-naphthoquinone (16a) in 10 mL THF (-78°C) under nitrogen atmosphere. The solution immediately developed a deep red color and was stirred for an additional 2 h before warming to rt and quenching with 10 % aqueous HCl. Extractive workup furnished 77 mg (72 %) of crude material whose spectral characteristics indicated hydroxyquinone **19**.

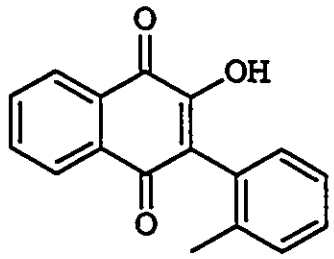


$C_{17}H_{12}O_3$ 264.28

**19**

**MS** (EI) m/e 264 $[M]^+$, 249, 246, 212.

**IR** ($CH_2Cl_2$) $\nu_{max}(cm^{-1})$ 3389 (Br), 1661 (s).

**$^1$H-NMR** ($CDCl_3$) δ(ppm) 1.56 (s, 1H); 2.18 (s, 3H); 7.10-7.33 (m, 4H); 7.76 (m, 2H); 8.16 (m, 2H).

**Photocyclization of 2-(2-methylphenyl)-1,4-naphthoquinone**

A solution of 25 mg (0.1 mmol) 2-(2-methylphenyl)-1,4-naphthoquinone (**16a**) in 1.0 mL of acetonitrile, contained in a quartz test tube, was suspended 10 cm from a Hanovia mercury lamp and irradiated for 12 h after which time tlc analysis (hexane:ethyl acetate 3:1) indicated complete conversion of the quinone. The crude mixture was resolved over 5 g 230-400 mesh silica gel which gave 19 mg (76 %) of purified **25**.

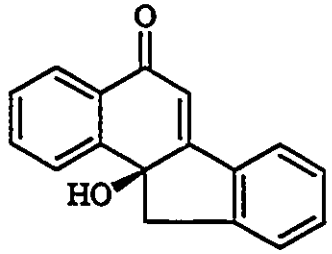


$C_{17}H_{12}O_2$ 248.08

**25**

**MS** (EI) m/e 248 $[M]^+$, 231, 230, 219, 202.

**HRMS** calcd for $C_{17}H_{12}O_2$ 248.0837 found 248.0864.

**IR** ($CH_2Cl_2$) $\nu_{max}(cm^{-1})$ 3315 (Br), 1683 (s).

**$^1$H-NMR** ($CDCl_3$) δ(ppm) 3.53 (q, 2H, $J$ = 15.9 Hz); 6.63 (s, 1H); 7.30-7.50 (m, 4H); 7.60-7.73 (m, 3H); 8.09 (d, 1H, $J$ = 8.1 Hz).

**Dehydration of 25**

A solution of 19 mg of **25** and a crystal of *p*-toluenesulfonic acid in 5 mL of dichloromethane was stirred for 12 h, during which time a deep red coloration developed. Analysis by tlc indicated complete

conversion of **25** and the formation of the highly fluorescent dehydration product **26**, which was purified by elution through a short silica gel plug with dichloromethane.

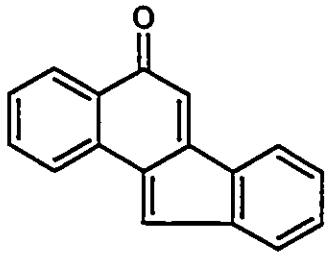

$C_{17}H_{10}O$ 230.07

**26**

**MS** (EI) m/e 230 $[M]^+$, 202, 149.

**HRMS** calcd for $C_{17}H_{10}O$ 230.0732 found 230.0709.

**Preparation of dicarbamate 32**

A saturated aqueous solution of $Na_2S_2O_4$ was added, dropwise, to a stirred solution of 400 mg (1.3 mmol) 2-(2-methoxy-4-methylphenyl)-5-methoxy-1,4-naphthoquinone (**16c**) in 20 mL of THF until the solution's color changed from brilliant orange to pale yellow. The THF solution was transferred to a separatory funnel, washed with 10 mL water, partitioned over brine solution, then dried over $MgSO_4$. After filtration, the THF solution of the hydroquinone was transferred to a 50 mL round bottomed flask and flushed with nitrogen. The solution was subsequently cooled to 0°C before 60 mg of NaH (60 % disp in mineral oil) was added. The mixture was warmed to rt, stirred until gas evolution ceased, then returned to the ice bath. A solution of 180 mg (1.3 mmol) of diethylcarbamoyl chloride in 5 mL THF was added, via a

dropping funnel, over 2 min. The mixture was warmed to rt and stirred overnight. Workup consisted of quenching the reaction with 10 % aqueous HCl followed by the usual extractive procedure which afforded 526 mg of crude material. Flash chromatography (hexane:ethyl acetate 1:1) furnished the starting quinone and 152 mg (23 %) of the dicarbamate **32.**

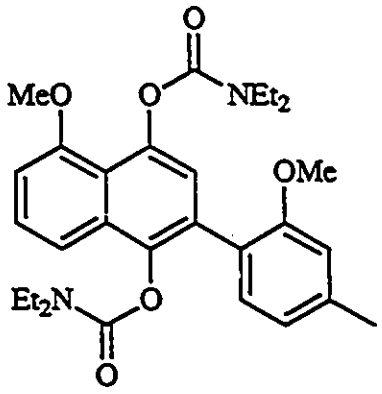


$C_{29}H_{36}N_2O_6$ 508.26

**32**

**MS** (EI) m/e 508 $[M]^+$, 149, 100.

**HRMS** calcd for $C_{29}H_{36}N_2O_6$ 508.2573 found 508.2603.

**$^1$H-NMR** ($CDC_3$) δ(ppm) 0.85-1.40 (m, 12H); 2.35 (s, 3H); 3.10-3.60 (m, 8H); 3.69 (s, 3H); 3.86 (s, 3H); 6.70-6.85 (m, 3H); 7.06 (s, 1H); 7.15-7.48 (m, 3H).

# Chapter 8

## Recommendations for Further Research

### 8.1 Further studies based on 1,4-dioxygenated-*o*-quinodimethanes.

In chapter 5 it was rationalized that the *o*-QDM **18e** (scheme 8.1) failed to cyclize due to a combination of two factors: First, because of the low

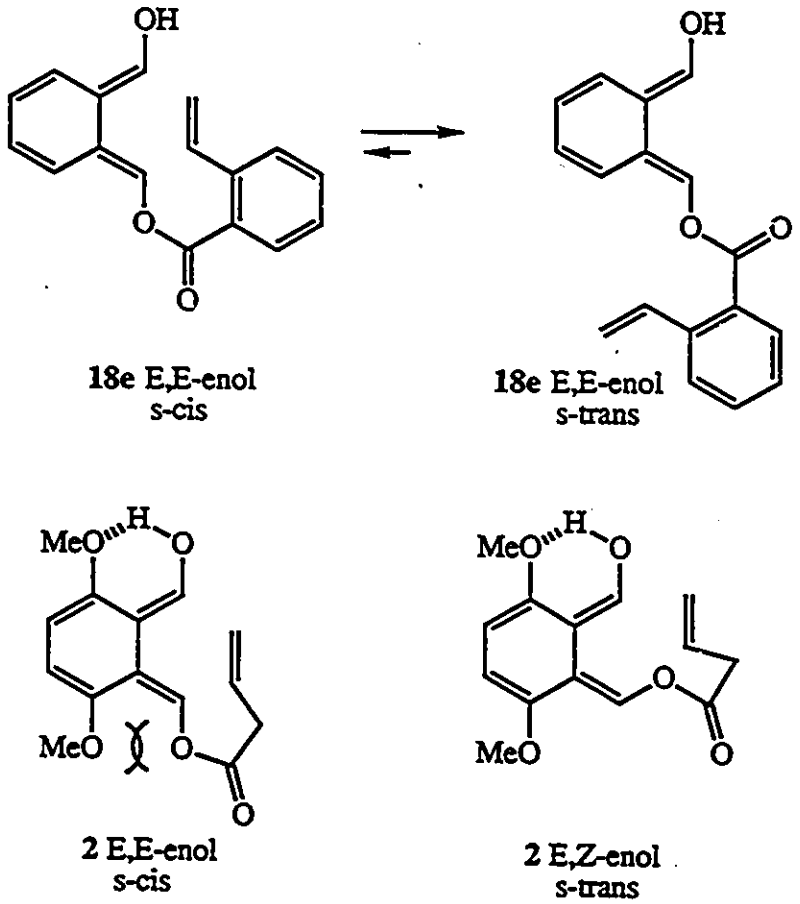


Scheme 8.1: Kraus's model vs model **18e**

proportion of the disfavoured s-cis rotamer with the geometry of the ester required for cycloaddition, and second, due to the poor reactivity of the styryl dienophile.

In an effort to account for the surprising results reported by Kraus *et al.*,[47] the cycloaddition of *o*-quinodimethane **2** was postulated to occur from the E,Z-enol (scheme 8.1), possibly, due to the buttressing effect of the *o*-methoxy group. The intramolecular H-bond present in **2** should stabilize the photoenol, suppressing side reactions and the reversion to precursor aldehyde. Thus it is also possible that the cycloaddition of **2** did, in fact, occur from the s-cis E,E-enol due to the increased photoenol lifetime.

Scheme 8.2 illustrates three new models designed to address the problems of ester conformation, *o*-QDM stability and photoenol geometry.

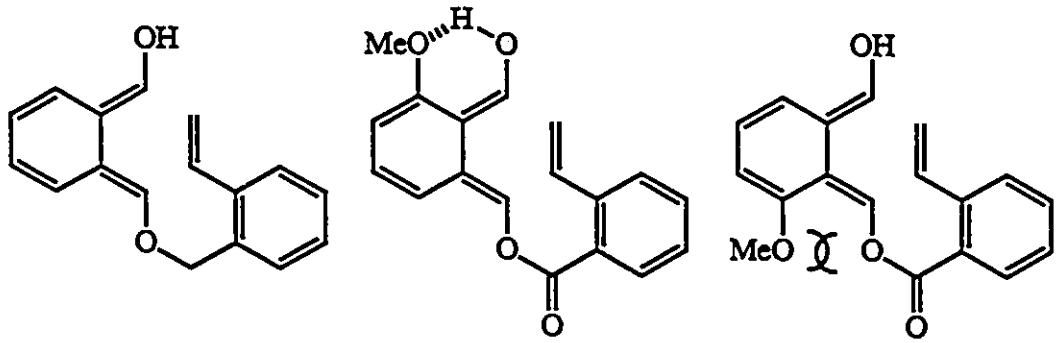


**18f** E,E-enol **18g** E,E-enol **18h** E,E-enol

Scheme 8.2: Proposed photoenols **18f**, **18g** and **18h**.

The ether tether present in photoenol **18f** should offer more conformational freedom and facilitate closer approach of the styryl

double bond. The parent aldehyde should be readily available starting from 2-(bromomethyl)stryrene and *o*-xylenol.

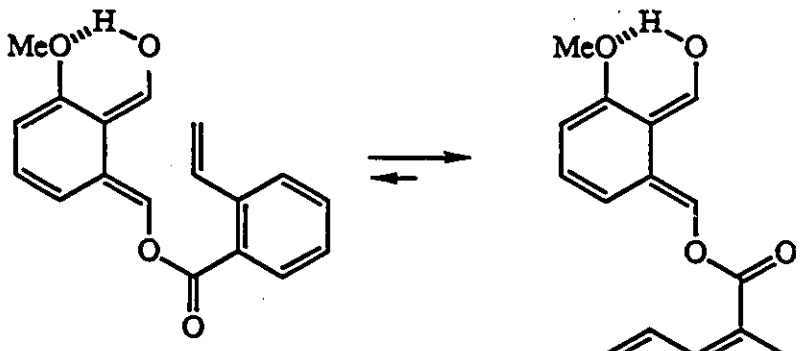


**18g** E,E-enol s-cis

**18g** E,E-enol s-trans

Scheme 8.3: s-cis and s-trans rotamers of **18g**

The *o*-methoxy group present in **18g** should stabilize the photoenol, suppress side reactions, and thus, increase the likelihood of cycloaddition occurring from the less stable s-cis conformer.

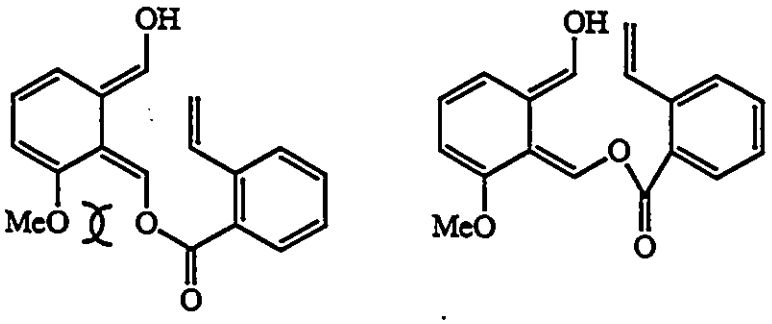


**18h** E,E-enol

**18h** E,Z-enol

Scheme 8.4: E,E vs E,Z-photoenols

If irradiation of the aldehyde precursor to **18h** yields cycloaddition products, the ratio of 1,4 syn to 1,4 anti isomers

observed would reveal the extent to which the photoenol geometry was influenced by the buttressing effect of the *m*-methoxy group.

The aldehyde precursors to **18g** and **18h** should be available employing the methodology described by Kraus *et al.*[47]

## 8.2 Quinone methide electrocyclization.

As described in chapter 7, attempts to cyclize the quinone methide anion **17** at -78°C, were unsuccessful (scheme 8.5), likely due

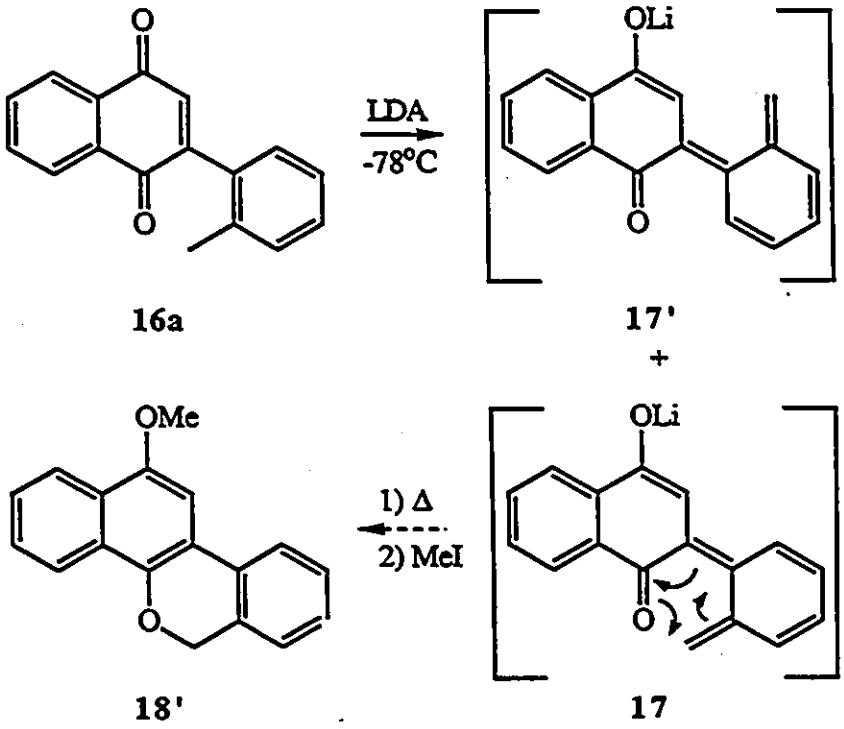


Scheme 8.5: Cyclization of 17 to 18'

to the predominant formation of **17'**. It may yet be possible, however, to accomplish some degree of electrocyclization if anion **17** was refluxed in the presence of MeI; trapping the oxygen anion with MeI might retard isomerization of the naphthol back to the quinone methide.

Scheme 8.6 depicts an analogous sequence with the more appropriately substituted precursor **16b**. Quinone **16b** is of greater

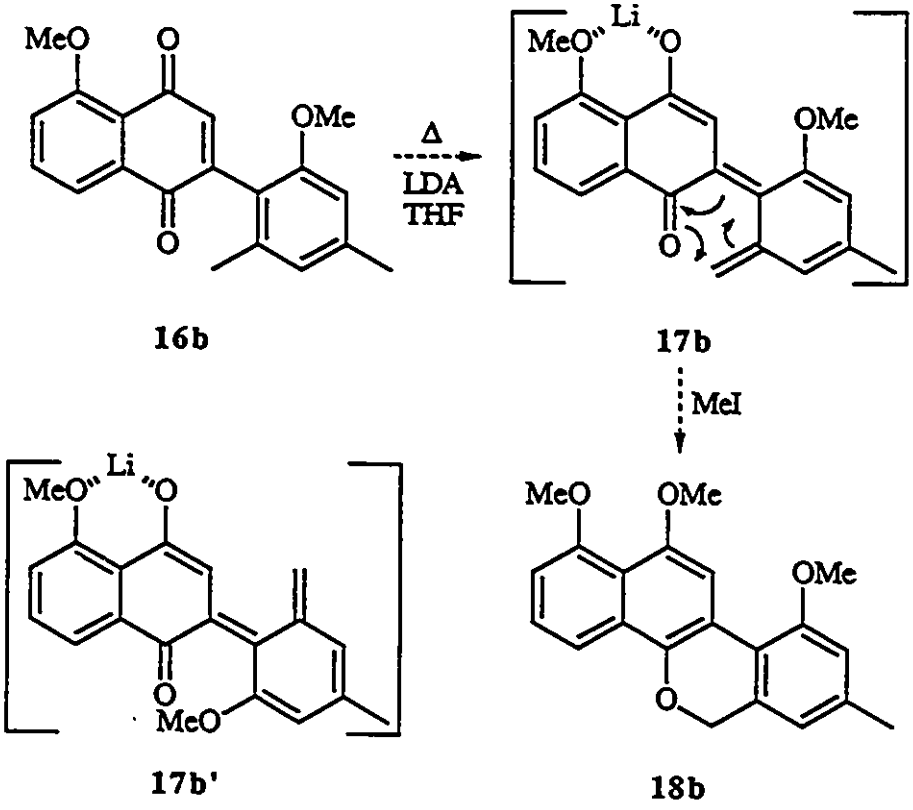


**16b** **17b** **17b'** **18b**

Scheme 8.6: Cyclization of **17b** to **18b**.

interest because of its structural similarity to defucogilvocarcin M, and because of the expectation that electrostatic repulsion should minimize the contribution of **17b'**.

Several methods for the synthesis of quinone **16b** were considered but, because of time limitations, were only briefly investigated. The retrosynthetic analysis, illustrated in scheme 8.7, begins with electrocyclization of the dianion **24**, which should be available via base treatment of the cyanoketone **23a**. Compound **23a**

could be prepared by 1,4 addition of HCN to the chalcone **22a**, obtained by condensation of **20a** and **21**.

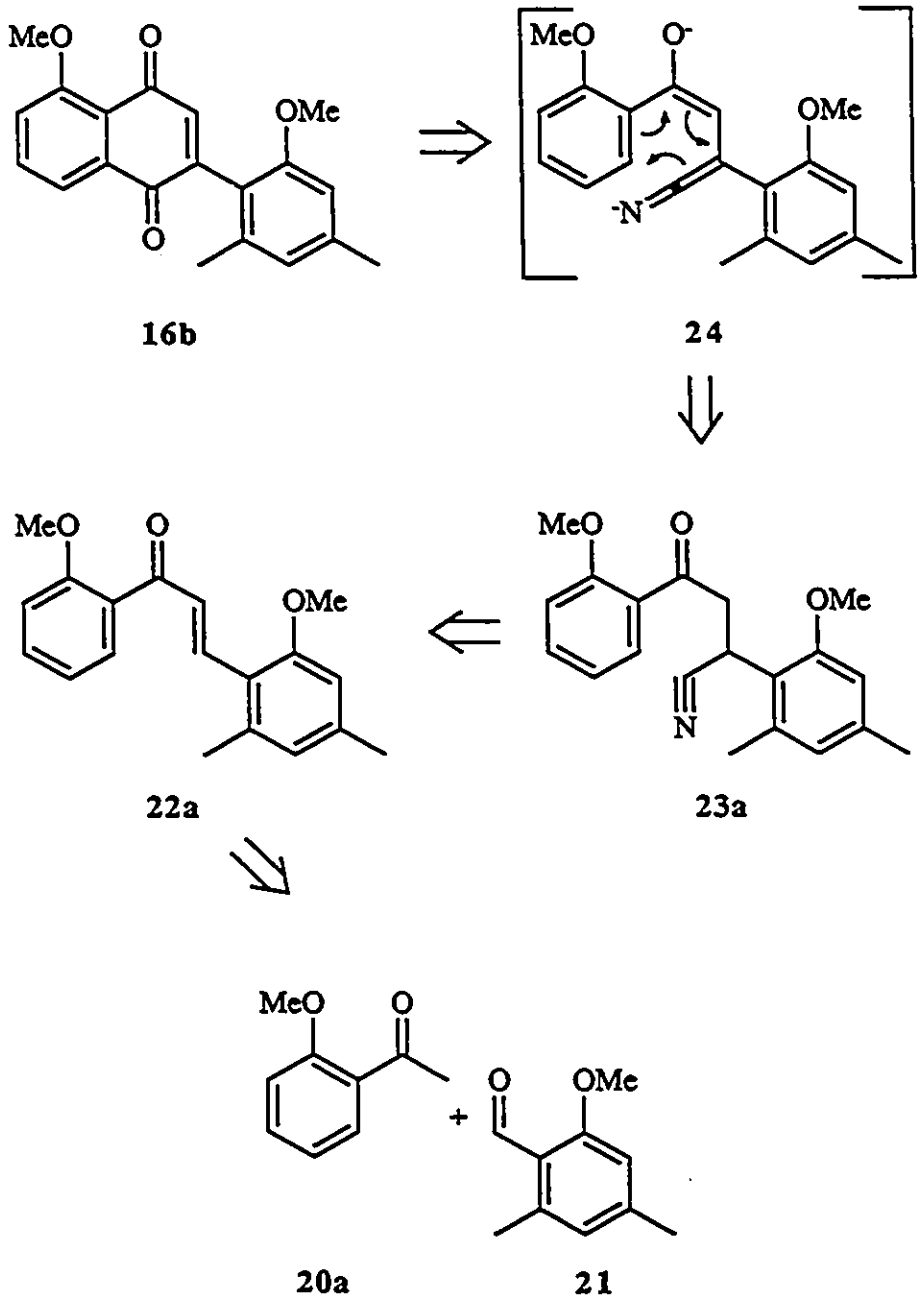


Scheme 8.7: Retrosynthetic analysis of quinone **16b**

During preliminary investigations, it was found that the chalcones **22a** and **22b** could be prepared in excellent yield by treatment of methanol or THF solutions of **20a/b** and **21** with benzyltrimethylammonium hydroxide (BTAH) (scheme 8.8).

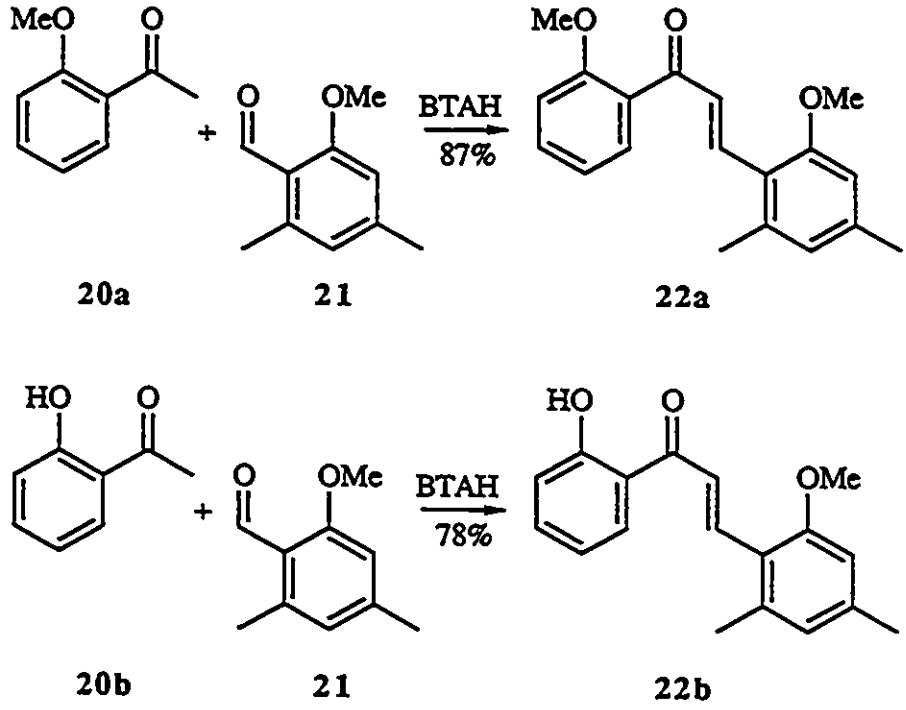


Scheme 8.8: Synthesis of chalcones 22a and 22b

The structures of chalcones **22a** and **22b** were determined on the basis of the $^1$H-NMR and mass spectral data. The chalcones have the advantage of facile preparation from readily available starting materials and incorporate much of the structure of defucogilvocarcin M.

The conjugate addition of cyanide to chalcones **22a** and **22b** was accomplished readily by treatment with acetone cyanohydrin in MeOH in

the presence of 0.25 eq $Na_2CO_3$ (scheme 8.9). Again, the structures of compounds **23a** and **23b** followed from the $^1$H-NMR and mass spectral data.

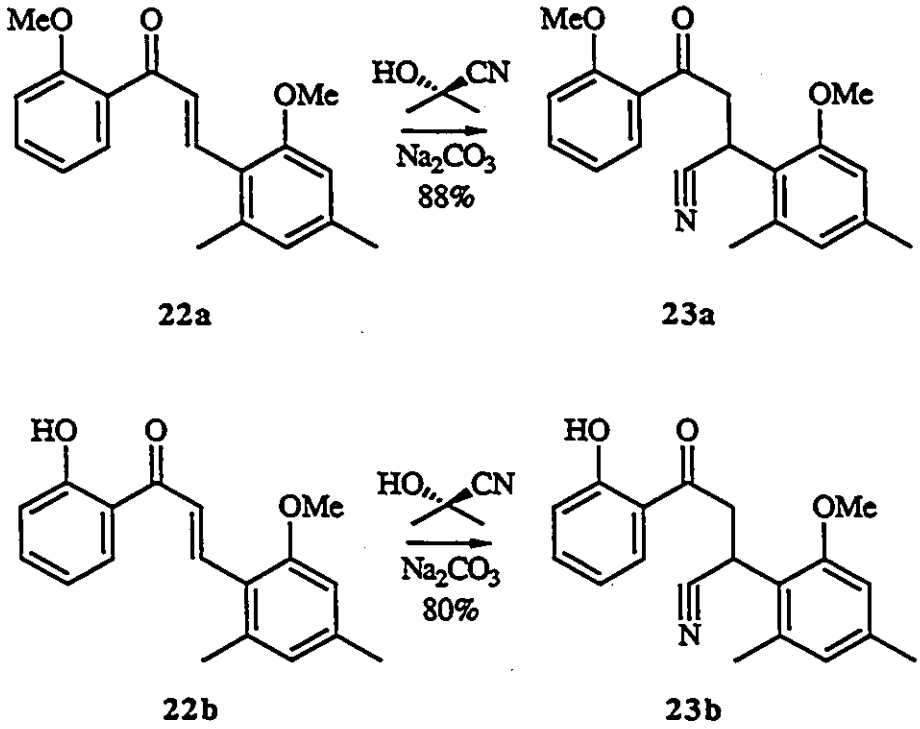


Scheme 8.9: Synthesis of 23a and 23b.

While time limitations did not allow for further investigation of either the chalcones **22a** and **22b** or the cyanoketones **23a** and **23b**, the potential for application to a defucogilvocarcin synthesis merits further attention. For example, TMSCN is known to add to α,β-unsaturated ketones in a conjugate manner in the presence of Lewis acids such as triethylaluminum, aluminum chloride or $SnCl_2$.[89] Thus similar treatment of **22a** should lead to the enol ether **24**, then upon

reaction with base, to anion **25** (scheme 8.10). Quinone **16b** would follow upon electrocyclic ring closure, hydrolysis and oxidation.

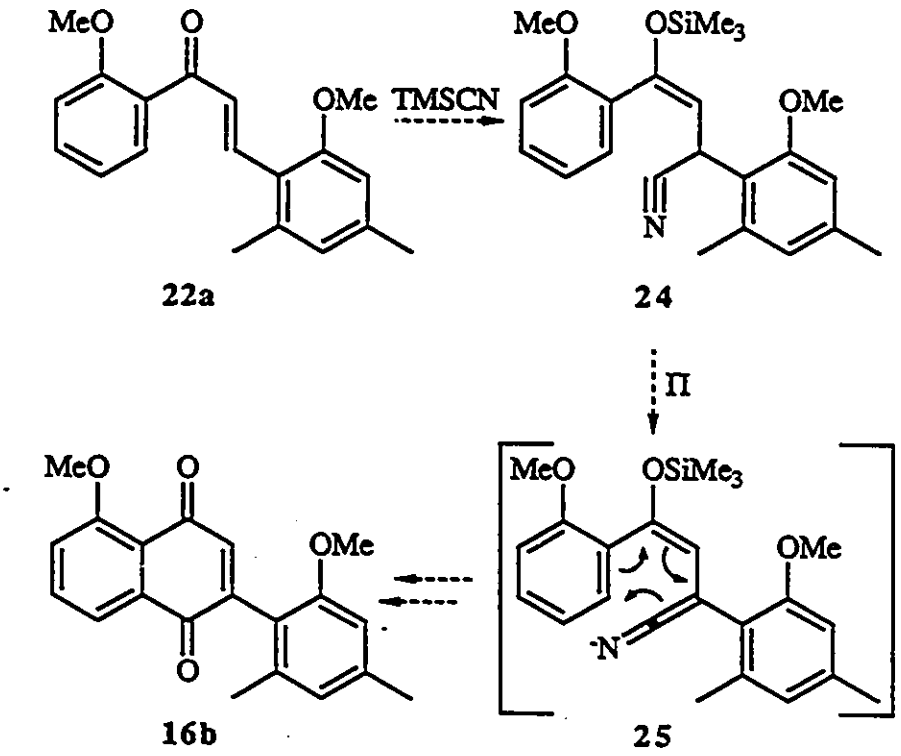


Scheme 8.10: Potential synthesis of **16b** involving TMSCN

Perhaps, a more likely scenario might begin with the phenolic cyanoketone **23b** (scheme 8.11). Compound **23b** should react with dichlorodimethylsilane to give the conformationally more constrained enol ether **26**, which should form anion **27** upon base treatment. The anionic intermediate **27** should undergo electrocyclic ring closure more efficiently than **25**, due to conformational limitations, and after electrocyclization, could be transformed to the hydroxyquinone **16e** via the same sequence described in the previous example.

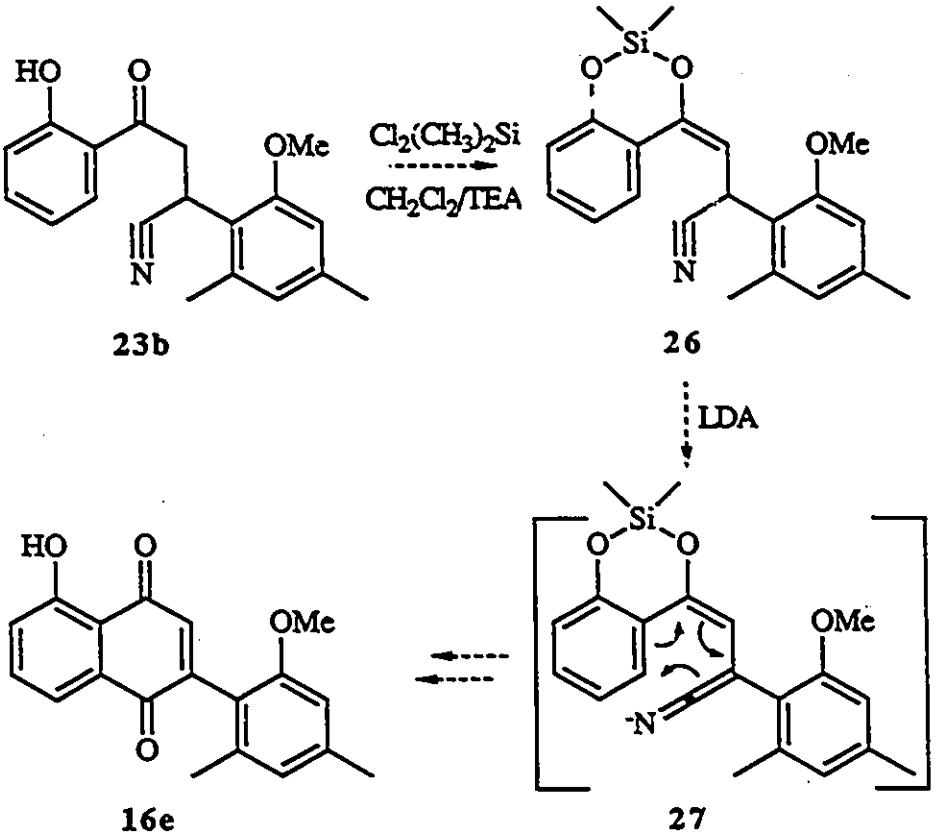


Scheme 8.11: Potential synthesis of **16e**

Another attractive, though highly speculative, possibility beginning with compound **23a** is depicted in scheme 8.12. The α,β-unsaturated cyanoketone **28** should be available by oxidation of **23a**. Herzig *et al.*,[90] in fact, have reported the synthesis of 3-cyano-1,3-diphenylprop-2-en-1-one by dehydrogenating 3-benzoyl-2-phenylpropiononitrile with $SeO_2$. Treatment of **28** with base should lead to the anion **29** which, upon reflux, should cyclize to **30**. Oxidation of **30** to the isoquinolone would open up possibilities for some interesting derivatives of defucogilvocarcin M carrying with it the

potential for installation of various molecular recognition elements at the amide nitrogen.

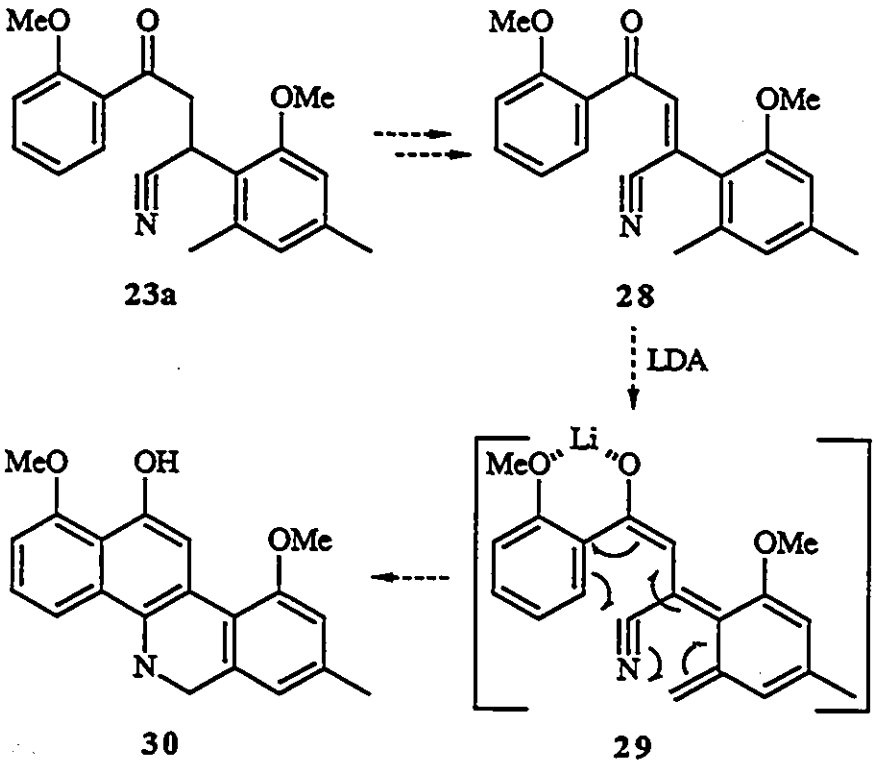


Scheme 8.12: Potential isoquinolone analogues of defucogilvocarcin M

The last sequence considered in this category is depicted in scheme 8.13 beginning with the 2,6-disubstituted acetophenone **20c** and aldehyde **21**. Chalcone **31** has already been prepared in excellent yield via Triton B; treatment of **31** with LDA should lead to the *o*-QDM **32**, which should then cyclize to the tetralone **33**. Aromatization of **33** and subsequent oxidation should afford the quinone **16b**.

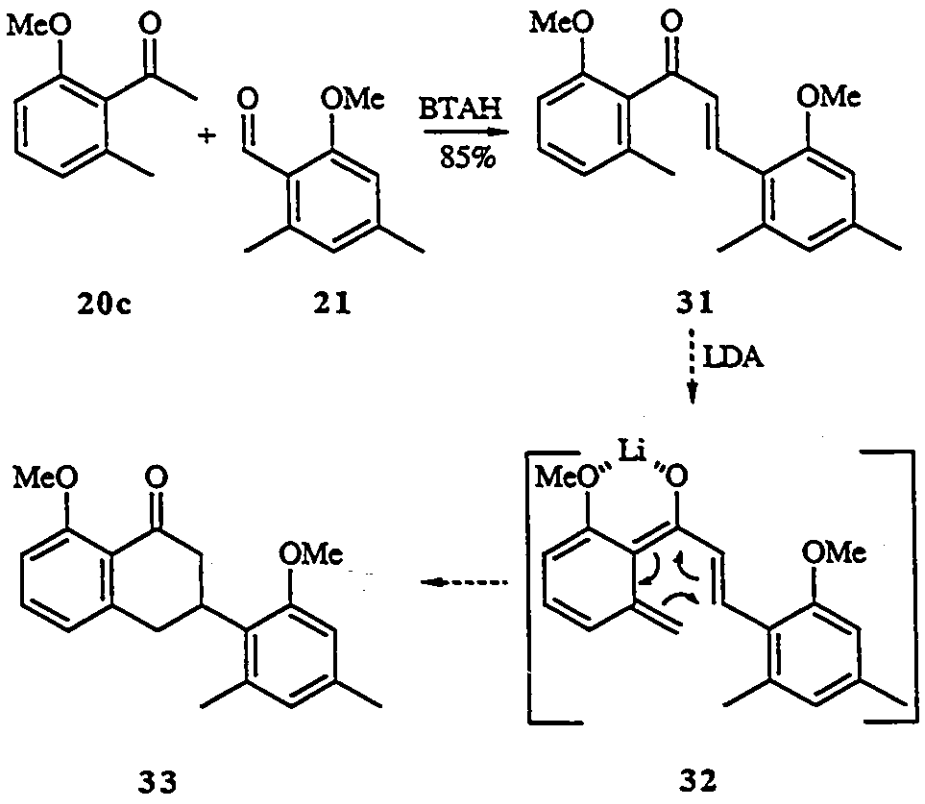


Scheme 8.13: Electrocyclic ring closure leading to compound 33

## 8.3 Quinone photochemistry

All of the possibilities described in the previous section evolved from the efforts outlined in scheme 8.5 which involved the attempted electrocyclic ring closure of anion **17**. In chapter 7, quinone **16a** was

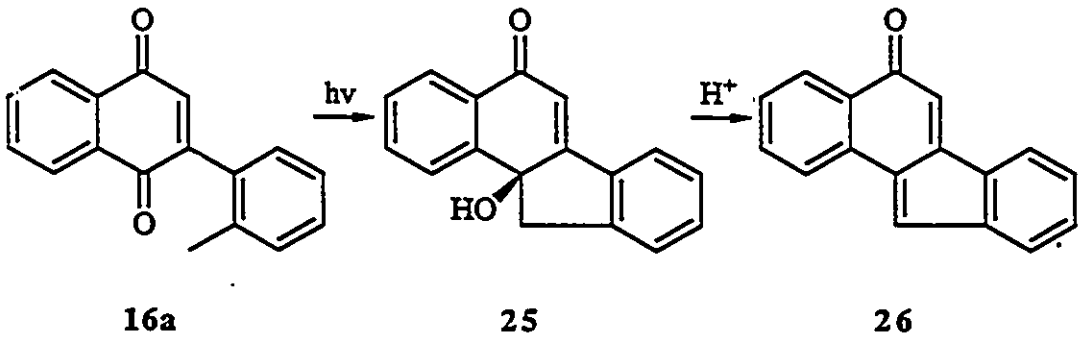


Scheme 8.14: Photochemical reactivity of quinone **16a**

shown to form the tertiary alcohol **25** upon irradiation, which was converted to **26** on acid treatment; It was suggested that compounds such as **26** might be biologically active because of the potential for DNA intercalation. The quinone methide entity present in **26** should also be susceptible to nucleophilic attack. An amine nitrogen from guanine, for example, could add as indicated in scheme 8.15, leading to alkylation of the host DNA. A similar reaction scheme involving a

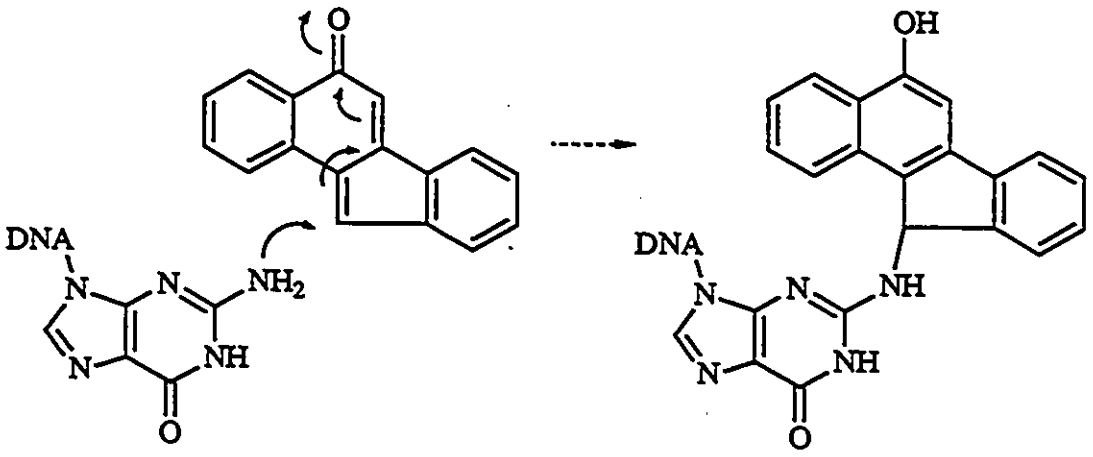


Scheme 8.15: Potential DNA alkylating agent

benz[a]pyrene epoxide has been suggested to account for the carcinogenicity observed with benz[a]pyrenes and other carcinogenic benzenoid hydrocarbons. Thus it should become apparent that a similar photochemical sequence as that depicted in scheme 8.14, beginning with quinones such as **16b**, could provide access to some interesting defucogilvocarcin derivatives with potentially useful biological activities (scheme 8.16).

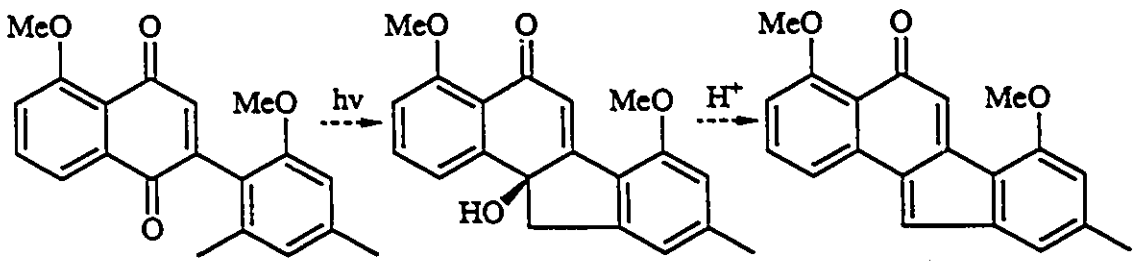


16a 34 35

Scheme 8.16: Quinone methide defucogilvocarcin M analogues

## 8.4 Extension of the remote metallation approach.

In chapter 7, two alternative pathways were proposed to prepare intermediate **31**. It was hoped that remote metallation of **31** would precipitate ring to ring carbamoyl transfer followed by cyclization to the benzonaphthopyranone **36**.

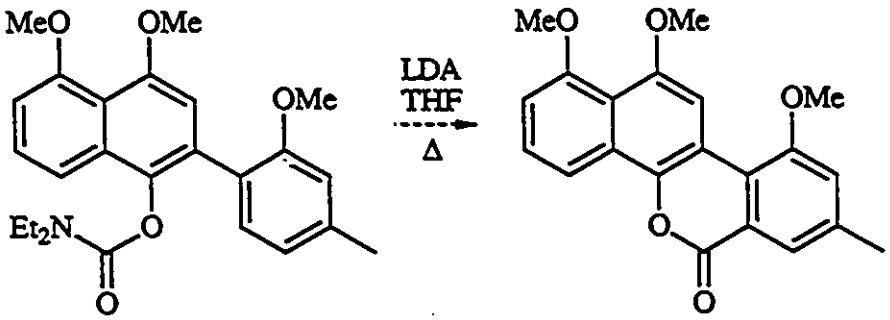


31 36

Scheme 8.17: Remote carbamoyl transfer leading to **36**

Unfortunately only pathway a, which repeatedly furnished the dicarbamate, was attempted. To complete the picture, pathway b, which involved a selective ether formation, should also be investigated. The peri-methoxy group present in compound **38** should provide a means of

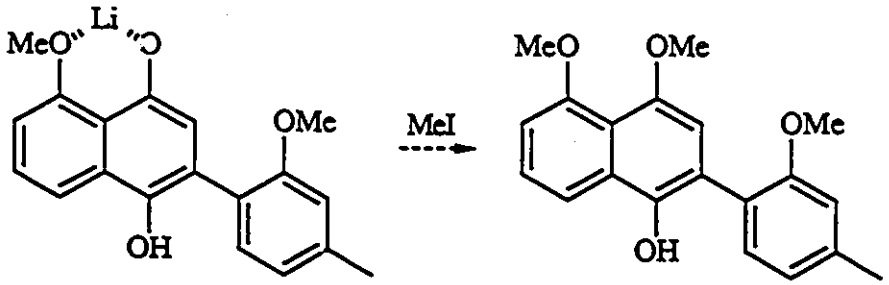


38 39

Scheme 8.18: Methylation of hydroquinone 38

selectively protecting the northern hydroxyl group (scheme 8.18). The monoprotected intermediate **39** could then be converted to the monocarbamate and the remote carbamoyl transfer attempted.

## 8.5 Experimental section

**General:** The same general experimental considerations which were described in chapters 5 and 6 may be applied to the following procedures a well.

### 8.5.1 Chalcone $22_a$

A solution of 1.0 g (6.7 mmol) 2'-methoxyacetophenone and 1.1 g (6.7 mmol) 2-methoxy-4,6-dimethylbenzaldehyde in 15 mL benzyltrimethylammonium hydroxide (40 % solution in MeOH) was stirred at 50 $^{o}$C for 30 min, after which time tlc analysis (3:1 hexane:ethyl acetate) indicated complete conversion of the starting materials. After evapouration of the solvent, the crude product was purified over 20 g of 70-230 mesh silica gel, employing 5:1

hexane:ethyl acetate as eluent, furnishing 1.8 g (87 %) of **22a** as a pale yellow oil.

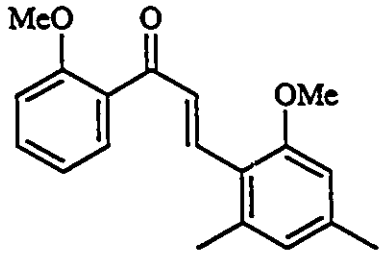


$C_{19}H_{20}O_3$ 296.14

**22a**

**MS** (EI) m/e 296 $[M]^+$, 282, 265, 249, 189.

**HRMS** calcd for $C_{19}H_{20}O_3$ 296.1412 found 296.1397.

**$^1$H-NMR** ($CDCl_3$) δ(ppm) 2.30 (s, 3H); 2.37 (s, 3H); 3.83 (s, 3H); 3.85 (s, 3H); 6.58 (s, 1H); 6.64 (s, 1H); 6.95 (d, 1H, $J$ = 8.2 Hz); 7.00 (t, 1H, $J$ = 7.4 Hz); 7.42 (t, 1H, $J$ = 8.4 Hz); 7.58 (d, 1H, $J$ = 7.5 Hz); 7.67 (q, 2H, $J$ = 16.1 Hz).

### 8.5.2 Chalcone 22b

A solution of 415 mg (3.0 mmol) 2'-hydroxyacetophenone and 500 mg (3.0 mmol) 2-methoxy-4,6-dimethylbenzaldehyde in 5 mL benzyltrimethylammonium hydroxide (40 % solution in MeOH) was treated as described above furnishing 671 mg (78 %) of **22b** as a brilliant yellow oil.

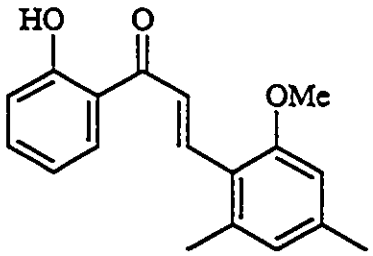


$C_{18}H_{18}O_3$ 282.13

**22b**

**MS** (EI) m/e 282 $[M]^+$, 267, 251, 231, 219.

**HRMS** calcd for $C_{18}H_{18}O_3$ 282.1256 found 282.1252.

**$^1$H-NMR** ($CDCl_3$) δ(ppm) 2.32 (s, 3H); 2.46 (s, 3H); 3.92 (s, 3H); 6.63 (s, 1H); 6.67 (s, 1H); 6.91 (t, 1H, *J* = 7.7 Hz); 6.99 (d, 1H, *J* = 8.4 Hz); 7.45 (t, 1H, *J* = 7.8 Hz); 7.88 (d, 1H, *J* = 8.1 Hz); 8.04 (q, 2H, *J* = 15.4 Hz).

### 8.5.3 Chalcone 31

A solution of 190 mg (1.2 mmol) 2-methoxy-6-methylacetophenone and 190 mg (1.2 mmol) 2-methoxy-4,6-dimethylbenzaldehyde in 2 mL benzyltrimethylammonium hydroxide (40 % solution in MeOH) was treated as described above furnishing 305 mg (85 %) of **31** as a yellow oil.

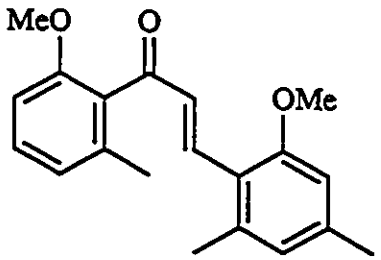


$C_{20}H_{22}O_3$ 310.16

**31**

**MS** (EI) m/e 310 $[M]^+$, 298, 279, 212, 189.

**HRMS** calcd for $C_{20}H_{22}O_3$ 310.1569 found 310.1559.

**$^1$H-NMR** ($CDCl_3$) δ(ppm) 2.21 (s, 3H); 2.22 (s, 3H); 2.28 (s, 3H); 3.74 (s, 3H); 3.81 (s, 3H); 6.56 (s, 1H); 6.60 (s, 1H); 6.76 (d, 1H, $J$ = 8.4 Hz); 6.81 (d, 1H, $J$ = 7.7 Hz); 7.22 (dd, 1H, $J$ = 7.9, 9.8 Hz); 7.33 (q, 2H, $J$ = 16.3 Hz).

### 8.5.4 Cyanoketone 23a

A stirred solution of 1.5 g (5.1 mmol) **22a**, 1.1 g (1.2 mL, 12.7 mmol) acetone cyanohydrin and 1.3 mL (1.3 mmol) 1.0 M aqueous $Na_2CO_3$ in 20 mL MeOH was refluxed for 12 hrs after which time tlc analysis (3:1 hexane:ethyl acetate) indicated complete conversion of **22a**. The mixture was cooled to rt, diluted with 10 mL water, and extracted with two 20 mL portions of dichloromethane. After drying the dichloromethane solution over $MgSO_4$, evapouration of the solvent gave 1.4 g (88 %) of **23a** as a light brown oil.

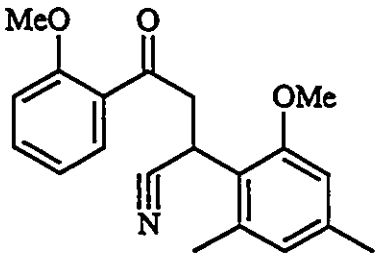


$C_{20}H_{21}NO_3$ 323.15

**23a**

**MS** (EI) m/e 323 $[M]^+$, 290, 212.

**HRMS** calcd for $C_{20}H_{21}NO_3$ 323.1521 found 323.1526.

**$^1$H-NMR** ($CDCl_3$) δ(ppm) 2.27 (s, 3H); 2.39 (s, 3H);

3.65 (dq, 2H, $J$ = 5.6, 8.2, 18.3 Hz); 3.84 (s, 3H);
3.85 (s, 3H); 4.84 (dd, 1H, $J$ = 5.6, 8.2 Hz); 6.58 (s, 1H);
6.60 (s, 1H); 6.93 (d, 1H, $J$ = 8.2 Hz); 6.96 (t, 1H, $J$ = 8.1 Hz);
7.45 (t, 1H, $J$ = 7.8 Hz); 7.73 (d, 1H, $J$ = 7.7 Hz).

### 8.5.5 Cyanoketone 23b

A stirred solution of 250 mg (0.9 mmol) **22b**, 189 mg (202 µL, 2.2 mmol) acetone cyanohydrin and 220 µL (0.2 mmol) 1.0 M aqueous $Na_2CO_3$ in 10 mL MeOH was treated as described above (with the exception that $Et_2O$ was used for the extraction in workup as dichloromethane formed emulsions) giving 220 mg (80 %) of **23b** as a pale yellow oil.

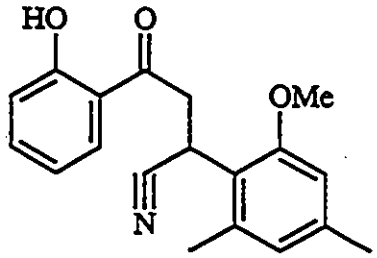


$C_{19}H_{19}NO_3$ 309.14

**23b**

**MS** (EI) m/e 309 $[M]^+$, 291, 264, 212, 174.

**HRMS** calcd for $C_{19}H_{19}NO_3$ 309.1365 found 309.1389.

**$^1$H-NMR** ($CDCl_3$) δ(ppm) 2.28 (s, 3H); 2.39 (s, 3H);
3.70 (dq, 2H, $J$ = 5.7, 8.1, 18.0 Hz); 3.88 (s, 3H);
4.78 (dd, 1H, $J$ = 5.7, 8.1 Hz); 6.60 (s, 1H); 6.62 (s, 1H);
6.86 (t, 1H, $J$ = 6.9 Hz); 6.95 (d, 1H, $J$ = 8.5 Hz);
7.45 (t, 1H, $J$ = 7.7 Hz); 7.64 (d, 1H, $J$ = 8.1 Hz); 11.92 (s, 1H).

# Claims to Original Research

## Chapter 5:

1) 2-(methoxymethyl)benzaldehyde (**11**), 2-(acetoxymethyl)-benzaldehyde (**14a**), 2-(benzoyloxymethyl)benzaldehyde (**14b**) and 2-(pyvaloyloxymethyl)benzaldehyde (**14c**) were found to generate 1,4-dioxygenated-*o*-quinodimethanes upon irradiation, which participated in Diels-Alder reactions with several reactive dienophiles.

2) Lithium chloride was found to act as a Lewis acid catalyst in the photochemically induced Diels-Alder cycloaddition of 2-(benzoyloxymethyl)benzaldehyde (**14b**) and methyl acrylate. Lewis acid catalysis employing LiCl was also observed with dimethylacetylene dicarboxylate and, to a lesser extent, with diethylfumarate as dienophiles. This represented the first example of a Lewis acid catalysed Diels-Alder reaction between a photochemically generated *o*-quinodimethane and a reactive dienophile.

## Chapter 6:

3) 2-Methylbenzoyl cyanide (**1a**) was found to dimerize, with HCN loss, forming the 3,4-dihydro-3-cyano-3-(2-methylphenyl)-1H-2-benzopyran-1-one **6a** when irradiated in the absence of a dienophile. Aroyl cyanide **1a**, as well as several other substituted acyl cyanides (including acetyl cyanide) were found to participate both in dimerizations and mixed photochemical cycloadditions giving highly substituted adducts. The acyl cyanides were also demonstrated to participate in Diels-Alder reactions with thermally generated *o*-

quinodimethanes. These observations represented the first example in which an acyl cyanide had acted in such a capacity.

4) The photoenols derived from 2-methylbenzoyl cyanide (**1a**) and 2-methoxy-6-methylbenzoyl cyanide (**1b**) were trapped with $SO_2$ giving the 1-hydroxy-1-cyano-1,3-dihydrobenzo[c]thiophene-2,2-dioxides **19** and **20**.

**Chapter 7:**

5) A novel and versatile isoquinolone synthesis was developed which involves refluxing the 3,4-dihydro-3-cyano-3-(alkyl/aryl)-1H-2-benzopyran-1-ones, obtained by cycloaddition of the aroyl or alkyl cyanides, with a substituted amine then cyclizing in 50 % acetic acid.

6) A simple isocoumarin synthesis was developed which involved base catalysed elimination of HCN from the 3,4-dihydro-3-cyano-3-(alkyl/aryl)-1H-2-benzopyran-1-ones.

7) A synthesis of 3-substituted naphthols (and naphthoquinones) was developed which involved nucleophilic addition of methyl lithium to the 3,4-dihydro-3-cyano-3-(alkyl/aryl)-1H-2-benzopyran-1-ones followed by intramolecular cyclization.

8) Naphthoquinone **16a** was shown to undergo photocyclization, presumably via a 1,5-biradical intermediate, to form the interesting semiquinone **25**. Compound **25** on treatment with TsOH formed the quinone methide **26**.

9) A facile synthesis of the potential defucogilvocarcin intermediate **16c** was developed based on a photochemical intermolecular Diels-

Alder cycloaddition of aroyl cyanides **1b** and **1e** (chapter 6).

# Publications

1) Acyl Cyanides as Carbonyl Heterodienophiles.
R. Connors and T. Durst.
*Tetrahedron Lett.* **1992**, *33*, 7277.

2) Acyl Cyanides as Carbonyl Heterodienophiles: Application to the Synthesis of Naphthols, Isoquinolones, and Isocoumarins.
R. Connors, E. Tran and T. Durst.
*Can. J. Chem.* manuscript submitted.

## References

1) Hatano, K.; Hagashide, E; Kameda, Y.; Horii, S.; Shibata, M. *Abstracts of Papers* of the Annual Meeting of the Agricultural Chemical Society of Japan, 1-4 April, p.363 (1971); Takeda, Japan 71-271, 6, Jan. 1971; *Index of Antibiotics from Actinomycetes*, (edited by H. Umezawa), Vol II. p. 1123 University Park Press, Baltimore (1978).

2) Hatano, K.; Hagashide, E.; Shibata, M.; Kameda, Y.; Horii, S.; Mizuno, K. *Agric. Biol. Chem.* **1980**, *44*, 1157.

3) Takahashi, K.; Yoshida, M.; Tomita, F.; Shirahata, K. *J. Antibiot.* **1981**, *34*, 271.

4) Hirayama, N; Takahashi, K.; Shirahata, K.; Ohashi, Y.; Sasada, Y. *Bull. Chem. Soc. Jpn.* **1981**, *54*, 1338.

5) Jain, T.C.; Simolike, G.C.; Jackman, L.M. *Tetrahedron* **1983**, *39*, 599.

6) Balitz, D.M.; O'Herron, F.A.; Bush, J.; Vyas, D.M.; Nettleton, R.E.; Grulich, R.E.; Bradner, W.T.; Doyle, T.W.; Arnold, E.; Clardy, J. *J. Antibiot.* **1981**, *34*, 1544.

7) Strelitz, F.; Flon, H.; Asheshov, I.N. *J. Bacteriol.* **1955**, *69*, 280.

8) Weiss, U.; Yoshihira, K.; Highet, R.J.; White, R.J.; Wei, T.T. *J. Antibiot.* **1982**, *35*, 1194.

9) Sehgal, S.N.; Vezina, C. **1980**, U.S. Patent 4 230 692.

10) Findlay, J.A.; Liu, J.S. *Can. J. Chem.* **1981**, *59*, 3018.

11) Misra, R.; Tritch, H.R. III; Pandey, R.C.; *J. Antibiot.* **1985**, *38*, 1280.

12) a) Morimoto, M.; Okubo, S.; Tomita, F; Marumo, H. *J. Antibiot.* **1981**, *34*, 701; b) Tomita, F; Takahashi, K.; Tamaoki, T. *J. Antibiot.* **1982**, *35*, 1038; c) Sehgal, S.N.; Czerkawski, H.; Kudelski, A.; Pandev, K.; Saucier, R.; Vezina, C. *J. Antibiot.* **1983**, *36*, 355; d) Rakhit, S.; Eng, C.; Baker, H.; Singh, K. *J. Antibiot.* **1983**, *36*, 1490; e) Singh, K. *J. Antibiot.* **1984**, *37*,

71; f) Wei, T.T.; Byrne, K.M.; Warnick-Pickle, D.; Greenstein, M. *J. Antibiot.* **1982**, *35*, 545.

13) Elespuru, R.K.; Gonda, S.K. *Science (Washington D.C.)* **1984**, *223*, 69.

14) Elespuru, R.K.; Hitchins, V.M. *Photochem. Photobiol.* **1986**, *44*, 607.

15) McGee, L.R.; Misra, R. *J. Am. Chem. Soc.* **1990**, *112*, 2386.

16) Fridovich, I. *Annu. Rev. Pharmacol. Toxicol.* **1983**, *23*, 239.

17) Weishaupt, K.R.; Gomer, C.; Dougherty, T.J. *Cancer Res.* **1976**,*36*, 2326.

18) Riesz, P.; Alegria, A.E.; Krishna, C.M.; Elespuru, R.K. *Photochem. Photobiol.* **1989**, *49*, 257.

19) Findlay, J.A.; Daljeet, A.; Murray, P.J.; Rej, R.N. *Can. J. Chem.* **1987**, *65*, 427.

20) Danishefsky, S.J.; Nguyen, N.H.; Patten, A.D. *j. Org. Chem.* **1988**, *53*, 1003.

21) Jung, M.E.; Jung, Y.H. *Tetrahedron Lett.* **1988**, *29*, 2517.

22) Suzuki, A. *Pure Appl. Chem.* **1985**, *57*, 1749.

23) Martin, O.R.; Deshpande, P.P. *Tetrahedron Lett.* **1990**, *31*, 6313.

24) Hart, D.J.; Merriman, G.H. *Tetrahedron Lett.* **1989**, *30*, 5093.

25) McGee, L.R.; Confalone, P.N. *J. Org. Chem.* **1988**, *53*, 3695.

26) Hua, D.H.; Saha, S.; Roche, D.; Maeng, J.C.; Iguchi, S.; Baldwin, C. *J. Org. Chem.* **1992**, *57*, 399.

27) McKenzie, T.C.; Hassen, W.; Macdonald, S.J.F. *Tetrahedron Lett.* **1987**, *28*, 5435.

28) Parker, K.A.; Coburn, C.A. *J. Org. Chem.* **1991**, *56*, 1666.

29) Suzuki, K.; Matsumoto, T.; Hosoya, T. *J. Am. Chem. Soc.* **1992**, *114*, 3568.

30) a) Charlton, J.L.; Alauddin, M.M. *Tetrahedron* **1987**, *43*, 2873. b) Oppolzer, W. *Synthesis* **1978**, 793. c) Kametani, T.; Nemoto, H. *Tetrahedron* **1981**, *37*, 3.

31) Cava, M.P.; Napier, D.R. *J. Am. Chem. Soc.* **1957**, *79*, 1701.

32) Durst, T.; Kozma, E.C.; Charlton, J.L. *J. Org. Chem.* **1985**, *50*, 4829.

33) Macdonald, D.I.; Durst, T. *J. Org. Chem.* **1988**, *53*, 3663.

34) Klundt, I.L. *Chem. Rev.* **1970**, *70* , 471.

35) Houk, K.N.; Jefford, C.W.; Bernardinelli, G.; Wang, Y.; Spellmeyer, D.C.; Buda, A. *J. Am. Chem Soc.* **1992**, *114*, 1157.

36) Schiess, P.; Heitzmann, M. *Angew. Chem. Int. Ed. Engl.* **1977**, *16*, 469.

37) Moss, R.J.; Rickborn, B. *J. Org. Chem.* **1986**, *51*, 1992.

38) Funk, R.L.; Vollhardt, K.P.C. *Chem. Soc. Rev.* **1980**, *9*, 41.

39) Ito, Y.; Amino, Y.; Nakatsuka, M.; Saegusa, T. *J. Am. Chem. Soc.* **1983**, *105*, 1586.

40) Tseng, K.L.; Michl, J. *J. Am. Chem. Soc.* **1977**, *99*, 4840.

41) Quinkert, G.; Stark, H. *Angew. Chem. Int. Ed. Engl.* **1983**, *22*, 637.

42) Durst, T.; Tetreault-Ryan, L. *Tetrahedron Lett.* **1978**, 2353.

43) Sammes, P.G.; *Tetrahedron* **1976**, *32*, 405.

44) Durst, T.; Glinski, M.B. *Can. J. Chem.* **1983**, *61*, 573.

45) Oppolzer, W.; Keller, K. *J. Am. Chem. Soc.* **1971**, *93*, 3836.

46) Kessar, S.V.; Singh, P.; Vohra, R.; Pal Kaur, N.; Venugopal, D. *J. Org. Chem.* **1992**, *57*, 6716.

47) a) Kraus, G.A.; Chen, L. *Synlett* **1991**, 89. b) Kraus, G.A.; Chen, L. Synthetic Communications **1993**, *23*, 2041.

48) Wagner, P.J.; Park, B. *J. Am. Chem. Soc.* **1991**, *113*, 709.

49) Coll, G.; Costa, A.; Deya, P.M.; Flexas, F.; Rotger, C.; Saa, J.M.

*J. Org. Chem.* **1992**, *57*, 6222.

50) Kitaura, Y.; Matsuura, T. *Tetrahedron Lett.* **1967**, 3309.

51) a) Findlay, D.M.; Tchir, M.F.; *J. Chem. Soc. Faraday Trans. I* **1976**, *72*, 1096. b) Haag, R.; Wirz, J.; Wagner, P.J. *Helv. Chem. Acta* **1977**, *60*, 2595.

52) Arnold, B.J.; Sammes, P.G.; Wallace, T.W. *J. Chem. Soc., Perkin Trans. 1* **1974**, 415.

53) Ian Flemming. *Frontier Orbitals and Organic Chemical Reactions.* John Wiley & Sons, London (1976). chpt. 4.

54) Charlton, J.L.; Koh, K. *Tetrahedron Lett.* **1988**, *29*, 5595.

55) Charlton, J.L.; Durst, T. *Tetrahedron Lett.* **1984**, *25*, 5287.

56) See ref 32.

57) Mann, J.; Piper, S.E. *J. Chem. Soc. Chem. Commun.* **1982**, 430.

58) Arnold, B.J.; Sammes, P.G.; Wallace, T.W. *J. Chem. Soc., Perkin Trans. 1* **1974**, 401.

59) a) Alston, P.V.; Ottenbrite, R.M. *J. Org. Chem.* **1975**, *40* 1111. b) Houk, K.N.; Strozier, R.W. *J. Am. Chem. Soc.* **1973**, *95*, 4094.

60) Anh, N.T.; Seyden-Penne, *J. Tetrahedron* **1973**, *29*, 3259.

61) Kelly, T.R.; Meghani, P.; Ekkundi, V. *Tetrahedron Lett.* **1990**, *31*, 3381.

62) Oppolzer, W. *Angew. Chem. Int. Ed. Engl.* **1971**, *11*, 1031.

63) Kametani, T.; Kajiwara, M.; Takahashi, T.; Fukumoto, K. *J. Chem. Soc., Perkin trans. 1* **1975**, 737.

64) Koreeda, M.; Ciufilini, M.A. *J. Am. Chem. Soc.* **1982**, *104*, 2308.

65) Tagmazyan, K.T.; Mkrtchyan, R.S.; Babayan, A.T. Zh. Org. Khim. **1974**, *10*, 1657.

66) a) Kessar, S.V.; Singh, P.; Vohra, R.; Kaur, N.P.; Venugopal, D.

*J. Org. Chem.* **1992**, *57*, 6716. b) Kessar, S.V.

*Pure & Appl. Chem.* **1987**, *59*, 381.

67) Hunig, S.; Schaller, R. *Angew. Chem. Int. Ed. Engl.* **1982**, 36.

68) Hauser, F.M.; Ellenberger, S.R. *Synthesis* **1987**, 723.

69) C. Bensimon, University of Ottawa.

70) Charlton, J.L. *Can. J. Chem.* **1986**, *64*, 720.

71) Charlton, J.L.; Durst, T. *Tetrahedron Lett.* **1984**, *25*, 2663.

72) a) S.W. Pelletier. *Chemistry of the Alkaloids*. Van Nostrand Reinhold Co., New York (1970) p.77. b) M. Shamma, J.L. Moniot. *Isoquinoline Alkaloid Research*. Plenum Press, New York (1978) p.57.

73) Dyke, S.F. et al. *Tetrahedron* **1971**, *27*, 281.

74) Dyke, S.F.; Brown, D.W. *Tetrahedron* **1966**, *22*, 2429.

75) Iida, H.; Kawano, K.; Kikuchi, T.; Yoshimizu, F. *Yakugaku Zasshi* **1976**, *96*, 176.; *CA* **1976**, *84*, 135898.

76) Tirodkar, R.B.; Usgaonkar, R.N. *Indian J. Chem., Sect. B.* **1972**, *10*, 1060.

77) a) Belgaonkar, V.H.; Usgaokar, R.N. *Tetrahedron Lett.* **1975**, 3849. b) Stanoeva, E.; Haimova, M.; Ognyanov, V. *Liebigs Ann. Chem.* **1984**, 389.

78) Mali, R.S.; Kulkarni, B.K.; Shankaran, K. *Synthesis* **1982**, 329.

79) Couture, A.; Cornet, H.; Grandclaudon, P. *Tetrahedron* **1992**, *48*, 3857.

80) Oediger, H.; Muller, F.; Eiter, K.. *Synthesis* **1972**, 591.

81) Gray, T.L. et al. *Tetrahedron* **1979**, *35*, 2539.

82) Sakamoto, T. et al. *Chem. Pharm. Bull.* **1986**, *34*, 2754.

83) Barret, R.; Daudon, M. *Tetrahedron Lett.* **1990**, *31*, 4871.

84) K. Thomas Finley in *The Chemistry of the quinoid compounds* S. Patai (Ed.), John Wiley & Sons, London (1974) p. 880.

85) Kanaoka, Y.; Koyama, K. *Tetrahedron Lett.* **1972**, 4517.

86) a) Wagner, P.J.; Meador, M.A.; Zhou, B.; Park, B. *J. Am. Chem. Soc.* **1991**, *113*, 9630. b) Schaden, G. *Angew. Chem. Int. Ed. Engl.* **1977**, *16*, 50.

87) Snieckus, V.; Wang, W. *J. Org. Chem.* **1992**, *57*, 424.

88) Beak, P.; Meyers, A.I. *Acc. Chem. Res.* **1986**, *19*, 356.

89) Utimoto, K.; Wakabayashi, Y.; Horiie, T.; Inoue, M.; Shishiyama, Y.; Obayashi, M.; Nozaki, H. *Tetrahedron* **1983**, *39*, 967.

90) Herzig, J.; Gottlieb, H.E.; Nudelman, A. *J. Chem. Research* **1986**, 196.